UNIVERSITÀ DEGLI STUDI

DI MODENA E REGGIO EMILIA

Research Doctorate in Food and Agricultural Science, Technology and Biotechnology

XXXIII Cycle

Characterization of Emilia-Romagna wines by high resolution mass spectrometry and nuclear magnetic resonance: case study on commercial Lambrusco and minor variety wines of *Vitis vinifera* L. newly registered in the national register of varieties

Candidate: Leonardo Setti

Tutor: Prof. Andrea Antonelli

Co-Tutor: Prof. Francesca Masino

Coordinator: Prof. Alessandro Ulrici

Acknowledgements

Vorrei innanzitutto ringraziare i componenti del gruppo di ricerca: il prof. Andrea Antonelli, la dott.ssa Francesca Masino ed il dott. Giuseppe Montevecchi. Se dovessi valutarli, lo farei con una PCA, visto che le variabili da considerare sarebbero molteplici. Se ognuno di loro rappresentasse una componente principale, sono sicuro che ognuna spiegherebbe il 33% della varianza totale del gruppo. Siete stati dei fantastici compagni di viaggio, a tratti complicati, ma d'altronde, chi non è un po' complicato in questo mondo?

Rimanendo sul tema dell'analisi statistica, vorrei ringraziare il prof. Alessandro Ulrici, che più volte mi ha aiutato a capire come si fa ad andare d'accordo con le matrici. La stessa cosa per il prof. Davide Bertelli, non solo con la statistica, ma anche con l'intricato mondo della risonanza magnetica nucleare (NMR = non molto raccomandabileperrimaneresanidimente).

Grazie alla prof. Elvira Tamames e alla prof. Montserrat Riu, per avermi accolto all'Università di Barcellona, e per avermi poi presentato la prof. Cristina Minguillon. Mi avete permesso di fare un'esperienza incredibile. Muchisimas gracias por todo!

Se non ci fosse il CIGS non ci sarebbe nemmeno questa tesi. Grazie infinite ai dott. Maria Cecilia Rossi, Filippo Genovese e Diego Pinetti. Grazie per non aver mai ignorato la chiamata alla vista del mio numero!

Un ringraziamento particolare va anche ai dott. Giovanni Nigro, Stefano Giovannini, Fabrizio Bocedi e Franco Roccatello per aver sempre fornito i campioni (tra mille difficoltà) e le informazioni necessarie.

Questa esperienza ha permesso non solo di fare molte conoscenze sul lavoro, ma di stringere nuove amicizie. A tutti i nuovi amici (modenesi, toscani, messicani, cileni, sardi, catalani, piemontesi, veneti, romani, portoghesi, argentini e russi), grazie per aver aumentato la biodiversità delle mie conoscenze!

Un ringraziamento lo devo anche alle persone che mi hanno dato tanti consigli nel corso degli ultimi anni. Vorrei quindi ringraziare la prof.ssa Donatella Pavanelli, il prof. Marco Setti, la dott.ssa Federica Filippi ed il dott. Claudio Cavazza per avermi aiutato ad indirizzare la mia carriera.

L'ultimo ringraziamento va al motivo principale per cui ognuno si impegna: la famiglia e le persone care. Per tre anni mi avete visto super occupato e super impegnato. Finalmente, dal primo gennaio sarò disoccupato, ma per lo meno avrò un po' più di tempo per voi. Grazie infinite per quello che mi avete permesso di fare.

A papà, con affetto.

Riassunto

Il progetto è stato svolto con l'obiettivo di trovare nuovi metodi alternativi ed a basso impatto ambientale per la caratterizzazione dei vini, commerciali e minori. Infatti, le analisi eseguite presso il Centro Interdipartimentale Grandi Strumenti (CIGS) di Modena, hanno permesso di analizzare i vini della famiglia dei Lambruschi, diventati ormai tra i vini più consumati ed esportati al mondo; i vini della famiglia delle Malvasie, che sempre più si stanno affermando sul mercato; i vini meno conosciuti dell'Emilia-Romagna, prodotti dal Centro di Ricerca delle Produzioni Vegetali (CRPV) di Cesena, sia rossi che bianchi. In particolare, per quel che riguarda i vini rossi, la metabolomica si è rivelata un approccio efficace, e l'utilizzo di strumenti di avanguardia quale lo spettrometro di massa ad alta risoluzione Orbitrap Q Exactive, ha permesso di individuare oltre 100 molecole di antocianine. Tra esse, oltre a quelle glicosilate, acetil-glicosilate, coumaroil-glicosilate e caffeoil-glicosilate, sono state individuate molte altre forme derivate, come ad esempio i di-glucosidi, che sono caratteristici delle viti americane, ma sono presenti in tracce anche nelle varietà di *V. vinifera*, così come le combinazioni con le catechine e le gallocatechine, a più alto peso molecolare. Infatti, con i metodi analitici comuni quali la spettrofotometria UV o la cromatografia liquida UV, non permettono di vedere le molecole presenti in basse concentrazioni, a causa della minore sensibilità dei rivelatori. Inoltre, gli spettrofotometri UV permettono di individuare le molecole solo in base ai tempi di ritenzione di quest'ultime, che spesso co-eluiscono le une con le altre, nonostante il metodo cromatografico sia stato messo a punto in modo adeguato. Analizzando i dati tramite la Principal Component Analysis (PCA), l'Ancellotta è stata confermata, sia in termini di quantità, sia come stabilità produttiva, come la varietà più interessante per la produzione di vino da taglio. Anche i lambruschi Salamino, Grasparossa e Reggiano, sono facilmente distinguibili ed hanno dimostrato anch'essi un'ottima resa, in termini di colore. Dal punto di vista tecnologico, è stato possibile distinguere l'Ancellotta vinificata in rosso da quella vinificata in bianco. Infatti, quella vinificata in rosso, soprattutto nell'annata 2019, si distingue non solo per gli alti contenuti di antocianine glicosilate, che sono tipicamente le più ricercate dagli enologi, ma anche per la grande quantità di antocianine derivate citate precedentemente. Tra i vitigni minori, il Festasio si è rivelato il vino con delle caratteristiche molto simili a quelle dei vini già presenti in commercio, sia in termini qualitativi che quantitativi. Anche il Lambrusco di Fiorano (o Lambrusco del Pellegrino), tipico del Modenese, seppur con una colorazione meno abbondante, ha mostrato caratteristiche interessanti per la vinificazione del Lambrusco. Per quanto riguarda le analisi dei vini bianchi, è stata condotta un'analisi mediante Risonanza Magnetica Nucleare monodimensionale (H^1-NMR),

approccio tipico delle analisi “untargeted” delle matrici. Questo tipo di analisi, nonostante sia un’analisi più approssimativa rispetto alla spettrometria di massa, ha consentito di caratterizzare efficacemente i vini rossi minori descritti in precedenza, oltre ai vini bianchi minori di Caveccia, Vernaccia del Viandante, Bertinora e Vernaccina, un tempo diffuse soprattutto nelle province rivierasche del Mar Adriatico, e la Melara, originaria della provincia di Piacenza. In particolare, è stato possibile distinguere i vini minori dai vini già presenti in commercio, quali ad esempio i Lambruschi ed il Pignoletto. Di quest’ultimo, è stato inoltre possibile distinguere il prodotto commerciale, e quindi già rifermentato in bottiglia, dal prodotto non ancora rifermentato, con un contenuto alto di zuccheri residui, ed ancora di basso grado alcolico.

Abstract

The project was carried out with the aim of finding new alternative and low environmental impact methods for the characterization of commercial and minor wines. In fact, the analyzes carried out at the Centro Interdipartimentale Grandi Strumenti (CIGS) in Modena permitted to analyze the wines of the Lambrusco family, which have now become among the most consumed and exported wines in the world; the wines of the Malvasia family, which are increasingly establishing on the market; the lesser-known wines of Emilia-Romagna, produced by the Centro di Ricerca delle Produzioni Vegetali (CRPV) of Cesena, both red and white. Regarding to the red wines, metabolomics proved to be an effective approach, and the use of cutting-edge tools such as the high-resolution mass spectrometer Orbitrap Q Exactive, permitted to identify over 100 anthocyanin molecules. Among them, in addition to the most known forms such as glycosylated, acetyl-glycosylated, coumaroyl-glycosylated and caffeoyl-glycosylated, many other derivative forms were identified, such as di-glucosides, which are typical of American vines, but are present in traces also in the varieties of *V. vinifera*, as well as the combinations with catechins and gallocatechins, with higher molecular weight. In fact, with common analytical methods such as UV spectrophotometry or UV liquid chromatography, it is not possible to see the molecules present in low concentrations, due to the lower sensitivity of the detectors. In addition, UV spectrophotometers allow the identification of molecules only based on the retention times, which often co-elute with each other, even though the chromatographic method has been properly developed. By analyzing the data through the Principal Component Analysis (PCA), the Ancellotta was confirmed, both in terms of quantity and production stability, as the most interesting variety to produce blended wine. Even the Lambrusco Salamino, Grasparossa and Reggiano, are easily distinguishable and have also shown an excellent yield, in terms of color. From a technological point of view, it was possible to distinguish the Ancellotta vinified in red from that vinified in white. In fact, the red vinified one, especially in the 2019 vintage, stands out not only for the high contents of glycosylated anthocyanins, which are typically the most appreciated by winemakers, but also for the large number of derived anthocyanins mentioned above. Among the minor vines, Festasio proved to be the wine with characteristics very similar to those of the wines already on the market, both in qualitative and quantitative terms, and it can be used as blended wine. Lambrusco di Fiorano (or Lambrusco del Pellegrino), typical of the Modena province, even if with a less abundant color, also showed interesting characteristics for the vinification of Lambrusco. As for the analysis of white wines, an analysis was conducted using mono-dimensional Nuclear Magnetic Resonance (H^1-NMR), a typical approach of "untargeted" analysis. This type of analysis, despite being a more approximated

analysis than mass spectrometry, allowed the characterization of the minor red wines described above, as well as the minor white wines of Caveccia, Vernaccia del Viandante, Bertinora and Vernaccina, once widespread especially in the coastal provinces of the Adriatic Sea, and the Melara, originally from the province of Piacenza. Moreover, it was possible to discriminate minor wines from wines already on the market, such as Lambrusco and Pignoletto. Of the latter, it was also possible to distinguish the commercial product, and therefore already refermented in the bottle, from the product not yet refermented, and thus with a higher content of residual sugars, and still low in alcohol.

Table of contents

2.7 GC analysis for volatile aromatic compounds

2.7.1 Solid phase extraction (SPE) of the free aromatic compounds

2.7.2 Gas chromatographic method

2.7.3 Identification of volatile compounds

2.8 Preliminary metabolomic analyses

2.8.1 Identification of anthocyanins

2.8.1 Identification strategy

2.8.2 Anthocyanins quantitative analysis

2.9 Q-Exactive qualitative and quantitative analysis

2.9.1 Anthocyanins

2.9.2 Identification strategy

2.9.3 Identification strategy with the platform XCMS

2.10 Nuclear Magnetic Resonance

2.10.1 ^{1}H-NMR 400 MHz experiment

2.10.2 NMR 600 MHz experiment

2.11 Statistical analysis

3. Results and discussion

3.1 GC-MS analysis

3.2 Preliminary metabolomic analysis

3.2.1 Anthocyanins identification with ESI-LC-MS-IT

3.2.2 Anthocyanins quantification with HPLC

3.3 Orbitrap analyses

3.3.1 Identification of anthocyanins

3.3.2 Quantification of anthocyanins

3.3.3 XCMS analysis

3.4 NMR analysis

3.4.1 NMR 400 MHz analysis

3.4.2 NMR 600 MHz analysis

4. Conclusion

1 Introduction

1.1 Food science

Food science is the discipline that studies the processing, the composition and the deterioration of foods, and the improvements achievable for the consumers (www.ift.org). Nowadays, consumers put more attention to original foods and beverages that contain healthy and/or bioactive compounds, or with appreciable characteristics. For these reasons, reliable and reproducible analytical methods need to be developed and studied, in order to keep the high quality and safe foods production and to increase human health (Hatzakis, 2017).

1.2 Grape varieties

The export of Protected Designation of Origin (PDO) and Protected Geographical Indication (PGI) sparkling wines increased by about 7.9% and 6.7% in the last year, respectively (Ismea, 2017). Among sparkling wines, Lambrusco is one of the more exported. There are several kinds of PDO Lambrusco: L. di Sorbara, L. Grasparossa di Castelvetro, L. Salamino di Santacroce, L. Reggiano, L. di Modena, Colli di Scandiano e di Canossa and Colli di Parma (Ismea). The varieties used for each winemaking process are listed in the specification of Production and are widespread in all the Emilia-Romagna region. However, there are a lot of minor varieties, according to Maul et al. (2017), that could be cultivated for Lambrusco winemaking. Nevertheless, the law that controls the admitted varieties has become a limit for the conservation and the wide spreading of local varieties (Visser, 2002; Law CE 98/95). Grapevine (*Vitis vinifera* L.) cultivation is an agricultural activity of ancient date and is widespread in every part of the Emilia-Romagna region (Northern Italy). Almost all the production of the provinces of Reggio Emilia and Modena is now based on red grape varieties for the Lambrusco wine production (Montevecchi et al., 2016). The varieties Ancellotta, L. Grasparossa, L. Maestri, L. Marani, L. Salamino, L. di Sorbara, L. Viadanese, Malbo Gentile, Marzemino are the most widely cultivated. Some of these varieties started to be of interest for researchers and wine producers worldwide. Indeed, Malinovski et al. (2016) demonstrated that the “Ancellotta” variety, produced in the Santa Catarina State (Brazil), has shown interesting characteristics for quality wine production, while the “Lambrusco” variety was the one with the most constant phenology. Moreover, the Lambrusco wine produced in Emilia Romagna achieved significant commercial success in America during the 1970s (Catena, 2005), especially the L. Reggiano, produced from L. Salamino and Maestri varieties (Boccaci et al., 2005).

1.2.1 Commercial Italian red varieties

Ancellotta

The Ancellotta grape variety is mainly grown in the Reggio Emilia province, and is probably the most versatile for the winemaking of Lambrusco wine. Because of its bright red color, it is also known as "rossissimo" and is used in the blending of other wines, such as L. Salamino and L. Maestri, with a lower hue value. The resulting wine is characterized by low acidity, an intense red color and high sugar content, such as the "Lambrusco Salamino di Santa Croce DOC" and the

"Reggiano DOC" (Calò et al., 2010). The Ancellotta has large pyramidal bunches, with a peel that is very reminiscent of an intense dark blue. The vine grows mainly in clayey soils, has good resistance to drought and frost, as well as to diseases and pests such as botrytis and downy mildew. In the last 10-15 years, this variety spread even in Switzerland, to blend Pinot varieties, and Brazil, to produce both monovarietal (Don Guerino) and blended wine (Robinson et al., 2012).

Lambrusco Maestri

The L. Maestri (LM) variety is probably native of the province of Parma, and the DNA analyses suggest that is a possible parent-offspring of the variety Fortana (Robinson et al., 2012; Boccacci et al., 2005). Nowadays, it is especially cultivated in the Emilia-Romagna region, but (it is also cultivated in) also in the Mantua province (Lombardia, Italy), in Puglia, in the South Italy, and even in Argentina (Robinson et al., 2012; Zulini et al., 2002). This variety is usually used as a blending wine to produce “Lambrusco Reggiano DOC” and “Lambrusco Mantuano DOC”. However, the “Lambrusco dell’ Emilia IGT” is produced with 100% of L. Maestri and is a rustic and a tannic red sparkling wine with strawberry notes (Robinson et al., 2012).

Lambrusco Marani

The L. Marani (LMA) variety is probably closely related to the Fogarina variety (Boccacci et al., 2005). This variety is highly productive, vigorous and adapted to damp soils, but is susceptible to low winter temperature. Lambrusco Marani is especially widespread in the province of Reggio Emilia, but is also cultivated in the provinces of Parma, Mantua, and Bologna to produce both red and white wines. In fact, is a blending wine to produce “Rosso Reggiano DOC”, “Colli di Scandiano e di Canossa DOC”, and “Reggiano Bianco Spumante”. Usually, the resulting wine is dry or middle-dry, fresh, with tannic and fruity notes (Robinson et al., 2012).

Lambrusco Grasparossa

The L. Grasparossa (LG) variety is widespread, especially in the province of Reggio Emilia and Modena, in which is cultivated particularly to produce the wine “Colli di Scandiano e di Canossa DOC” and “Lambrusco Grasparossa di Castelvetro DOC” (Robinson et al., 2012). The resulting wine has an intense color, a higher alcohol content, and more fruity and tannic notes than other Lambrusco varieties. However, it can be used for both dry and semi-sweet wine production (Robinson et al., 2012).

Lambrusco Salamino

The name L. Salamino (LS) is due to the cylindrical shape of the bunches. Because of this characteristic, the berries are very close each other and this facilitates the development of downy and powdery mildew. This variety is native from the Santa Croce di Carpi (Modena, Italy), and is widespread throughout the provinces of Reggio Emilia, Modena, and with a lesser extension in Mantua, Bologna, and Ferrara (Italy). Especially in Modena, is a blended wine to produce the "Lambrusco di Sorbara DOC" and "Lambrusco Salamino di Santa Croce DOC", while being the main variety for the "Lambrusco Mantuano" and "Lambrusco Reggiano" (Robinson et al., 2012).

1.2.2 Commercial Italian white varieties

Pignoletto

The Pignoletto (PI) white grape variety is native from the province of Bologna, and its name is due to the shape of the bunches, that is like a pinecone. Several studies showed that Pignoletto has a closed genetic relationship with Spergola and Grechetto di Orvieto varieties, while it is genetically identical to Ribolla Riminese and Grechetto di Todi. Thus, it is cultivated in Emilia-Romagna, in Northern Italy, to produce "Colli Bolognesi DOC" and "Colli di Imola", while in Central Italy, in Marche, Lazio, Umbria, it is produced under the name Grechetto (Robinson et al., 2012).

Malvasia

The Malvasia family represents a wide group of varieties native to Greece and widespread in the Mediterranean area (Crespan et al., 2006). Then the cultivation has been expanded to North America (Bettiga et al., 2003), South America (Fielden, 2003; Ducati et al., 2009) and Australia. Several Malvasia varieties are characterized by specific aromatic compounds that give to the resulting wines a particular sensorial trait. Nowadays, in the Italian National Register of Grapevine varieties (are registered) 19 varieties are registered, native from several Italian geographical zones. In fact, they are cultivated in Northern Italy, such as in the Piedmont, Lombardia, Emilia-Romagna and Friuli-Venezia Giulia regions; in Central Italy, such as in the Lazio, Umbria, and Tuscany regions; in Southern Italy, such as the Basilicata, Puglia, and Molise regions; and finally, in the islands, Sardinia and Sicily (Mipaaf, Registro Nazionale delle Varietà di Vite, 2020). In particular, the wines analyzed in this study were obtained from the varieties cultivated in the Emilia-Romagna region, in the provinces of Parma, Reggio Emilia and Piacenza (Italy), and in the zone of Oltrepò

Pavese, in the Pavia province (Lombardia, Italy) (i.e., Malvasia Bianca, Malvasia Istriana, Malvasia Bianca di Candia, Malvasia di Candia Aromatica). The Malvasia di Candia aromatica (MCA) variety has been already studied in several agronomical, genetical, and metabolomic studies (Zamboni *et al.*, 2009; Bavaresco et al., 2008; Giust et al., 2005; Costacurta et al., 2005; Borsa et al., 2005; Lacombe et al., 2007; Meneghetti et al., 2012). Recently, Ruffa et al. (2016) have demonstrated that there is no parent-offspring relationship between the Malvasia di Candia Aromatica the White Muscat (Moscato bianco). Moreover, several studies on the sensorial and aromatic profiling studies have shown the main traits that make this variety so appreciated to the consumers, and thus requested on the market (Scalabrelli et al., 2008; Nicolini et al., 2009; Montevecchi et al., 2015).

1.2.3 Minor red varieties

Several cultivars are considered minor varieties and are usually cultivated on a limited surface (a few hectares or less) in a very old vineyard (30-40 years, or more). Moreover, not all are included in the National Register of Grape Varieties and, thus, considered "in danger of extinction", even if specific international indicators for cultivar biodiversity do not exist (FAO, 2009; FAO, 2002; Maul et al. 2017; MiPaaf, 2013). Because of the strong competition on the international wine market, new products have started to be sought by producers (Boccaci et al., 2005).
Minor grape varieties are widespread in all Emilia-Romagna region, and they can be produced for both white and red wines winemaking. These ancient grape varieties have been bred for the production in a specific area. Moreover, these varieties represent an important biodiversity source to increase high-quality wine production (Mattivi et al., 2002).

In the Fig. 1 is reported the geographical origin of the minor red grape varieties analyzed in this study.

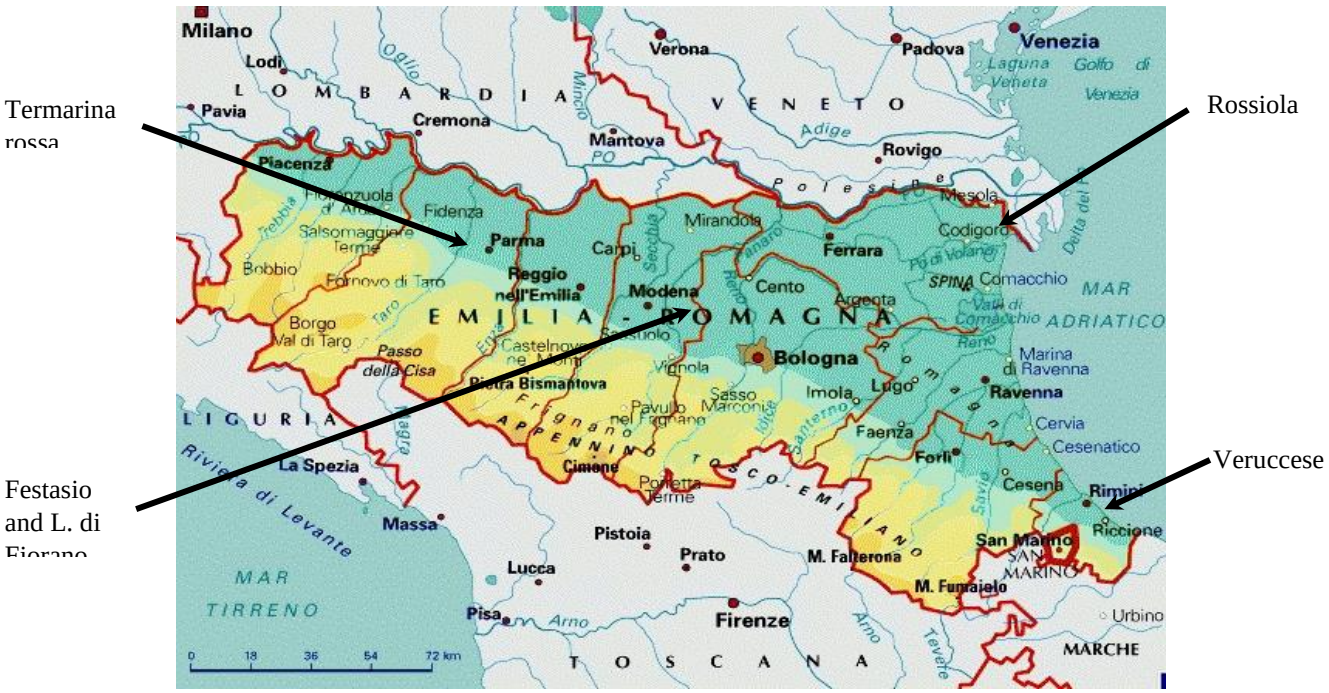

Figure 1. Origin of minor red grapes in the Emilia-Romagna region.

Veruccese

According to the Emilia-Romagna region website, there are only 220 cultivated plants of this grape variety, located in the Province of Rimini (Italy). The Veruccese (VE) or Verucchiese is a Sangiovese biotype, with very similar characteristics but with an earlier maturation (Bucci, 2007). In fact, the genomic diversity with Sangiovese has been confirmed through the DNA analysis (Nigro et al., 2010). This cultivar is used to produce a young wine ("Novello") and his cultivation is limited in the Verucchio town area (Nigro et al., 2010). The wine produced has a ruby red color with violet reflections, low acidity, but lightly bitter and sapid, and with an appreciable flavor profile, with notes of flowers and red fruits (Nigro et al., 2010).

Termarina rossa (or Termarina)

Termarina (TE) has been cultivated for a long time in the Emilia-Romagna region. Nevertheless, up to 2005 when a 1200 plant vineyard was planted in Parma, there were just a few dozen of plants in Ravenna and in Parma. Nowadays, it is cultivated in the provinces of Parma, Reggio Emilia, and Modena. Its name is due to his origin. In fact, this variety was probably imported in Italy from the Egeo sea because of the commercial exchanges of the old Republic of Venice. Several studies refuted the similarity between Termarina and the cultivar Corinto nero (Schneider and Torello Marinoni, 2003; Boccacci et al., 2005), even if they share the seedless berry character. The

Termarina grape was originally used to produce jam and raisin. Because of his low anthocyanin content, it produces a medium intense red wine with a good aromatic profile and a high alcohol content. By contrast, it is in danger because it is very prone to both powdery mildew (*Oidium tuckeri*) and grey mold (*Botrytis cinerea*) disease, and its low production.

Lambrusco di Fiorano (or Lambrusco del Pellegrino)

This variety is typical in the foothill region of Modena and Reggio Emilia provinces, but nowadays, there are only 105 plants of Lambrusco di Fiorano or Lambrusco del Pellegrino (PE) in Castelnuovo Rangone, Modena (Italy) and Ravenna province. The morphology of this variety is very similar to another one, Lambrusco oliva. For this reason, people call it Lambrusco oliva grosso, because the berries are bigger than the berries of Lambrusco oliva (RER, 2011). Nevertheless, Boccacci et al. (2005) compared the microsatellite profile of Lambrusco di Fiorano with a large group of Lambrusco varieties, and stated that is very different, as well as Grasparossa cultivar. Nigro et al. (2013) state that Lambrusco di Fiorano can produce both sparkling and non-sparkling wine, because of his oenological characteristics. In fact, it can produce an interesting ruby red wine with violet reflexes, a high acidity, a medium astringency, and with a flavor of species, red fruits and floral notes.

Festasio

Festasio (FE) is another variety native to Modena, and the remaining plants are cultivated in Marano sul Panaro, Modena (Italy). The main characteristics are low acid content and very high anthocyanic level. The high colour intensity increases the potential of this variety. The wine has an intense red colour with violet-blue reflexes, and the aromatic characteristics present red fruit, floral and spicy (pepper and liquorice) notes (Nigro et al., 2013).

Rossiola

All the plants of Rossiola (RO; about 650) are cultivated in Comacchio, Pomposa and Lido di Spina, in Ferrara province (Italy). It has been produced in this geographical area since XIX sec. This red wine is produced by local farmers that particularly appreciate it, but there are not many bibliographic references that describe this product.

1.2.4 Minor white varieties

In Fig. 2 is reported the geographical origin of the minor white grape varieties analyzed in this study.

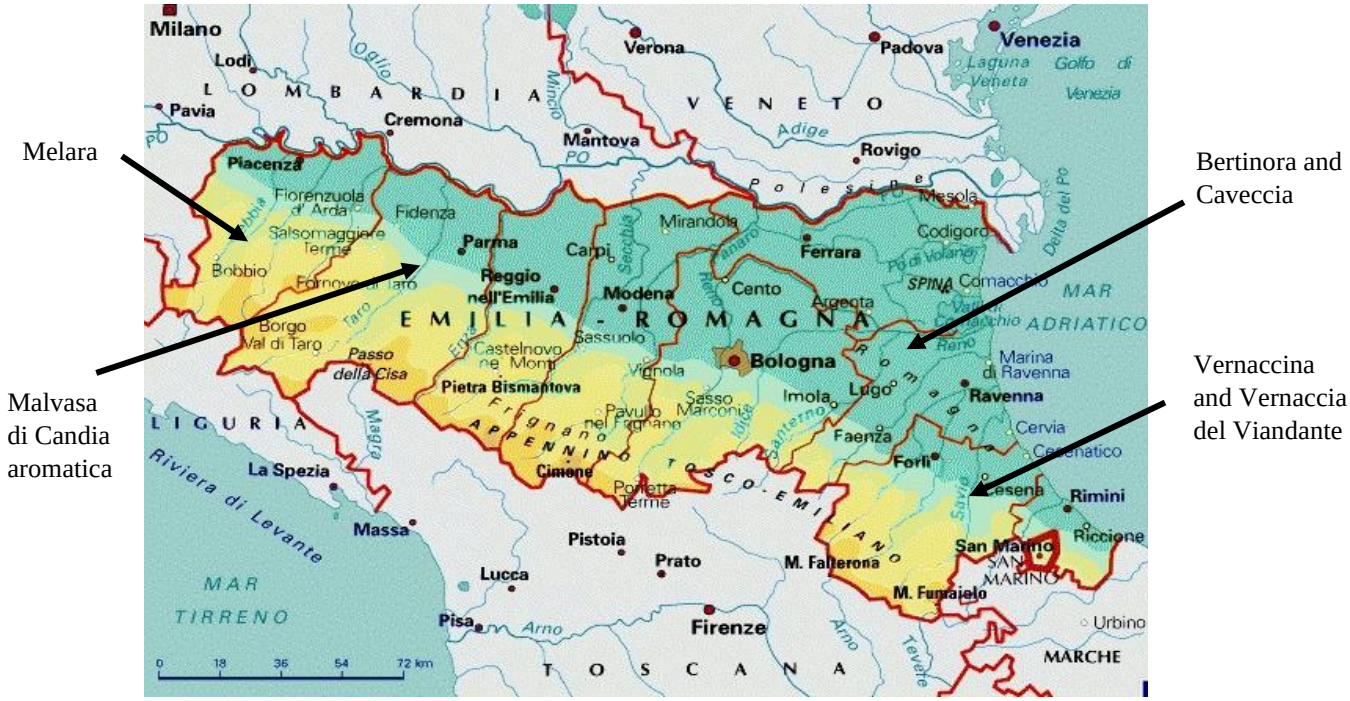

Figure 2. Distribution of minor white grapes in the Emilia-Romagna region.

Albana rosa

Albana rosa (AR) is a minor variety registered in the National Register of Grape Varieties since 2016 (G.U. 155 05/07/2016). This variety is characterized by a partial pigmented skin but is fundamentally a white grape used for white wine winemaking. In Rimini province, there is another native variety: the Albana bianca. This variety is widespread even in the province of Forlì-Cesena, and it is used to produce sweet-wines, dry non-sparkling wines, passito-wines, and even botrytized wines.

Bertinora

Nowadays, only 14 plants of Bertinora (BE) variety exist. It is cultivated in Tebano, in the Ravenna province (Italy) and in Bertinoro, in the Forlì-Cesena province (Italy), and is also named “Rossola” because when the berries are exposed to the sun, the skin turns to a light pink. Bertinora has

medium production, a late maturation, and it tolerates the downy mildew (*Plasmopara viticola*) disease.

Vernaccina

Vernaccina (VER) is a local white grape variety of the Rimini province. The cultivated vineyards are on the Rimini hills and they have been planted during the ’70, but nowadays only 35 plants exist. This variety is characterized by an early maturation and a medium-high vigor. The wine has a high alcohol content (13% - 14.5% vol.) and with a total acidity over 6.0 g/L. The color intensity is low, but it has a yellow-green reflex, while the flavor has notes of citrus fruits, exotic fruits and flowers (Nigro et al., 2010). Moreover, it has been demonstrated that this variety has a different isoenzymatic pattern from another cultivar registered in Italy, even if it is not possible to confirm the difference with Malvasia bianca di Basilicata and Zibibbo (Fontana et al., 2007).

Melara

Melara (ME) variety, or Lecco, is a white grape native from the Piacenza province and there are only 108 plants on a farm in Ziano Piacentino. Even if it is in danger of extinction, Melara variety is registered since 1999 in the National Register of Grape Varieties and it is used to produce the Vin Santo di Vigoleno (Robinson et al., 2012). According to Fregoni et al. (2002), the origin of Melara is unknown, but it was widespread around Val d’Arda. This name is probably due to the honey notes of the wine. It is a variety with low production, a medium maturation, with good sugar and acid content.

Santa Maria

Santa Maria (SM) is another white grape native from the Piacenza province and there are only 53 plants on a farm in Ziano Piacentino. As Melara, it is used to produce the Vin Santo di Vigoleno and it was cultivated in the Val d’Arda area, and its wine has a note of toasted hazelnut (Scienza et al., 2004). A study carried out by Cipriani et al. (2010) has shown that Santa Maria has probably been naturally bred from Vernaccia di Oristano and Pensicato, which is a red grape with unknown origin.

Vernaccia del Viandante

To the author's knowledge, there are no bibliographic references about Vernaccia del Viandante (VV).

1.2.5 Other varieties

Gewürztraminer (aromatic Traminer)

The Traminer is a very ancient variety with an ambiguous origin. In fact, it is probably native to the North-East region of France (Alsace, Lorraine, Champagne-Ardenne, Franche-Comptè) or to the South-West of Germany (Rheinland-Pfalz, Baden-Württemberg), more specifically to the Reno valley. Genetic analyses have demonstrated that it is strictly related to the Pinot variety, even if it is not clear which variety is the parent. Moreover, Traminer has been hybridized to create several widespread varieties, such as the “Manzoni rosa” in Italy and the “Traminette” in the North-East of the USA. Since it is an old variety, it also has various somatic variations synonyms. The first mention of Traminer dates back to 1242, in Bolzano, in which the document refers to the wine produced in Tramin (Termeno, in the Italian language) in South Tyrol (Italy), even if the Traminer variety was present in that area, and thus it was not used to produce any kind of wine at that time. Subsequently, the term Traminer appears as the name of a specific wine, produced in southern Germany (Württemberg), which thus has given the name to this grape variety. The 'Traminer' was later found to be the Savagnin that had long spread in the South-East of France, even if the name Sauvagnin appeared only in 1732 (Rézeau 1997; Krämer 2006; Robinson et al., 2012).

Alvarinho (Albariño)

The Alvarinho variety has originated in the border area between the North-eastern region of Portugal, in which is called Alvarinho, and the North-west region of Spain (Galicia), in which is called Albariño (AL) (Robinson et al., 2012). Because of its high morphological diversity, especially in Portugal, it is considered a very old variety, although its exact age is not clear (Boso et al., 2005; Santiago et al., 2005, 2007). Ibañez et al. (2003) stated that Alvarinho is genetically different from Albarìn blanco, and that it is not a color mutation of Alfrocheiro. Alvarinho is a moderately vigorous variety, with an early-mid ripening, susceptible to downy and powdery mildew and mites, and the resulting wine is fresh, with several floral and fruity aromas and flavors, such as lemongrass, honeysuckle, peach, and orange (Robinson et al., 2012). For these reasons, it has spread throughout all the Iberian Peninsula, and even in California, New Zealand, Australia, and Uruguay.

Merlot

The Merlot (MER) variety is included in the Carmenet ampelographic group, that has been originated in the area between the Gironde (French) and Basque Country (Spain) (Bordenave et al., 2007; Bisson et al., 2009). The studies of Regner (1999) and Boursiquot et al. (2009) demonstrated that Merlot derives from the breeding of Cabernet Franc and Magdeleine Noire. Indeed, they have given to Merlot, two important characteristics: the high-quality phenolic compounds; precocity and fertility, respectively (Boursiquot et al., 2009). Thus, the resulting wine is tannic, with caramel and cherry notes, and is often blended with Cabernet Sauvignon to balance the tannic taste and to highlight the fruity notes. The Merlot is widespread throughout the European Union, but it is produced especially in France and Italy. Outside the EU, it is cultivated in California, Canada, Australia, New Zealand, Argentina, Chile, Bolivia, South Africa, and other parts of the United States (Robinson et al., 2012).

Tempranillo

The Tempranillo (TEM) red grape variety is considered the noblest of the Spanish cultivars used for winemaking, and for this reason it is the most cultivated red wine variety in Spain. Moreover, it is a preferential or an authorized cultivar in 56 out of the 72 Spanish Denominations of Origin (D.O.). In Europe, it is cultivated even in Portugal, France, Italy, Greece, Malta, and Cyprus (Lacombe et al. 2011), while outside Europe, Tempranillo is cultivated in Argentina, Australia, Canada, Chile, Dominican Republic, Lebanon, Mexico, Morocco, New Zealand, South Africa, Turkey, Uruguay, and the United States. The Vitis International Variety Catalogue (VIVC, www.vivc.de) reports up to 66 synonyms for Tempranillo, and the most in Spain are Tinta del País (D.O. Ribera del Duero), Tempranillo de Rioja, Aragonés, Cencibel (La Mancha), Chinchillana, Escobera (Badajoz), Tinto Fino de Madrid (Madrid), Tinta de Toro (Zamora), Tinto Aragonés (Aragón), and Ull de Llebre (Cataluña). In addition, Tempranillo is known in Portugal by the names Aragonez and Tinta Roriz. The name Tempranillo refers to an early ("temprano", in the Spanish language) ripening and it has been used, with some spelling differences, for four different varieties: Tempranillo, Tempranilla, Temprano, and Temprana. The first written reference to the current Tempranillo dates back to the mid-18th century (Valcarcel 1791: the description is of a cultivar with a resistant berry skin, strong vine shoot, ripening 15 days earlier than Garnacha Tinta. An early 19th-century document (Rojas Clemente y Rubio 1807) reports a more complete description, even if the author proposed the name Cupani. The author stated that the variety was cultivated in Logroño (Rioja, northern Iberian Peninsula), and it was brought in Sanlúcar (Cádiz, southern Spain) in 1798, where it was less

productive. In 1905, Manso de Zúñiga described Tempranillo as the variety cultivated in Rioja (Spain) and included agronomic, ampelographic, and oenological data. Also, García de los Salmones (1914) has described the origin of Tempranillo in the Ebro River Valley (Rioja and Aragón).

Syrah

Bowers et al. (2000) have demonstrated that the Syrah (SY) variety has been bred from Mondeuse Blanche (mother) and Dureza (father). Syrah produces a complex wine, with several fruity notes (pineapple and berries), and even smoky and wood notes (Mayr et al., 2014). Moreover, wines made from Syrah grapes, and especially aged wines, contain high levels of dimethyl sulfide (DMS), which improve the fruity notes (Segurel et al., 2004). The Syrah is cultivated in France, Italy (especially in Sicily), Australia, New Zealand, United States, South America, and South Africa (Robinson et al., 2012).

Cabernet Sauvignon

Cabernet Sauvignon (CS) originates from Bordeaux, France, and is now planted worldwide, including Europe, the United States, South Africa, Chile, New Zealand, and China (Robinson et al., 2012b). In Europe it is principally cultivated in France, Italy and Spain. The resulting wine has a color that goes from blue to black with purple reflections, rich in tannins and aromatic substances, with notes of blueberries, blackcurrant and blackberry (Bowers and Meredith, 1997). Often, it also develops herbaceous, fruity and/or floral aroma, with roasted, wood-smoke, and cooked meat shade (Allen et al., 1990, 1994; Peynaud et al., 1980).

1.3 Wine: history and characteristics

The origins of wine are very ancient, and the first cultivation of vineyard has been attributed to Noah. Nevertheless, several studies have highlighted how wine is a native product of India, already reported in the Third Millennium BC, and then spreading throughout the Mediterranean basin, like in Mesopotamia, and in ancient Egypt, where it was already known in 2,500 BC. Then, the Egyptian influenced Jews, Arabs, and Greeks cultures in winemaking practices. Recently, traces of typical organic acids of grape and wine were found in several archeological samples (Neolithic) in Georgia (McGovern et al., 2017).

A Greek myth tells that the god Dionysus introduced grapevine cultivation among men, thus explaining the amazing typologies of wine produced in that period.

In the Mediterranean basin, winemaking was very important, especially during the Roman Empire. The first process developed was very easy: immediately after the harvest, the grapes were pressed in a tank, or *lacus*; the must was separated from the grape marc; finally, the must was transferred in the fermentation tank. However, three important events improved the forbidding of viticulture: the birth of Christianity; the decline Roman Empire; the spreading of Islamism between the 9th and the 13th century AD. Wine started being a source of inebriation and ephemeral pleasure.

Only during the Renaissance wine returned to Western culture, because during the 17th century, both glass bottles and cork stoppers were very cheap, and thus of common use, thus increasing both preservation and export of alcoholic beverages. Lately, during the 19th century, wine became a real rural tradition, and the studies conducted by renowned scientists like Louis Pasteur, remarkably increased the preparation of high-quality products. In 1866, Louis Pasteur stated that "*the wine is the healthiest and most hygienic of all beverages*" (Cianferoni, 2006).

Wine is the resulting beverage from grape processing (or some other fruit or vegetables) and the subsequent alcoholic fermentation. The minimum alcoholic variates according to the legislation of each region, and usually it is between 8.5% vol. to 7% vol. These thresholds change based on the characteristics of wine, which also change considerably as a consequence of the climate, soil management, cultivar, particular qualitative factors, local traditions, and crop management (International Organization of Vine and Wine, 2006). Usually, the real ethyl alcohol content variates from 80 and 140 mL L^{-1}.

Another crucial characteristic of wine is the acidity. Indeed, about 600 acid substances have been found in wine, and they can be classified as: fixed acids (i.e. tartaric, malic, succinic, and many others) and volatile acids (acetic acid, propionic acid, lactic acid, formic acid and many others). The quantification and the sum of both fixed and volatile acidity gives the total acidity, that generally varies from 4 to 8 g L^{-1}. These acids can also form the corresponding salts (tartrate, malate, succinate, acetate), that are responsible for the formation of precipitates as K tartrate. In wine there are also several kinds of alcohols, glycerin, amino acids, proteic substances, vitamins, minerals, volatile organic compounds (VOCs), carbon dioxide, especially in sparkling wines, and the phenolic compounds (Mipaaf, 2019).

In accordance with FAO Investment Centre Division (2009), wine quality can be investigated by the determination of the following criteria:

- total alcoholic content (from 9 to 15%);
- total acidity (from 5.25 to 8.5 g L^{-1}, expressed as tartaric acid);

- total residual sugar;
- volatile acidity (lower than 0.6 g L^{-1} for white wine, and 1.1 g L^{-1} for red wine, expressed as acetic acid);
- pH (ranging from 2.8 and 3.8);
- total SO_2 content (about 70–120 mg L^{-1} for dry wines);
- free SO_2 content (about 25–40 mg L^{-1} for dry wines).

1.3.1 Winemaking process

Winemaking process is defined as the production of wine and all its connected operations, such as crushing, destemming, roughing, pressing, etc. During this process, the grape is transformed in must, which in turn is transformed into wine after the alcoholic fermentation. During the fermentation process the sugars, mostly represented by fructose and glucose, are transformed into alcohol, CO_2 and other secondary products, such as glycerin, succinic and acetic acids, volatile compounds, which influences the wine taste and aroma.
Winemaking process may be subdivided as follows (FAO Investment Centre Division, 2009):

- mechanical operations (reception, crushing and destemming);
- transfer to fermentation tanks;
- primary alcoholic fermentation and maceration (in case of red winemaking);
- final fermentations (alcoholic and malolactic fermentation).

One of the most important steps of the winemaking process is the maceration of grapes. During this operation, which is realized together with alcoholic fermentation, the solid part (grape marc) and the liquid part (must) are kept in contact for a variable time, depending on the necessities of the winery (International Organization of Vine and Wine, 2006). This procedure distinguishes red winemaking, in which the maceration is accomplished, from the white winemaking, in which the grape marcs are separated from the must after the grape crushing. Generally, red winemaking is the typical processing of red grapes. However, as in the case of Champagne, red grapes may also not be macerated to obtain white wines. In addition to this, the maceration process is also used to assure aroma, body, and color to wine, because of the presence of polyphenols and aromatic substances in the peel of the berries (Blouin and Peynaud, 2001; OIV, 2006).

1.3.1.1 Microvinification process

According to the Italian Law (Mipaaf, 2008), the micro-winemaking process is mandatory when a new grape variety is studied. In fact, the law indicates that starting from the 4th year of cultivation, each variety needs to be evaluated for the oenological potential. Then, a quantity of 50-300 Kg of grape is processed, depending on the kind of variety (white or red), the final product that the researcher wants to obtain, the number of analyses of the product. Finally, (are studied) the physical-chemical characteristics are studied such as pH, ethanol, ash, density, hue, and acidity by using the common analysis techniques, and the sensorial pattern, through a panel test. The whole procedure is fundamental for the final subscription of the evaluated variety in the National Register of the Grape Variety.

1.3.1.2 Charmat winemaking

The Charmat is one of the most known methods to produce white sparkling wine of the kind "spumante". The process is very similar to the champenoise method, but the re-fermentation is done in an airtight vat, the yeasts are eliminated after a few days, and the fermentation temperature is kept low (10-18 °C). This process is typically used for the winemaking of Champagne which has not been vinified outside the original production area, but it is also used for the vinification of other wines, like Malvasia and Muscat, and for lower quality grapes (Ribéreau-Gayon et al., 2006).

1.3.2 Polyphenols

One of the most important classes of compounds in oenology is represented by the phenolic compounds, or polyphenols. In fact, they affect all color differences between red and white wines, but they are also essential for the determination of the aroma. Polyphenols are located in different parts of grapefruits and they are extracted during the maceration process. Among these compounds, some of most abundant in grapes and wines are the cinnamic and benzoic acid derivatives, and their concentrations vary from 10 to more than 500 mg L^{-1}. In particular, the benzoic acids can be found in their free forms, especially as anthocyanidins, as well as in their glycosides and esters adducts (Galvin, 1993). Also, the cinnamic acids can form esters adducts with alcohols, or they can be present in their free form (Ribereau-Gayon, 1965). Cinnamic acids can also form the coumarins that particularly affect the physicochemical traits of red wood-aged wine.

Since polyphenols have various origins, structure, and biological function, they can be classified in different subclasses on the basis of the number and the position of the aromatic rings, the elements bounded with the aromatic rings, and their substitutes (Ribereau-Gayon, 1959; Ribereau-Gayon P, 1964):

- non-flavonoids
- flavonoids.

The stilbenes are non-flavonoids compounds formed by two benzene rings bounded by an ethylene group. They have been found in grape skins, wine and oak wood (Langcake, 1981).

Tannins are complex flavonoids resulting from the polymerization of catechins with other phenols, thus reaching a high molecular weight (Moutounet et al., 1989). Astringency, color hue, and instability are some of their properties. For these reasons, tannins are very important in red and white wines, especially when aged in oak barrels (Pocock et al., 1994; Vivas and Glories, 1993; Vivas and Glories, 1996; Burger et al., 1990).

Flavonoids, depending on the oxidation, are responsible for different yellow shades to white wines. However, they also give color and astringency to red wines. Furthermore, they have many nutritional and pharmacological properties that may promote health benefits attributable to a moderated consumption of wine. Their chemical skeleton is flavene linked by several types of hydroxyl groups, that permit the classification of flavonoids in flavones, flavanols, flavanones, flavanonols and anthocyanins (Figure 3).

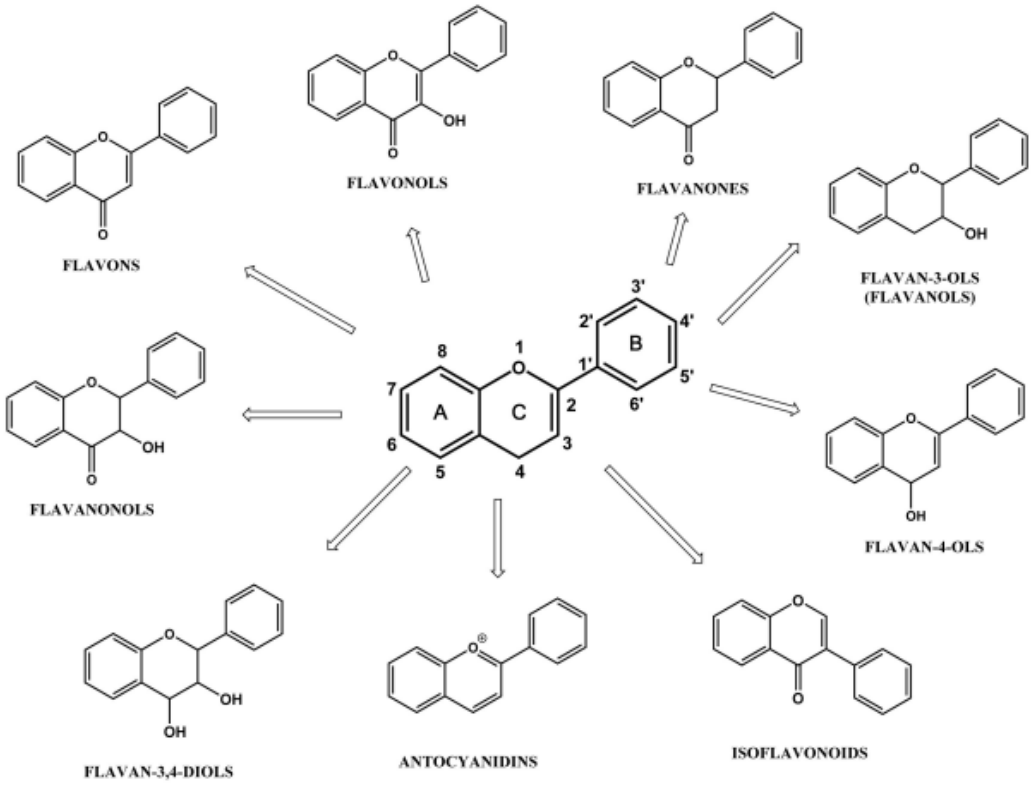

Figure 3. Different structures of polyphenols with a flavene backbone or structure.

Flavanols and flavanonols are polyphenols situated in the peel of both red and white grapes, and they are respectively yellow and bright yellow. It is important to highlight that they are present in the glycosylated form in grape, while during the winemaking process they are transformed into the respective aglycone form (Ribereau-Gayon, 1964; Ollivier, 1987). All the red wines are very rich in flavonoids, and especially flavanols, which include monomers (catechins), as well as oligomeric and polymeric PAs (Rasmussen et al., 2005).

The anthocyanins are another important type of flavonoids responsible for the red color in grape. In grapes, anthocyanins are mainly located in the hypodermal tissue of the peel, but a small percentage can also be found in the flesh (Piovan et al., 1998), while they are accumulated in the leaves at the end of the growing season. Moreover, anthocyanins are important for their benefits on health, because of their effects against the free radical activity and cardiovascular diseases, and not only for wine quality (Ghiselli et al., 1998). The anthocyanidins are polyhydroxy- and polymethoxy-derivatives of 2-phenyl-1-benzopyrylium salts (flavylium cation), consisting in an acyl group(s), sugar(s) and an aglycone (anthocyanidin). On the basis of the kind of aglycone and on the substituent (i.e. OH and OCH_3) of the lateral nucleus, five main molecules are formed: cyanidin, peonidin, petunidin, delphinidin, and malvidin (Fig. 4).

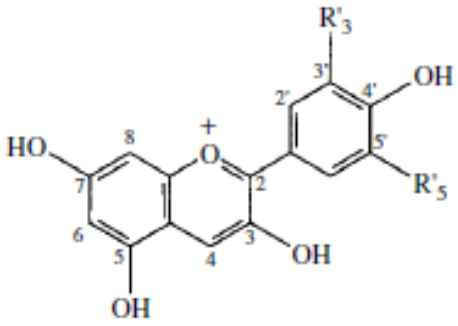

R'_3	R'_5	Name of aglycone
OH	H	Cyanidin
OCH_3	H	Peonidin
OH	OH	Delphinidin
OH	OCH_3	Petunidin
OCH_3	OCH_3	Malvidin

Figure 4. Formula of the five main anthocyanidins found in grapes.

Their color can be violet-blue, red, green or yellow-orange (Fig.5), depending on different factors, such as pH, SO_2, molecular structure, formation of adducts with other polyphenols (i.e. phenolic acids, flavonoids) (Amrani-Joutei, 1993). Generally, their quantities and percentage depend on the cultivar (varietal pattern) (Mazza and Miniati, 1993) and on the environment (Price et al., 1995; Larice et al., 1989).

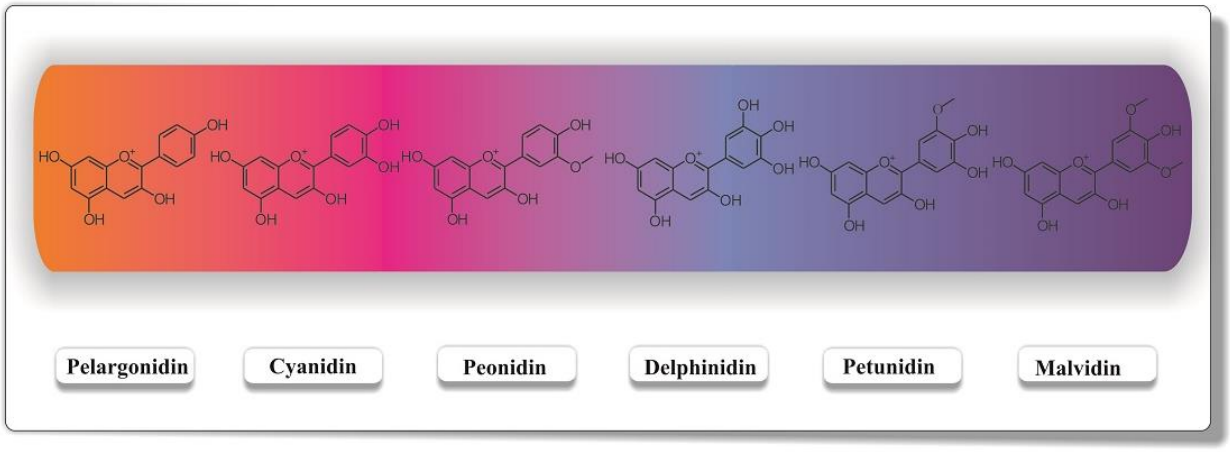

Figure 5. Different colors that are attributed to anthocyanidins.

It has been demonstrated that their interaction with carbohydrates affects pigment stability and modify the equilibrium and rate constants of the flavylium network (Cavalcanti et al., 2011; Fernandes et al., 2013; Lewis et al., 1995; Mazzaracchio et al., 2004).

Malvidin (or oenin) is typically the most abundant, representing the 50% - 90% of the total amount, and its quantity varies because of cultivar (Castagnino and Vercauteren, 1996). On the B-ring, the anthocyanins have several substituents: OH or OCH_3 responsible of their different hue. Moreover, they can be glycosylated with different monosaccharides (glucose, fructose, xylose, rhamnose, galactose, arabinose, and many others). Thus, they can be classified as 3-monoglycosides and 3,5-diglycosides, if one or two molecules of sugars are bound to the anthocyanidin. Some studies have

reported the detection even of the 3,7-diglycosides or 3,5,7-triglycosides forms. Additionally, the sugar residues can be linked with cinnamic acids (p-coumaric, caffeic, sinapic, ferulic), aliphatic acids (malic, acetic, oxalic, malonic, succinic) and benzoic acids (gallic acid) (Clifford, 2000). The anthocyanins of *Vitis vinifera* are mostly in 3-monoglucosides form, and usually do not contain substantial amounts of 3,5-*O*-diglucosides. By contrast, in many grape varieties are present interesting amounts of 3-*O*-acetylglucoside, 3-*O*-*p*-coumaroylglucoside and 3-*O*-caffeoylglucoside forms (Ribereau-Gayon, 1959). Indeed, the anthocyanins contained in the Grenache, Carignan and Cabernet Sauvignon grapes are classified in four groups: anthocyanidin-3-glucosides, -3-*O*-(6''-acetylglucosides), -3-*O*-(6''-*p*-coumaroylglucosides), and -3-*O*-(6''-caffeoylglucosides) (Monagas et al., 2003).

1.3.3 Aromatic compounds

Aromatic compounds are fundamental to investigate both aroma and quality of wine. They can be subdivided in three groups:

- the first group originates from the grapes, and it can be influenced during the grape processing;
- the second group is constituted by the compounds originated throughout the fermentation process;
- the third group results from wine aging, and it forms the bouquet.

However, aromatic components can change according to environmental factors, variety, crop management, fermentation process (pH, temperature, must nutrients, yeasts), or post-fermentation processes (clarification, blending, etc.) (Rapp and Manderey, 1986).

Generally, grapes are rather poor in volatiles. There are only a few alcohols, such as benzyl alcohol phenyl ethanol as well as modest quantities of other substances, generally under the perception threshold. The exceptions are the aromatic varieties, which are characterized by the presence of terpenols, free and bound to sugars (Rapp and Knipser, 1980; Schreier et al., 1976). The esters occur in small amounts in grapes, and the contribute to the aroma of *V. vinifera* cultivars is principally due to acetate esters of short chain alcohols. On the contrary, the esters create the characteristic aroma of the American species *V. labrusca*, such as the methyl anthranilate, and *V. rotundifolia* (muscadine) (Neudoerffer et al., 1965; Stern et al., 1967; Stevens et al., 1965).

Aldehydes are an important group of aromatic substances in both grape and juice. Indeed, C_6-aldehydes and alcohols are enzymatically generated during the grape crushing because of the cell destruction. However, both saturated and unsaturated aldehydes have been found during experiments of enzymatic inhibition (Schreier et al., 1976). In fact, trans-2-hexenal and n-hexanal are important aromatic compounds of the Grenache and Sultana varieties (Ramshaw and Hardy, 1969; Stevens et al., 1967).

Alcoholic compounds are mainly composed of C_4 to C_{11} chain length n-alcohols; however, there are even branched and unsaturated short chain alcohols, such as benzyl alcohol, 1- and 2-phenylethanol and monoterpenols (Schreier, 1979). For example, the flavor of *V. rotundifolia* grape is characterized by the attendance of isoamyl alcohol, hexanol, benzaldehyde, 2-phenylethanol and its derivation products (Welch et al., 1982). The only sesquiterpene alcohols that have been detected in wine are α-cadinol and farnesol. Nevertheless, monoterpene alcohols and their derivatives are also

very important for the typical aroma of the Muscat cultivars, such as Muscat d'Alexandrie, Morio-Muscat and Muscat Blanc, and other aromatic varieties like Riesling and Scheurebe (Rapp and Mandery, 1986). Up to today, more than 50 monoterpene molecules in either grapes and wines have been identified. In aromatic cultivars the typical terpene alcohols are linalool, geraniol, nerol, citronellol, α-terpineol and hotrienol (linalool oxide derivatives, nerol oxide, rose oxide and the ethers) (Ohloff, 1978), which form the base of several essential oils together with their derivatives. In fact, both linalool and geraniol are the main terpene fraction of Muscat aroma (Ribéreau-Gayon et al., 1975).

In several aromatic cultivars, their particular aroma is due to slight differences in terpene profiles. The oxides of geraniol, nerol, α-terpineol and the linalool constitute typical patterns in various *V. vinifera* white varieties (Terrier et al., 1972), that permits their discrimination. Furthermore, monoterpene alcohols are distributed in different ways in both peel and pulp. In fact, in the peel of Muscat d'Alexandrie variety are located the most quantity of geraniol and nerol, while the linalool is uniformly distributed in both pulp and skin (Bayonove et al., 1974; Cordonnier and Bayonove, 1978, 1981). For these reasons, the maceration process influences the intensity and quality of the aroma, even if the quantity of terpenes of the primary grape aroma are not affected (Rapp et al., 1985a).

Terpene compounds are also precursors of other molecules. Indeed, the oxidation of linalool and linalool oxides produces the 2-vinyl-2-methyl-tetrahydrofuran-5-one. The biodegradation of diterpenes and carotenoids forms the norisoprenoids. Both α- and β-ionone have a very low perception threshold (Buttery et al., 1971; Keith and Powers, 1968) and thus are used to compound fruit flavors (Naves, 1947). The spiroether or vitispirane, has been firstly found as aromatic compounds of grape juice (Simpson et al., 1977). The Z-isomer of the β-damascenone has been occasionally found in wine studies, but the E-isomer is considered an important aromatic compound, especially for red wines, giving the notes of apple or baked apple (Robinson et al., 2011; Pineau et al., 2007; Kotseridis and Baumes, 2000; Ferreira et al., 2002; Aznar et al., 2001). Even if both theaspirane and dihydroactinidiolide have been found in grape juice, several fruits, tea and some essential oils, their role in wine aroma is still not clear (Caven-Quantrill and Buglass, 2007; Ohloff, 1978).

The perception threshold values of nerol and α-terpineol is higher than linalool (100 μg L^{-1}), while their oxides have a perception threshold of 3000-5000 μg L^{-1}. However, the perception threshold of mixtures of these compounds is lower than the threshold of each single compound because of the additive effects (Ribéreau-Gayon et al., 1975).

Grey powdery mildew disease of grapes (*Botrytis cinerea* Pers.) causes the decrease of monoterpenes in muscat varieties (Boidron, 1978). However, in specific climatic conditions it develops a noble rot, that is a specific characteristic of the botrytised wines, hence their particular aroma. The noble rot transforms the linalool into some other monoterpenes and it produces terpenoids only in varieties that already contain terpenes (Shimizu et al., 1982). Even if there are quantitative aromatic differences between the botrytised and the normal wines, two peculiar aromatic compounds of the botrytised ones have been found (Masuda et al., 1984): the ethyl 9-hydroxy-nonanoate and the 4, 5-dimethyl-3-hydroxy-2(5H)-furanone (sotolone). The first one, with a perception threshold of 2.5 ppb, gives the sweet, and caramel note; the second one, in the botrytised wine has a concentration of about 5-20 ppb, while in the normal ones is below 1 ppb, and it gives a flavor of sugar molasses, aged rice wine and flour sherry (Masuda et al., 1984). Moreover, an increased quantity of l-octen-3-ol in noble rot-infected grapes and wines has been observed (a.k.a. mushroom alcohol) (Rapp, 1980).

The principal part of the aromatic compound of wine emerges during the fermentation process, in which the aroma of grape juice is substituted by the fermentation aroma, that gives the typical aroma to wine. In wine, ethanol and glycerol are the most abundant alcohols. Then, there are also diols, higher alcohols (or fusel alcohols) and esters, with a concentration of 0.2-1.2 g L-1 in white wines and 0.4-1.4 g L-1 in red wines (Bertrand, 1975). About 50% of these quantities are represented by n-propanol, n-butanol, 2-methylbutanol, 3-methylbutanol, phenylethanol, ethyl acetate and ethyl lactate. The ethanol defines the viscosity or “body”, equilibrates the taste and fixes the odours of wine. The concentration of the higher alcohols is greater than their sensory perception threshold; in particular, below 300 mg L^{-1} they provide the appreciated aromatic complexity of wine, but when the concentration rises (above 400 mg L-1) is considered a negative quality (Montevecchi et al., 2015).

The concentration of terpene alcohols and oxides is slightly influenced during yeast fermentation (Mandery, 1978), and are related to non-volatile monoterpene glycosides that have been found in grapes and wines (Williams et al., 1982b). As well as for terpene alcohols, even the quantity of monoterpene ethers is moderately influenced during yeast fermentation (Rapp et al., 1984). Moreover, they are independent from the geographical origin (Rapp and Hastrich, 1978), and they have been used to discriminate varieties of grapes and wines (Drawert and Schreier, 1978; Gfintert, 1984; Rapp t al., 1985b: Rapp and Hastrich, 1978; Schreier et al., 1976).

Most of the aldehydes present in grapes or must are probably reduced to alcohol after the initial phase of fermentation (Rapp and Mandery, 1985). Nevertheless, furfural and 5-

hydroxymethylfurfural can originate from carbohydrate degradation, vanillin and cinnamaldehyde originate from lignin. Moreover, aldehydes can also be formed during wine aging.

Most of the ketones that have been detected in grapes have also been found in wines, but in smaller quantities. The whole ketones, α-diketones and α-hydroxyketones that occur during yeast fermentation (i.e acetone, acetoin, 2, 3-pentanedione) have a very low sensory impact on wine, except for the diacetyl, that gives buttery odor.

γ-Butyrolactone and 4-hydroxy-2-pentenoic acid-γ-lactone have been identified by GC-MS techniques in dried Sultana grapes (Nagy and Powers, 1968). The second one probably results from the must heating process.

Volatile phenols of wine are formed by yeast or bacterial metabolism, or from hydrolysis of higher molecular weight phenols. In facts only the acetovanillone is present in grapes (Schreier, 1979), while the 4-vinylguaiacol and 4-vinylphenol can be originated from the p-coumaric and ferulic acid by enzymatic or thermal decarboxylation (Albagnac, 1975; Steinke and Paulson, 1964).

Up to today, no evidence has been presented that nitrogen compounds, such as amines or N-alkyl acetamides, are created during the fermentation process However, during the crushing or the maceration process, several compounds like small peptides or the 2-methoxy-3-isobutylpyrazine can be extracted from the grape skins, seeds and stalks (Riberéu-Gayon et al., 2018a).

The only volatile organic acids which contribute to odor of wine are acetic acid (vinegar note), propanoic acid (goat note), butanoic acid (rotten butter note) and lactic acid, but they generally have a lower concentration than their perception threshold, except for the acetic acid in old or ruined wines.

Volatile organic sulfur compounds are of remarkable importance for aromas because they usually have extraordinarily low perception thresholds. Among them, hydrogen sulfide has a recognition threshold below 1 μg L^{-1} and causes the ‘rotten egg' odor during the initial fermentation steps. The most abundant is 3-methylpropanol. Its formation is due to the 'Ehrlich pathway' out of the amino acid methionine (Schreier et al., 1976). Other sulfur compounds with an intensive odor in wine are (Güntert, 1984; Rapp et al., 1985a; Schreier, 1979; Schreier et al., 1976b):

- thioethers (dimethylsulphide, diethylsulphide);
- thiols, such as ethanethiol (fecal and formic aldehyde), 4-methylthio-l-butanol);
- thiolanes, such as 2-methylthiolane-3-one, 2-methylthiolane-3-ols (onion);

- esters of sulphurated acids (methyl and ethyl-3-methylthiopropionate);
- thiazols;
- mercaptal, such as the methyl-2-hydroxy-ethyl mercaptal (Rapp et al., 1985a).

Esters are present in a small quantity in grapes. During the alcoholic fermentation, the generation of both acetate and fatty acid ethyl esters crosses the ethanol pathway. Hence, they are important components of young wine. The main ester is ethyl acetate, even though there are other esters (called 'fruit esters') of fusel alcohols and short chain fatty acids. The fatty acid ethyl esters such as the ethyl butanoate, caproate, caprylate, caprate and laurate, are characteristic of white wines, but they can be found even in other kinds of wines. Their total quantity is usually about 1-10 mg L^1, while their perception threshold is about 10 times lower. The ethyl caproate has a fruit-like odor, but when the carbon chain increases, the odor becomes softer and soap-like.

Yeast strain has a significant impact on the production of esters, as well as the fermentation conditions. Indeed, lower fermentation temperatures have a positive effect on the total quantity of esters (Avakyants et al., 1981).

During the storage conditions, various chemical reactions influence the aromatic profile of wine, transforming the aroma into the bouquet. The bouquet can be distinguished in oxidation bouquet, formed by aldehydes and acetals, and the reduction bouquet, generated after aging in bottles (Ribéreau-Gayon, 1978). The aroma of red wines aged in wooden barrels receives various aromatic elements of wood that enrich its character, such as the phenolic compounds from the degradation of lignin, as well as the diastereomers of 3-methyl-γ-octalactone (Masuda and Nishimura 1971) and vanillin. These compounds have been found in wines aged in wooden barrels (Kepner et al., 1972; Schreier et al., 1976b), in whiskey (Nishimura and Masuda, 1971), and brandy (Guymon and Crowell, 1972; Otsuka et al., 1974; Schreier et al., 1979).

Oxygen, as well as the components extracted or created during the aging process, causes important flavor changes. Moreover, the wine aging increases the levels of volatile acidity and ethyl acetate (Ribereau-Gayon, 1971), as well as the concentration of acetaldehyde (Bayer, 1966) and some other, higher aldehydes (Baro and Quiros Carrasco, 1977; Wildenradt and Singleton, 1974).

Acetals are generated from aldehydes and alcohols in wine, mainly acetaldehyde acetals as this aldehyde is the most abundant. About 20 molecules of this kind have been identified in wine, with diethoxyetanale as the most relevant. Usually, these compounds are almost irrelevant for the bouquet of wine, but for certain wine they can give vegetal and fruity notes (Ribéreau-Gayon et al.,

2018; Güntert, 1984; Mandery, 1983; Schreier and Drawert, 1974; Schreier et al., 1976d; Arctander, 1969).

Acetates contribute to the fruity aroma of novel wines and are enzymatically produced beyond their equilibrium concentrations. Then, during the storage they gradually hydrolyze until they reach the equilibrium with the corresponding acid and alcohol. Thus, their decreased concentration in wine may result in the loss of freshness and fruitiness. Conversely, the quantity of the fatty acid ethyl esters remains fairly constant during storage, because of the slow hydrolyzation of the ethyl esters, compared to the acetate esters (Ramey and Ough, 1980). Probably the esters, fatty acids and ethanol are produced by the yeasts in very equilibrated concentration.

Ethyl esters of diprotic acids show regular increase of concentration during aging, because of esterification.

Carotenoid degradation during the aging forms some interesting compounds: the norisoprenoid substances. In fact, the quantity of the vitispiranes increases with storage, highlighting the camphoraceous eucalyptus-like odor (Simpson et al., 1977; Simpson, 1978b). Damascenone (rose) and β-ionone (violet) are other compounds resulting from carotene breakdown, whose concentration declines during aging (Güntert, 1984).

Several furane derivatives are degradation products carbohydrate in young wines, such as furfural and ethyl furoate. By contrast, the molecules like 2-acetylfuran, furfuryl alcohol, 2-ethoxymethyl-5-furfural, 2-hydroxymethyl-5-furfural and levulinic acid ethyl ester originate after some years of aging. Also furfural greatly increases during bottle aging as well, and thus has been proposed as storage time index (Nagy and Dinsmore, 1974; Nagy and Randall, 1973).

In white wine the monoterpenes change considerably during the aging:

- monoterpene alcohols (linalool, geraniol and citronellol) decrease;

- the linalool oxides, nerol oxide, hotrienol, hydroxylinalool and hydroxycitronellol increase;

- the 2,6,6-trimethyl-2-vinyl-tetrahydropyran, anhydrolinalool oxides, 2,2-dimethyl-5 (1-methylpropyl)-tetrahydrofuran and cis-1,8-menthandiol are formed (Buttery et al., 1971; Hennig and Villforth, 1942).

The hatched diols have been found only in muscat-type wines (Rieth, 1984).

As a result, the increases in linalool oxides do not deteriorate the aromatic properties (Ribéreau-Gayon et al., 1975; Terrier, 1972), while an enhanced quantity α-terpineol may negatively affect the bouquet.

In wine, the olfactory perception threshold of monoterpenes compounds is not constant (100 to 700 μg L^{-1}), because the additive effects reduce the olfactory threshold (Ribéreau-Gayon, 1978). The prediction of the changing pattern of the aroma during the aging is not easy. Regarding) As for the red wines, this problem does not exist because they usually contain a very small amount of monoterpenes. However, during storage both red and white wines are affected by a decrease in acetate amounts.

1.4 Technical approach for food characterization

Metabolic profiling is an approach that provides information on the technological potential of grape varieties. Among them, phenolic and aromatic compounds are the most popular (Moreno-Arribas et al., 2009). Especially the anthocyanins and the flavanols, that belong to the flavonoid family, are particularly abundant in the skin of grapes (Mattivi et al., 2006). These compounds are involved in both color and taste of red wine during the winemaking process (Moreno-Arribas et al., 2009). Among the industrial applications of anthocyanin compounds, oenocyanin is the oldest known commercial product extracted from the skin of red grapes, and is used as a food colorant (Marakakis, 1982). The anthocyanin composition of red grapes is a phenotypic distinctive trait of variety. Indeed, the anthocyanin profile is appreciably stable, even if it changes throughout the different vintages because of environmental and agronomical factors. For these reasons, its determination can be used as an indicator for the evaluation of grape authenticity, wine adulteration and chemotaxonomic studies (Flamini, 2013; Montevecchi et al., 2016).

1.4.1 Gas chromatography

Gas chromatography (GC) technology was developed in the 1950s. In fact, several organic and fatty acids from mixtures have been separated in the study of James and Martin (1954), by using nitrogen as carrier gas and 10% stearic acid in silicone/diatomaceous earth as stationary phase (Bartle and Myers, 2002). Since GC technology development, there have been enormous progress and improvements in the hardware, software, and consumables which have determined GC as an important instrument for the isolation and the analysis of chemical constituents from complex matrices in the food, chemicals, environmental, biological and medical sciences (Jennings et al., 1987). For example, fused silica capillary columns of different stationary phases and dimensions have replaced packed columns because of their better separation efficiency and resolution. Moreover, the modern GC instruments are equipped with pneumatics and microfluidic devices, allowing a precise control of gas flows that provides reliable chromatographic retention times (Mommers et al., 2011), and also permit a multiplicity of sample injection and maintenance techniques, such as the large volume or programmed temperature vaporization (PVT) injection (Saito et al., 2004), column backflushing (Maštovská and Wylie, 2012), and sophisticated GC methods such as low pressure, fast capillary and multidimensional (GCxGC) GC techniques (González-Rodríguez et al., 2002; Korytár et al., 2002; Kirchner et al., 2005; Matisová and Hrouzková, 2012). The integration of the computer in the hardware of the modern GC instruments

strengthens the optimization of the working conditions and facilitate the acquisition and storage of both chromatography and mass spectra data, as well as their processing.

The union of all these technological improvements has permitted to integrate sampling devices such as headspace, thermal desorption, solid-phase microextraction (SPME) and stir bar sorptive extraction, and automated sample preparation workstations, developing an increased sample throughput and further diversity of GC and gas chromatography–mass spectrometry applications (GC-MS).

Due to its high sensitivity, resolution and sample reproducibility, GC-MS is the most used instrument for volatile metabolite analysis. Moreover, the accessibility of spectral libraries such as Wiley, AMDIS, NIST and METLIN, based on the mass spectra and the retention time or index of each molecule, makes the identification of biomarkers more effective, especially for the studies of the biological mechanisms and pathology alterations, and cheaper, at the same time (Schauer et al., 2005; t'Kindt et al., 2009; https://metlin.scripps.edu/; http://chemdata.nist.gov; Majchrzak et al., 2018; Theodoridis et al., 2012; Dagan, 2000).

Although its lower cost and reduced operation, when the target molecules are non-volatile, GC-MS analysis requires laborious sample preparation to increase the volatility and the thermal stability of the target compounds. Thus, several derivatization reactions can be used to preserve the functional groups, such as alkylation, acylation, and silanization (Fiehn, 2002; Zhang et al., 2016). However, during the derivatization process different metabolites can variate or form byproducts, affecting the efficiency of the analysis, and increasing the risk of misinterpretation of the data (Zhang et al., 2016; Kanani et al., 2008). Consequently, an automated high-throughput sample derivatization or a robust analytical approach can increase the linearity and the reproducibility of the analysis (Hadi et al., 2017; Zhao et al., 2017; Yan et al., 2016).

The wide spreading of comprehensive GC (GCxGC) techniques increased the sensitivity, and thus the identification of metabolites (Wong et al., 2014; Chin and Marriott, 2014; Mostafa et al., 2012). In GCxGC, there is a secondary column that performs a second independent separation of the molecules eluted from the primary column (Cortes et al., 2009). Usually, the first and the second column have a nonpolar and a polar stationary phase, respectively. Hence, different compounds with a similar boiling point can be separated, increasing the separation efficiency power, as well as the quantity of detectable compounds (Ryan et al., 2005; Miyazaki et al., 2017).

Generally, the gas-phase eluate that comes from the column, or columns, in the case of GCxGC, contains:

1. mobile phase (H_2 or He);
2. sample;
3. volatile components;
4. decomposition molecules of the stationary phase (usually cyclic siloxanes).

1.4.1.1 Mass spectrometry

Mass spectrometry is one of the main instrumental analytical techniques used for the identification of unknown compounds from a given matrix. It is based on the ionization of compounds in the gas phase. A typical mass spectrometer consists of an ion source to produce the ions of analytes of interest, a mass analyzer, which separates the ions and measures the mass-charge ratio (*m/z*) and a detector to register the ions at each *m/z* ratio.

Based on the ionization technique, the intact molecules, or ions, may have enough energy to fragmentate in ions with a smaller mass. Generally, in GC/MS most of the formed ions have only a single charge. In fact, only the aromatic hydrocarbons that receive the electron ionization (EI), which are lowly abundant, form double-charge ions. The ions are separated in the mass spectrometers depending on their mass-to-charge ratio (*m*/*z*) values. Hence, in the case of the single charge, the *m*/*z* value transformed in GC/MS is also the corresponding mass of the ion (Sparkman et al., 2011). After the formation of ions, they are fragmented in less than a microsecond. Then, they are accelerated out of the ion source into the *m*/*z* analyzer with a constant energy.

EI technique was developed in the 1930s by Arthur Jeffery Dempster (Kiser, 1965), and it was originally called *electron impact*. An electron beam is generated by accelerating electrons against a positive charged trap facing the ion volume (~1 cm^3). A fixed magnet is located at the source to transmit a helical path to the electron beam, thus improving the chance of contact between the electron and the energy cloud, in which most of the molecular volume of the analyte is contained (Sparkman et al., 2011). In Figure 6 the structure of a general EI device is represented.

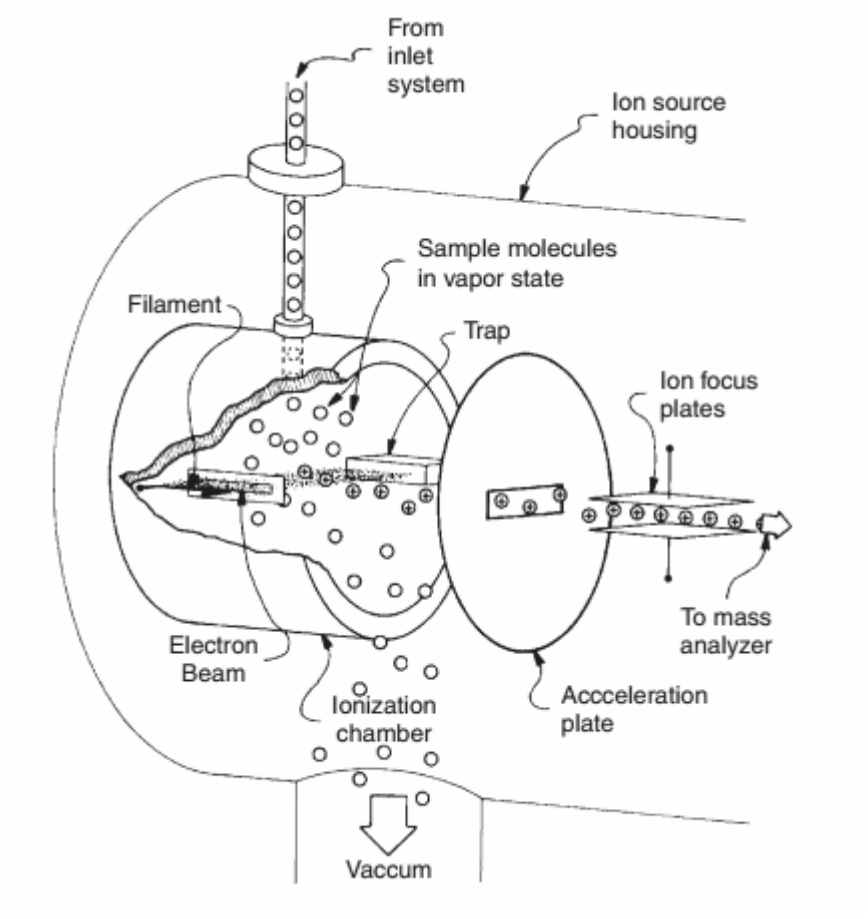

Figure 6. Scheme of an EI source in its housing.

Molecules are constituted mainly of open space with a systematic dispersion of atomic nuclei and electrons that are, within certain limits, in motion. Even though an ionizing electron can come in contact with a nucleus or an electron of an atom, the mass of the ionizing electron is very small, and thus it is possible to transmit a little kinetic energy to the analyte (Busch, 1995). Thus, even more than one molecule can be stimulated. Thus, the stimulated molecule wants to reach a lower energy state and it expels an electron and as a consequence is acquired the positive-charge molecular ion. Then, the electron expelled by the analyte is attracted and neutralized by the positively charged trap (Sparkman et al., 2011).

It is important to highlight that the efficiency of EI is between 0.01% and 0.001%. For this reason, mass spectrometry is considered the experimental approach that produces more information from fewer samples, compared with other techniques. Moreover, the large commercial availability databases of EI spectra increased its utilization, such as the NIST08 Mass Spectral Database (192,262 compounds) or the Wiley Registry, 9^{th} ed. (668,092 spectra) (Sparkman et al., 2011).

Depending on the chemical structure of the molecular ions, a considerable number is fragmented, and the abundances of the fragment ions detected produce the specific EI mass spectrum of the

molecule (“EI fingerprint”). Nevertheless, sometimes the energy of the formed molecular ions is too high, and their mass spectra do not show a M^+ peak. For this reason, supplementary soft ionization techniques can provide the molecular weight of the analyte, considering even their lack of fragment-ion formation (Sparkman et al., 2011).

Usually, the fragmentation of the ions of the intact molecule determines the structure of the analyte. In fact, the *m*/*z* values of both fragments and dark matter (the elemental compositions suggested by the difference in the *m*/*z* values of two mass spectral peaks), and the *m*/*z* value of the molecular ion, are essential for structure determinations (Sparkman et al., 2011). The mass spectra resulting from a GC/MS analysis are acquired one after another at a regular rate, and their coordinates are represented by the *m*/*z* value of the ion, as the x axis, and by the abundance of the ion, as y axis. (Fig. 7).

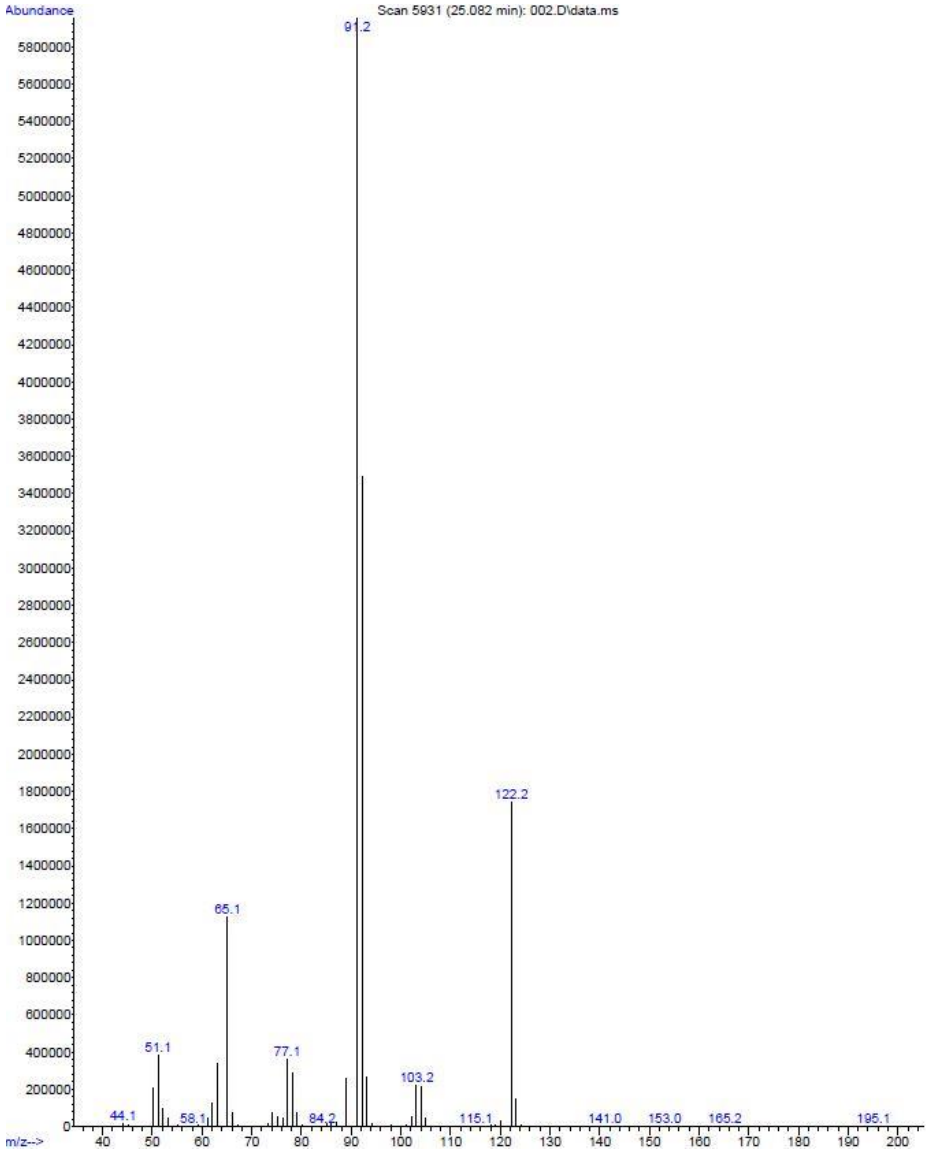

Figure 7. Mass spectra of the phenethyl alcohol detected in wine.

Sometimes, the intensity information values are collected every 1/20 of a *m*/*z* unit, and then summed. When both the sum and the actual 1/20 value of a *m*/*z* unit are recorded in the point with the greatest intensity, the so-called centroid data are obtained. To obtain these data, it is also possible to record the intensity only at the *m*/*z* value (in the 20 *m*/*z* unit range) in which occurs the maximum intensity or recording the data every 20 steps up to the position that probably coincides with the maximum intensity of the peak. Otherwise, the spectra can be displayed as profile data, representing each intensity value of the 20 steps recorded, or in a tabular format, representing the *m*/*z* values and the corresponding intensities as couples of numbers (Sparkman et al., 2011).

Both a single mass spectrum and a series of spectra averaged together can be displayed as a unique spectrum and subtracting another reference spectrum or another averaged series of spectra as background correction. Moreover, a series of spectra can be shown by summing all the intensities in each spectrum in comparison with the spectrum number. Thus, the x axis (spectrum number) is related to time, because each spectrum is acquired at a constant rate, while the y axis relates to the concentration of the analyte in the ion source, because it represents the abundance of each ion in the mass spectrum. Hence, a chromatogram is the resulting plot of the quantity of analyte as a function of time and is also called "reconstructed total ion current" (TIC) chromatogram (Fig. 8) (Sparkman et al., 2011).

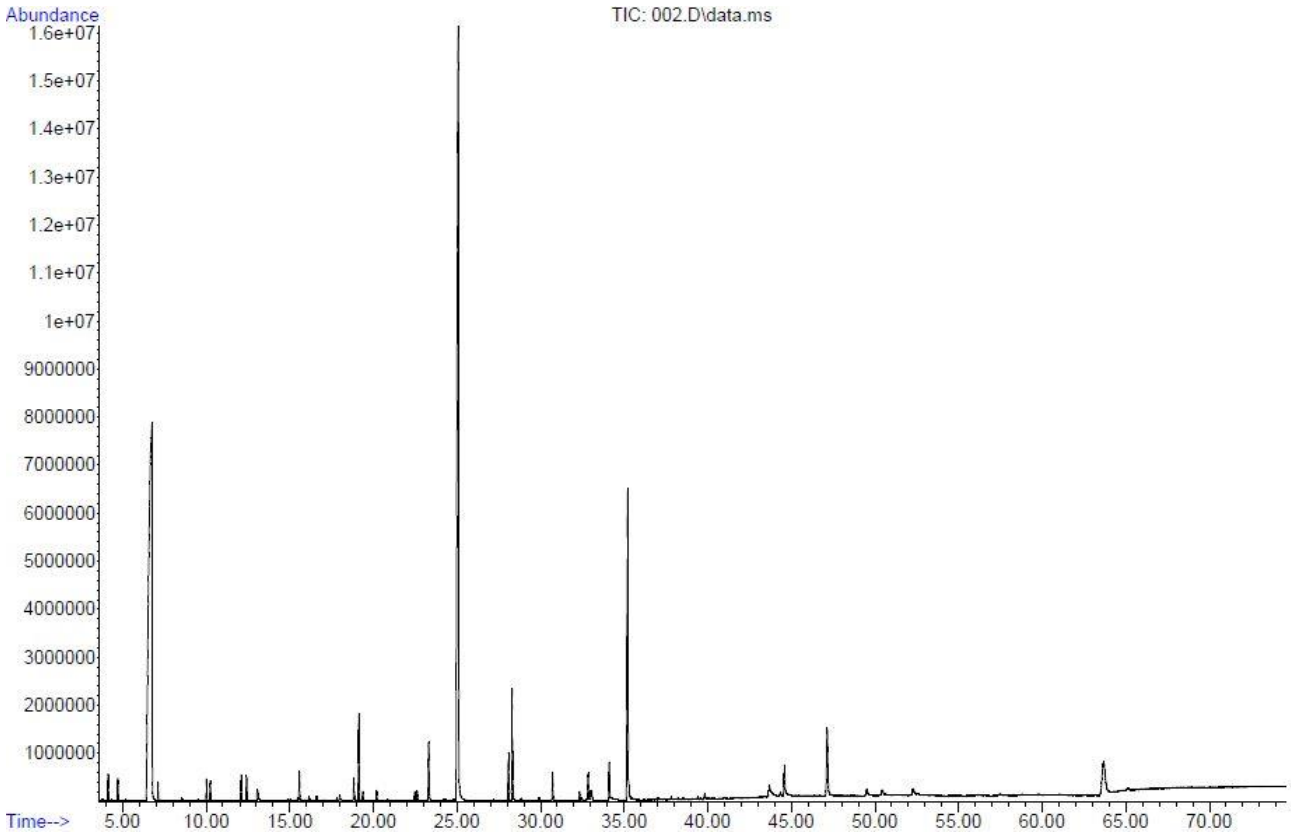

Figure 8. Example of a TIC of the aromatic profile of a wine.

Mass spectral data can also be shown as the plot of the ion current for a single *m/z* value, a small range of *m/z* values, or the sum of several *m/z* values as a function of time and are called mass chromatograms or extracted ion current (EIC) (Fig. 9) chromatograms (Sparkman et al., 2011).

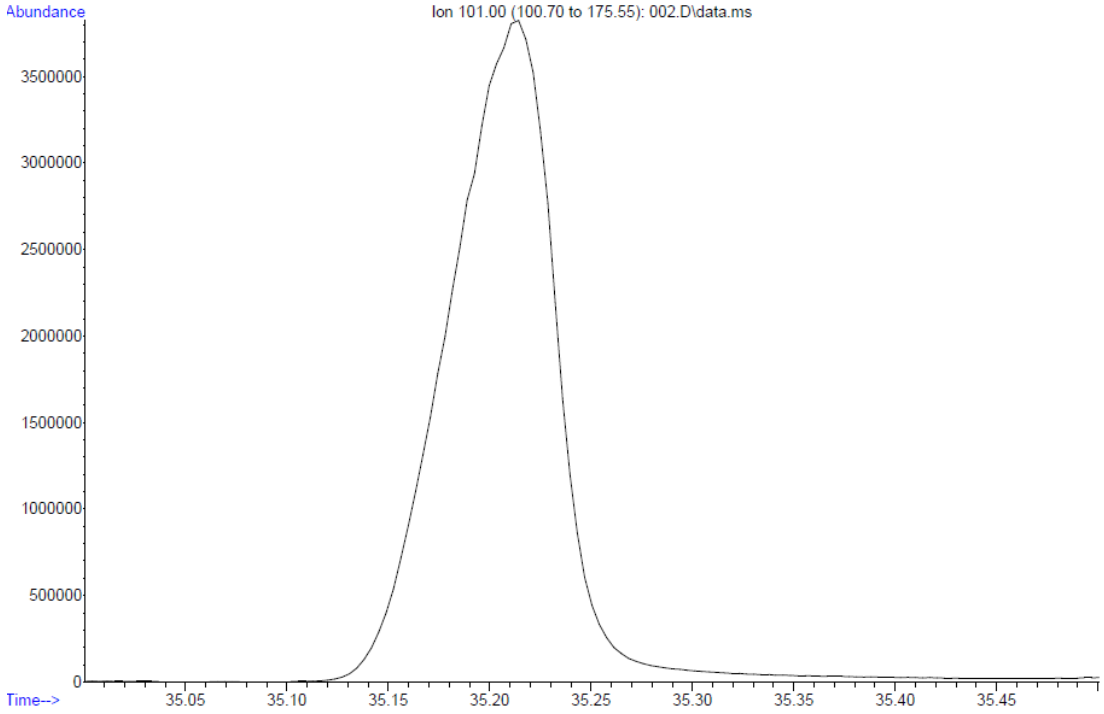

Figure 9. Example of the EIC of the Monoethyl-succinate in wine.

The quadrupole mass filter (QMF) has been a consequence of these studies, and almost after its commercialization in the late 1960s, it has become the reference instrument for GC/MS. QMF uses both direct current and alternating current (DC and AC, respectively) in the form of radio frequency (RF) electric field to separate ions, depending on their *m*/*z* values, from a complex ion beam that constantly flows from the ion source to the detector. The QMF is built up by four electrical poles working as conducting surfaces (Fig. 10).

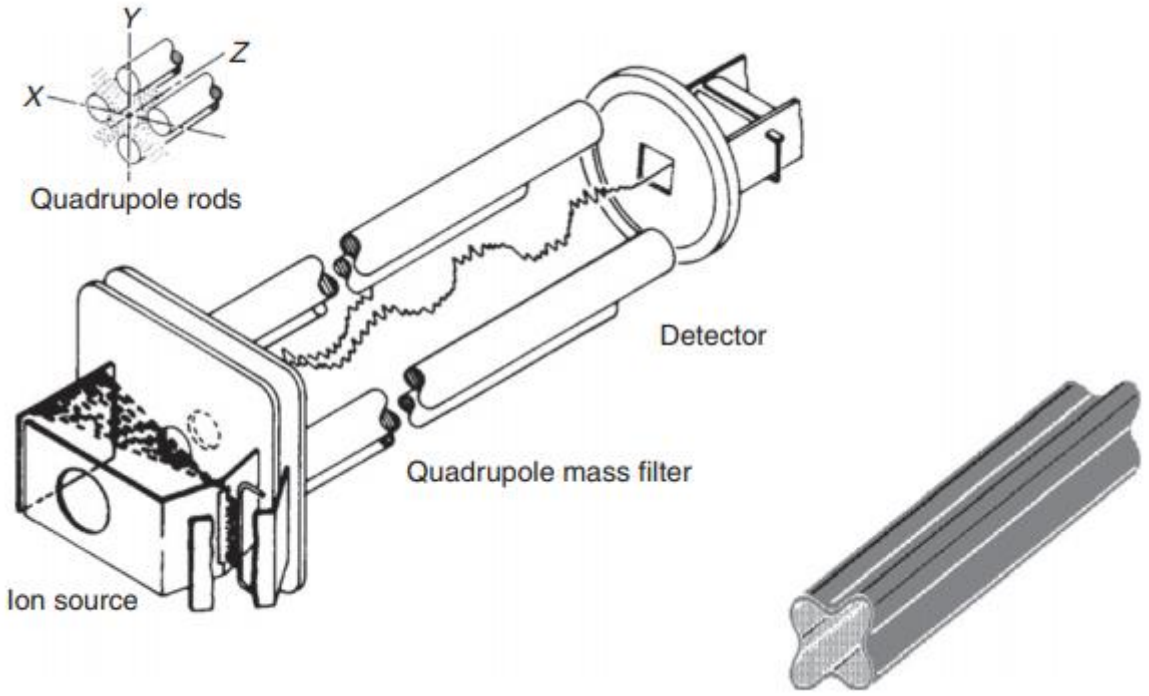

Figure 10. General structure of QMF and orientation of the rods (Sparkman et al., 2011).

These poles are arranged along both x axis and y axis, creating a x–y plot of two orthogonal hyperbolic functions: one with a positive DC potential and the other with a negative DC potential. Simultaneously, a fixed-frequency RF voltage is applied to both the set of poles, creating an alternated electric field that pushes and pulls the ions through the z axis. As a consequence, at a specific RF/DC ratio only the ions of a certain *m*/*z* value remain in the ion beam, while the others receive the push-pulling effect up to they are expelled from the ion beam. Finally, the mass spectrum is obtained by keeping a constant DC/RF amplitude ratio, while increasing or decreasing simultaneously the two amplitudes. The required RF depends on the size of the poles, whose distance varies with the design of the instrument, and thus, by changing the frequency of the RF generator changes, the instrument does not work.

After exiting from the mass analyzer, the ions hit the detector that generates a dropping of electrons (or photones) that produce the signal, whose intensity is directly proportioned to the abundance of the ions with a certain *m*/*z* value. The primary release is due to the kinetic energy of the ions ($Ek= mv^2/2$), that in the QMFinstruments is ∼15 eV or lesser, resulting in an extensive range of responses when the detector is hit by ions of different *m*/*z* values (Sparkman et al., 2011).

The optimal performance of an electron multiplier (EM) is the production of about 10^5 electrons per ion. However, the voltage applied to the EM needs to be intensified during its lifetime to keep this performance. In fact, the EM needs to be substituted when the lowest signal level is not

distinguishable from the noise. The types of EM can be distinguished in continuous dynode and discrete dynode, and both devices have an electron emitting surface consisting in a lead-doped glass (Sparkman et al., 2011).

Data acquisition in GC/MS approach refers to the continuous measurement of spectra and selected-ion-monitoring (SIM) (Budde, 2001; Eichelberger et al, 1975). During SIM process the ions of a certain *m/z* values are controlled for a fraction of the data acquisition time. Therefore, spending more time of the acquisition cycle on a few ions, more of them can be detected providing a stronger signal, and thus reducing the LOD of target compounds (Sparkman et al., 2011). For these reasons, SIM can increase the quantitative precision by defining the chromatographic peak with a higher number of data points, thus reducing the LOQ. In addition, some QMF GC-MS instruments can alternate the full-scan acquisition with the SIM acquisition (Sparkman et al., 2011).

In both SIM and full-scan mode, the delay time between the injection and the spectral acquisition is an important point. Indeed, during the delay time both ion-source filament and detector are turned off to avoid the detection of the solvent, that is the first material eluted from the column, whose abundance is usually higher than the analyte, and thus preserving the detector lifetime (Sparkman et al., 2011).

Commonly, data acquisitions start at *m/z* 35 or 40, in order to avoid peaks at *m/z* 18, 28, and 32, that are due to air leaks. In fact, air can seriously damage the stationary phase of the column, especially if it is in a hot oven. Another important source of air contamination is the overused injection septa, which must be changed every 50–100 injections. Nevertheless, it is important to highlight that peaks at *m/z* 30 and 31 represent aliphatic amines and alcohols, respectively, and thus is necessary to start the analysis at the lowest value possible (Sparkman et al., 2011).

Most of GC/MS systems have a maximum *m/z* range between 650 and 1,000. Thus, both acquisition range and acquisition rate can be changed during the analysis, because usually the analytes eluted at a low acquisition time have also a lower nominal mass than the compounds eluted at the end of the analysis. Even if the oven temperature is programmed, the peaks of the early eluted compounds are usually narrower than the compound eluted later. As a consequence, at the beginning of the analysis a short *m/z* range can be used, which can be expanded later (Sparkman et al., 2011).

1.4.1.2 The application of gas chromatography in food science

GC techniques have been applied in each step of the wine production chain. However, many studies have mainly characterized the base wine aromatic compounds, such as the main fermentation derived esters, alcohols and acids (de Villers et al., 2012). Usually, these compounds are analyzed daily by standard GC methods coupled with FID or MS detection. For what concern the determination of compounds such as terpenes, volatile phenols, sulfur compounds, norisoprenoids, pyrazines and many others, have been developed several extraction, separation and detection techniques (de Villers et al., 2012). In particular, the relevance of isoamyl acetate as a typical fermentation aroma of young Pinotage wines, has been firstly described by Van Wyk et al. (1979). Nowadays, much research has been conducted on major volatile compounds to distinguish wines by variety (Tredoux et al., 2008; Weldegergis et al., 2011) and vintage (Weldegergis and Crouch, 2008). Another important research topic has been the correlation between fermentation yeast and the aromatic traits of wines and derived products (Pretorius, 2000; Swiegers et al., 2006; Louw et al., 2006; Masino et al., 2008), such as the effect of esterase activity (Lilly et al., 2000, 2006a), or the branched-chain amino acid transaminase activity (Lilly et al., 2006b). A study about the liberation of free monoterpenoids, has been conducted by Zietsman et al. (2011), by using the effect of co-expression of selected glucosidase and furanosidase genes in *Saccharomyces cerevisiae*. Also the 1,1,6-trimethyl-l,2-dihydronaphthalene (TDN) has been analyzed by GC–MS, since it is probably one of the aromatic compounds that give a kerosene taint to aged Riesling wines, with a perception threshold of 20 ppb (de Villers et al., 2012).

1.4.2 Application of Nuclear Magnetic Resonance (NMR)

Nuclear Magnetic Resonance (NMR) spectroscopy is an instrumental analytical technique that allows to obtain detailed information on the structure of molecules by observing the behavior of atomic nuclei in a magnetic field. After immersing the molecule under examination in a strong magnetic field, the absorption of a radio frequency radiation (from 100 to 1000 MHz) is measured, which causes nuclear spin transitions in particular atoms such as ^{1}H or ^{13}C.

Each NMR systems usually includes: 1) the magnet to generate the static magnetic field (B_0); 2) the probe that produce the RF pulses (B_1 field) and contain the sample; 3) the control console for generation of B_1, signal detection, and sample temperature control; 4) a computer to control the hardware and for data processing (Fig. 11).

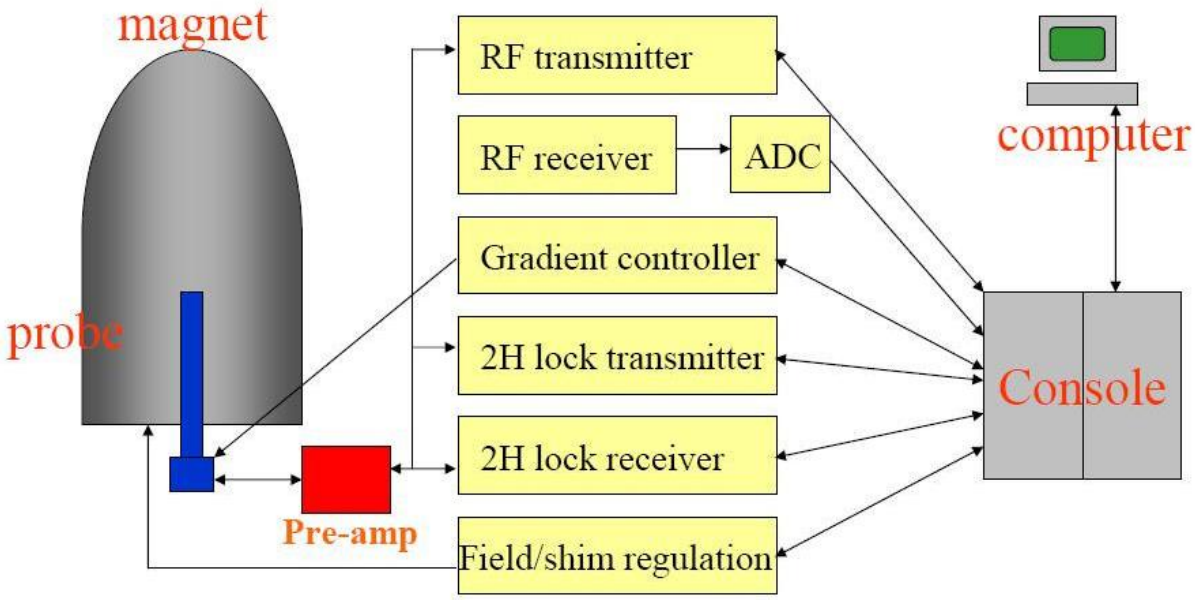

Figure 11. General scheme of an NMR working station.

The magnet is a cylindrical shaped container formed by different concentric tanks. The internal one generates B_0 by a superconducting coil along the z-axis. Because some studies require high spectral resolution and sensitivity, superconductivity is necessary to generate the appropriate magnetic fields. In the internal tank, the solenoid coil, built in niobium–titanium, is maintained at 4K by a liquid helium bath, to achieve superconductivity. This container is enclosed in another vacuum tank, surrounded by an external dewar, containing liquid nitrogen, that reduces the helium evaporation.

The probe is placed in the center of the magnet through a hole, and it contains both transmitters that are the RF coil that stimulates the sample contained in the NMR tube, and the signal receiver. Basically, there are there are two NMR probes:

- inverse probes, in which the coil is close to the internal coil, and thus to the sample, and it permits the excitation of proton frequencies, while the external one is used for heteronuclei;
- observe probes, built with an inverse structure.

In fact, the first type is recommended when there are detected proton nuclei, as in 1D ^{1}H NMR or the most common 2D NMR experiments. Regarding the second type, it is effective for the detection of heteronuclei (i.e. ^{13}C and ^{31}P) in the internal coil, while in the less-sensitive outer coil can be easily detected the much more abundant protons. Thus, since heteronuclei have a high spectral resolution, they may be effective in food technology application (Williamson and Hatzakis, 2017).

1.4.2.1 Analyses and experiments applied in NMR spectroscopy

The NMR analyses most applied are:

- relaxometry, which investigates the different magnetic relaxation of the compounds (Capitani et al., 2017a; Tavares, 2017);
- diffusometry, which measures the translational diffusion of molecules (Mariette, 2009);
- imaging technique (Ablett, 1992; Hills, 1998);
- high-resolution NMR spectroscopy (Laghi et al., 2014; Mannina et al., 2012; Spyros and Dais, 2013).

NMR spectroscopy is based on the magnetic properties of the nuclei, which can have an odd mass number as well as an even mass number. However, these nuclei have an odd atomic number and a nuclear spin (S), that is the angular momentum without a macroscopic analogue described through the nuclear spin quantum number (I) (Levitt, 2005). The nuclei can be studied by the interaction between μ and the external magnetic field (B_0) generated by the magnet of the NMR. In food science, ^{1}H, ^{13}C, and ^{31}P are the most investigated nuclei. Without a magnetic field, the energy of each nuclear orientation is the same, but applying B_0 the states are separated, splitting the different nuclear spin levels (Zeeman effect) (Levitt, 2005).

NMR experiments measure the macroscopic (net or bulk) magnetization, that is an intrinsic property of the analyzed sample, due to the average of each magnetic moment of all spins (Keeler, 2010). At this point, the magnetization starts the oscillation, generating a voltage to a coil in the x-y plane. The voltage represents the first NMR signal, the free induction decay (a.k.a. FID) (Fig. 12). Once the RF pulse is ended, B_0 oscillates and decreases up to zero because of longitudinal relaxation (T_1), transverse relaxation (T_2) mechanisms. Then, the FID is transformed in a frequency domain signal (NMR spectrum), that is commonly used in high-resolution NMR approaches, by using the Fourier transform (FT), as widely described in many studies (Lambert, Mazzola and Ridge, 2018; Spyros et al., 2013). The acquisition and processing parameters that are commonly used in NMR studies are the chemical shift (δ), the scalar coupling (J coupling), and the signal area. Then, from the signal other parameters can be determined, such as the dipolar coupling, T_1, T_2, and translational diffusion.

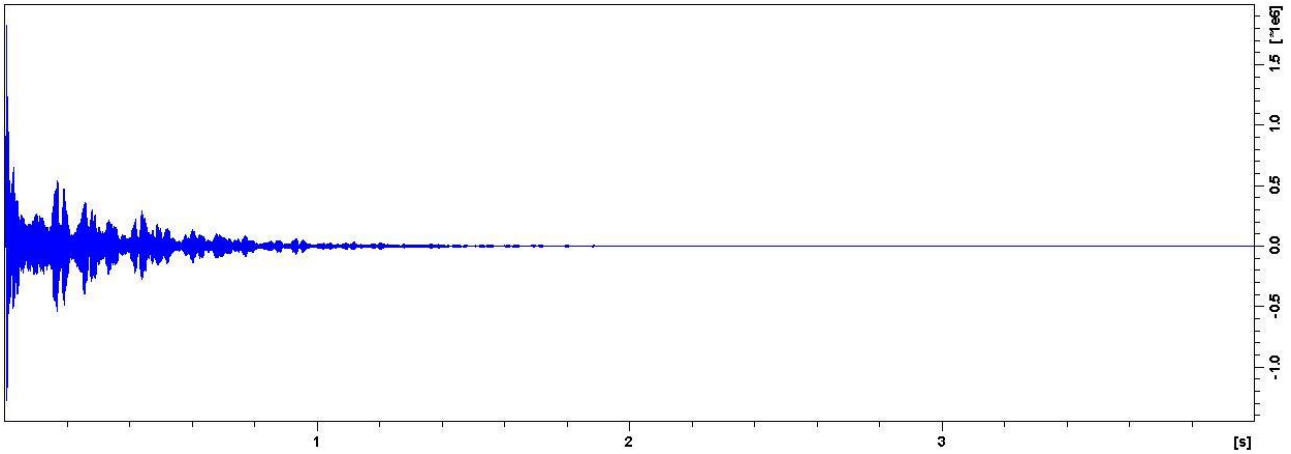

Figure 12. Example of a FID of a white wine.

The δ is obtained by plotting the signal intensity on the y-axis, and frequency on the x-axis, and is typically shown by one-dimensional (1D) NMR spectrum (Fig. 13). Thus, it shows the position of each signal in the spectrum, giving information about the chemical environment of nuclei. The δ is expressed in ppm and is referenced to an internal standard (IS), that typically are the tetramethylsilane (TMS) or the trimethylsilylpropanoic acid (TSP) and are used to set to 0 ppm (spectra calibration). Representing δ in ppm rather than Hz makes data obtained in different instruments easily comparable. The δ occurs because all the nuclei encounter both B_0 and local magnetic fields. The last one is the result of the chemical environment, such as the electrons surrounding the nucleus, even considering a single molecule. Hence, δ is directly proportional to B_0, and the different nuclei receive energy at several resonance frequencies because of the variability of the electron density. For these reasons, δ gives information about the functional groups of a molecule (H, OH, COOH, etc.) present in the chemical environment.

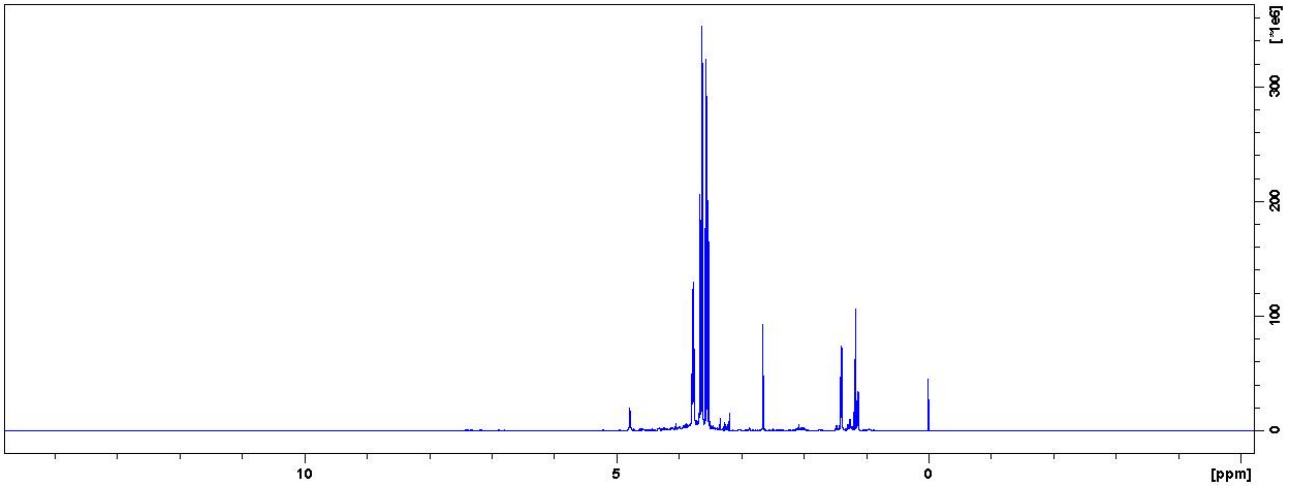

Figure 13. Example of a 1D-^{1}H NMR spectrum of a white wine.

Nuclei that tend to resonate in lower δ are shielded from B_0 because of the high-density electron cloud. By contrast, if a nucleus is near to an electronegative atom, such as oxygen or halogens, is de-shielded and thus has a high-frequency signal, because to cause the resonance is necessary a stronger B_0. For instance, the methyl group (CH_3) of a fatty acid in a triglyceride compound is shown at ~0.9 ppm in an ^{1}H NMR spectrum, while the glyceridic proton on the *sn*-2 position is shown at ~5.3 ppm, because it is close to the oxygen atoms of the ester bonds and the hydroxylic groups. Values of δ vary from 0 to 12 ppm for ^{1}H NMR, from 0 to 220 ppm for ^{13}C and from -30 to 200 ppm for ^{31}P. In food authentication the site-specific natural isotope fractionation-NMR is used, that investigates the δ value for ^{2}H (SNIF-NMR; Martin, Akoka, and Martin, 2006).

The J coupling causes the signal splitting, and it is the results of the interacting adjacent spins mediated via bonding electrons. This parameter is very important for structural characterization since its amplitude rely on the specing and the relative orientation (dihedral angle) between nuclei. J coupling value (expressed in Hz) is independent by the B_0 strength and can be positive or negative. The splitting pattern of a certain nucleus is calculated as $2nI+1$; where n is the number of neighbouring protons; I is the nuclear spin quantum number. If a nucleus has spin 1⁄2 the rule is simplified to $n+1$ such as the anomeric proton ^{1}H of monosaccharides (for example, glucose), the splitting due to the neighbouring proton H^2 shows it as a couple. However, this last rule is applicable just for weakly coupled spins, in which the different δ between the nuclei is bigger than J. This happens because the H^2 proton has two energy states, α and β, that respectively add and subtract to the magnetic field shown by H^1, that resonates in two different frequencies divided by the J coupling constant. About 98.9% of the protons present in nature are bound to the NMR inactive ^{12}C isotope, while the remaining 1.1% are ^{13}C isotope, and the splitting due to the adjacent carbon is not visible.

Usually, in ^{13}C and ^{31}P experiments, the effect of J coupling is suppressed with the "broadband decoupling" technique. Then, the NMR spectra appear like chromatographs because these nuclei consist of singlets (Shaka et al., 1983; Shaka et al., 1985).

Nuclear overhauser effect (NOE) corresponds to the modification of the signal intensities produced by the dipole-dipole coupling interactions, that are through-space contributions. In fact, broadband proton decoupling increases the intensity of the ^{13}C or ^{31}P signal. Therefore, the decoupling pulses cause the disturbance in the stability of the population of protons (which is affected in turn), as well as the signal intensities of the neighbouring ^{13}C or ^{31}P nuclei, which are dipolar coupled to protons, causing their T_1 relaxation. Since NOE depends on the spacing between nuclei, it is very useful to study both chemical structure and molecular interactions (Silipo et al., 2012; Wang et al., 2011).

T_1 relaxation mechanism is also known as spin-lattice relaxation. Based on the equation $M_z(t) = M_0 (1 - e^{-t/T1})$, it is correlated to its settlement along the direction of B_0 (z-axis), and it constitutes the introduction of the Gaussian population distribution of α and β spin states in B_0. T_1 changes depending on the nucleus, the molecular weight, the temperature, the size of B_0 and is a priority process generated by the transient magnetic fields, as a result of the molecular motion (Keeler, 2010). Moreover, T_1 settles the delay time between each RF pulse, that must permit the relaxation of the before the next pulse. Then, it is of fundamental importance for absolute quantification purposes (Levitt, 2005).

The excited magnetization decay is a mechanism of dephasing of each magnetic component and the depletion of phase coherence. This mechanism is called transverse or spin–spin relaxation or T_2. As well as for T_1, the T_2 relaxation time is due to the transient magnetic field. T_2 is typically calculated with the experiment known as CPMG (Meiboom and Gill, 1958).

NMR spectra can be mono-dimensional, if they have only one frequency dimension (1D), or multidimensional (i.e. 2D), when they have more than one frequency dimension (Fig. 14). Both 1D and 2D approaches are utilized in food science studies. In fact, several compounds commonly present in food samples, such as sugars and organic acids can be quickly identified by their particular NMR signals. The techniques typically used in 1D NMR are:

- simple pulse-acquire 1D ^{1}H experiment;
- CPMG pulse sequence (for signals suppression of high molecular weight molecules);
- 1D experiments (detection of heteronuclei, i.e. ^{13}C and ^{31}P).

2D NMR experiments permit the study of neighbouring nuclei through the correlation peaks, which are cross peaks with two frequencies representing the correlation, or coupling, between two different nuclei. Both homonuclear or heteronuclear experiments can be applied, depending on the kind of nuclei connected, the same in the first case, or different in the second one. These experiments are based on polarization transfer between different nuclei. Generally, the resolution of 2D experiments is better than 1D NMR because of the two frequency dimensions. Indeed, they are a good approach if complex molecules or samples are analyzed, but they need longer experimental times because they are composed of a series of 1D experiments. The COSY, TOCSY, HSQC, and HMBC are 2D experiments commonly used in food science. Among the most advanced experiments there are HSQC-TOCSY, ULTRA-FAST sequences, constant time experiments, diffusion, and many others (Nilsson et al., 2004; Orfanakis et al., 2013; Dais et al., 2015; Dal Poggetto et al., 2017; Schievano et al., 2017).

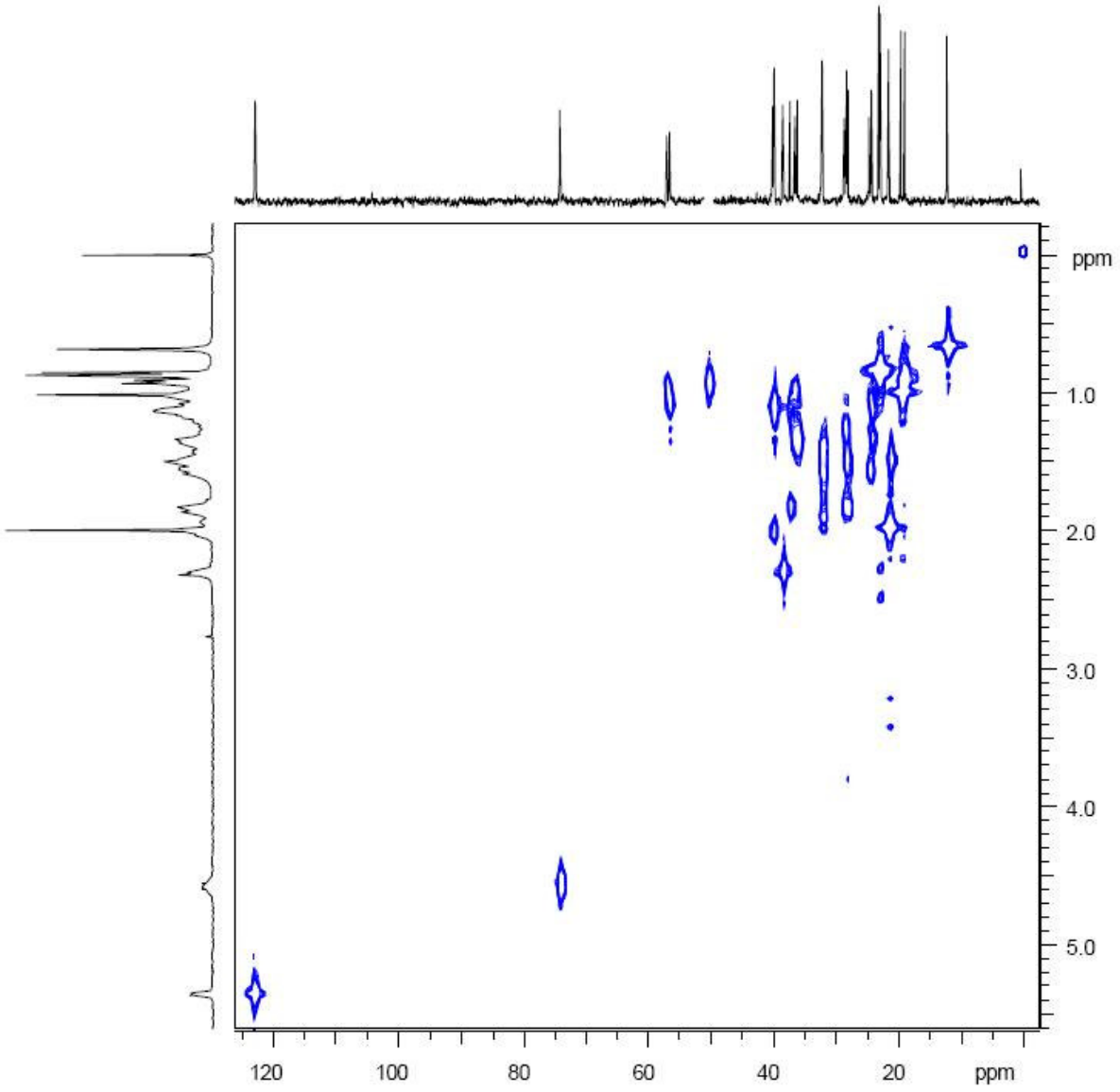

Figure 14. Example of a 2D experiment.

Since often it is required the quantification of food constituents, qNMR approach has been adopted in many applications in foods and beverages (Dais and Hatzakis, 2013; Vlahov, 1999). Thus, to prevent the polarization transfer from ^{1}H to ^{13}C through the NOE, the broadband proton decoupling must be used only in the course of the acquisition (Vlahov, 1998; Williamson and Hatzakis, 2017).

qNMR tool has shown an excellent repeatability and reproducibility in food analysis purposes (Dais et al., 2007). The relative quantification is obtained through the comparison between the peak area of each target compound, normalized for the number of nuclei contributing to the signal. The combining relationships that join the different signal areas are used when non-equivalent groups of protons represent two or more compounds (Williamson and Hatzakis, 2017).

Another important point in NMR analyses is the suppression of solvents, such as water. Usually, water is removed by lyophilization processes, even if it is not completely extracted from the sample. Furthermore, lyophilization significantly enhances the experimental time and in some cases even the alteration of the sample. Thus, water suppression can be an effective solution. Generally, the signal of the solvent is much higher than the analytes, causing interferences with the detection of less concentrated compounds, limiting the analog-to-digital converter (ADC). The most used water suppression experiments in food approaches are pre-saturation (Hoult, 1976), WATERGATE (Piotto et al., 1992), and the 1D version, when the NOESY experiment is used, that is widely used in metabolomics because of the low baseline distorted spectra produced, in particular near to the suppressed peak (McKay, 2011). In other cases, multiple signals need a supplementary suppression (for example, ethanol in beer), applied with shaped pulses and continuous wave (CW)-decoupling on ^{13}C nuclei (Mannina et al., 2016).

1.4.2.2 NMR in food science

Foods are complex matrices because they are made up of hundreds or even thousands of organic and inorganic molecules metabolized by plants, microorganisms, and animals, or resulting from the interactions between other constituents, or from the effects of external factors (for example, storage, transport, and processing). Then, human metabolism can also create additional new and/or more complex compounds (Laghi et al., 2014). However, this great complexity and variability are commonly detected by NMR analysis. Thus, the resulting spectra contain an enormous number of information that cannot be easily interpreted with a common univariate analysis. This approach belongs to the "foodomics" (Cifuentes, 2009; Laghi et al., 2014), in which data are interpreted by multivariate statistical analysis (MVSA) to completely describe a food product based on the quality, origin, processing, storage history and sensory characteristics, or to investigate how a specific nutritional approach influences human metabolism and health. In NMR-based metabolomics (called metabonomics) the two main approaches are targeted and untargeted analysis (Roberts et al., 2012). In the first approach, the objective is the quantification of the metabolites, and their quantities are used as variables in the statistical analysis. Thus, biomarkers are often predefined. In the second approach, the discrimination of each sample occurs by comparing the whole spectral pattern (Cloarec et al., 2005).

The use of as many variables as possible simultaneously by using MVSA (chemometrics), permits the extraction the maximum number of significant information contained in a big dataset, usually constituted by many variables, but not necessarily by many observations, decreasing its

dimensionality (Hatzakis, 2019; Hand et al., 2001; Massart, 1988; Monakhova et al., 2013). Therefore, MVSA permits the translation from thousands of variables system to a two- or three-dimensional graphical analysis. Thus, food metabolomics can provide a global view of the whole dataset, compare different groups of samples, apply regression modelling between various datasets to build prediction models on food composition, and many other applications. Some examples of metabolomics approaches are the study of the metabolic profiling of genetically modified (GM) foods (Le Gall et al., 2003), the quality control of beverages (Mannina et al., 2016; Lee et al., 2010; Lee et al., 2015), the control of the evolution of wine during the fermentation process and the metabolic characterization of the commercial product, (Hong, 2011; Mazzei et al., 2013; Skogerson et al., 2009), the authentication of comestible oils (Alonso-Salces et al., 2010a, 2010b), and fruit juices (Vogels et al., 1996), the classification of fruits and vegetables (Vermathen et al., 2011; Sobolev et al., 2010), and also the interrelationship between the spectral pattern and aroma (Malmendal et al., 2011).

For what concern the sample preparation, that should be randomized to avoid the bias effect, several steps can be included: the extraction of target compounds by using a specific solvent and/or technique; lyophilization; buffering and homogenization (Spyros and Dais, 2013). In the specific case of liquid-state NMR, the extracted sample is commonly resuspended in a specific solvent, such as deuterium oxide (D_2O), containing also the adequate IS for nonpolar solvents (i.e. TMS) or for polar solvents (i.e. TSP). Then, after the data acquisition a series of FIDs is acquired, and after being converted into spectra, they can finally be processed all with the same standard procedures, such as Fourier transform, phase and baseline correction, and signal referencing (Xi and Rocke, 2008; Rusilowicz et al., 2014).

To compare different samples, a pre-processing step is often required before the application of MVSA. The most common pre-processing steps are the spectral alignment, binning (or bucketing), sample scaling (or normalization), data scaling, and spectral editing.

Even if a standardized NMR data processing includes signal referencing, several aspects such as pH variation, the presence of paramagnetic cations, and ionic strength, can be a source of variations in δ values, and thus a source of error during data analysis. However, these sources of errors can be easily fixed by using buffer solution (such as hydrochloric acid and ammonium oxalate) and chelators, such as EDTA, or with a further optimization to correct the signal alignment with softwares, such as ICOSHIFT (Savorani et al., 2010; Izquierdo-Garcìa et al., 2011; Vu and Laukens, 2013). Nevertheless, by binning (also called bucketing) the small variations of the chemical shifts of the spectra can be efficiently corrected (Ellinger et al., 2013). Binning technique

permits data reduction by segmenting the spectrum in pieces (bins or buckets) typically ranging from 0.01 to 0.05 ppm (usually 0.04 ppm) (Beckonert et al., 2003). However, it is important to highlight that data reduction also means a decreased spectral resolution, and that it is possible that signals of some analyte is splitted in more bins, needing an additional data treatment (Smolinska et al., 2012).

Usually, in metabolomics the most significant differences have been shown by the less abundant biomarkers. Nevertheless, the biomarkers with a high signal intensity have also a wider variance, and thus require data scaling pre-treatment, such as mean-centring (Craig et al., 2006). Regarding the data scaling, the procedures that are commonly used in food metabolomics are the auto-scaling, or unit variance scaling, whereby standard deviation (SD) represents the scaling factor, and Pareto-scaling, in which each variable is divided by $\sqrt{SD}$ (Eriksson et al., 2001). The first approach leads to a variance equal to one for each variable and thus an equal importance, minimizing the effects of the metabolites with a high concentration. The second approach softly reduces the influence of big variances. Then, data-output appears like a table with rows and columns suitable for statistical analysis softwares (Hatzakis, 2019).

In NMR analysis, principal components (PCs) represent the linear combinations of the signal intensities explaining a specific quantity of variance. Thus, if it is necessary to study the variance attributable to a particular factor, a supervised technique can be an effective solution, because the principal component analysis (PCA) plot represents the entire variance of the dataset. For this purpose, the loadings may be plotted as a line loadings plot, recreating the real spectrum (Hatzakis, 2019). Conversely to PCA, in PLS-DA can be used for classification purposes because the class membership is known (Wold, 1966). In PLS-DA procedure, there are two related matrices (X and Y) containing observations and variables (i.e. samples and bins) (Hatzakis, 2019).

Both identification NMR and q-NMR approaches can be used to perform composition studies of foods, since they give important information for structural explanation. In fact, they have been efficiently to study lipids in oils (Dais and Hatzakis, 2013; Monakhova and Diehl, 2016a, 2016b; Tsiafoulis et al., 2014), carbohydrates (Kazalaki et al., 2015; Merkx et al., 2018; Singh et al., 2016), amino acids (Belton et al., 1996), alcohols (Hatzakis et al., 2007; Nilsson et al., 2004), organic acids (Berregi et al., 2007), polyphenols (Agiomyrgianaki and Dais, 2012a, 2012b; Charisiadis et al., 2010), vitamins (Ackermann et al., 2017; Dais et al., 2015; Shumilina et al., 2015), terpenes (Dais et al., 2017), phospholipids (Hatzakis et al., 2008; Kaffarnik et al., 2013), colorants (Scotter, 2009; Venkatachalam et al., 2018), rather than contaminants (Lachenmeier et al., 2009). Moreover,these

compounds have been studied in different foods, such as oils (Dais and Hatzakis, 2013; Siddiqui et al., 2003), beverages (Kidric, 2008; Ryu et al., 2017; Zurriarrain et al., 2015), meats (Garcıa-Garcıa et al., 2018), dairy products (Gangwar et al., 2018; Maher and Rochfort, 2014; Tociu et al., 2018). In particular, the application of 2D techniques is necessary to characterize the chemical structure, as well as the availability of spectroscopic databases and model compounds. In fact, it permits unambiguous NMR assignments, since the molecular conformation, δ, and vicinal J couplings, can be influenced by the matrix, as demonstrated by various studies (Cheng and Neiss, 2012; Dais and Hatzakis, 2013; Fotakis et al., 2013; Kazalaki et al., 2015; Mannina et al., 2015; Marcone et al., 2013; Petersen et al., 2014a; Spyros and Dais, 2013; Zhao et al., 2017).

Generally, 1D NMR spectroscopy is used in qNMR food-related studies. Indeed, 2D NMR have been used only for a few qNMR studies (Hu et al., 2007), even if it remains an effective high-resolution technique for composition analysis, as a consequence of some recent improvements (Giraudeau, 2014). Probably, the underuse of 2D NMR for compositional analysis is due to several disadvantages:

- it consumes more time than 1D ^{1}H NMR;
- the TOCSY and HSQC experiments, working on magnetization transfer through "J" coupling, in which much value cannot be completely fulfilled by mixing the experimental time, since the spinning time can interact;
- NMR equipment is very expensive and requires very specialized people for data interpretation.

Polysaccharides, since they remarkably influence both functions and formulations of foods, are among the most studied compounds in composition analysis and structural characterization (Cheng and Neiss, 2012). Indeed, they are responsible of several physicochemical properties, stabilization of foam, binding of aroma, and shelf life, therefore affecting food quality and sensory properties (Saha and Bhattacharya, 2010; Schmitt and Turgeon, 2011; Wang et al., 2015; Cook et al., 2018). Nevertheless, their characterization is intricated because of their molecular complexity, as well as the different molecular weights when compared with other food components (Lovegrove et al., 2017). In fact, 2D NMR allows the study of branching and the glycosidic bonds. Furthermore, liquid-state NMR can be applied as a fast approach to analyze of soluble polysaccharides extracted from coffee (D'Agostina et al., 2004; Gniechwitz et al., 2008; Nunes et al., 2008), potatoes (Khodaei and Karboune 2013; Nilsson et al., 1996), and many other matrices (Cheng and Neiss, 2012; Kang et al., 2011; Kang et al., 2018).

In food authentication studies the NMR spectroscopy is considered a new approach (Ellis et al., 2012). In fact, the site-specific natural isotopic fractionation (SNIF) NMR, is the official method used by the European Commission for the authentication of wine and vinegar (EC regulation 2676/90 2347/91, 2348/91, OIV; Martin et al., 2006). Another example is the application of an AOAC (http://www.eoma.aoac.org/) method for the authentication of fruit juices and vanillin (Bensaid et al., 2002; Caytan et al., 2007; Remaud and Akoka, 2017). Other approaches, such as SNIF-NMR, that measures the isotopic ratio for D/H or $^{13}C/^{12}C$ on each position of the molecule, have been used for the authentication of honey (Bertelli et al., 2010), fruits and vinegar (Ko et al., 2013), wine (Košir et al., 2001; Ogrinc et al., 2001), and spirits (Jiang et al., 2015; Perini et al., 2018). This sudden notice about the NMR spectroscopy is due to the concern of producers and consumers for authentic products, as well as for the creation of a safe market and for its economic and health consequences. However, the final food composition depends on various factors: geographical origin, agronomic practices, vintage, harvest period, variety, type of production, and possible adulteration (Capitani et al., 2017b; Agiomyrgianaki et al., 2012b; Papotti et al., 2013; Picone et al., 2016; Akanbi and Barrow, 2018; Girelli et al., 2016). Moreover, in most cases more than one biomarker is necessary to classify and characterize a specific food, thus making its authentication complicated. For this reason, the combination of untargeted or targeted NMR analysis with MVSA is crucial for food authentication (Esslinger et al., 2014; Lopez et al., 2014).

All the different combinations of analytical techniques previously described can simplify food classification extremely. In fact, NMR can rapidly analyze a complex mixture, and thus more compounds simultaneously, and its use in the food industry, analytic laboratories and regulation agencies, is expected to raise (Marcone et al., 2013). Despite this, the lack of standardized protocols for sample preparation, available libraries and of classification and prediction statistical models needs to be filled, as well as the high cost and the low sensitivity (Hatzakis, 2019).

1.4.3 The liquid chromatography-mass spectrometry (LC-MS) technique

Liquid chromatography (LC) can easily identify polyphenols, sugars, organic acids, and other metabolites (Andersen and Markham, 2006; Mazza et al., 2004; da Costa et al., 2000). When the LC is combined with mass spectrometry (MS) instruments such as Ion Trap (IT), the resulting instrument (LC-MS) can give a selective identification of unknown metabolites in a complex matrix (Fig. 15) (Kong et al., 2003). In addition, LC-MS approach has become fundamental for quantification purposes (Hopfgartner et al., 2004). In fact, in complex samples high accuracy is

reached with the detection of the abundances of the precursor ions and their respective fragments. Moreover, quantification performance is usually adequate when the variation of concentration (VC) is below a certain threshold, e.g., 10%, and thus due to the statistical variability. Accordingly, High Resolution Mass Spectrometers (HRMS) permit to reach an additional specificity because of the dependable separation of the overlapping isobaric peaks.

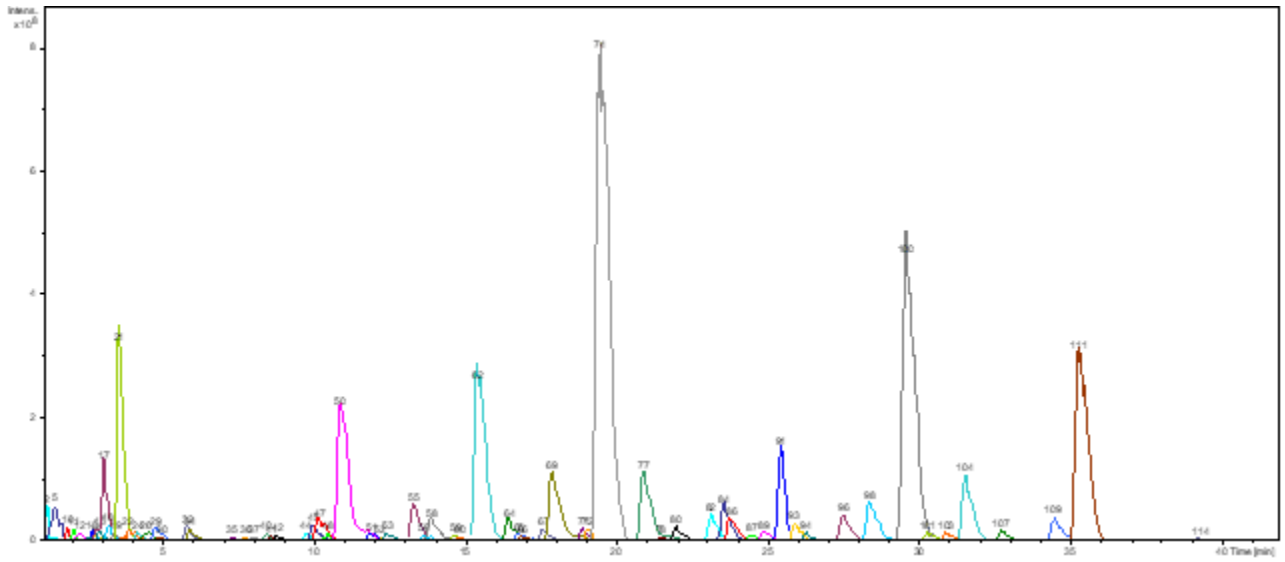

Figure 15. Example of the anthocyanins profile of a red must. 114 different masses have been automatically detected after an LC-MS-IT analysis.

Among the HRMS devices, the Orbitrap is one of the most used in food science, pharmacology, toxicology, and other researching fields. However, the higher transmission of the Orbitrap analyzer permits it to reach the required VC, but with a lower fragment intensity threshold.

The Orbitrap analyzer is a component of an instrument that has been built by Thermo Masslab Ltd (Manchester, UK), and it is well described even in other studies (Makarov, 1999, 2000; Hardman and Makarov, 2003). The main components of the instrument are shown in Fig. 16.

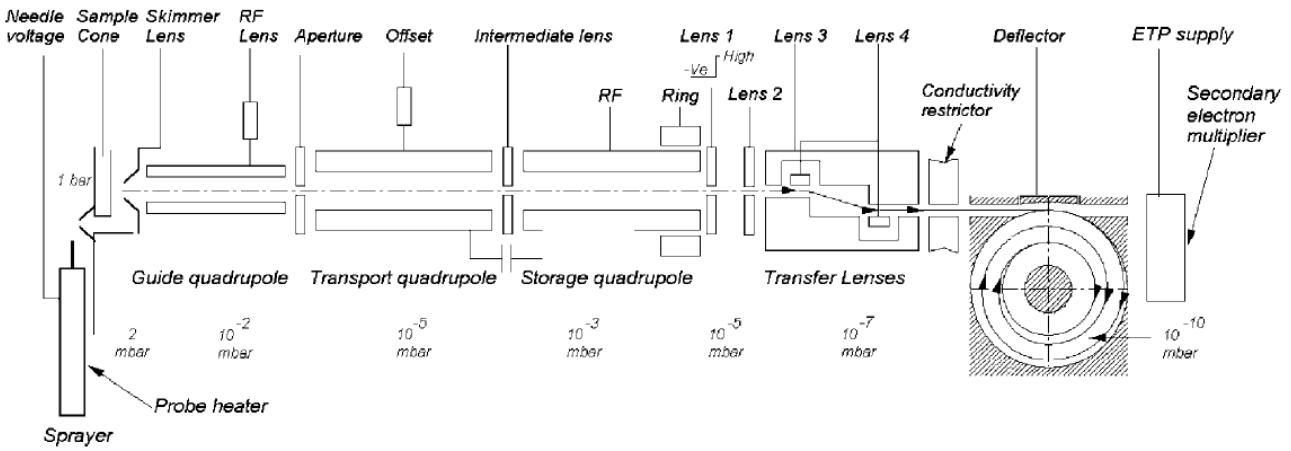

Figure 16. The scheme of the Orbitrap mass spectrometer reported by Hu et al. (2005).

In the Orbitrap mass analyzer the ions enter with a specific velocity, perpendicularly to the *z*-axis. By injecting in a position offset from its equator corresponding to $z = 0$, the potential energy is given to the ions in the *z*-direction (Fig. 17) (Hu et al., 2005).

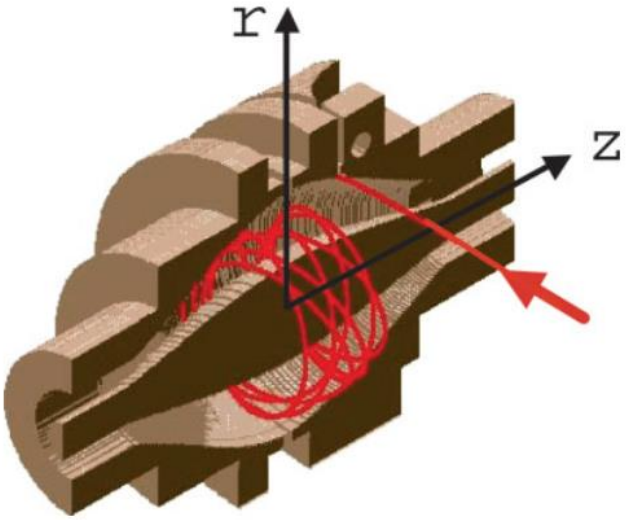

Figure 17. Section of the Orbitrap mass analyzer and ions trajectories (Hu et al., 2005).

Receiving enough collisions from a bath gas (~10^{-4} Torr), the ions are slowed down and grouped as small ions packages of a few mm. Then, the backwards lens of Q_2 is pulsatory opened, when enough ions have been accumulated (usually in 0–400 ms), and an intense electric field is created through the Q_2 axis to rapidly extract the ions, and then sent in 100–200 ns to the Orbitrap (Hardman and Makarov, 2003; Makarov et al., 2002). Here, the ions are speeded up by the ion optical deflection lens system on the Orbitrap circumference and injected by switching to a suitable value the voltage applied to the deflector lens. From $z = 0$ starts a harmonic axial oscillation without any supplementary excitation. All ions have equal amplitude, even if the ion packets of various *m*/*z* carry out their axial oscillations depending on the respective frequencies (ω), according to the formula: $\omega = \sqrt{z/m} \cdot k$ (rad s^{-1}) (Makarov, 2000).

Detecting an ion image current on the basis of its motion through *z*-axis is possible when the ion packets maintain the spatial coherence (i.e. phase coherence and small spatial extension) along the *z*-axis direction (Makarov, 2000). The external electrode is split in half at $z = 0$, permitting the collection of the ion image current. Each half of the external electrode amplifies differently the current, that is then converted analog-to-digital to be processed and collected by customized control and acquisition software (Orbitrap Tune Program, Mike Senko, Thermo Electron, San Jose, CA). Recent Orbitrap analyzers have a smaller dimension than the previous ones, with a maximum

diameter of the internal electrode of 8 mm, and a maximum internal diameter of the external electrode of 20 mm (Hardman and Makarov, 2003; Makarov et al., 2002).

Data collection time can reach 1600 ms, while the delay time is ~100 ms (i.e. the time necessary for the stabilization of the high-voltage amplifier of the central electrode). At this point, the time-domain signal has a 'transient' form. The collision between the ion and the background gas molecules, despite the ultra-high vacuum level (2 x 10^{-10} mbar), causes a loss of phase coherence (ion packet dephasing), or a loss of ion from the trap, or even both, resulting as a transient with a decreased signal intensity. Moreover, a partial dephasing may be due to the space charge. Finally, the transient is Fourier-transformed by the program MIDAS, creating the mass spectrum (Senko et al., 1996).

Even though the Orbitrap is a new device, it is describable as a modified 'Knight-style' Kingdon trap, in which both internal and external electrodes have a special shape, or also as a quadrupole IT with a different form. However, in the Orbitrap is used a static electrostatic field, while in the IT is used a dynamic electric field with an oscillation of ~1 MHz (Schwartz et al., 1990). The axially symmetric electrodes of the Orbitrap generate a combined 'quadrologarithmic' electrostatic potential, according to the following formula (Makarov, 2000):

$$u\,(r,z) = \frac{k}{2}\,(z^2 - \frac{r^2}{2}) + \frac{k}{2}\,.(R_m)^2\,.ln\left[\frac{r}{R_m}\right] + C \qquad (1)$$

Where *r* and *z* are the axis of the Orbitrap, *C* is a constant, *k* represents the curvature of the field, and *Rm* is the characteristic radius. An unwavering ion trajectory is obtained by the orbital motion of the ions around the central electrode (*r*, φ-motion, where φ is the angular coordinate), and the contemporaneous oscillations along the *z*-direction.

Even though both radial and angular frequencies are mass-dependent, ω is totally independent from the energy and the spatial spreading of the ions, giving to the Orbitrap enough mass resolution (up to 150000) and accuracy to perform high-performance mass (HRM) analysis. The mass resolution (MR) measured at the full width of each peak at half of its maximum height (FWHM) is

$$MR = m/Dm \quad (2)$$

where m is the measured or experimental mass, and Dm is the theoretical mass (Dm) (Junot et al., 2014).

In addition to this, compared to other instruments, the Orbitrap has an increased space charge capacity for higher *m*/*z* values, as a consequence of both independent trapping potential on *m*/*z* ratio and the bigger trapping volume (Hu et al., 2005). For these reasons, the Orbitrap-based analyses are applied in several research fields, such as food safety and environmental analysis (Self et al., 2011; Blay et al., 2011; Zachariasova et al., 2010), metabolomics studies (Lim et al., 2007; Werner et al., 2008; Griffiths et al., 2008; Madalinski et al., 2008; Olszewski et al., 2010; Storm et al., 2011; Amador-Noguez, 2010), clinical analysis (Henry et al., 2012; Franke et al., 2011; Li and Franke, 2011), bioanalysis (Zhang et al., 2012; Ruan et al., 2011), doping control (Moulard et al., 2011; Thomas et al., 2012; Virus et al., 2008), and lipidomics (Schuhmann et al., 2011, 2012; Schwudke et al., 2007; Ejsing et al., 2009).

Generally, the mass accuracy of HRMS is lower than 5 ppm, while the mass resolution is usually higher than 10,000 (Zubarev and Makarov, 2013). HRMS devices are represented by FT-ICR, Orbitrap and time of flight (TOF) analyzers, which reach a mass resolution of over 1,000,000 (at *m*/*z* 400), up to 240,000 and up to 60,000 (at *m*/*z* 200), respectively (Junot et al., 2014). Because of these performances, they are widely used in metabolomic studies for their high resolving power, the increased mass accuracy, and they also permit a better precision in the adduct identification (Brown et al., 2005). For what concern the limit of detection (LOD), it is usually calculated on the basis of the inner noise of the pre-amplifier, that in the recent instruments it is about 2-4 elementary charges in 1 s of acquisition time. As a result, in the case of charge states higher than 5-10, it can be reached with the single-ion detection (Rose et al., 2012). Especially in complex matrices, HRMS can perform measurements with ppm and sub-ppm errors, and thus providing mass spectrum with minor interference due to overlapping molecules that minimizes the ambiguity of molecular formula assignments (Brown et al., 2005). Moreover, both FT-ICR and Orbitrap devices have become commonly used in direct infusion mass spectrometry (DIMS) applied in metabolomics and lipidomics because of the ultrarapid data acquisition (Aharoni et al., 2002; Raterink et al., 2013; Soltow et al., 2013). As a result, the fast replication of the analysis on the same sample increases the reproducibility of the experiment, and finally improves the accuracy of the statistical analysis (Dettmer et al., 2007).

The HRMS devices are also highly adaptable to the heated-electrospray ionization (HESI), to matrix assisted laser desorption ionization (MALDI) ion sources (Kuehnbaum and Britz-McKibbin 2013; Nagornov et al., 2014; Brown et al., 2005; Junot et al., 2014; Lei et al., 2011; Moco et al., 2007) and also to other fragmentation techniques, including the collision induced dissociation (CID) or the high-energy collisional dissociation (HCD) (Junot et al., 2014). This high adaptability allows

the stepwise fragmentation in the experiments of multiple stage mass spectrometry (MSn), in order to obtain more trusting identification or characterization of unknown metabolites (Rojas-Cherto et al., 2012).

As in any FT analyzer, the resolving power in the Orbitrap is inversely proportional to the speed. Hence, an improved FT permits to choose to double the speed at the same resolving power, as well as to double the resolving power without changing the speed (Zubarev and Makarov, 2013). The limit is due to the duration of the transient, that is very strict for ions with high *m*/*z*, and is mainly affected by vacuum conditions in the trap and by the near ion optics (Makarov and Denisov, 2009).

1.4.3.1 Orbitrap applied to wine adulteration and analysis

Wine has been subjected to several kinds of fraud worldwide, such as label fraud, in which occurs the mislabeling of the varietal or growing area of wine, or the blending with other varieties (Everstine et al., 2013). For instance, in 2008 and 2009, in Italy almost 2 million liters of high-quality wine have been impounded for having been produced with unauthorized grapes (Asimov, 2009). Another enormous fraud occurred in 2002 in the Bordeaux region (France), in which the producers have vinified wine with the Bordeaux designation of origin with grapes imported from other regions (Paris, 2002). Thus, even if a combined method, by coupling the QuEChERS extraction with UHPLC-Q-Exactive, was developed by Jia et al. (2014) for the identification of 69 dyes in wines, the control of the authenticity and/or adulteration of wines is a challenging purpose (Everstine et al.,2013).

Numerous polyphenols have been detected in red wine extracts, such as phenolic acids and anthocyanins, by using an LTQ Orbitrap Velos instrument (Vallverdú-Queralt et al., 2015). In addition, Cavaliere et al. (2019) have identified and also quantified several flavonoids and anthocyanins with a Hybrid Quadrupole Orbitrap in rosè wine, and thus with the polarity set in both positive and negative mode. A Q-Orbitrap instrument has been also used to analyze tannins in grape skins and grape marc by using an untargeted approach (Barnaba et al., 2019), and to identify and quantify the phenolic compounds in French red wines (Damoc et al., 2009). Boido et al. (2019) used a Q-Exactive Orbitrap for the characterization of commercial and minor grape Uruguayan varieties. Orbitrap instruments have also been used to determine the mycotoxins (for example, ochratoxin A) in wine (Li et al., 2012), as well as for the quantification of casein in white wine (Monaci et al., 2011a, 2011b).

1.5 XCMS data processing

In the last decades, the untargeted metabolomics approach has remarkably increased the interest of the investigators in several research fields. Nevertheless, each metabolomics study needs a deep knowledge of the different techniques that can be used, such as GC-MS or LC-MS, as well as strong informatic skills for the use of the software to control the instrument and for the processing of raw data (i.e. mass spectra), and also the familiarity with the different statistical analysis techniques, such as ANOVA and MVSA, and software. In addition to this, not all investigators have the possibility to use the specific software of the instrument with which they have obtained the raw data. Indeed, it is necessary to buy the license of the software, or to use an open-source software, especially in case of students. However, even with these solutions, the entire data processing workflow may be very challenging, as well as highly time-consuming. For these reasons, in the last two decades several online platforms that permit an easy analysis of complex matrices, such as MetaboAnalyst (Xia et al., 2009) and XCMS Online (Tautenhahn et al., 2012), have been developed. In fact, the XCMS Online platform was created in 2004, in parallel with the METLIN database, that nowadays contains more than 500,000 standard compounds, analyzed through an MS-MS approach in both positive and negative polarity (https://metlin.scripps.edu/). Besides, there are also other databases connected to XCMS, specifically for metabolomics purposes, such as the Human metabolome Database (HMDB, https://hmdb.ca/), the National Institute of Standard and Technology database (NIST, https://webbook.nist.gov/chemistry/), and finally the MassBank database (http://www.massbank.jp/), that is the official database of the Mass Spectrometry Society of Japan. Furthermore, for proteomic and genetic studies, is possible to do further researches by using the KEGG database (https://www.kegg.jp/kegg/kegg2.html), while for lipidomic studies, the LIPID MASS database (https://www.lipidmaps.org/) is available.

Tautenhahn et al. (2012) has described the workflow steps of XCMS Online as follows:

1. uploading of raw data: the outputs data of the instrument used (typically, RAW file) are directly charged in the working session created on the platform;

2. selection of the parameters: in this section the default parameters can be used for each instrument (and analyzer) that is selectable on the platform, for both GC- and LC-MS techniques. However, on the basis of the type of research, the complexity of the sample, and the quality of the mass spectra, each of this parameter needs to be optimized *ad hoc*, such as the retention time alignment, statistical analysis, or TIC correction;

3. view and/or download of the results: in the final step the results can be visualized as a table, in which the retention time, the medium *m/z* ratio and the quantity of each compound (feature) are reported, if a “Single” job has been selected. On the other hand, when a more complex job is the output of the analysis, such as a “Pairwise” job or a “Multigroup” job, in the table the p-value of each feature are also reported, and an automatic PCA is showed in the “iPCA” section.

AIM OF THE STUDY

The project involves the metabolic characterization of red and white wines produced from ancient *Vitis vinifera* cultivar of Emilia-Romagna region, not yet or newly registered in the National Register of Vine Varieties. These varieties are in the brink of extinction (medium-high risk) and they need to be carefully studied to allow their valorization. Thus, the comparison between minor wines and commercially established wines managed with different cultivation regimes, such as organic and integrated farming, is the best approach. In fact, in the Emilia-Romagna region Lambrusco varieties are among the most commercially established. Moreover, Ancellotta variety is particularly widespread to produce blending wines (Rossissimo) and worldwide exported. In addition, the evaluation of the most cultivated varieties in Europe, such as Tempranillo, Cabernet Sauvignon, Merlot, Syrah and Gewürztraminer compared to the minor wines covered by this study, could increase the knowledge oenological potential of new products (collaboration with University of Barcelona). Given the experience of the group about Lambrusco and aromatic wines (Malvasia family), the aim of the PhD project is the characterization of minor and commercial wines through innovative and uncommon techniques, expanding the experience of the group. Such techniques, like HRMS and NMR, permit qualitative and quantitative analysis of a wide range of compounds. Moreover, most of these techniques are already included in the official protocols of analysis in characterization and adulteration studies, giving an added value to the project.

2. Materials and methods

2.1 Chemicals

GC analysis: dichloromethane (≥ 99.5%) and methanol (≥ 99.8%) were purchased from VWR International Srl (Milan, Italy). Absolute ethanol (≥ 99.8%), sodium sulfate anhydrous (Na_2SO_4), 2-octanol (≥ 97%), and the standards for the GC analyses were purchased from Sigma-Aldrich (Milan, Italy).

LC analysis: malvidin-3-*O*-glucoside was purchased from Sigma-Aldrich (Milan, Italy); acetonitrile and formic acid were purchased from VWR International Srl (Milan, Italy).

NMR analysis: 3-(trimethylsilyl)-propionate acid-d4 (TSP) and deuterium oxide (99.8 %) and the sodium oxalate (≥ 99.9%) were purchased from Sigma-Aldrich (Milan, Italy); sulfuric acid (96%) was purchased from Carlo Erba Reagents (Cornaredo, Italy).

The deionized water used for each analytical procedure was obtained by using the purification system Elix^{3UV} (Merk, Milan, Italy), while for the ^{1}H-NMR 400 MHz the deionized water was obtained from a Labostar Milli-Q® water from EVOQUA Water Technologies (Günzburg, Germany).

2.2 Samples analyzed during the preliminary metabolomics and GC-MS analysis

Samples representing commercial products were L. Salamino, L. Grasparossa, both conventional and organic, produced by the Cantine Riunite of Campegine (Reggio Emilia, Italy). Samples representing minor wines (L. di Fiorano, Festasio and Albana Rosa) were produced and provided by CRPV of Cesena. The whole dataset (Table 1) is referred to the vintage 2017 and the vinification processes are described in section 2.5.

Sample	Wine	Vintage	Winery	Origin
FE	Red sparkling	2017	CRPV	Modena
PE	Red sparkling	2017	CRPV	Modena
AR	White still	2017	CRPV	Forlì-Cesena
LSC	Red sparkling	2017	Riunite	Modena/Reggio Emilia
LSO	Red sparkling	2017	Riunite	Modena/Reggio Emilia
LGC	Red sparkling	2017	Riunite	Modena/Reggio Emilia
LGO	Red sparkling	2017	Riunite	Modena/Reggio Emilia

Table 1. Dataset for preliminary analysis. FE = Festasio; PE = L. di Fiorano or Pellegrino; AR = Albana rosa; LSC = L. Salamino conventional; LSO = L. Salamino organic; LGC = L. Grasparossa conventional; LGO = L. Grasparossa organic.

2.3 Samples analyzed with the Orbitrap and agrometeorological data

Veruccese, Bertinora, Rossiola, Termarina rossa, L. di Fiorano and Festasio were produced c/o Astra – Innovazione e Sviluppo based in Tebano (Emilia-Romagna, Italy) – experimental winery (CRPV of Cesena). Actually, Bertinora is a white grape with a partial pigmented peel.

L. Reggiano conventional, L. Reggiano organic, L. Grasparossa conventional, L. Grasparossa organic, Ancellotta organic, and Ancellotta conventional were provided from Cantine Riunite & CIV of Campegine. Among these wines, L. Reggiano is a mixture of several varieties, according to its specification of production. In fact, it can contain up to 85% of Lambrusco varieties, such as L. Marani, L. Maestri, L. Salamino, L. Montericco, L. di Sorbara, L. Grasparossa, L. Viadanese, L. oliva and L. Barghi. The remaining 15% is constituted by Ancellotta, Malbo gentile, L. a foglia frastagliata and Fogarina. All the other wines are single-variety.

Rossissimo organic T7, Rossissimo organic T17, Rossissimo organic T95, Rossissimo organic T96, Rossissimo conventional T308, Salamino conventional T52, Salamino conventional T309 were provided from Cantina di San Martino in Rio (SMR) (Reggio Emilia, Italy) and were all single-varietal wines.

The list of the whole dataset is reported in Table 2, while the specific vinification process is described in Section 2.5.

The production area of the wineries is very wide, with both flat land and hills productions, throughout the provinces of Modena and Reggio Emilia. Moreover, vineyards are managed with different pruning techniques, such as the horizontal spurred cordon, overhead system (Pergola or Semibelussi), Sylvoz and GDC, in the flat zones, and especially the Guyot in the hilly areas, in both organic and conventional production. The typical rootstocks in the flat zone are Kober 5BB, SO4 and 420A, because they are adaptable at different kinds of soils. In the hills production the Kober 5BB is not used: instead, SO4 and 420A, but also Golia, 110 Richter and 1103 Paulsen are used, all more adaptable to less fertile soils. In the flat zones, the soil is grassed-managed in the inter-row and it is mechanically hoed (organic farming) or weeded (integrated farming). In the hilly areas the soil is predominantly hoed. In the flat zones, the high-water availability permits irrigation during the period of *veraison* (from the middle of July up to the middle of August), while in the hills zones the irrigation practice is rare. The pest management varies according to the integrated pest management and the organic farming production. For what concern the oenological process, organic red wine can contain a maximum of 100 mg L^{-1} of SO_2 (Reg. CE 203/12).

Regarding the meteorological data, they were collected from the website of Arpae Emilia-Romagna (https://www.arpae.it/). In particular, the average values of temperatures and the rainfall of the vintages 2018 and 2019 were collected during the *veraison* period of grape (3rd decade of July and the 1st decade of August), which is the crucial period for the accumulation of the anthocyanins.

All the samples were collected during the vintages 2018 and 2019, with two bottles representing two replications of the wine analyses. Then, all samples were analyzed as soon as possible to avoid any kind of modification of the product as far as possible.

Sample	Wine	Vintage/s	Winery	Origin
VE	Red still	2018-2019	CRPV	Rimini
BE	White still	2018-2019	CRPV	Forlì-Cesena
ROS	Red still	2018	CRPV	Ferrara
FE	Red sparkling	2018-2019	CRPV	Modena
PE	Red sparkling	2018	CRPV	Modena
TE	Red still	2019	CRPV	Parma
RO7	Red sparkling tank 7	2018-2019	SMR	Reggio Emilia/Modena
RO17	Red sparkling tank 17	2018	SMR	Reggio Emilia/Modena
RO95	Red sparkling tank 95	2018	SMR	Reggio Emilia/Modena
RO96	Red sparkling tank 96	2018	SMR	Reggio Emilia/Modena
RC308	Red sparkling tank 308	2018-2019	SMR	Reggio Emilia/Modena
LSC52	Red sparkling tank 52	2018-2019	SMR	Reggio Emilia/Modena
LSC309	Red sparkling tank 309	2018	SMR	Reggio Emilia/Modena
LRC	Red sparkling	2018	Riunite	Reggio Emilia/Modena
LRO	Red sparkling	2018	Riunite	Reggio Emilia/Modena
LGC	Red sparkling	2018	Riunite	Reggio Emilia/Modena
LGO	Red sparkling	2018	Riunite	Reggio Emilia/Modena
AO	Red sparkling	2018-2019	Riunite	Reggio Emilia/Modena
AC	Red sparkling	2018-2019	Riunite	Reggio Emilia/Modena
LSC	Red sparkling	2018	Riunite	Reggio Emilia/Modena

Table 2. List of wines analyzed through Q-Exactive Orbitrap. VE = Veruccese; BE = Bertinora; ROS = Rossiola; FE = Festasio; PE = L. di Fiorano or Pellegrino; TE = Termarina; RO7 = Rossissimo organic from tank 7; RO17 = Rossissimo organic from tank 17; RO95 = Rossissimo organic from tank 95; RO96 = Rossissimo organic from tank 96; RC308 = Rossissimo conventional from tank 308; LSC52 = L. Salamino conventional from tank 52; LSC309 = L. Salamino conventional from tank 309; LRC = L. Reggiano conventional; LRO = L. Reggiano organic; LGC = L. Grasparossa conventional; LGO = L. Grasparossa organic; AO = Ancellotta organic; AC = Ancellotta conventional; LSC = L. Salamino conventional.

2.4 Wine analyzed by 400 MHz NMR experiment

The dataset (Table 3) consisted of minor red wines (Veruccese, Rossiola, and Festasio) and minor white wines (Vernaccina, Bertinora, Melara, Vernaccia del Viandante and Caveccia) which were provided by CRPV. All the Lambrusco samples analyzed are those described in section 2.3. Pignoletto organic and conventional wines were provided by Cantine Riunite & CIV of Campegine. Cantine Riunite of Castelfranco (Bologna, Italy) provided additional samples of both Pignoletto conventional and organic, the Pignoletto of Righi brand and the Pignoletto Brut.

About 100 mL of each wine was withdrawn and put into a PE bottle (100 mL) filled up to the very top, in order to prevent the oxidation process, and sent to the University of Barcelona.

Finally, the Spanish red wines (Cabernet Sauvignon, Tempranillo, Merlot and Syrah) and the Spanish white wines (Gewürztraminer and Albariño) were provided by Codorníu, based in Haro (La Rioja, Spain) which has the main production in the Catalonia region (Spain).

Sample	Wine	Vintage	Winery	Origin
VE	Red still	2018	CRPV	Rimini
VR	White still	2018	CRPV	Rimini
BE	White still	2018	CRPV	Forlì-Cesena
ROS	Red still	2018	CRPV	Ferrara
ME	White still	2018	CRPV	Piacenza
VV	White still	2018	CRPV	Forlì-Cesena
CA	White still	2018	CRPV	Ravenna
FE	Red sparkling	2018	CRPV	Modena
RO7	Red sparkling	2018	SMR	Reggio Emilia/Modena
RO17	Red sparkling	2018	SMR	Reggio Emilia/Modena
RO95	Red sparkling	2018	SMR	Reggio Emilia/Modena
RO96	Red sparkling	2018	SMR	Reggio Emilia/Modena
RC308	Red sparkling	2018	SMR	Reggio Emilia/Modena
LSC52	Red sparkling	2018	SMR	Reggio Emilia/Modena
LSC309	Red sparkling	2018	SMR	Reggio Emilia/Modena
PTO	White sparkling	2018	Riunite	Modena
PTC	White sparkling	2018	Riunite	Modena
LRC	Red sparkling	2018	Riunite	Modena
LRO	Red sparkling	2018	Riunite	Modena
LGC	Red sparkling	2018	Riunite	Modena
LGO	Red sparkling	2018	Riunite	Modena
AO	Red sparkling	2018	Riunite	Modena
AC	Red sparkling	2018	Riunite	Modena
CS	Red still	2018	Codorníu	Spain
TP	Red still	2018	Codorníu	Spain
MT	Red still	2018	Codorníu	Spain
SY	Red still	2018	Codorníu	Spain
GE	White still	2018	Codorníu	Spain

AL	White still	2018	Codorníu	Spain
PTCC	White sparkling	2018	Riunite	Castelfranco Emilia
PTOC	White sparkling	2018	Riunite	Castelfranco Emilia
PTCR	White sparkling	2018	Riunite	Castelfranco Emilia
PTOR	White sparkling	2018	Riunite	Castelfranco Emilia
PTB	White sparkling	2017	Riunite	Castelfranco Emilia

Table 3. List of wines analyzed by 400 MHz NMR at University of Barcelona. VE = Veruccese; VR = Vernaccina; BE = Bertinora; ROS = Rossiola; ME = Melara; VV = Vernaccia del Viandante; CA = Caveccia; FE = Festasio; RO7 = Rossissimo organic from tank 7; RO17 = Rossissimo organic from tank 17; RO95 = Rossissimo organic from tank 95; RO96 = Rossissimo organic from tank 96; RC308 = Rossissimo conventional from tank 308; LSC52 = L. Salamino conventional from tank 52; LSC309 = L. Salamino conventional from tank 309; PTO = Pignoletto organic; PTC = Pignoletto conventional; LRC = L. Reggiano conventional; LRO = L. Reggiano organic; LGC = L. Grasparossa conventional; LGO = L. Grasparossa organic; AO = Ancellotta organic; AC = Ancellotta conventional; LSC = L. Salamino conventional; CS = Cabernet Sauvignon; TP = Tempranillo; MT = Merlot; SY = Syrah; GE = Gewürztraminer; AL = Albariño; PTCR = Pignoletto conventional from Castelfranco Emilia; PTOC = Pignoletto organic from Castelfranco Emilia; PTCR = Pignoletto conventional with Righi brand; PTOR = Pignoletto organic with Righi brand; PTB = Pignoletto brut.

2.5 Winemaking processes

All the wines supplied by CRPV were produced by a micro-vinification process according to the Italian law (Mipaaf, 2008). In particular, (the) red wines Veruccese, Rossiola and Festasio were obtained by maceration of grape marc (red winemaking), while Bertinora was made without maceration of grape mark (white winemaking). The red micro-vinification process was carried out through destalking, grape crushing (100 Kg), and adding 6 g q^{-1} of SO_2.

Selected yeasts (20 g hL^{-1}, Zymaflor F15, Laffort Italia S.r.l., Greve in Chianti, Italy) and biological activator VitaDrive®F3 (10 g hL^{-1}, Erbsloh, Geisenheim GmbH, Geisenheim, Germany), composed of inactive yeast, yeast cell walls (14%), diammonium hydrogen phosphate (1%) and thiamine (0.13%) were added to the mass grape must in order to permit the fermentation of must during the maceration. The must racking and the pressing of grape marc were done when the alcohol level was at 9°, before the ending of the fermentation process. Then, the must was decanted, added with SO_2 and bentonite, and stabilized at -4 °C in saturated condition with inert gas, and finally decanted for a final filtration up to 0.65 μm.

For what concern the white micro-vinification process, the same steps were followed, but without the grape marc maceration. During the crushing 6 g q^{-1} of SO_2 were added, while during the fermentation process the fermentation adjuvant were added.

L. Reggiano conventional, L. Reggiano organic, L. Grasparossa conventional, L. Grasparossa organic, Ancellotta organic and Ancellotta conventional were provided from Cantine Riunite & CIV of Campegine. The harvest was both manual and mechanical (95% and 5%, respectively). The red winemaking process consisted of the following main phases:

1. grape crushing and destalking;
2. SO_2 (70-80 mg L^{-1}), in the form of gas or salt and enzymes for color extraction;
3. pre-fermentation maceration (12 to 72 hours), with two slight pumping-overs per day;
4. racking and pomace cap elevation;
5. filtration (flour rotative filter);
6. SO_2;
7. fermentation at 19 °C with selected yeasts;
8. topping;
9. racking;
10. re-fermentation;

11. centrifuge;
12. filtration;
13. blending according to the specification of production;
14. storage.

Concerning the samples of Rossissimo and L. Salamino provided by SMR, the same vinification steps listed above were followed but without the maceration process (white winemaking process).

Pignoletto wines were produced according to the white winemaking process. The phases are the following:

1. grape crushing and destalking;
2. SO_2 (70-80 mg L^{-1}), in the form of gas or salt;
3. draining;
4. pressing;
5. racking;
6. filtration (flour rotative filter);
7. clarification, with fining agents (the quantity variates according to the properties of each lot) and clarification operation to prevent *casse* and other defects;
8. cold settling;
9. fermentation at 18-22 °C with selected yeasts of concentrated musts or rectified concentrated musts;
10. fining operations (racking, re-fermentation, centrifuge, filtration, concentration) to enhance the clarity and the conservation of wine;
11. blending according to the specification of production;
12. storage.

Regarding the Spanish wines, several vinification processes were applied, depending on the variety (https://www.codorniu.com/).

Cabernet Sauvignon single-varietal wine was produced through a cold maceration step in steel tanks after which the fermentation was carried out for 10 days at 25-28 °C. Contemporaneously, lees stirrings were carried out several times. The maceration was kept even in post-fermentation. Finally, after the draining of wine, the pressing and then the malolactic fermentation were applied.

Merlot wine was made through a traditional red winemaking, with a short cold maceration process of a few hours in a steel tank. Then the fermentation was started and once finished, the wine was transferred to perform the malolactic fermentation and finally refined for a few months.

Tempranillo wine was produced by a traditional red winemaking, with a fermentation at 28 °C and a maceration of 2 weeks. Eventually, the wine was aged in American oak barrels for 12 months.

Syrah wine was obtained through a cold maceration at 10 °C for 12-24 hours and a fermentation at 28 °C. Then, after a clarification process the wine was bottled.

Gewürztraminer was harvested in two different periods: during the first one, grapes showed more herbaceous characteristics, while during the second one, grapes showed spicier characteristics. Then grapes were immediately pressed and naturally clarified for 24-48 hours at low temperatures and transferred into a steel tank for fermentation at 16-18 °C.

Albariño grapes were separately harvested at the optimal ripening. Then, the low temperature fermentation was carried out to extract the citrus aroma, while the fermentation on the lees in a separate tank occurred, thus obtaining a product with more “body”. Finally, wines were aged in barrels for 10 months, stabilized, filtered and finally bottled.

2.6 Malvasia wines analyzed by 600 MHz NMR experiment

The dataset was composed of 15 wine samples replicated twice (Table 4).

Wine 01 is produced starting from a grapevine pruned with a Guyot with a density of 4000 plants Ha^{-1}, and a total yield of 70-90 q Ha^{-1}. The grapes are then softly crushed and a cryo-maceration of 24 hours was applied before the first fermentation at 16-18 °C.

The grapes to produce the wine 02 is softly crushed and then directly vinified without maceration. The process consists of a long Charmat winemaking and a refining step into a steel tank. The only agronomic information is that the vineyards are located 200-350 m a.s.l.

The vineyards for the production of wine 03 are located at 250 m a.s.l. and are pruned as Guyot with a density of 1800 plants Ha^{-1}. The harvest is late (about the middle of September) and gives a yield of 55 q Ha^{-1}. Grapes are crushed and macerated for 7-10 days, pressed and finally fermented in acacia barrels for 9 months.

Wine 04 is produced by a soft crushing and a long Charmat winemaking. Also in this case, the only agronomic information is that the vineyards are located 200-250 m a.s.l.

The grapes to produce wine 05 are lately harvested and subsequently vinified with a Charmat method at 18 °C. The final product has a sugar content of 90 g L^{-1}.

Wine 06 is produced from vineyards cultivated with a Guyot pruning giving a yield of 60 q Ha^{-1}. Grapes harvested are then used in the percentage of 80% for the Charmat winemaking, while the remaining 20% is refined for 6 to 9 months in wood barrels.

Wine 07 is produced with a Charmat winemaking at 15 °C for 3 months, with a final sugars content of 90 g L^{-1}. In this case, no agronomic information is available.

The vineyards to produce wine 08 are 53 years old, with 3700 plants Ha^{-1} and late harvested, giving a yield of 100 q Ha^{-1}. Then, grapes are crushed, shortly cryo-macerated and partially fermented.

Wine 09 is produced from vineyards located at 300 m a.s.l., cultivated in a Guyot form with 6000 plants Ha^{-1}. Grapes are selectively harvested at the end of August (or in mid-September). Then the first fermentation occurs for 20 days at 18 °C.

Wine 10 is produced through a short cryo-maceration of a few hours and a fermentation of one month at 12 °C. The vineyards are cultivated in a Guyot form with a late harvest.

The vineyards to produce wine 11 are located at 400 m a.s.l. They are cultivated in a Guyot form with 3300 plants Ha^{-1}. The cultivation and the winemaking are based on the specification of organic production.

Wine 12 is produced from vineyards managed in the same way as wine 09, but they are located at 230-300 m a.s.l. The main winemaking steps are the fermentation at 18 °C for 20 days and the refining for 3 months in the steel tank.

Wine 13 is produced through the pellicular maceration of grapes at 7-8°C for 4 hours and a fermentation in a steel tank. The only agronomic information is that the vineyards are cultivated in a Guyot form.

Wine 14 is produced from differently managed vineyards. The 85% are cultivated in a Guyot form and the 15% are cultivated in the Casarsa form, that is a variation of the Sylvoz pruning. Moreover, the 75% are cultivated with 5,000 plants Ha^{-1}, while the 25% are cultivated with 2200 plants Ha^{-1}. In addition to this, bunches are thinned at a 30 to 45%. All vineyards are late harvested and are located at 180 to 210 m a.s.l. Finally, grapes are softly pressed and fermented at 14-15 °C for 5 months with batonnage. Both winemaking and cultivation follow the specifications of organic production.

Wine 15 is produced from vineyards cultivated at Guyot with a yield of 60 q Ha^{-1} and located at 230-300 m a.s.l. Winemaking consists of a fermentation of 20 days and a refining process of 6 months in a steel tank with batonnage.

ID	Producers	Commercial name	Vintage	Kind of wine	Designation of origin	%Vol.	Variety
01	Perini & Perini	Quattro Valli	n.d.	Sweet spumante	DOC - Colli Piacentini	6.0	MCA
02	Ariola Vigne e Vini	Forte Rigoni	n.d.	Sweet sparkling	IGP Emilia	7.0	Malvasia and MCA
03	Lusenti	Bianca Regina	2014	White still	DOC - Colli Piacentini	13.0	MCA
04	Cantina Valtidone	Venus	2018	Sweet spumante	DOC - Colli Piacentini	7.0	MCA
05	Ca' de' Medici	Rubigalia Gold	n.d.	Sweet aromatic spumante	IGT Malvasia dell'Emilia	6.0	MCA
06	Torre Fornello	Donna Luigia	2016	White still	DOC - Colli Piacentini	13.0	MCA
07	Bonelli	MIMì	2018	Sweet sparkling	DOC - Colli Piacentini	7.0	MCA
08	Azienda Oinoe	Sabitu 14.0	2018	White sparkling	DOC - Colli di Parma	13.0	MCA
09	Monte dell Vigne	Malvasia Selezione	2018	Brut spumante	DOC - Colli di Parma	11.5	MCA
10	Puianello	Le Foglie	n.d.	Dry sparkling	Colli di Scandiano e Canossa DOC	10.5	MCA
11	Vigna Cunial	Monteroma	n.d.	Brut spumante	IGT Malvasia dell'Emilia	12.0	Malvasia
12	Monte delle Vigne	Poem	2016	White still	DOC - Colli di Parma	12.5	MCA
13	Santa Giustina	Malvasia	2017	White still	DOC - Colli Piacentini	12.5	MCA
14	La Tosa	Sorriso di cielo	2018	White still	DOC - Colli Piacentini	13.0	MCA
15	Monte delle Vigne	Callas	n.d.	Dry still	Emilia IGT	13.5	MCA

Table 4. Main description of the wine analyzed by 600 MHz NMR. MCA = Malavasia di Candia Aromatica.

2.7 GC analysis for volatile aromatic compounds

2.7.1 Solid phase extraction (SPE) of free aromatic compounds

Each 25 mL/5 g C18 cartridge (ISOLUTE®, Biotage, Uppsala, Sweden) was washed with 50 mL of dichloromethane, then activated with 50 mL of methanol and finally 100 mL of deionized water.

A quantity of 50 µL of 2-octanol solution (10000 ppm) was added into a 50-mL volumetric flask using a graduated syringe and filled up with wine. The sparkling wines were previously degassed for 10 min (Elma® ultrasonic degasser).

The samples were loaded on the cartridge, and the aromatic fraction was eluted with 20 mL dichloromethane using a vacuum pump and a flow rate of 2 mL min^{-1} Extracted aromatic fractions were collected into a tube and stored at -20°C (for 60 min), to freeze the remaining water that was removed by filtering it off with paper filter (Whatman®, Cytiva, Marlborough, USA), filled with anhydrous sodium sulfate. The solvent was removed using a Kuderna-Danish equipment set at the temperature of 50 °C and finally it was reduced to 500 µL under a stream of pure N_2.

2.7.2 Gas chromatographic method

The extract (1 µL) was manually injected with a 10-µL syringe onto a Hewlett-Packard (HP) 6890 series GC-MS instrument (Hewlett-Packard, Waldbronn, Germany). The instrument was equipped with a Stabilwax®-DA (Crossbond Carbowax Polyetileneglicole, Restek Corporation, Bellefonte, PA, USA) 30-m column (ID0.25 mm, 0.25 µm fd). The carrier gas, He, flowed at a rate 0.9 mL min^{-1}. The oven temperature was set at 45 °C, held for 3 min, and then raised up to 230 °C (4.25 °C min^{-1}), and was maintained for 20 min. Then it was increased to 245 °C at 15 ° C/min and was maintained at this temperature for 10 min (76.5 min of analysis). The injector temperature was 250 °C and the molecular fragmentation was obtained by electron impact ionization (EI). The data were obtained in full scan mode and the mass-to-charge ratio (*m*/*z*) was recorded between 33 and 300 at an ionization voltage of 70 eV with a solvent delay of 3 min. The ion source temperature was set at 230 °C, the quadrupole temperature at 150 °C, and the transfer line at 240 °C. The chromatograms were acquired and processed using Enhanced Chem Station software (G1701AA Version A.03.00, Hewlett Packard©).

2.7.2 Identification of volatile compounds

The identification of aromatic compounds was carried out, according to Montevecchi et al. (2015) and Masino et al. (2008), by the comparison of the retention times and mass spectra with that of the reference pure standards when available, injected under the same conditions as the samples. The other substances were tentatively identified by comparing their spectra with those of the NIST/EPA/NIH Mass Spectral library (2002 version with a minimum of ≥80% correspondence). The unknown compounds were tentatively identified through data system libraries (Wiley 7th Edition Library and NIST-14) and/or literature. When an unacceptable reliable match was found in the libraries, each compound was independently checked, while in the case of coelution, the molecular ion, the base ion, and the fragmentation patterns were collected, and finally reporting the compound as 'unknown'. A semi-quantitation was carried out by considering the average values of the absolute peak areas.

2.8 Preliminary metabolomic analyses

2.8.1 Identification of anthocyanins

For the qualitative analysis of anthocyanins and flavonoids an Agilent 6310A Ion Trap LC-MS was used. The analyses were carried out using an electrospray (ESI) interface operating in positive mode, scanning from 200 *m/z* to 2200 *m/z*, and using the following conditions: drying gas flow, 10 L min^{-1}; nebulizer pressure, 35 psi; gas drying temperature, 350 °C; capillary voltage, 4000 V. All samples (20 μL) have been injected once without dilution while ten dilution was carried out for flavonoids. The elution solvents were HPLC-grade water and formic acid 90% + 10% (solvent A), acetonitrile, water and formic acid 45% + 45% + 10% (solvent B). Linear gradient elution was as follows: from 97% to 70% A in 20 min, from 70% to 46% A in 17 min, then 0 at 42 min, from 0% to 97% A at 52 min. Time run was 65 min. The flow was 0.35 mL min^{-1}. Flow was 0.35 mL min^{-1}. The column was an Agilent Poroshell SB-C18 (100 mm x 3.0 mm, 2.7-Micron) set at 30 °C in a column oven (Agilent 1100/1200 Column Thermostat 1).

2.8.2 Anthocyanins quantitative analysis

The analysis was carried out using an HPLC Jasco model UV-Vis at 520 nm. All samples were diluted 10 times with distilled water, and then injected twice (20 μL). Elution solvents, linear gradient elution, running, flow and column were the same described in chapter 2.8.1.

2.9 Q-Exactive qualitative and quantitative analysis

2.9.1 Anthocyanins

The LC-MS/MS system was a UHPLC Ultimate 3000 (Thermo Fisher Scientific, Waltham, MA) with a Q Exactive™ Hybrid Quadrupole-Orbitrap mass spectrometer with low-mass accuracy (< 3 ppm) and a high mass range (*m*/*z* 350 to 80,000) (Thermo Fisher Scientific, Waltham, MA).

All samples were centrifuged at 13,000 rpm for 5 min and diluted 20 times with a solution of deionized water, acetonitrile and formic acid (95:3:2), in order to avoid any damage to the sensor caused by the most abundant molecules. The temperature of the autosampler was 15 °C. The analyses were carried out using a heated electrospray ionization source (HESI) operating in positive mode, using the following conditions: scan range: 300 *m/z* to 3000 *m/z* in full scan mode; resolving power: 140,000 FWHM (*m*/*z* 200); microscans: 1; AGC 1*E6; maximum IT: 200 ms. Spray parameters were: sheath gas: 40 au; auxiliary gas: 30 au; spray voltage: 3 kV; capillary temperature: 320 °C; S-lens voltage: 25 V; skimmer voltage: 15V; probe heater temperature: 290 °C. The confidence range of the instrument was 3 ppm. Mobile phases were: solution A (water + formic acid, 100:1), solution B (water + acetonitrile + formic acid, 50:50:1). The column was an Agilent Poroshell Bonus (100 mm × 3.0 mm, 2.7 µM) thermostated in an oven at 30 °C. Runtime was 65 min and the gradient started at 10% of B, then at 30% of B at 20 min, then at 54% of B at 37 min, then at 100% of B at 42 min up to 49.9, then at 10% at 50 min up to 65 min. Flow was set at 0.35 mL min^{-1}, kept by a Binary Pump HPG 3400RS. Samples were injected with a well plate autosampler WPS 3000RS with an injection volume of 20 µL.

The quantification results were expressed as mg L^{-1} of malvidin-3-*O*-glucoside (Sigma-Aldrich Corporation, St. Louis, MO), which was used as an external standard. The dilutions of the standard for the calibration curve of each were: 50, 25, 10, 5, 2, 0.5, 0.250, 0.100, 0.050, 0.025, 0.010, 0.005, 0.001 ppm. The equation used for the quantification Y = -21857+8.03693e+007*X, R^2 = 0.9957, and it was obtained with the standard replicated during the two years of analysis. The equation was calculated with the software Xcalibur (Thermo Fischer Scientific, Waltham, MA) using a linear curve index and a weighting index of $1/x^2$. LOD and LOQ were calculated according to Shrivastava and Gupta (2011): LOD = $3S_a/b$, LOQ = $10S_a/b$, in which S_a is the standard deviation of the intensity of the peaks of all dilution analyzed and b is the slope of the equation. Then, results were used to determine the sums of glycosylated, acetyl glycosylated, and coumaroyl glycosylated

anthocyanins, and to calculate the indexes of F3′5′OH Activity, 3′ OMT Activity, 5′ OMT Activity (Mattivi et al., 2006), and the (dp+cy+pt/pn+mv) × 10 ratios (Vasile Simone et al., 2013).

2.9.2 Identification strategy

The identification was done with the software Xcalibur (Thermo Fisher Scientific, Waltham, MA) using the condensed formula of each compound found in the literature (Hornedo-Hortega et al., 2017; Sun et al., 2012; Vallverdú-Queralt et al., 2015; Roman et al., 2019; Willemse et al., 2015; HMDP) to determine theoretical experimental accurate mass and retention time of each compound. Then, fragments and accurate mass of each compound were confirmed.

2.9.3 Identification strategy with the platform XCMS

The whole dataset obtained on both vintages was processed through the XCMS On-line platform by aMultigroup Job mode, which permit the contemporaneous analysis of more than two datasets. Job Parameters were set based on the UPLC-Q-Exactive default parameters of the platform, then modified and adjusted according to Benton et al. (2014) and Tautenhahn et al. (2012). General parameters were set as an analysis in positive mode. Molecules (named features on the platform) detection was set with a maximal tolerated *m*/*z* deviation of 5 ppm, a minimum chromatographic peak width of 10 s, a maximum peak width of 120 s, a minimum difference in *m*/*z* for peaks with overlapping retention times of 0.015 ppm, a prefilter peaks of 10, a prefilter intensity of 100,000, and a noise filter of 10,000. The retention time correction was done with a step size of 1 *m*/*z*. The alignment was done with an overlapping width of 0.015 *m*/*z* and a retention time deviation of 15 s. The identification was performed on the $[M+H]^+$ adducts with a tolerance of 5 ppm.

2.10 Nuclear Magnetic Resonance

2.10.1 ^{1}H-NMR 400 MHz experiment

The dataset was composed of 34 wine samples (20 red and 14 white). The analyses for wine characterization were performed using a ^{1}H-NMR analysis with a 400.1399 MHz Bruker system at a temperature of 300 K with T2 filter. A pre-freezing process at -80 °C and an overnight lyophilization was carried out for 1 mL of each sample (Viggiani et al., 2008). Then, 400 µL of D_2O, 140 µL of buffer solution at pH 4.00 (sodium oxalate), and 60 µL of internal standard, IS (TSP 5mM) were added in the Merck NMR tubes (5 mm class B borosilicate, 203 mm L, 100 MHz) (Papotti et al., 2012). ^{1}H NMR data were acquired using the Bruker spin-echo sequence “cpmgpr

1d" (Carr−Purcell−Meiboom−Gill, Bruker Library), and an 8-fold suppression of the signals of water and ethanol was conducted. The data were acquired manually under the control of ICON-NMR (Bruker Biospin, Rheinstetten, Germany). The complete sequence of commands was as follows: temperature equilibration, LOCK, ATMA, TOPSHIM, TOPSHIM_with_z_corr, PULSECAL, ZGPR, shape calculation using sample specific H_2O, ZGPR and CPMGPR 1D. Setting parameters were: time domain = 64100; dummy scans = 16; number of scans = 256; spectral width = 20.0249 Hz; acquisition time = 3.9 s; FIDRES = 0.2500 Hz; D1 = 4.0 s. Calibration, phase correction, alignment and binning (0.04 ppm) of each spectrum was carried out with the MNova version 10.0 software (Mestrelab Research, Santiago de Compostela, Spain).

2.10.2 NMR 600 MHz experiment

Each wine (30 ml) was pH-adjusted at pH 2 with a solution at 30% (w/w) of sulfuric acid. Then, 550 µL of wine added with TSP as internal standard and 50 µL of D_2O were introduced directly into NMR tubes (Wilmad, 5 mm class A, 178 mm L, 600 MHz). The analyses for wine were carried out with a ^{1}H-NMR analysis with a 600 MHz Bruker system FT-NMR AVANCE III HD 600 MHz coupled with a CryoProbe BBO H&F 5 mm at a temperature of 300 K and non-spinning. ^{1}H NMR data were acquired using the Bruker spin-echo sequence "noesy gpps 1d" (Carr−Purcell−Meiboom−Gill, Bruker Library), and an 8-fold suppression of the signals of water and ethanol was conducted. The data were acquired manually under the control of ICON-NMR (Bruker Biospin, Rheinstetten, Germany). The complete sequence of commands was as follows: temperature equilibration, LOCK, ATMA, TOPSHIM, TOPSHIM_with_z_corr, PULSECAL, ZGPR, shape calculation using sample specific H_2O, ZGCPPR and NOESY GPPS 1D. Setting parameters were: time domain = 65536; dummy scans = 5; number of scans = 32; spectral width = 9009.009 Hz; acquisition time = 3.6 s; fidres = 0.2500 Hz; D1 = 2.0 s. Total acquisition time was 6 min.

The assignments of the compounds were carried out based on the ^{13}C-NMR, ^{1}H–^{13}C heteronuclear multiple-bond correlation (HMBC), and ^{1}H–^{13}C heteronuclear single-quantum coherence (HSQC) experiments. Acquisition parameters of the ^{13}C-NMR were: time domain = 131072; dummy scans = 4; number of scans = 512; spectral width = 37593.984 Hz; acquisition time = 1.74 s; fidres = 0.57 Hz; D1 = 4.0 s. Total acquisition time was 50 min.

Acquisition parameters of the HMBC were: F2 (^{1}H) time domain = 4096; F1 (^{13}C) time domain = 256; dummy scans = 16; number of scans = 16; F2 (^{1}H) spectral width = 6602.113 Hz; F1 (^{13}C) spectral width = 31692.758 Hz; acquisition time = 0.31 s; fidres = 3.22 Hz; D1 = 1.5 s. Total acquisition time was 2 h 45 min.

Acquisition parameters of the HSQC were: F2 (^{1}H) time domain = 2048; F1 (^{13}C) time domain = 256; dummy scans = 16; number of scans = 32; F2 (^{1}H) spectral width = 6602.113 Hz; F1 (^{13}C) spectral width = 31692.758 Hz; acquisition time = 0.15 s; fidres = 6.45 Hz; D1 = 2.0 s. Total acquisition time was 2 h 14 min.

The peak intensities are directly proportional to concentrations of nuclei. Thus, ^{1}H NMR spectra were used as absolute intensity value for each spectral point. Generated spectra were phased and calibrated (accordingly to TSP signals) using TopSpin 4.0.9. Finally, they were analyzed by chemometric methods.

2.11 Statistical analysis

Principal component analysis (PCA) of the autoscaled dataset, the analysis of variance (ANOVA) and Tukey's test were carried out with the Statistica v8.0 (StatSoft Inc., Tulsa, OK, USA). The statistical analysis of the automatic XCMS experiment was performed with a Kruskal-Wallis non-parametric test, a *p-value* threshold for highly significant and significant features of 0.01 and 0.05, respectively. Concerning the NMR analyses, the PCA was carried out by using PLS_Toolbox and MATLAB R2020b academic version.

3 Results and discussion

3.1 GC-MS analysis

The GC-MS analysis permitted the identification of 78 aromatic compounds. The analysis of variance (ANOVA) of each compound is reported in Table 5.

ID	Compound	Festasio		L. del Pellegrino		Albana rosa		L. Salamino conventional		L. Salamino organic		L. Grasparossa conventional		L. Grasparossa organic	
1	ethyl isovalerate	0.03	ab	**0.04**	**a**	**0.04**	**a**	0.00	c	0.01	bc	0.00	c	0.01	bc
2	isobutanol	1.66	ab	1.41	ab	**1.88**	**a**	0.79	ab	0.55	c	0.68	ab	0.73	ab
3	3-methyl-1-butyl acetate	0.39	c	0.39	c	2.01	bc	8.22	a	7.28	a	4.60	ab	4.63	ab
4	1-butanol	**0.62**	**a**	0.32	ab	0.53	ab	0.34	ab	0.43	ab	0.24	c	0.26	c
5	isoamyl alcohols	121.93	n.s.	136.48	n.s.	152.02	n.s.	133.68	n.s.	102.31	n.s.	99.46	n.s.	112.64	n.s.
6	ethyl hexanoate	0.44	c	0.50	c	1.68	b	2.13	b	2.05	b	1.52	b	**2.84**	**a**
7	3-methyl-3-buten-1-ol*	**0.04**	**a**	0.03	b	0.02	b	0.00	c	0.00	c	0.01	b	0.02	b
8	hexyl acetate	0.00	c	0.00	c	0.04	c	**0.58**	**a**	**0.77**	**a**	0.27	b	0.29	b
9	ethyl ethoxyacetate	0.00	b	0.00	b	0.00	b	0.00	b	0.00	b	0.02	a	0.02	a
10	acetoin	**5.11**	**a**	0.38	b	0.12	b	0.64	b	0.52	b	0.61	b	1.34	b
11	(Z)-3-hexen-1-yl acetate	0.00	c	0.00	c	0.00	c	0.03	b	**0.06**	**a**	0.01	c	0.02	bc
12	4-methyl-1-pentanol*	0.09	cd	0.11	c	**0.18**	**a**	0.08	de	0.06	e	0.09	cd	0.15	b
13	(Z)-2-penten-1-ol*	**0.07**	**a**	0.00	d	0.00	d	0.02	b	0.00	d	0.01	c	0.02	b
14	3-methyl-1-pentanol*	0.11	d	0.25	b	**0.38**	**a**	0.17	c	0.14	cd	0.17	c	0.28	b
15	ethyl lactate	**49.35**	**a**	13.81	b	11.29	b	2.49	b	2.46	b	6.29	b	6.46	b
16	1-hexanol	**5.11**	**a**	1.67	d	2.59	c	3.70	b	3.51	b	2.53	c	2.84	c
17	(E)-3-hexen-1-ol	0.06	ab	0.02	c	0.05	b	0.07	a	0.06	ab	**0.07**	**a**	0.05	b
18	3-ethoxy-1-propanol	0.42	b	0.25	bc	0.03	d	1.12	a	**1.14**	**a**	0.15	cd	0.32	bc
19	Z-3-hexenol	0.05	e	0.06	e	0.06	e	0.27	b	**0.35**	**a**	0.10	d	0.19	c
20	(E)-2-hexen-1-ol	0.05	n.s.	0.00	n.s.	0.17	n.s.	0.00	n.s.	0.32	n.s.	0.01	n.s.	0.02	n.s.
21	ethyl octanoate	0.46	e	0.82	e	3.12	d	4.23	bc	4.58	ab	3.41	cd	**5.13**	**a**
22	1-octen-3-ol	**0.14**	**a**	0.00	c	0.09	b	0.00	c	0.00	c	0.00	c	0.00	c
23	acetic acid	**9.25**	**a**	1.35	c	6.12	ab	3.32	bc	3.39	bc	2.42	bc	2.81	bc
24	ethyl 3-hydroxybutanoate	0.05	b	0.07	b	**0.16**	**a**	0.06	b	0.05	b	0.06	b	0.06	b
25	2-methyltetrahydrothiophen-3-one*	0.15	c	0.20	b	0.05	e	0.11	d	0.05	e	0.12	cd	**0.31**	**a**
26	benzaldehyde	0.00	b	0.00	b	0.01	b	0.06	a	0.01	b	0.04	a	0.00	b
27	unknown	0.28	ab	0.27	ab	**0.29**	**a**	0.03	e	0.03	e	0.07	c	0.05	d
28	2,3-butanediol	**25.01**	**a**	13.96	ab	11.70	ab	5.55	b	13.66	ab	4.49	b	8.38	ab
29	linalool	**0.25**	**a**	0.14	ab	0.12	b	0.06	b	0.05	b	0.04	b	0.08	b
30	linalyl acetate	0.00	d	0.01	b	**0.02**	**a**	0.00	d	0.00	d	0.01	c	0.01	c
31	2-methylpropanoic acid	0.41	ab	0.41	ab	**0.54**	**a**	0.16	d	0.19	d	0.36	b	0.49	ab
32	isoamyl lactate	**0.41**	**a**	0.09	b	0.00	d	0.00	d	0.00	d	0.04	c	0.00	d
33	ethyl decanoate	0.11	c	0.19	bc	0.86	b	**1.98**	**a**	**2.43**	**a**	2.21	a	2.34	a
34	γ-butyrolactone	**0.91**	**a**	**0.69**	**a**	0.37	b	0.13	b	0.10	b	0.13	b	0.14	b
35	3-methyl-butanoic acid	**2.14**	**a**	**2.12**	**a**	1.77	b	1.30	c	1.21	c	1.67	b	**2.18**	**a**
36	diethyl succinate	14.39	b	**31.68**	**a**	**33.96**	**a**	0.64	d	0.64	d	7.39	c	8.08	c
37	3-(methylthio)-1-propanol	**1.85**	**a**	**1.89**	**a**	0.63	b	0.38	b	0.26	b	0.90	b	0.52	b

38	unknown	0.14	c	0.14	c	0.07	c	**0.51**	**a**	0.42	ab	0.33	b	0.41	ab
39	geranyl acetate	0.05	n.s.	0.04	n.s.	0.04	n.s.	0.02	n.s.	0.02	n.s.	0.03	n.s.	0.03	n.s.
40	citronellol	**0.02**	**a**	0.01	b	0.01	b	0.00	c	0.00	c	0.01	b	0.00	c
41	ethyl 4-hydroxybutanoate	**2.13**	**a**	0.96	b	0.74	b	**2.18**	**a**	**2.18**	**a**	1.58	ab	**2.25**	**a**
42	phenethyl acetate	0.21	c	0.55	c	0.83	c	**5.47**	**a**	4.89	ab	4.77	ab	3.83	b
43	ethyl laurate	0.00	c	0.00	c	0.02	c	0.08	b	0.14	b	**0.28**	**a**	**0.16**	**a**
44	hexanoic acid	4.37	d	4.09	d	9.30	c	17.04	ab	**20.21**	**a**	13.47	b	**20.56**	**a**
45	benzyl alcohol	0.36	c	0.05	e	0.08	de	0.10	d	0.13	d	**0.63**	**a**	0.47	b
46	N-(3-methylbutyl)acetamide	**1.40**	**a**	0.05	bc	0.19	c	1.27	a	0.22	bc	0.45	b	0.07	bc
47	phenethyl alcohol	148.14	n.s.	194.43	n.s.	123.68	n.s.	147.79	n.s.	114.06	n.s.	156.73	n.s.	151.48	n.s.
48	(Z)-2-hexenoic acid	0.18	b	0.02	c	0.05	c	0.17	b	**0.27**	**a**	0.04	c	0.03	c
49	γ-nonalactone*	**0.24**	**a**	0.00	c	0.00	c	0.00	c	0.00	c	0.05	b	0.06	b
50	diethyl malate	2.05	c	**12.66**	**a**	5.39	b	0.76	c	1.05	c	0.55	c	0.83	c
51	octanoic acid	2.30	b	3.31	b	9.00	bc	22.59	a	27.39	a	17.68	ab	26.80	a
52	unknown lactone	**4.93**	**a**	**6.16**	**a**	**4.71**	**a**	0.26	b	0.25	b	0.50	b	0.30	b
53	ethyl acetamidoacetate	**0.20**	**a**	0.16	ab	0.12	bc	0.05	cd	0.04	d	0.12	bc	0.09	bcd
54	2- or 3-ehtylphenol*	0.01	cd	0.00	d	0.00	d	0.00	d	0.02	b	**0.05**	**a**	0.01	bc
55	2-methoxy-4-vinylphenol*	0.23	n.s.	0.02	n.s.	0.17	n.s.	0.03	n.s.	0.06	n.s.	0.05	n.s.	0.05	n.s.
56	ethyl palmitate	0.00	c	0.04	c	0.04	c	0.00	c	0.04	c	**0.60**	**a**	0.24	b
57	unknown lactone	1.01	bc	1.99	a	1.87	ab	0.46	c	0.38	c	0.81	c	0.56	c
58	decanoic acid	0.34	b	0.49	b	1.99	b	7.18	a	9.56	a	6.69	a	8.80	a
59	ethyl 2-hydroxy-3-phenylpropanoate	**0.95**	**a**	**1.08**	**a**	**1.02**	**a**	0.46	b	0.32	b	0.35	b	0.15	b
60	unknown	0.00	c	**0.91**	**a**	0.36	bc	0.00	c	0.00	c	0.53	ab	0.75	ab
61	geranic acid	0.07	ab	0.01	bc	0.00	c	0.03	bc	0.07	ab	**0.12**	**a**	0.03	bc
62	2(4H)-benzofuranone	0.00	e	0.00	e	0.00	e	0.01	d	0.01	c	0.01	b	**0.02**	**a**
63	monoethyl succinate	0.15	d	80.85	b	48.69	c	8.94	d	9.71	d	76.42	b	**94.90**	**a**
64	4-vinylphenol	**1.34**	**a**	0.00	c	0.20	ab	0.12	ab	0.33	ab	0.16	ab	0.23	ab
65	benzoic acid	0.13	ab	0.05	d	0.05	cd	0.08	cd	0.10	bc	0.14	ab	**0.17**	**a**
66	unknown	**0.23**	**a**	0.00	c	0.02	bc	**0.18**	**a**	0.06	bc	0.07	b	0.02	bc
67	dodecanoic acid	0.00	n.s.	0.00	n.s.	0.46	n.s.	0.19	n.s.	0.37	n.s.	0.27	n.s.	0.31	n.s.
68	benzeneacetic acid*	**1.04**	**a**	0.33	b	0.14	b	0.34	b	0.37	b	0.36	b	0.30	b
69	N-(2-phenylethyl)-acetamide	**0.40**	**a**	0.04	c	**0.42**	**a**	0.14	bc	0.08	c	0.29	ab	**0.42**	**a**
70	unknown	**1.25**	**a**	**1.43**	**a**	**0.94**	**a**	0.09	b	0.10	b	**0.94**	**a**	**1.32**	**a**
71	4-hydroxy-3-methoxy benzoate	**1.01**	**a**	0.25	b	0.05	c	0.08	c	0.11	bc	0.16	bc	0.10	bc
72	3-oxo-α-ionol*	0.11	ab	0.15	ab	0.02	b	0.07	ab	0.08	ab	0.18	ab	**0.20**	**a**
73	1-(4-hydroxy-3-methoxyphenyl)ethanone*	0.41	abc	0.18	d	0.19	d	0.23	cd	0.29	bcd	**0.53**	**a**	0.48	ab
74	n-hexadecanoic acid	0.27	n.s.	0.19	n.s.	0.15	n.s.	0.26	n.s.	0.39	n.s.	0.44	n.s.	0.63	n.s.
75	N-acetyltyramine	0.00	b	0.00	b	0.00	b	**0.36**	**a**	**0.52**	**a**	**0.60**	**a**	**0.67**	**a**
76	4-hydroxyphenylethanol	13.82	n.s.	15.92	n.s.	14.51	n.s.	12.08	n.s.	13.78	n.s.	19.95	n.s.	24.07	n.s.
77	1H-indole-3-ethanol*	19.69	n.s.	19.55	n.s.	2.34	n.s.	17.14	n.s.	17.10	n.s.	21.63	n.s.	15.65	n.s.
78	ethyl p-hydroxycinnamate	**5.18**	**a**	0.79	b	0.40	b	0.00	b	1.01	b	0.22	b	0.30	b

Table 5. Results of the one-way analysis of variance (ANOVA) expressed in mg L^{-1}. Letters indicate the significance for $p<0.05$. ID numbers are referred to retention times. * Substances identified by GC-MS library only.

To the authors' knowledge, this is the first time that the profile of free aromatic compounds of Festasio, L. di Fiorano and Albana rosa is reported.

Among the analyzed molecules, only the isoamyl alcohols (5), geranyl acetate (39), (E)-2-hexen-1-ol (20), phenethyl alcohol (47), 4-hydroxyphenylethanol (75), 1H-indole-3-ethanol (76), and n-hexadecanoic acid (73) showed no significant differences among the different kinds of wines. However, isoamyl alcohols (5), which typically are the most representative alcohols, as well as geranyl acetate (70) (note of rose), showed interesting values in minor wines, even higher than L. Salamino and Grasparossa ones (Gómez-Plaza et al., 1999; Rapp and Mandery, 1986).

Esters & Lactones. Festasio showed the highest values for molecules ethyl lactate (15), isoamyl lactate (32), γ-butyrolactone (34), diethyl succinate (36), ethyl 4-hydroxybutanoate (41), γ-nonalactone (49), ethyl 2-hydroxy-3-phenylpropanoate (59), ethyl 4-hydroxy-3-methoxy benzoate (70), ethyl *p*-hydroxycinnamate (77). L. di Fiorano (L. del Pellegrino) showed the highest values for ethyl isovalerate (1), γ-butyrolactone (34), diethyl malate (50), and ethyl 2-hydroxy-3-phenylpropanoate (59), while the diethyl succinate (36) is similar to that found in Albana rosa and γ-butyrolactone (34) content is similar to Festasio. Albana rosa showed the highest values only for ethyl 3-hydroxy butanoate (24), while ethyl 2-hydroxy-3-phenylpropanoate (59) content is similar to found in Festasio and L. di Fiorano.

All L. wines showed the highest value for ethyl decanoate (33) except for L. di Fiorano, as well as for ethyl 4-hydroxybutanoate (41) except for Festasio wine that showed a value for this compound similar to that of Lambruschi. Finally, L. Grasparossa conventional showed the highest values for ethyl laurate (43) and ethyl palmitate (56), while L. Grasparossa organic showed the highest values for ethyl hexanoate (6) octanoate (21), and monoethyl succinate (62). However, both L. Grasparossa wines showed the presence of ethyl ethoxyacetate (9) when compared with others.

Acetates. These compounds were mainly representative of L. Salamino wines with 3-methyl-1-butyl acetate (3) that was the most concentrated substance, while phenethyl acetate (42) is the compound most abundant in all Lambruschi.

Ketones and aldehydes. L. Grasparossa organic showed the highest value for 2(4H)-benzofuranone (62) that was not detected in minor wines, and for 2-methyltetrahydrothiophen-3-one (25). L. Grasparossa conventional showed the highest value for 1-(4-hydroxy-3-methoxyphenyl)ethanone (72). Festasio showed the highest value for acetoin (10).

The only aldehyde detected was benzaldehyde (26), which was distinctive for both L. Salamino and L. Grasparossa conventional wines.

Alcohols. They were the main class of compounds, represented by 24 different molecules. In particular, Festasio showed the highest values for molecules 1-butanol (4), 3-methyl-3-buten-1-ol (7), (Z)-2-penten-1-ol (13), 1-hexanol (16), 1-octen-3-ol (22), 2,3-butanediol (28), 3-(methylthio)-1-propanol (37), and 4-vinylphenol (63). L. di Fiorano showed a similar value for molecule 3-(methylthio)-1-propanol (37) as for Festasio. This last compound, that gives an aroma of burnt garlic or cooked cabbage, significantly exceeded its perception threshold (0.5-1 mg L^{-1}). Albana rosa showed the highest values for molecules isobutanol (2) but are not significantly different from that found in Festasio and L. di Fiorano. On the contrary, 4-methyl-1-pentanol (12), and 3-methyl-1-pentanol (14) were most representative. L. Salamino conventional and organic showed the highest values for molecules (E)-3-hexen-1-ol (17), 3-ethoxy-1-propanol (18), while only L. Salamino showed the highest value of Z-3-hexenol (19). L. Grasparossa conventional showed the highest values for molecules benzyl alcohol (45), and ehtylphenol (47), among the Lambrusco wines. Alcohols with six carbons are important because of their herbaceous aroma. Moreover, they are considered pre-fermentative compounds, even if they are probably involved in yeasts metabolism (Masino et al., 2008).

Terpenes. This class is a set of very fragrant compounds present in the skins and characterize the wines obtained from aromatic cultivars (Montevecchi et al., 2015) giving flowers or fruit notes (i.e. rose, geranium, lemon, orange). Festasio showed the highest values for molecules linalool (29)**,** citronellol (40), while Grasparossa organic showed the highest value only for molecule 3-oxo-α-ionol (71) while Grasparossa conventional showed showed the highest value for molecule as geranic acid (61). 3-oxo-α-ionol typically gives tobacco notes, but its perception threshold is higher than its concentration (R).

Acids. Festasio showed the highest values for molecules as acetic acid (23) but is below the total acidity limit and benzeneacetic acid (67), while 3-methyl-butanoic acid (35) is most abundant both Festasio and L. di Fiorano Albana rosa showed the highest value only for molecule 2-methylpropanoic acid (31), however without showing significant differences with some Lambruschi and Festasio All Lambrusco wines showed the highest values for decanoic acid (58). Both L. Salamino wines and L. Grasparossa organic showed the highest values for molecule 51. Both organic wines showed the highest value for molecules as hexanoic acid (44), octanoic acid (51), and decanoic acid (58), probably because of the minor concentration of SO_2 used during the fermentation process (Riberéu-Gayon et al., 2018a; Reg. CE 203/12). Then, L. Salamino organic showed the highest value for molecule (Z)-2-hexenoic acid (48), 3-methyl-butanoic acid (35) and benzoic acid (64). The total concentration of molecules hexanoic acid (44), octanoic acid (51) and decanoic acid (58) give pleasant aroma, up to a certain threshold (4 to 10 mg L^{-1}), as for Festasio

and L. di Fiorano, while above the threshold of 20 mg L^{-1}, as for all Lambrusco type wines, they give unpleasant aroma (Shinohara, 1985). Since the fermentation temperature was lower than 25 °C, the biosynthesis of long-chain fatty acid was very scarce, while the concentration of medium-chain and short-chain fatty acids was significantly higher (Molina et al., 2007; Beltran et al., 2008).

Ammides & Ammines. These compounds were represented by only 4 compounds. Molecule N-(3-methylbutyl)acetamid (46) distinguished L. Salamino conventional and Festasio, while molecule N-(2 - phenylethyl)-acetamide (68) distinguished Festasio, Albana rosa and L. Grasparossa organic. Finally, Festasio showed the highest values for ethyl acetamidoacetate (53), N-Acetyltyramine (74) was the only molecule detected that was quantified only in Lambrusco wines.

In order to gain a better comprehension of the whole variability of the results, PCA was applied to the whole aroma data set. The first two PCs (Figure 18) explained 62.79% of the total variance of the data set, while PC3 added a further 15.57% (78.36%). PC1 (41.44%) mainly expresses the effect of fermentation as many substances come from yeast metabolism (i.e. most ethyl esters, some alcohols, fatty acids, lactones, etc.). However, some varietal compounds (i.e. terpenic compounds) complete the weight of this PC that, as a matter of fact, include the most important contribution to variability (Figure 18 and Table 6).

PC2 (21.35%) is mainly characterized by compounds of different origin (Figure 20 and Table 6)**:** acetoin (10), 3-methyl-1-pentanol (14), 1-hexanol (16), linalyl acetate (30), (Z)-2-hexenoic acid (48), γ-nonalactone (49), monoethyl succinate (62), benzeneacetic acid (67)**,** 4-hydroxy-3-methoxybenzoic acid (70).

Benzyl alcohol (45), ethyl palmitate (56), benzoic acid (64), 4-hydroxy-3-methoxybenzoic acid (70), 3-oxo-α-ionol (71), and 4-hydroxyphenylethanol (75) are the compounds that mainly characterized the PC3 (15.57%).

The first two PCs show 3 well-separated clusters (Figure 19). FE in the lower left corner, while PE and AR are well separated on PC2. The first wine is strongly influenced by a higher value of C6 compounds, γ-nonalactone (49), ethyl p-hydroxycinnamate (77), and some minor acids, while the second ones by a higher value of 3-methyl-1-pentanol (14), and linalyl acetate (30). All the other wines are grouped on the extreme right with a slight separation of the organic samples (LGO and LSO) from the relative conventional wines (LGC and LSC). In other words, the cultivar prevails on the technology. The important variables affecting these wines are mainly acetates, and esters with positive sign (e.g. 3-methyl-1-butyl acetate (3), ethyl hexanoate (6), ethyl octanoate, (21)) with the

addition of octanoic and decanoic acids (86 and 95), and alcohols with negative sign (e.g. isobutanol (2).

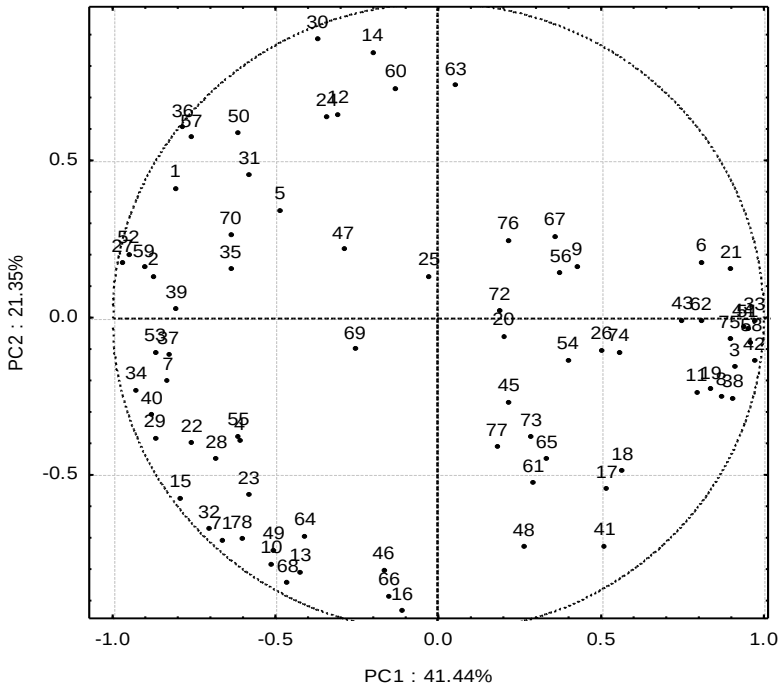

Figure 18. Loadings (see table 5) plot of PC1×PC2 of aromatic compounds (for details see 2.2).

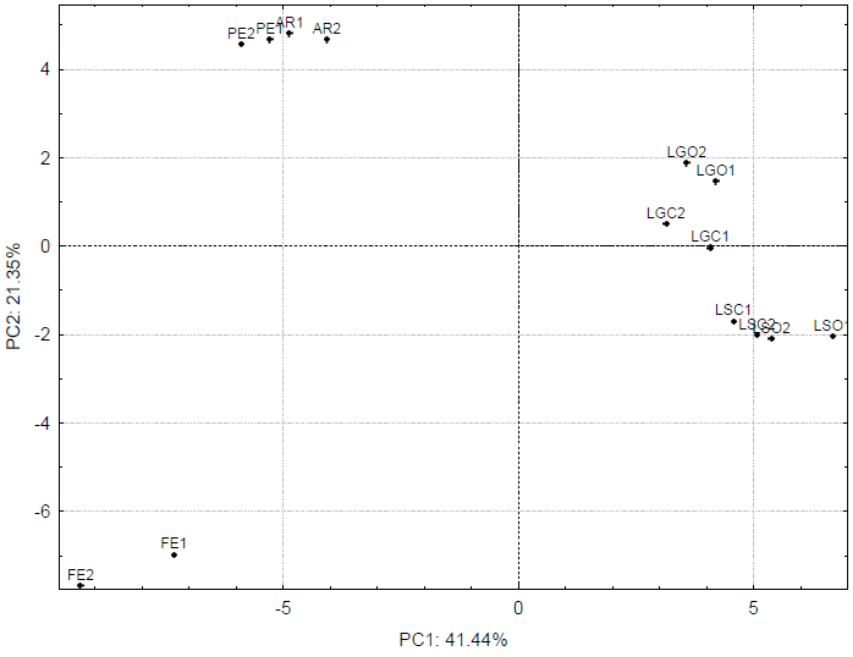

Figure 19. Score plot of PC1×PC2 of the volatiles of some commercial products (for details see 2.2). FE = Festasio; PE = L. di Fiorano or Pellegrino; AR = Albana rosa; LSC = L. Salamino conventional; LSO = L. Salamino organic; LGC = L. Grasparossa conventional; LGO = L. Grasparossa organic.

n.	variable	PC1	PC2	PC3	n.	variable	PC1	PC2	PC3
1	**ethyl isovalerate**	**-0.808**	0.413	-0.159	**40**	**citronellol**	**-0.879**	-0.309	0.208
2	**isobutanol**	**-0.875**	0.133	-0.187	41	ethyl 4-hydroxybutanoate	0.511	-0.727	0.175
3	**3-methyl-1-butyl acetate**	**0.910**	-0.155	-0.284	**42**	**phenethyl acetate**	**0.970**	-0.136	-0.008
4	1-butanol	-0.610	-0.391	-0.423	43	ethyl laurate	0.750	-0.008	0.519
5	isoamyl alcohols	-0.487	0.342	-0.447	44	hexanoic acid	0.936	-0.030	0.014
6	**ethyl hexanoate**	**0.808**	0.176	0.036	**45**	**benzyl alcohol**	0.216	-0.267	**0.871**
7	**3-methyl-3-buten-1-ol**	**-0.831**	-0.200	0.470	46	N-(3-methylbutyl)acetamide	-0.169	-0.803	-0.162
8	**hexyl acetate**	**0.869**	-0.249	-0.370	47	phenethyl alcohol	-0.292	0.217	0.332
9	unknown	0.426	0.164	0.844	48	**(Z)-2-hexenoic acid**	0.263	**-0.729**	-0.552
10	**acetoin**	-0.512	**-0.781**	0.264	49	**γ-nonalactone**	-0.505	**-0.737**	0.417
11	**(Z)-3-hexen-1-yl acetate**	**0.794**	-0.236	-0.438	50	diethyl malate	-0.613	0.587	-0.154
12	4-methyl-1-pentanol,	-0.308	0.648	0.186	**51**	**octanoic acid**	**0.950**	-0.033	0.026
13	(Z)-2-penten-1-ol	-0.423	-0.808	0.247	**52**	**unknown lactone**	**-0.951**	0.203	-0.109
14	**3-methyl-1-pentanol**	-0.202	**0.844**	-0.011	**53**	**ethyl acetamidoacetate**	**-0.869**	-0.109	0.413
15	**ethyl lactate**	**-0.792**	-0.572	0.167	54	2- or 3-ethylphenol	0.398	-0.134	0.531
16	1-hexanol	-0.111	**-0.932**	-0.145	55	2-methoxy-4-vinylphenol	-0.613	-0.377	-0.039
17	E-3-hexen-1-ol	0.517	-0.545	-0.050	56	**ethyl palmitate**	0.376	0.143	**0.722**
18	3-ethoxypropanol	0.566	-0.486	-0.560	**57**	**unknown lactone**	**-0.758**	0.573	-0.071
19	**Z-3-hexenol**	**0.837**	-0.228	-0.373	**58**	**decanoic acid**	**0.962**	-0.078	0.089
20	(E)-2-hexen-1-ol	0.201	-0.059	-0.469	59	ethyl 2-hydroxy-3-phenylpropanoate	-0.904	0.160	-0.289
21	**ethyl octanoate**	**0.900**	0.156	-0.015	60	unknown	-0.130	0.730	0.580
22	**1-octen-3-ol**	**-0.757**	-0.397	-0.069	61	geranic acid	0.293	-0.525	0.380
23	acetic acid	-0.582	-0.565	-0.131	**62**	**2(4H)-benzofuranone**	**0.806**	-0.010	0.435
24	ethyl 3-hydroxybutanoate	-0.342	0.640	-0.291	**63**	**monoethyl succinate**	0.054	**0.738**	0.650
25	2-methyltetrahydrothiophen-3-one	-0.028	0.133	0.703	64	4-vinylphenol	-0.409	-0.694	0.104
26	benzaldehyde	0.501	-0.102	-0.169	65	**benzoic acid**	0.334	-0.448	**0.776**
27	**unknown**	**-0.970**	0.176	-0.081	**66**	**unknown**	-0.151	**-0.886**	-0.124
28	2,3-butanediol	-0.682	-0.449	-0.100	67	dodecanoic acid	0.358	0.261	-0.087
29	linalool	**-0.870**	-0.381	0.076	**68**	**benzeneacetic aci**d	-0.463	**-0.844**	0.205

30	**linalyl acetate**	-0.371	**0.887**	0.137	69	N-(2-phenylethyl)-acetamide	-0.256	-0.101	0.494
31	2-methylpropanoic acid	-0.580	0.454	0.456	70	unknown	-0.638	0.264	0.679
32	**isoamyl lactate**	**-0.703**	-0.672	0.196	**71**	**4-hydroxy-3-methoxybenzoic acid**	-0.665	**-0.708**	0.205
33	**ethyl decanoate**	**0.971**	-0.010	0.131	**72**	**3-oxo-α-ionol**	0.188	0.021	**0.837**
34	γ-butyrolactone	-0.928	-0.229	0.029	73	1-(4-hydroxyOH-3-methoxyphenyl)ethanone	0.285	-0.378	0.845
35	3-methyl-butanoic acid	-0.638	0.154	0.523	74	n-hexadecanoic acid	0.554	-0.108	0.659
36	**diethyl succinate**	**-0.784**	0.605	-0.049	**75**	**N-acetyltyramine**	**0.894**	-0.068	0.420
37	**3-(methylthio)-1-propanol**	**-0.830**	-0.117	0.268	**76**	**4-hydroxyphenylethanol**	0.214	0.248	**0.799**
38	**unknown**	**0.905**	-0.256	0.005	77	1H-indole-3-ethanol	0.180	-0.412	0.417
39	**geranyl acetate**	**-0.804**	0.028	-0.004	**78**	**ethyl p-hydroxycinnamate**	-0.604	**-0.704**	0.100

Table 6. Loadings of the first three PCs related to aroma. In boldface values higher than |0.700|.

Despite the poor contribution of PC3 on explained variability (Figure 20 and 21), it is worth mentioning the fact that this PC can separate the two cultivars of Lambrusco wines from each other. On the contrary, no separation is shown between organic and conventional wines.

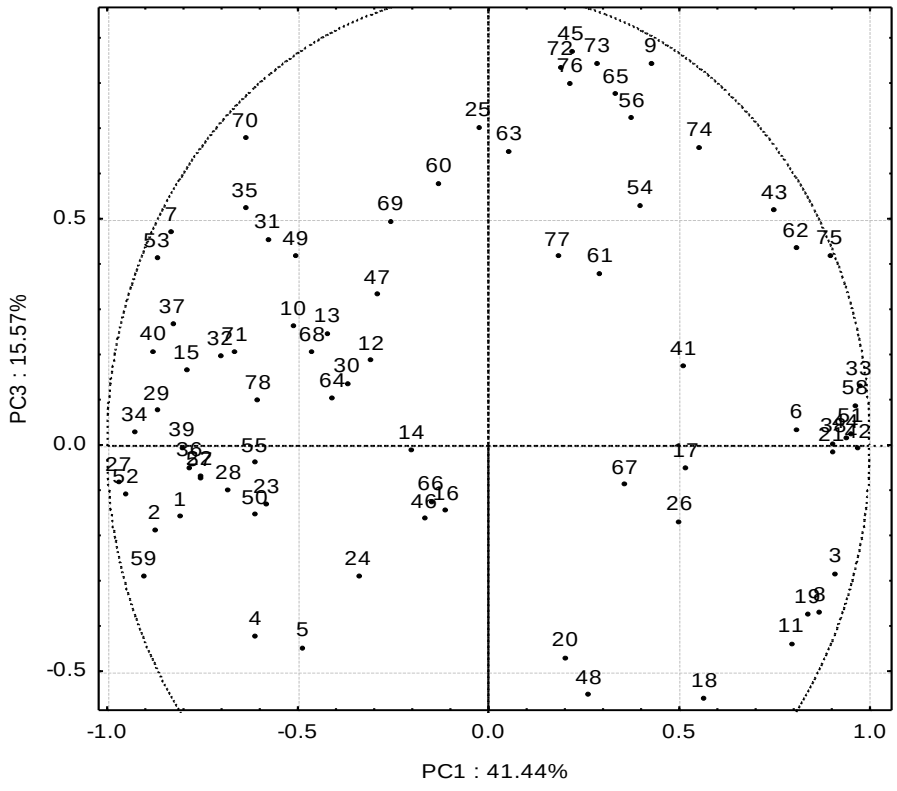

Figure 20. Loading plot of PC1×PC3of the aromatic compounds.

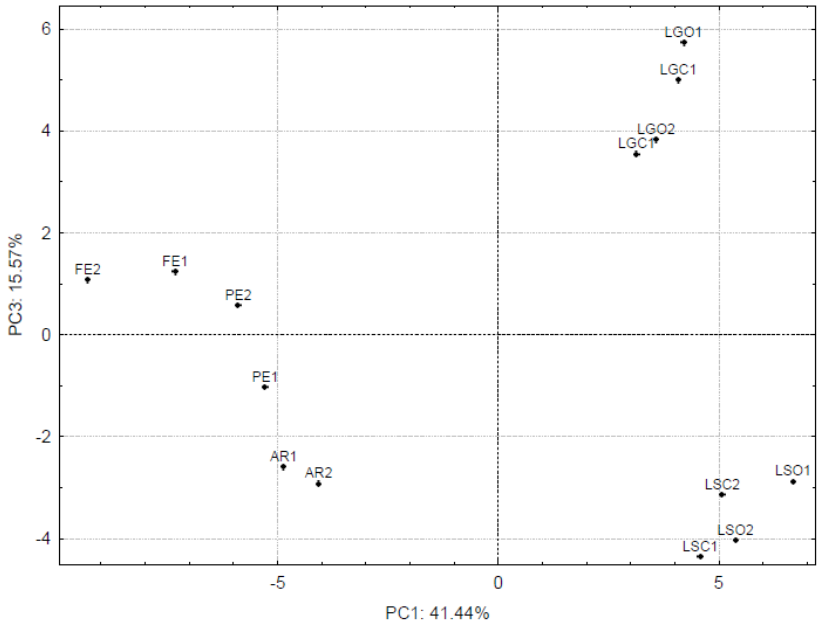

Figure 21. Score plot of PC1×PC3 of the aromatic compounds. FE = Festasio; PE = L. di Fiorano or Pellegrino; AR = Albana rosa; LSC = L. Salamino conventional; LSO = L. Salamino organic; LGC = L. Grasparossa conventional; LGO = L. Grasparossa organic.

In conclusion, the different agronomic treatments and the different concentration of SO_2 slightly affected the biosynthesis pathways of both varietal compounds (terpenes and norisoprenoids), pre-fermentative compounds (C6 aldehydes and alcohols), fermentative compounds (ethanol, other higher alcohols, short-chain fatty acids and their esters, lactones, terpenes, aldehydes and ketones). Also post-fermentative compounds (esters and acetals; Riberéu-Gayon et al., 2018a) seemed scarcely affected by organic treatments. In addition to this, the synthesis of aromatic compounds also depends on the agronomic practices, such as topping, irrigation and fertilization, and it is also affected by the environmental conditions, such as the slope of the soil, the exposition of the vineyard, the presence of biotic and abiotic stresses (Riberéu-Gayon et al., 2018a). Thus, further studies are needed to assess the variation of aromatic compounds in different environmental conditions and agronomic management.

3.2 Preliminary metabolomic analysis

3.2.1 Anthocyanins identification with ESI-LC-MS-IT

In Table 7, the anthocyanins tentatively identified through the LC-MS-IT analyses are reported.

ID	Compound	tR	Parent ion	Product ion
1	Delphinidin-3-*O*-glucoside	10.8	465.2	303.1
2	Cyanidin-3-*O*-glucoside	13.3	449.1	287.1
3	Petunidin-3-*O*-glucoside	15.4	479.2	317.1
4	Malvidin-3-*O*-glucoside-di(epi)catechin (F-A type)	15.5	1069.3	619.2
5	Peonidin-3-*O*-glucoside	17.8	463.2	301.1
6	Malvidin-3-*O*-glucoside	19.4	493.2	331.1
7	Delphinidin-3-*O*-(6"-acetyl-glucoside)	20.8	507.2	303.1
8	Vitisin A	21.9	561.1	399.1
9	Malvidin-ethyl-di(epi)catechin	22.6	1097.4	357.1
10	Malvidin-3-*O*-(6"-acetylglucoside)	23.1	535.2	331.1
11	Cyanidin 3-*O*-(6"-acetylglucoside)	23.5	491.1	287.1
12	A-type vitisin of Malvidin-3-*O*-(6"-acetylglucoside)	23.6	603.2	399.2
13	Vitisin B	23.7	517.2	355.1
14	Petunidin-3-(6"-acetylglucoside)	25.3	521.2	317.1
15	Acetylvitisin B	25.6	559.2	355.1
16	*trans*-Delphinidin-3-*O*-(6-*p*-coumaroylglucoside)	27.3	611.2	303.1
17	Peonidin-3-*O*-(6"-acetylglucoside)	28.2	505.2	301.1
18	Malvidin-3-*O*-(6-*p*-coumaroylglucoside)	28.7	639.3	331.1
19	Malvidin-3-*O*-(6"-acetyl-glucoside)	29.4	535.2	331.1
20	Cyanidin-3-*O*-(6-*p*-coumaroylglucoside)	30.0	595.2	287.1
21	*trans*-Malvidin-3-*O*-(6"-caffeoylglucoside)	30.6	655.2	331.1
22	Malvidin-3-*O*-(6"-caffeoylgalactoside)	31.2	663.2	355.1
23	Coumaroylvitisin A	31.3	625.3	317.1
24	*trans*-Petunidin-3-*O*-(6-*p*-coumaroylglucoside)	31.6	625.2	317.1
25	Malvidin-3-*O*-glucoside-di(epi)catechin (A-F type)	31.9	1071.2	357.1
26	*trans*-Peonidin-3-*O*-(6-*p*-coumaroylglucoside)	34.2	609.2	301.1
27	*trans*-Malvidin-3-*O*-(6-*p*-coumaroylglucoside)	35.1	639.3	331.1

Table 7. Anthocyanins compounds identified.

All the parent ions were reported and confirmed according to the literature (Chinnici et al., 2009; He et al., 2012; Papouskova et al., 2011; Willemse et al., 2015). As expected, monoglucosides, acetyl- and *p*-coumaroyl-derivatives of the main molecules were easily detected (Alcalde-Eon et al., 2006; Chinnici et al., 2009). As for high molecular weight molecules, such as the compounds 4, 9 and 25, parent ions were not present in the literature (Willemse et al., 2015). This can be due to the complexity of the anthocyanins, their low concentration in wines and the presence of different types of hardly recognizable stereoisomers (Andersen and Markham, 2006; Ribéreau-Gayon, 2018a).

3.2.2 Anthocyanins quantification with HPLC

One-way ANOVA of the quantification results of the anthocyanins is reported in Table 8.

Compound	1	2	3	4	5	6	7
Delphinidin-3-O-glucoside	7.09d	7.36d	2.64e	23.14a	16.57b	**20.95a**	12.29c
Cyanidin-3-O-glucoside	**3.87a**	**4.08a**	2.64c	2.94bc	3.26b	3.27b	2.89bc
Petunidin-3-O-glucoside	8.77d	8.98d	2.65e	**29.78a**	21.69b	23.43b	14.36c
Peonidin-3-O-glucoside	0.00e	4.98cd	2.63d	6.56c	5.38c	20.68a	11.36b
Malvidin-3-O-glucoside	50.86c	25.24cd	2.72d	**134.15a**	98.33b	**148.65a**	92.49b
Delphinidin-3-O-(6"-acetylglucoside)	**15.33a**	**15.84a**	2.64c	8.80b	6.52b	9.29b	6.68b
Delphinidin-3-O-(6"-acetylgalactoside)	**21.58a**	4.89b	2.65c	3.97bc	3.55bc	3.84bc	4.18bc
Cyanidin--3-O-(6"-acetyl-glucoside)	0.00b	**5.85a**	0.00b	4.35ab	2.90ab	4.78ab	5.19ab
Petunidin-3-O-(6"-acetyl-glucoside)	9.76b	0.00d	0.00d	**12.81a**	9.98b	6.70c	6.42c
trans-Delphinidin-3-O-(6-p-coumaroylglucoside)	**3.81a**	**4.11a**	0.00c	**3.79a**	3.11ab	**4.25a**	3.38ab
Peonidin-3-O-(6"-acetyl-glucoside)	**7.24a**	**5.73a**	0.00b	**5.19a**	**4.02a**	**5.64a**	**4.59a**
Malvidin-3-O-(6"-acetyl-glucoside)	0.00f	6.50e	0.00f	**38.35a**	29.69b	15.42c	11.72d
Cyanidin-3-O-(6-p-coumaroylglucoside) + *trans*-Malvidin-3-O-(6"-caffeoylglucoside)	0.00c	0.00cd	0.00c	0.00c	3.37b	0.00c	**3.68a**
trans-Petunidin-3-O-(6-p-coumaroylglucoside)	0.00c	0.00c	0.00c	0.00c	2.75b	**3.84a**	**3.63a**
trans-Peonidin-3-O-(6-p-coumaroylglucoside)	0.00d	2.81c	0.00d	2.91bc	2.70c	**5.05a**	3.25b
trans-Malvidin-3-O-(6-p-coumaroylglucoside)	6.62bc	3.47cd	0.00d	10.09b	7.10bc	**18.21a**	8.72b

Table 8. Quantification results of anthocyanins. The data are expressed in mg L^{-1}. Differences are classified for $p<0.05$. 1: Festasio, 2: L. del Pellegrino, 3: Albana rosa; 4: L. Salamino conventional; 5: L. Salamino organic; 6: L. Grasparossa conventional; 7: L. Grasparossa organic.

Malvidin-3-*O*-glucoside was the most abundant anthocyanin in all red samples. However, Festasio and L. del Pellegrino showed lower relative amounts of Malvidin-3-*O*-glucoside and a corresponding higher level of delphinidin-3-*O*-(6"-acetylglucoside). Albana rosa is a faintly pink colored minor grape and possesses a basic pattern of the main anthocyanins with very low concentrations.

In any case, all molecules showed significant differences. In particular, for the delphinidin-3-*O*-glucoside, L. Salamino conventional (23.14 mg L^{-1}) and L. Grasparossa conventional (20.95 mg L^{-1}) showed the highest values, 80% and 63% above the average, respectively. In the case of cyanidin-3-*O*-glucoside, Festasio (3.87 mg L^{-1}) and L. del Pellegrino (4.08 mg L^{-1}) showed the highest values, 18% and 24% above the average, respectively. Concerning the petunidin-3-*O*-glucoside, L. Salamino conventional showed the highest value (29.79 mg L^{-1}), 90% above the average. L. Grasparossa conventional showed the highest value of peonidin-3-*O*-glucoside (20.68 mg L^{-1}), 181% above the average. The highest values of malvidin-3-*O*-glucoside were shown by L.

Salamino conventional (134.15 mg L^{-1}) and L. Grasparossa conventional (148.65 mg L^{-1}), 70% and 88% above the average, respectively. Festasio and L. del Pellegrino showed the highest values of delphinidin-3-*O*-(6"-acetylglucoside) (15.33 mg L^{-1} and 15.84 mg L^{-1}, respectively), 65% and 70% above the average, respectively. Festasio also showed the highest value of malvidin-3-*O*-(6"-acetylgalactoside) (21.58 mg L^{-1}), 238% above the average. Concerning the cyanidin-3-*O*-(6"-acetylglucoside) L. del Pellegrino showed the highest value (5.85 mg L^{-1}), 77% above the average. The highest value of petunidin-3-*O*-(6"-acetylglucoside) was shown by L. Salamino conventional (12.81 mg L^{-1}), 96% above the average. Regarding the *trans*-delphinidin-3-*O*-(6-*p*-coumaroylglucoside), Festasio (3.81 mg L^{-1}), L. del Pellegrino (4.11 mg L^{-1}), L. Salamino conventional (3.79 mg L^{-1}) and L. Grasparossa conventional (4.25 mg L^{-1}) showed the highest values, 19%, 28%, 18% and 33% above the average, respectively. L. Salamino conventional showed the highest value for malvidin-3-*O*-(6"-acetylglucoside) (38.35 mg L^{-1}), 164% above the average. L. Grasparossa organic showed the highest value for the sum of cyanidin-3-*O*-(6-*p*-coumaroylglucoside) and *trans*-malvidin-3-*O*-(6"-caffeoylglucoside) (3.68 mg L^{-1}), 265% above the average. Concerning the *trans*-petunidin-3-*O*-(6-*p*-coumaroylglucoside), L. Grasparossa conventional and L. Grasparossa organic showed the highest values (3.843 mg L^{-1} and 3.633 mg L^{-1}, respectively), 163% and 148% above the average. Thus, this compound might be a distinctive molecule of the L. Grasparossa variety. L. Grasparossa conventional also showed the highest values of *trans*-peonidin-3-*O*-(6-*p*-coumaroylglucoside) (5.051 mg L^{-1}) and *trans*-malvidin-3-*O*-(6-*p*-coumaroylglucoside) (18.21 mg L^{-1}), 112% and 135% above the average, respectively.

Generally speaking, these results suggest that conventional farming yields a higher anthocyanins content. Moreover, even if Festasio and L. del Pellegrino showed high values for certain molecules, they could not reach the levels of the other cultivars. Hence, they may be used for single-variety wine production, as well as for blended wines, such as L. Reggiano. Finally, the precise determination of the blending potential of both Festasio and L. del Pellegrino needs an experimentation of more than one year, since the anthocyanins content is severely affected by the vintage effect (Riberéu-Gayon et al., 2018a). However, these are results of a single vintage. The lack of replications makes speculative these observations.

3.3 Orbitrap analysis

3.3.1 Identification of anthocyanins

A library of 110 compounds was created (Table 9). Identified compounds are listed according to their elution time.

ID	Compound	Molecular formula $[M]^+$	t_R (min)	Measured accurate mass (*m*/*z*)	Error (ppm)	Calculated exact mass (*m*/*z*)	MS^E fragment	Reference
1	Delphinidin-3-*O*-rhamnoside-5-*O*-glucoside	$C_{27}H_{31}O_{16}$	4.67	611.1605	-0.31	611.1607	287.0551	HMDB
2	Delphinidin-3,5-*O*-diglucoside	$C_{27}H_{31}O_{17}$	7.86	627.1556	0.1	627.1556	303.0492	Roman et al., 2019; HMDB
3	Malvidin-3-*O*-glucoside-(epi)gallocatechin (F-A type)	$C_{38}H_{37}O_{19}$	8.82	797.1920	-0.49	797.1924	n.d.	Willemse et al., 2015
4	Delphinidin-3-*O*-glucoside	$C_{21}H_{21}O_{12}$	12.51	465.1027	-0.15	465.1028	303.0495	Hornedo-Hortega et al., 2017; Sun et al., 2012; Willemse et al., 2015
5	Peonidin-3-*O*-galactoside-4-vinylphenol	$C_{30}H_{27}O_{12}$	12.54	579.1493	-0.71	579.1497	287.0544, 301.0703, 409.0913	tentatively identified
6	Delphinidin-3-*O*-glucoside-acetaldehyde	$C_{23}H_{21}O_{12}$	13.01	489.1028	0.12	489.1028	327.0493, 195.3988	Willemse et al., 2015
7	Catechin-malvidin-3-*O*-glucoside (F-A type)	$C_{38}H_{37}O_{18}$	13.66	781.1970	-0.57	781.1974	619.149	Willemse et al., 2015
8	Cyanidin-3-*O*-glucoside	$C_{21}H_{21}O_{11}$	14.34	449.1079	0.13	449.1078	287.0547	Hornedo-Hortega et al., 2017; Vallverdú-Queralt et al., 2015; Willemse et al., 2015
9	Petunidin-3-*O*-glucoside	$C_{22}H_{23}O_{12}$	15.28	479.1184	0.07	479.1184	317.0651	Sun et al., 2012; Vallverdú-Queralt et al., 2015; Willemse et al., 2015
10	Malvidin-3,7-*O*-diglucoside	$C_{29}H_{35}O_{17}$	15.7	655.1870	0.12	655.1869	331.0795	Willemse et al., 2015
11	Malvidin-3-*O*-glucoside-di(epi)catechin (F-A type)	$C_{53}H_{49}O_{24}$	16.24	1069.2608	0.01	1069.2608	n.d.	Willemse et al., 2015
12	Pelargonidin-3-*O*-glucoside	$C_{21}H_{21}O_{10}$	16.26	433.1131	0.42	433.1129	n.d.	Hornedo-Hortega et al., 2017; Willemse et al., 2015
13	Peonidin-3-*O*-glucoside	$C_{22}H_{23}O_{11}$	17.07	463.1235	0.01	463.1235	301.0703	Hornedo-Hortega et al., 2017; Sun et al., 2012; Willemse et al., 2015
14	Malvidin-3,5-*O*-diglucoside	$C_{29}H_{35}O_{17}$	17.25	655.1857	-1.84	655.1869	331.0808	Roman et al., 2019; Willemse et al., 2015

15	Peonidin-3-*O*-glucoside-4-vinylphenol	$C_{301}H_{27}O_{12}$	17.28	579.1494	-0.51	579.1497	287.0544, 301.0707, 409.0915	Willemse et al., 2015
16	Malvidin-3-*O*-glucoside	$C_{23}H_{25}O_{12}$	17.58	493.1342	0.17	493.1341	331.0808	Sun et al., 2012; Vallverdú-Queralt et al., 2015; Willemse et al., 2015
17	Pyranone-malvidin-3-*O*-(6-*p*-coumaroylglucoside)	$C_{34}H_{31}O_{15}$	18.24	679.1655	-0.38	679.1658	n.d.	Willemse et al., 2015
18	Malvidin-3-*O*-glucoside-(epi)catechin-(epi)gallocatechin	$C_{53}H_{51}O_{25}$	19.01	1087.2710	0.03	1087.2714	n.d.	Willemse et al., 2015
19	Malvidin-3-*O*-glucoside-acetaldehyde (Vitisin B)	$C_{25}H_{25}O_{12}$	19.32	517.1343	0.4	517.1341	355.0807, 339.0486, 311.0536, 283.3947	Willemse et al., 2015
20	Petunidin-3-*O*-glucoside-pyruvic acid	$C_{25}H_{23}O_{14}$	19.53	547.1084	0.25	547.1082	385.0524, 375.0303	Willemse et al., 2015
21	(epi)catechin-(C4-C6)-malvidin-3-*O*-galactoside (F-A type)	$C_{38}H_{37}O_{18}$	19.82	781.1972	-0.3	781.1974	329.0663	Willemse et al., 2015
22	(epi)catechin-malvidin-3-*O*-galactoside (F-A type)	$C_{38}H_{37}O_{18}$	20.13	781.1971	-0.43	781.1974	329.0656	tentatively identified
23	Malvidin--3-*O*-glucoside-vinyl-(epi)gallocatechin	$C_{40}H_{37}O_{19}$	20.68	821.1913	-1.27	821.1924	n.d.	Willemse et al., 2015
24	Peonidin-3-*O*-glucoside-pyruvic acid	$C_{25}H_{23}O_{13}$	22.03	531.1135	0.36	531,1133	369.0592	Willemse et al., 2015
25	Delphinidin-3-*O*-(6"-acetyl-glucoside)	$C_{23}H_{23}O_{13}$	22.06	507.1135	0.44	507.1133	303.0495	Roman et al., 2019; Willemse et al., 2015
26	(epi)catechin-(C4-C6)-malvidin-3-*O*-glucoside (F-A type)	$C_{38}H_{37}O_{18}$	22.12	781.1971	-0.47	781.1974	329.0641	Willemse et al., 2015
27	Petunidin-3-*O*-glucoside-ethyl-epicatechin	$C_{39}H_{39}O_{18}$	22.38	795.2127	-0.47	795,2131	343.0797, 525.7787, 149.0751	Willemse et al., 2015
28	Malvidin-3-*O*-glucoside-pyruvic acid (Vitisin A)	$C_{26}H_{25}O_{14}$	22.6	561.1239	0.09	561.1239	399.0699	Willemse et al., 2015
29	Catechin-(C4-C6)malvidin-3-*O*-glucoside (F-A type)	$C_{38}H_{37}O_{18}$	22.72	781.1971	-0.4	781.1974	329.0653	Willemse et al., 2015
30	Malvidin-3-*O*-(6"-acetyl-glucoside)-(epi)-catechin (F-A type)	$C_{40}H_{39}O_{19}$	22.88	823.2078	-0.29	823.2080	n.d.	Willemse et al., 2015

31	Malvidin-3-O-(6-p-coumaroylglucoside)-vinylcatechol	$C_{40}H_{35}O_{16}$	23.12	771.1916	-0.45	771.1920	n.d.	Willemse et al., 2015
32	Petunidin-3-O-glucoside-ethyl-catechin	$C_{39}H_{39}O_{18}$	23.2	795.2131	-0.29	795.2131	343.0816	Willemse et al., 2015
33	Pyranone-malvidin-3-*O*-galactoside	$C_{25}H_{25}O_{13}$	23.3	533.1269	0.79	533.1290	312.8526, 254.4459, 115.8772	tentatively identified
34	Malvidin-3-*O*-glucoside-di(epi)catechin (A-F type)	$C_{53}H_{51}O_{24}$	23.38	1071.2765	0.02	1071.2765	631.1626, 469.1114, 383.1218	Willemse et al., 2015
35	Petunidin-3-*O*-glucoside-vinylcatechol	$C_{30}H_{27}O_{14}$	23.45	611.1396	0.16	611.1395	303.0492	Willemse et al., 2015
36	Malvidin-ethyl-di(epi)catechin-isomer 1	$C_{55}H_{53}O_{24}$	24.11	1097,2924	0.25	1097.2921	n.d.	tentatively identified
37	Cyanidin-3-*O*-(6"-acetyl-glucoside)	$C_{23}H_{23}O_{12}$	24.27	491.1186	0.49	491,1184	287.0547	Hornedo-Hortega et al., 2017; Willemse et al., 2015
38	Malvidin-3-*O*-glucoside-(C4−C6)-ethyl-(epi)catechin	$C_{40}H_{41}O_{18}$	24.42	809.2284	-0.48	809.2287	357.0967, 519.1446	Willemse et al., 2015
39	Petunidin-3-*O*-(6"-acetyl-glucoside)	$C_{24}H_{25}O_{13}$	24.49	521.1292	0.49	521,1290	317.0651	Roman et al., 2019; Willemse et al., 2015
40	Malvidin-3-*O*-glucoside-(C4-C6)-(epi)catechin (A-F type)	$C_{38}H_{39}O_{18}$	24.72	783.2128	-0.42	783.2131	469.1131, 331.0847	Willemse et al., 2015
41	Malvidin--3-*O*-(6"-acetyl-glucoside)-pyruvic acid (Acetylvitisin A)	$C_{28}H_{27}O_{15}$	24.8	603.1345	0.5	603.1345	399.0711, 333.8062	Willemse et al., 2015
42	Malvidin--3-*O*-(6"-acetyl-glucoside)-(epi)catechin (A-F type)	$C_{40}H_{41}O_{19}$	24.97	825.2231	-0.61	825.2237	n.d.	Willemse et al., 2015
43	Peonidin-3-*O*-(6-p-coumaroylglucoside)-vinylcatechol	$C_{39}H_{33}O_{15}$	25.4	741.1813	-0.1	741.1814	n.d.	Willemse et al., 2015
44	Malvidin-ethyl-di(epi)catechin-isomer 2	$C_{55}H_{53}O_{24}$	25.54	1097.2921	-0.06	1097.2921	357.0950, 519.1499, 619.5068, 669.5162, 447.1047	tentatively identified
45	Malvidin-3-*O*-glucoside-ethyl-epigallocatechin	$C_{40}H_{41}O_{19}$	25.54	825.2230	-0.8	825,2237	357.0974, 519.1498	Willemse et al., 2015
46	Malvidin-3-*O*-glucoside-(C4-C6)-ethyl-catechin	$C_{40}H_{41}O_{18}$	25.55	809.2282	-0.64	809.2287	357.0964, 423.8505, 267.5872	tentatively identified

47	Malvidin-3-*O*-glucoside-ethyl-gallocatechin	$C_{40}H_{41}O_{19}$	25.72	825.2234	-0.31	825.2237	n.d.	Willemse et al., 2015
48	Malvidin-3-*O*-(6"-acetyl-glucoside)	$C_{25}H_{27}O_{13}$	26.32	535.1449	0.6	535,1446	331.0807, 287.0542	Willemse et al., 2015
49	Peonidin-3-*O*-(6"-acetyl-glucoside)	$C_{24}H_{25}O_{12}$	26.48	505.1340	-0.04	505.1341	301.0702	Roman et al., 2019; Willemse et al., 2015
50	Malvidin-ethyl-di(epi)catechin	$C_{55}H_{53}O_{24}$	26.69	1097.2922	0.03	1097.2921	357.0964, 519.1500	Willemse et al., 2015
51	Malvidin-ethyl-di-catechin	$C_{55}H_{53}O_{24}$	26.94	1097.2922	0.07	1097.2921	357.0967, 519.1504	tentatively identified
52	Malvidin-3-*O*-glucoside-ethyl-(epi)catechin	$C_{40}H_{41}O_{18}$	26.95	809.2284	-0.48	809.2287	357.0964, 519.1498	Willemse et al., 2015
53	Malvidin-3-*O*-glucoside-ethyl-catechin	$C_{40}H_{41}O_{18}$	27.1	809.2284	-0.47	809.2287	357.0962, 519.1505	tentatively identified
54	Malvidin-3-*O*-glucoside-(C4-C6)-catechin (A-F type)	$C_{38}H_{39}O_{18}$	27.13	783.2129	-0.21	783.2131	n.d.	Willemse et al., 2015
55	Petunidin-3-*O*-(6-*p*-coumaroylgalactoside)	$C_{31}H_{29}O_{14}$	27.73	625.1553	0.24	625.1552	317.0656	tentatively identified
56	Malvidin-3-*O*-glucoside-vinyl-di(epi)catechin	$C_{55}H_{49}O_{24}$	28.6	1093.2612	0.38	1093.2608	n.d.	Willemse et al., 2015
57	Petunidin-3-*O*-(6-*p*-coumaroylglucoside)-pyruvic acid	$C_{34}H_{29}O_{16}$	29.14	693.1451	0.14	693.1450	n.d.	Willemse et al., 2015
58	Malvidin-3-*O*-glucoside-vinyl-di-catechin	$C_{55}H_{49}O_{24}$	29.16	1093.2606	-0.33	1093.2608	n.d.	Willemse et al., 2015
59	Malvidin-3-*O*-glucoside-vinylsyringol	$C_{33}H_{33}O_{15}$	29.22	669.1808	-0.94	669.1814	n.d.	tentatively identified
60	Delphinidin--3-*O*-(6"-acetyl-galactoside)-vinyl-(epi)catechin	$C_{40}H_{35}O_{19}$	29.29	819.1767	-0.01	819.1767	n.d.	tentatively identified
61	Peonidin-3-*O*-(6-*p*-coumaroylglucoside)-(epi)catechin (F-A type)	$C_{46}H_{41}O_{19}$	29.48	897.2234	-0.24	897.2237	n.d.	Willemse et al., 2015
62	Malvidin-3-*O*-(6-*p*-coumaroylglucoside)-catechin (F-A type)	$C_{47}H_{43}O_{20}$	29.73	927.2344	0.17	927.2342	n.d.	Willemse et al., 2015
63	Malvidin-3-*O*-glucoside-(epi)catechin (A-F type)	$C_{38}H_{39}O_{18}$	29.75	783.2128	-0.26	783.2131	469.1122, 343.0810	Willemse et al., 2015

64	Malvidin-3-*O*-(6-p-coumaroylglucoside)-epicatechin (F-A type)	$C_{47}H_{43}O_{20}$	30.01	927.2342	-0.05	927.2342	619.1365	Willemse et al., 2015
65	Malvidin-3-*O*-glucoside-catechin (A-F type)	$C_{38}H_{39}O_{18}$	30.03	783.2128	-0.36	783.2131	469.1125, 343.0819, 505.1287	Willemse et al., 2015
66	Malvidin-3-*O*-(6"-acetyl-glucoside)-vinyl-di(epi)catechin	$C_{57}H_{51}O_{25}$	30.05	1135.2721	0.64	1135.2714	n.d.	Willemse et al., 2015
67	Malvidin-3-*O*-(6"-acetyl-glucoside)-ethyl-(epi)catechin	$C_{42}H_{43}O_{19}$	30.19	851.2390	-0.38	851.2393	357.0959, 561.1544, 327.2170	Willemse et al., 2015
68	Delphinidin-3-*O*-(6-*p*-coumaroylglucoside)	$C_{30}H_{27}O_{14}$	30.23	611.1396	0.07	611.1395	303.0495	Roman et al., 2019; Willemse et al., 2015
69	Malvidin-3-*O*-(6"-caffeoylglucoside)	$C_{32}H_{31}O_{15}$	30.41	655.1659	0.24	655.1658	331.0805	Willemse et al., 2015
70	Malvidin-3-*O*-(6-*p*-coumaroylglucoside)-acetaldehyde (Coumaroylvitisin B)	$C_{34}H_{31}O_{14}$	30.42	663.1709	0.15	663.1708	355.0802,	Willemse et al., 2015
71	Malvidin-3-*O*-(6"-acetyl-glucoside)-ethyl-(epi)catechin isomer 1	$C_{42}H_{43}O_{19}$	30.46	851.2391	-0.2	851.2393	357.0972, 781.9293	Willemse et al., 2015
72	Malvidin-3-*O*-(6"-acetyl-glucoside)-vinyl-di-catechin	$C_{57}H_{51}O_{25}$	30.5	1135.2718	0.36	1135.2714	n.d.	tentatively identified
73	Malvidin-3-*O*-(6"-acetyl-glucoside)-ethyl-(epi)catechin isomer 2	$C_{42}H_{43}O_{19}$	30.67	851.2391	-0.23	851.2393	357.0954, 847.2078, 435.8372, 501.7649	tentatively identified
74	Malvidin-3-*O*-glucoside-vinylcatechol (Pinotin A)	$C_{31}H_{29}O_{14}$	30.69	625.1554	0.32	625.1552	n.d.	Willemse et al., 2015
75	Delphinidin-3-*O*-(6"-acetyl-galactoside)-vinyl-catechin	$C_{40}H_{35}O_{19}$	30.71	819.1766	-0.17	819.1767	n.d.	tentatively identified
76	Malvidin-3-*O*-(6-*p*-coumaroylgalactoside)	$C_{32}H_{31}O_{14}$	31.21	639.1709	0.1	639.1708	331.0806	tentatively identified
77	Malvidin-3-*O*-(6-*p*-coumaroylglucoside-pyruvic acid (Coumaroylvitisin A)	$C_{35}H_{31}O_{16}$	31.74	707.1608	0.17	707.1607	399.0703, 373.9021, 410.9676, 431.7963	Willemse et al., 2015
78	Petunidin-3-*O*-(6-*p*-coumaroylglucoside)	$C_{31}H_{29}O_{14}$	32.01	625.1553	0.13	625.1552	317.0651	Roman et al., 2019; Willemse et al., 2015

79	Melphinidin-3-*O*-(6"-acetyl-glucoside)-vinyl-(epi)catechin	$C_{40}H_{35}O_{19}$	32.02	819.1773	0.7	819.1767	n.d.	Willemse et al., 2015
80	Peonidin-3-*O*-glucoside-vinylguaiacol	$C_{31}H_{29}O_{13}$	32.04	609.1604	0.24	609.1603	n.d.	Willemse et al., 2015
81	Malvidin-3-*O*-(6"-acetyl-glucoside)-ethyl-catechin	$C_{42}H_{43}O_{19}$	32.12	851.2390	-0.33	851.2393	357.0960	tentatively identified
82	Cyanidin-3-*O*-(6-*p*-coumaroylglucoside)	$C_{30}H_{27}O_{13}$	32.13	595.1447	0.11	595.1446	287.0546	Willemse et al., 2015
83	Delphinidin-3-*O*-(6"-acetyl-glucoside)-vinyl-catechin	$C_{40}H_{35}O_{19}$	32.21	819.1765	-0.28	819.1767	n.d.	Willemse et al., 2015
84	Petunidin-3-*O*-glucoside-vinylphenol	$C_{30}H_{27}O_{13}$	32.65	595.1448	0.33	595.1446	433.0913	Willemse et al., 2015
85	Malvidin-3-*O*-glucoside-vinyl-(epi)catechin	$C_{40}H_{37}O_{18}$	33.06	805.1973	-0.21	805.1974	491.0965	Willemse et al., 2015
86	Malvidin-3-*O*-(6-*p*-coumaroylgalactoside)-ethyl-(epi)catechin	$C_{49}H_{47}O_{20}$	33.31	955.2653	-0.24	955.2655	357.0952, 665.1879	tentatively identified
87	Malvidin-3-*O*-(6-*p*-coumaroylglucoside)	$C_{32}H_{31}O_{14}$	33.48	639.1707	-0.26	639.1708	331.0808	Roman et al., 2019; Willemse et al., 2015
88	Malvidin-3-*O*-glucoside-epicatechin (A-F type)	$C_{38}H_{39}O_{18}$	33.51	783.2122	-1.09	783.2131	621.1585, 607.1702, 469.1174	Willemse et al., 2015
89	Peonidin-3-*O*-(6-*p*-coumaroylglucoside)-ethyl-(epi)catechin	$C_{48}H_{45}O_{19}$	33.51	925.2546	-0.34	925.2550	n.d.	Willemse et al., 2015
90	Peonidin-3-*O*-(6-*p*-coumaroylglucoside)-ethyl-catechin	$C_{48}H_{45}O_{19}$	33.71	925.2554	0.52	925.2550	n.d.	Willemse et al., 2015
91	Peonidin-3-*O*-(6-*p*-coumaroylglucoside)	$C_{31}H_{29}O_{13}$	33.87	609.1604	0.27	609.1603	301.0702	Roman et al., 2019
92	Malvidin-3-*O*-(6-*p*-coumaroylglucoside)-ethyl-gallocatechin	$C_{49}H_{47}O_{21}$	34.19	971.2613	0.94	971,2604	n.d.	Willemse et al., 2015
93	Malvidin-3-*O*-glucoside-vinylphenol (Pigment A)	$C_{31}H_{29}O_{13}$	34.42	609.1606	0.49	609.1603	447.1074	Willemse et al., 2015
94	Pyranone-malvidin-3-*O*-glucoside	$C_{25}H_{25}O_{13}$	34.61	533.1293	0.65	533.1290	371.0760, 349.6219	Willemse et al., 2015
95	Malvidin-3-*O*-glucoside-vinyl-catechin	$C_{40}H_{37}O_{18}$	34.75	805.1950	-2.15	805.1974	n.d.	Willemse et al., 2015

96	Petunidin-3-*O*-(6"-acetyl-glucoside)-vinyl-catechin	$C_{41}H_{37}O_{19}$	34.81	833.1924	0.01	833.1924	n.d.	HMDB
97	Malvidin-3-*O*-glucoside-vinylguaiacol	$C_{32}H_{31}O_{14}$	35.16	639.1711	0.39	639.1708	331.0809	Willemse et al., 2015
98	Malvidin-3-*O*-(6"-acetyl-glucoside)-vinyl-(C4-C6)-(epi)catechin	$C_{42}H_{39}O_{19}$	35.71	847.2079	-0.11	847.2080	n.d.	Willemse et al., 2015
99	Malvidin-3-*O*-(6-*p*-coumaroylglucoside)-ethyl-(epi)catechin	$C_{49}H_{47}O_{20}$	36.15	955.2655	-0.02	955.2655	357.0962, 665.1808	Willemse et al., 2015
100	Malvidin-6-(6-*p*-coumaroyl-galactoside)-4-vinylphenol	$C_{40}H_{35}O_{15}$	36.37	755.1971	0.05	755.1970	n.d.	tentatively identified
101	Malvidin-3-*O*-(6-*p*-coumaroylgalactoside)-vinyl-(epi)catechin	$C_{49}H_{43}O_{20}$	36.61	951.2343	0.05	951.2342	n.d.	tentatively identified
102	Malvidin-3-*O*-(6"-acetyl-glucoside)-vinyl-(epi)catechin	$C_{42}H_{39}O_{19}$	36.68	847.2080	-0.01	847.2080	n.d.	Willemse et al., 2015
103	Malvidin-3-*O*-(6"-acetyl-glucoside)-vinyl-catechin	$C_{42}H_{39}O_{19}$	36.79	847.2079	-0.25	847.2080	n.d.	tentatively identified
104	Malvidin-3-*O*-(6-*p*-coumaroylglucoside)-ethyl-catechin	$C_{49}H_{47}O_{20}$	36.96	955.2656	0.05	955.2655	357.0959, 791.2314, 489.3846, 467.1928	tentatively identified
105	Peonidin-3-*O*-(6"-acetyl-glucoside)-(epi)catechin	$C_{41}H_{37}O_{18}$	36.99	817.1975	0.01	817.1974	n.d.	Willemse et al., 2015
106	Malvidin-3-*O*-(6"-acetyl-glucoside)-vinylphenol	$C_{33}H_{31}O_{14}$	37.01	651.1710	0.26	651.1708	447.1078, 337.9287	Willemse et al., 2015
107	Malvidin-3-*O*-(6-*p*-coumaroylglucoside)-vinyl-(epi)catechin	$C_{49}H_{43}O_{20}$	37.26	951.2344	0.18	951.2342	n.d.	Willemse et al., 2015
108	Peonidin-3-*O*-(6"-acetyl-glucoside)-catechin	$C_{41}H_{37}O_{18}$	37.4	817.1974	-0.08	817.1974	n.d.	Willemse et al., 2015
109	Pyranone-malvidin-3-*O*-(6"-acetyl-glucoside)	$C_{27}H_{27}O_{14}$	38.13	575.1397	0.38	575.1395	n.d.	Willemse et al., 2015
110	Malvidin-6-(6-*p*-coumaroylglucoside)-4-vinylphenol	$C_{40}H_{35}O_{15}$	40.37	755.1974	0.42	755.1970	447.1078	Willemse et al., 2015

Table 9. n.d. = not detected; error = difference between experimental and theoretical accurate mass in parts per million (ppm); t_R = retention time of the molecule.

Even if the literature about identification and quantification of anthocyanins is particularly diverse, there are very few correspondences about the accurate mass of molecules. For these reasons, only a few studies were taken into consideration.

The experimental mass of each molecule identified showed an error (or mass measurement accuracy) lower than 3 ppm, suggesting the high closeness of the measured mass to the exact mass, as well as of the accuracy of the elemental composition (Brenton and Godfrey, 2010; Strupat et al., 2016). In addition to this, most of the molecules showed the same fragmentation pattern described in previous studies (Hornedo-Hortega et al., 2017; Roman et al., 2019; Sun et al., 2012; Vallverdú-Queralt et al., 2015; Willemse et al. 2015). However, molecules 24 and 40 showed a different fragmentation, compared to the literature, while the experimental mass was correct (Willemse et al., 2015). Moreover, since the mass spectra of molecules 15, 21, 38, 50, 52, 94, 99, 102, 107, 110 showed many peaks with the same *m/z* ratio and fragmentation pattern, 21 compounds were tentatively identified as their possible isomers. Compound 5 showed a measured accurate mass similar to the compound 15, showing also the same fragmentation pattern. Compound 22 showed a measured accurate mass similar to the compound 21, as well as the same fragment. Compound 46 showed a measured accurate mass similar to the compound 38, but a different fragmentation pattern. Compounds 44 and 36 showed a measured accurate mass similar to the compound 50, while only the compound 44 showed the same fragmentation pattern of the compound 50. Compound 53 showed a measured accurate mass similar to the compound 52, as well as the same fragments. Compound 33 showed a measured accurate mass similar to the compound 94, but a different fragmentation pattern. Compounds 86 and 104 showed a measured accurate mass similar to the compound 99. According to Willemse et al., (2015), two compounds (86 and 99) showed the same fragmentation pattern (357.0952 and 665.1879), while compound 104 showed only the fragment 357.0959 that confirm the similarity with the other two molecules. Compounds 103 and 101 showed a measured accurate mass similar to the compound 102 and 107, respectively, but any fragment of these compounds was detected. Compound 100 showed a measured accurate mass similar to the compound 110. The first one did not show a fragmentation pattern, while the second showed a fragment of 447.1078, according to Willemse et al., (2015).

All molecules found can be divided in 11 classes of anthocyanins according to Willemse et al., (2015), since anthocyanins can form new adducts with other polyphenols present in wine through the copigmentation through non-covalent bonds, typically not detectable by a traditional HPLC technique (Ribéreau-Gayon, 2018a). All compounds were detected in both vintages since they were all above the LOD (0.44 ppb).

The first class was represented by the main anthocyanin monoglucosides and their corresponding acetyl, *p*-coumaroyl and caffeoyl derivatives, that are typically the most abundant in wine (Ribéreau-Gayon, 2018a). For this reason, they were taken into consideration to characterize each wine through statistical analysis (see chapter 3.3.2). The fragmentation of monoglucosides, acetyl, *p*-coumaroyl and caffeoyl derivatives caused neutral losses of *m/z* 162, 204, 308, and 324, respectively (Alberts et al., 2012).

The second class was constituted by anthocyanins diglucosides (molecules 1, 2, 10, 14). Even if diglucosides are considered specific of certain American grape species, such as *V. riparia* and *V. rupestris* (Ribéreau-Gayon, 1959), they have already been found in *V. vinifera* grapes (Roggero et al., 1984), although in low concentrations. For this reason, in France these molecules are used as a quality control method and for the protection of PDO wine production (Ribéreau-Gayon, 2018a).

Class of direct anthocyanins-tannins adducts was represented by 19 molecules: 3, 7, 11, 18, 21, 22, 26, 29, 30, 34, 40, 42, 54, 61-65 and 88. Indeed, flavanol-anthocyanins (F-A type) and anthocyanins-flavanol (A-F type) adducts were already detected in wine (Sanchez-Ilarduya et al., 2014), but the presence of several isomers may explain the high number of compounds detected (Ribéreau-Gayon, 2018a).

Class of acetaldehyde-mediated tannins adducts was represented by 22 molecules: 27, 32, 36, 38, 44-47, 50-53, 67, 71, 73, 81, 86, 89, 90, 92, 99 and 104. Their formation is due to the condensation of anthocyanins and flavonols (catechins and procyanidins) through an ethyl unit during fermentation (Marquez et al., 2013; Ribéreau-Gayon, 2018a).

Class of anthocyanin-vinylflavanol condensation products was constituted by 17 molecules: 23, 56, 58, 60, 66, 72, 75, 79, 83, 85, 95, 96, 98, 101-103 and 107. This class of compounds is formed by the cycloaddition of vinylflavanols and anthocyanins and is usually present in low concentration, then rising during wine aging (Marquez et al., 2013; Ribéreau-Gayon, 2018a).

Oxovitisins class was represented by only 4 molecules: 17, 33, 94 and 109. Their formation is probably due to the oxidation of the pyran ring of vitisins through the addition of a hydroxyl group (He et al., 2010).

Anthocyanin-pyruvic acid products (Vitisin A) were constituted by 5 molecules: 24, 28, 41, 57, 77. This class of anthocyanins is commonly found in wine and is formed during fermentation (Chinnici et al., 2009; Ribéreau-Gayon, 2018a).

Anthocyanin-acetaldehyde products (Vitisin B) were represented only by 3 molecules: 6, 19 and 70. Also this class of anthocyanins is commonly found in wine and is formed during fermentation (Chinnici et al., 2009; Ribéreau-Gayon, 2018a).

Anthocyanin-vinylcatechol derivatives were represented by 4 molecules: 31, 35, 43, 74. This class of compounds is formed by the C4/C5 cycloaddition of vinylflavanols and anthocyanins and it is low concentrated in young wines (Marquez et al., 2013; Ribéreau-Gayon, 2018a).

Anthocyanin-vinylphenol derivatives were constituted by 7 molecules: 5, 15, 84, 93, 100, 106 and 110. This class of compounds is formed by the cycloaddition of 4-vinylphenol, resulting from the decarboxylation of *p*-coumaric acid mediated by yeasts, and anthocyanins (Ribéreau-Gayon, 2018a).

Anthocyanin-vinylguaiacol derivatives were represented by only 2 molecules: 80 and 97. This class of compounds is formed by the cycloaddition of 4-vinylguaiacol, resulting from the decarboxylation activity of yeasts, and anthocyanins (Ribéreau-Gayon, 2018a).

In anthocyanin-vinylsyringol derivatives only the compound 59 was detected. This class of compounds is rarely detected in wine, since their presence is already low in grapes (Chatonnet et al., 1993; Schwarz et al., 2003).

3.3.2 Quantification of the anthocyanins

All molecules quantified showed a response higher than LOQ (1.45 ppb).

During the two years of experiments some wine was not replicated. Indeed, L. Reggiano (conventional and organic) and L. Grasparossa (conventional and organic) were analyzed only in 2018, while L. di Fiorano and Termarina rossa were analyzed only in 2019. To discuss and compare these wines with the respective dataset of each year one-way ANOVA was used.

Concerning the vintage 2018 (Table 10), L. Grasparossa conventional showed the highest values for both 3'OMT activity and 5′ OMT activity. L. Reggiano conventional and organic showed the highest values for the 3'5'OH activity. These indexes were widely used in literature to describe the flavanol pattern. However, they were rarely used in studies about red wines, especially about Lambrusco type wines (Forester and Waterhouse, 2009; Mattivi et al., 2006). Hence, having a large quantity of different cultivars not investigated, the use of these tools may be useful to explore all the possible differences. In fact, L. Grasparossa conventional showed a completely different anthocyanins pattern as compared to the other wines, due to the low content of cyanidin-3-*O*-glucoside (3'OMT activity) and delphinidin-3-*O*-glucoside (5′ OMT activity). In fact, all the other wines were characterized by a higher level of 3'5'OH activity and a lower level of 3'OMT activity and 5′ OMT activity. Concerning the L. Reggiano wines, the higher level of 3'5'OH activity suggests an increased stability of the color (Mattivi et al., 2006). Nevertheless, the data about these wines are poor, since the analyses were done only during the first year and because the L. Reggiano wine is a particularly blended wine, resulting from the mixture of several varieties.

ID	Compound	BE	ROS	VE	FE	AC	AO	RC308	RO95	RO96	RO17	RO7	LSC52	LSC309	LGC	LGO	LRC	LRO
4	Delphinidin-3-*O*-glucoside	0.00f	0.27f	1.79ef	12.15de	12.81de	**47.00a**	25.91bc	30.50b	30.77b	30.43b	33.68b	15.16d	13.93cd	3.91def	2.20ef	4.90def	5.35def
8	Cyanidin-3-*O*-glucoside	0.00e	0.12e	0.86de	0.87de	0.62e	**3.36a**	**3.48a**	2.00bcd	2.07bc	2.17bc	2.50ab	1.04cde	1.12cde	0.17e	0.12e	0.31e	0.39e
9	Petunidin-3-*O*-glucoside	0.01f	0.40f	3.45cef	15.39bcde	15.07bcde	**44.67a**	21.69bc	25.86b	26.15b	26.19b	28.25b	19.15bcd	18.50bcd	5.55def	2.95ef	7.72cdef	7.80cdef
12	Pelargonidin-3-*O*-glucoside	0.00f	0.01ef	0.01ef	0.02de	0.02de	0.04ab	**0.05a**	0.03cd	0.03cd	0.03cd	0.03bc	0.01ef	0.01def	0.01ef	0.01ef	0.01ef	0.01ef
13	Peonidin-3-*O*-glucoside	0.01e	0.67e	8.05bcde	7.54bcde	6.74bcde	**25.26a**	12.16bcd	11.56bcd	11.93bcd	12.41bc	13.57b	3.57cde	4.18bcde	5.86bcde	2.70de	1.63e	1.49e
16	Malvidin-3-*O*-glucoside	0.03e	2.88de	22.64cde	121.05ab	86.32bcde	**195.31a**	76.47bcde	86.62bcde	89.14bcd	90.74bcd	96.70bc	68.70bcde	70.66bcde	48.31bcde	24.91 cde	42.02bcde	37.26bcde
25	Delphinidin-3-*O*-(6"-acetylglucoside)	0.00f	0.03f	0.26ef	5.25bcd	3.60cdef	**13.21a**	4.15bcde	7.24bc	7.27bc	7.23bc	7.80b	3.71cdef	3.09def	0.33ef	0.22ef	1.51def	1.42def
37	Cyanidin-3-*O*-(6"-acetylglucoside)	0.00e	0.02e	0.74cde	0.67cde	0.72cde	**2.55a**	0.71cde	1.59abc	1.63abc	0.75cds	1.73abc	0.74cde	0.61cde	0.07e	0.06e	0.38de	0.36de
39	Petunidin-3-*O*-(6"-acetylglucoside)	0.00c	0.03c	0.42c	7.38b	4.32bc	**14.96a**	4.42bc	7.09b	7.29b	7.25b	7.73b	5.40bc	4.65bc	0.50c	0.32c	2.68bc	2.41c
48	Malvidin-3-*O*-(6"-acetylglucoside)	0.00c	0.17c	2.22c	57.74ab	23.97c	**77.44a**	19.12c	26.14c	26.98c	27.12c	28.64bc	20.48c	18.87c	3.39c	1.99c	12.96 c	10.34c
49	Peonidin-3-*O*-(6"-acetylglucoside)	0.00d	0.05d	1.83bcd	3.89bcd	3.19bcd	**11.19a**	2.53bcd	4.41bc	4.51bc	4.55bc	4.82b	1.31bcd	1.31bcd	0.72bcd	0.30cd	0.77bcd	0.55bcd
55	Petunidin-3-*O*-(6-*p*-coumaroylgalactoside)	0.00g	0.02efg	0.00g	0.01efg	0.04ef	0.04e	**0.43a**	0.25b	0.26b	0.26b	0.26b	0.10d	0.15c	0.01fg	0.01fg	0.01fg	0.01efg
68	Delphinidin-3-*O*-(6-*p*-coumaroylglucoside)	0.01c	0.02c	0.30c	1.15c	1.17c	**4.26a**	**3.17a**	**3.25a**	**3.29a**	3.00ab	**3.46a**	1.35bc	0.89c	0.30c	0.13c	0.31c	0.31c
69	Malvidin-3-*O*-(6"-caffeoylglucoside)	0.00d	0.01d	0.05cd	**0.60a**	0.11cd	0.39b	0.15cd	0.16cd	0.17cd	0.17cd	0.18c	0.12cd	0.12cd	0.08cd	0.03cd	0.06cd	0.05cd
76	Malvidin-3-*O*-(6-*p*-coumaroylgalactoside)	0.00f	0.03ef	0.01ef	0.03ef	0.11e	0.10ef	**1.24a**	0.57b	0.57b	0.58b	0.57b	0.23d	0.38c	0.02ef	0.01ef	0.02ef	0.02ef
78	Petunidin-3-*O*-(6-*p*-coumaroylglucoside)	0.01c	0.02c	2.40ab	1.42c	1.35c	**5.02a**	3.05ab	2.91ab	2.95ab	2.73ab	3.20ab	1.70ab	1.29c	0.34c	0.14c	0.44c	0.43c
82	Cyanidin-3-*O*-(6-*p*-coumaroylglucoside)	0.01e	0.03e	**1.28a**	0.25de	0.38bcde	**1.33a**	0.84abcd	1.02ab	1.02ab	0.96abc	**1.10a**	0.39bcde	0.28cde	0.10e	0.04e	0.11e	0.12e
87	Malvidin-3-*O*-(6-*p*-coumaroylglucoside)	0.01c	0.09c	2.55bc	12.28bc	8.97bc	**32.77a**	12.98bc	14.33bc	14.62bc	14.42bc	15.75b	8.59bc	8.13bc	3.60bc	1.44bc	2.50bc	2.17bc
91	Peonidin-3-*O*-(6-*p*-coumaroylglucoside)	0.00d	0.05cd	2.59abcd	1.14bcd	1.53bcd	**5.27a**	2.74abc	2.65abcd	2.69abcd	2.62abcd	2.90ab	0.80bcd	0.75bcd	0.91bcd	0.26bcd	0.21cd	0.18cd
	Sum glucosides	0.04e	4.34de	36.80cde	157.05b	121.58bcde	**316.20a**	140.23bcd	156.99bc	160.53b	162.42b	175.21b	107.75bcde	108.53bcde	63.82bcde	32.95de	56.59 bcde	52.31bcde
	Sum acetylglucosides	0.00f	0.30f	5.48def	74.92b	35.80bcde	**119.36a**	30.94bcdef	46.46bcde	47.69bcd	46.90bcde	50.70bc	31.64bcdef	28.54cdef	5.02def	2.89ef	18.31cdef	15.08cdef
	Sum coumaroylglucosides	0.05d	0.26d	9.13bcd	16.28bcd	13.55bcd	**48.79a**	24.46bc	24.97bc	25.39bc	24.58bc	27.23ab	13.17bcd	11.86bcd	5.28bcd	2.03d	3.59cd	3.23cd
	3'5'OH activity	5.88h	4.52hi	3.13i	17.67d	15.59e	10.04f	7.95g	10.54f	10.44f	10.12f	9.87f	22.37b	19.49c	9.61f	11.06f	**28.26a**	**26.67a**
	3'OMT activity	0.00d	5.78cd	9.35cd	8.70cd	10.77bc	7.52cd	3.46cd	5.72cd	5.68cd	5.66cd	5.36cd	3.44cd	3.62cd	**34.47a**	20.53b	5.19cd	3.77cd
	5'OMT activity	0.00f	10.67ab	**12.63a**	9.97abc	6.68cd	4.16de	2.92ef	2.80ef	2.84ef	2.95ef	2.81ef	4.54de	4.87de	**12.27a**	10.89ab	8.47bc	6.92cd
	(dp+cy+pt/pn+mv) × 10 activity	1.68e.	2.21cde	1.99de	2.21cde	3.10bcde	4.33abcde	5.89ab	**6.15a**	**6.06a**	**5.93a**	**6.05a**	4.89abc	4.81abcd	1.80e	1.99de	3.01cde	3.52abcde

Table 10. One-way ANOVA of minor and commercial wines for the vintage 2018. All values are expressed in mg L^{-1} for molecules and sums. The values of all the indexes are absolute values. Classification was done for $p<0.05$.

About the vintage 2019 (Table 11), L. di Fiorano showed the highest values for 3’5’OH activity, 3′ OMT activity and 5′ OMT activity. This trend was due to the high level of malvidin-3-*O*-glucoside, and also because of the low level of the low content cyanidin-3-*O*-glucoside (3’OMT activity) and delphinidin-3-*O*-glucoside (5′ OMT activity). In addition, the fact that the 3’5’OH activity was higher than 3’OMT activity and 5′ OMT activity, which were strong as well (Mattivi et al., 2006), suggest that the characteristics of this variety are similar to other Lambrusco type wines. Termarina rossa showed the highest value for (dp+cy+pt/pn+mv) × 10, that indicates the highest relative content of the anthocyanins with antioxidant properties, despite the low anthocyanins content as compared to Ancellotta and Festasio wines (Vasile Simone et al., 2013).

This is the first time that the data about these minor varieties are reported. However, further studies are needed to evaluate their oenological potential during different vintages.

ID	Compound	BE		ROS		TE		VE		PE		FE		AC		AO		RC		RO		LSC		LSCR	
4	Delphinidin-3-*O*-glucoside	0.00	f	1.34	f	5.62	ef	2.37	f	13.61	ef	64.88	b	**147.76**	**a**	43.95	cd	54.43	bc	47.73	cd	34.46	d	18.68	e
8	Cyanidin-3-*O*-glucoside	0.01	g	0.56	g	4.83	c	2.07	ef	0.54	g	2.93	def	**15.05**	**a**	3.23	de	6.01	b	4.51	c	3.29	d	1.95	f
9	Petunidin-3-*O*-glucoside	0.00	f	1.73	ef	3.06	ef	4.79	fg	21.51	def	77.28	b	**133.70**	**a**	41.02	cd	46.33	c	38.85	cde	37.63	cde	19.54	efg
12	Pelargonidin-3-*O*-glucoside	0.00	g	0.00	g	0.02	efg	0.03	cde	0.01	fg	0.04	cd	**0.15**	**a**	0.04	c	0.07	b	0.08	b	0.02	def	0.03	cde
13	Peonidin-3-*O*-glucoside	0.00	f	4.26	f	5.67	f	18.82	de	8.15	fg	37.82	b	**65.02**	**a**	21.35	cd	30.72	bc	21.66	cd	6.74	f	8.80	ef
16	Malvidin-3-*O*-glucoside	0.10	e	11.12	de	9.03	de	29.91	cde	173.22	b	**515.84**	**a**	**441.65**	**a**	151.99	bc	154.89	b	130.08	bcd	128.91	bcd	81.62	bcde
25	Delphinidin-3-*O*-(6"-acetylglucoside)	0.00	d	0.02	d	0.50	d	0.32	d	2.46	cd	**22.79**	**a**	**25.93**	**a**	9.74	bc	8.85	b	7.00	b	5.76	bc	2.67	cd
37	Cyanidin-3-*O*-(6"-acetylglucoside)	0.00	h	0.02	h	0.82	efg	1.62	cd	0.35	gh	2.99	b	**4.58**	**a**	1.87	c	1.76	cd	1.16	de	1.15	def	0.49	fgh
39	Petunidin-3-*O*-(6"-acetylglucoside)	0.00	d	0.04	d	0.40	cd	0.60	cd	4.48	bcd	**32.13**	**a**	**32.57**	**a**	10.89	b	10.04	b	7.78	bc	8.71	b	3.95	bcd
48	Malvidin-3-*O*-(6"-acetylglucoside)	0.00	c	0.13	c	1.42	c	2.90	c	29.93	c	**228.94**	**a**	126.12	b	44.34	c	41.00	c	33.69	c	30.02	c	14.58	c
49	Peonidin-3-*O*-(6"-acetylglucoside)	0.00	d	0.07	d	0.47	d	4.56	bcd	2.53	bcd	**19.20**	**a**	**15.06**	**a**	6.58	bc	6.75	b	4.49	bcd	1.64	cd	1.28	d
55	Petunidin-3-*O*-(6-*p*-coumaroylgalactoside)	0.00	g	0.00	g	0.00	g	0.00	g	0.01	g	0.02	g	0.59	b	0.05	f	0.32	c	**0.80**	**a**	0.21	d	0.17	e
68	Delphinidin-3-*O*-(6-*p*-coumaroylglucoside)	0.00	e	0.05	e	0.29	de	0.30	de	1.53	de	5.97	b	**12.87**	**a**	3.84	**c**	5.77	b	5.50	b	1.71	e	1.01	de
69	Malvidin-3-*O*-(6"-caffeoylglucoside)	0.00	c	0.01	c	0.03	c	0.04	c	0.31	c	**1.93**	**a**	0.82	b	0.25	c	0.24	c	0.18	c	0.17	c	0.10	c
76	Malvidin-3-*O*-(6-*p*-coumaroylgalactoside)	0.00	f	0.01	f	0.01	f	0.01	f	0.03	ef	0.00	f	1.38	b	0.12	e	0.81	c	**2.07**	**a**	0.46	d	0.44	d
78	Petunidin-3-*O*-(6-*p*-coumaroylglucoside)	0.00	d	0.04	d	0.14	d	0.43	de	2.05	d	6.57	b	**12.68**	**a**	3.84	c	4.99	bc	4.64	c	2.00	d	1.04	de
82	Cyanidin-3-*O*-(6-*p*-coumaroylglucoside)	0.00	g	0.13	fg	1.02	d	2.31	b	0.41	ef	1.20	d	**3.24**	**a**	1.12	d	1.69	c	1.25	d	0.50	e	0.26	efg
87	Malvidin-3-*O*-(6-*p*-coumaroylglucoside)	0.00	f	0.11	f	0.39	f	2.46	f	17.52	cde	50.94	b	**70.16**	**a**	20.49	cd	24.45	d	22.37	cd	9.68	def	5.62	ef
91	Peonidin-3-*O*-(6-*p*-coumaroylglucoside)	0.00	g	0.20	g	0.37	fg	5.19	bc	2.01	ef	5.49	b	**10.21**	**a**	3.27	de	5.40	b	3.71	cd	0.74	fg	0.80	fg
	Sum glucosides	0.11	d	19.02	d	28.36	d	57.98	cd	217.41	bc	**698.95**	**a**	**804.44**	**a**	262.07	b	293.02	b	243.48	b	211.36	bc	130.85	bcd
	Sum acetylglucosides	0.00	d	0.28	d	3.60	cd	10.00	cd	39.74	cd	**306.05**	**a**	204.27	b	73.43	c	68.40	cd	54.12	cd	47.28	cd	22.98	cd
	Sum coumaroylglucosides	0.00	g	0.53	g	2.22	g	10.71	fg	23.56	def	70.19	b	**111.14**	**a**	32.72	cde	43.43	c	40.33	cd	15.30	efg	9.35	fg
	3'5'OH activity	10.88	d	2.95	h	1.69	i	1.78	i	**24.01**	**a**	16.20	c	9.03	ef	9.65	f	6.97	g	8.27	f	20.04	b	11.16	d
	3'OMT activity	0.00	g	7.64	d	1.17	f	9.10	c	**15.21**	**a**	12.82	b	4.32	e	6.61	d	5.10	e	4.80	e	2.05	f	4.51	e
	5'OMT activity	0.00	h	8.31	b	1.61	g	**12.61**	**a**	**12.72**	**a**	7.92	b	2.99	ef	3.46	de	2.84	ef	2.73	f	3.76	cd	4.37	c
	(dp+cy+pt/pn+mv) × 10 activity	0.92	g	2.36	ef	**9.19**	**a**	1.89	f	1.97	f	2.63	e	5.85	b	5.10	c	5.76	b	6.00	b	5.54	bc	4.44	d

Table 11. One-way ANOVA of minor and commercial wines for the vintage 2019. All values are expressed in mg L^{-1} for molecules and sums. The values of all the indexes are absolute values. Classification was done for $p<0.05$. N.s. = not significant.

According to the two-way ANOVA of the monoglucosides anthocyanins the second vintage (2019) showed the highest values (Table 12). In fact, it is known that anthocyanins content of the same variety can duplicate or triplicate, depending on the vintage and the environmental condition (Ribéreau-Gayon et al., 2018a). Concerning the sums and indexes only the 3′ OMT activity, 5′ OMT activity and the (dp+cy+pt/pn+mv) × 10 ratios showed no significant differences. However, all the calculated ratios showed significant differences among the various samples. In fact, despite the biosynthesis of anthocyanins in grape is both tissue- and species-specific, the anthocyanin biosynthetic pathway is regulated by different mechanisms among cultivars and tissues (Ageorges et al., 2006; Falginella et al., 2012).

ID	Compound	2018		2019		BE		ROS		VE		FE		AC		AO		LSC		RO		RC	
4	Delphinidin-3-*O*-glucoside	19.57	b	**44.10**	**a**	0.00	e	0.80	e	2.08	e	38.51	bc	**80.28**	**a**	45.47	b	21.18	d	34.62	c	40.17	bc
8	Cyanidin-3-*O*-glucoside	1.55	b	**4.18**	**a**	0.00	g	0.34	f	1.46	f	1.90	e	**7.83**	**a**	3.29	c	1.81	f	2.65	d	4.75	b
9	Petunidin-3-*O*-glucoside	18.83	b	**42.37**	**a**	0.00	e	1.07	e	4.12	e	46.33	b	**74.39**	**a**	42.84	bc	25.09	d	29.06	d	34.01	cd
12	Pelargonidin-3-*O*-glucoside	0.02	b	**0.05**	**a**	0.00	f	0.00	f	0.02	de	0.03	d	**0.08**	**a**	0.04	c	0.02	e	0.04	c	0.06	b
13	Peonidin-3-*O*-glucoside	9.05	b	**22.93**	**a**	0.00	d	2.46	d	13.43	c	22.68	b	**35.88**	**a**	23.30	b	4.83	d	14.23	c	21.44	b
16	Malvidin-3-*O*-glucoside	77.48	b	**173.83**	**a**	0.06	d	7.00	d	26.27	d	**318.45**	**a**	**263.98**	**a**	173.65	b	89.42	c	98.66	c	115.68	bc
25	Delphinidin-3-*O*-(6"-acetyl-glucoside)	4.83	b	**8.94**	**a**	0.00	e	0.02	e	0.29	e	14.02	ab	**14.77**	**a**	11.48	b	4.19	d	7.31	c	6.50	cd
37	Cyanidin-3-*O*-(6"-acetyl-glucoside)	0.96	b	**1.68**	**a**	0.00	d	0.02	d	1.18	bc	1.83	ab	**2.65**	**a**	**2.21**	**a**	0.84	c	1.37	bc	1.24	bc
39	Petunidin-3-*O*-(6"-acetyl-glucoside)	5.46	b	**11.42**	**a**	0.00	d	0.04	d	0.51	d	**19.75**	**a**	**18.45**	**a**	12.93	b	6.25	c	7.43	c	7.23	c
48	Malvidin-3-*O*-(6"-acetyl-glucoside)	25.30	b	**56.35**	**a**	0.00	d	0.15	d	2.56	d	**143.34**	**a**	75.05	b	60.89	b	23.13	cd	28.51	c	30.06	c
49	Peonidin-3-*O*-(6"-acetyl-glucoside)	3.35	b	**6.48**	**a**	0.00	d	0.06	d	3.20	bc	**11.54**	**a**	**9.13**	**a**	**8.88**	**a**	1.42	cd	4.56	b	4.64	b
55	Petunidin-3-*O*-(6-*p*-coumaroylgalactoside)	0.14	b	**0.22**	**a**	0.00	e	0.01	e	0.00	e	0.01	de	0.31	b	0.04	d	0.15	c	**0.36**	**a**	**0.38**	**a**
68	Delphinidin-3-*O*-(6-*p*-coumaroylglucoside)	1.95	b	**4.00**	**a**	0.01	d	0.04	d	0.30	d	3.56	b	**7.02**	**a**	4.05	b	1.32	c	3.70	b	4.47	b
69	Malvidin-3-*O*-(6"-caffeoylglucoside)	0.17	b	**0.40**	**a**	0.00	e	0.01	e	0.04	de	**1.26**	**a**	0.46	b	0.32	bc	0.14	de	0.17	cd	0.19	cd
76	Malvidin-3-*O*-(6-*p*-coumaroylgalactoside)	0.34	b	**0.54**	**a**	0.00	f	0.02	ef	0.01	f	0.01	f	0.74	c	0.11	e	0.36	d	0.87	b	**1.02**	**a**
78	Petunidin-3-*O*-(6-*p*-coumaroylglucoside)	2.16	b	**3.91**	**a**	0.01	c	0.03	c	1.41	c	3.99	b	**7.02**	**a**	4.43	b	1.66	c	3.28	b	4.02	b
82	Cyanidin-3-*O*-(6-*p*-coumaroylglucoside)	0.68	b	**1.27**	**a**	0.01	f	0.08	de	**1.79**	**a**	0.73	c	**1.81**	**a**	1.22	b	0.39	cd	1.07	b	1.27	b
87	Malvidin-3-*O*-(6-*p*-coumaroylglucoside)	11.19	b	**22.30**	**a**	0.01	f	0.10	f	2.50	ef	31.61	ab	**39.57**	**a**	26.63	bc	8.80	e	16.30	d	18.71	cd
91	Peonidin-3-*O*-(6-*p*-coumaroylglucoside)	1.98	b	**3.80**	**a**	0.00	d	0.13	d	3.89	bc	3.32	bc	**5.87**	**a**	4.27	b	0.76	d	2.91	c	4.07	bc
	Sum glucosides	126.74	b	**287.83**	**a**	0.08	d	11.68	d	47.39	d	**428.00**	**a**	**463.01**	**a**	289.13	b	142.54	c	179.73	c	216.63	bc
	Sum acetylglucosides	39.90	b	**84.87**	**a**	0.00	e	0.29	e	7.74	de	**190.49**	**a**	120.04	b	96.39	b	35.82	cd	49.17	c	49.67	c
	Sum coumaroylglucosides	18.44	b	**36.04**	**a**	0.02	e	0.40	e	9.92	de	43.24	b	**62.35**	**a**	40.76	b	13.44	d	28.50	c	33.95	bc
	3'5'OH activity	9.53	b	**11.35**	**a**	8.38	ef	2.45	g	3.73	g	16.94	b	12.31	c	9.85	de	**20.63**	**a**	9.85	d	7.46	f
	3'OMT activity	5.77	n.s.	5.83	n.s.	0.00	g	6.71	c	9.23	b	**10.76**	**a**	7.54	c	7.06	c	3.03	f	5.44	d	4.28	e
	5'OMT activity	4.96	n.s.	5.22	n.s.	0.00	f	9.49	b	**12.62**	**a**	8.94	b	4.84	c	3.81	cd	4.39	c	2.83	e	2.88	de
	(dp+cy+pt/pn+mv) × 10 activity	4.01	n.s.	4.25	n.s.	1.30	c	2.28	c	1.94	c	2.42	c	4.48	b	4.71	b	5.08	ab	**6.04**	**a**	5.83	ab

Table 12. Two-way ANOVA of minor and commercial wines of vintages 2018 and 2019. All values are expressed in mg L^{-1} for molecules and sums. The values of all the indexes are absolute values. Classification was done for $p<0.05$. n.s. = not significant.

Both vintages were characterized by high temperatures. Indeed, during 2018, the maximum temperatures in the provinces of Modena and Reggio Emilia increased to about 2 °C, as compared to the reference period of 1961-1990. The warm days (with a temperature over 30 °C) in the flat and hill zone were about 60-70 days and 50-60 days, respectively (Arpae, 2019). Moreover, there was a decrease in the total rainfall in both flat and hilly zones, up to -550 mm. For what concern the tropical nights (minimum temperature over 20 °C), values of 5-10 in the hilly zone, and up to 20 in the flat zone were recorded. During the whole *veraison* period, the temperatures were over 30 °C, with absolute temperatures between 36 and 37 °C, in the whole flat zone, while the rainfall events were occasional. During 2019, the maximum temperatures in the provinces of Modena and Reggio Emilia increased to about 1.7 °C, as compared to the reference period of 1961-1990. The warm days in the flat and hilly zones were about 35-50 days and 10-30 days, respectively. However, 2019 showed a positive rain balance (+173 mm), but without a significant variation as compared to the reference period of 1961-1990 (Arpae, 2020). For what concern the tropical nights (minimum temperature over 20 °C), were recorded values of 5-15 in the hills zone, and up to 30 in the flat zone. During the *veraison* period, the temperatures rose above 30 °C just for ten days, with peaks up to 37-38 °C, in the whole flat zone, while the intensive rainfall events increased the water availability, thus interrupting the warm period. The main characteristics are represented in Figure 22.

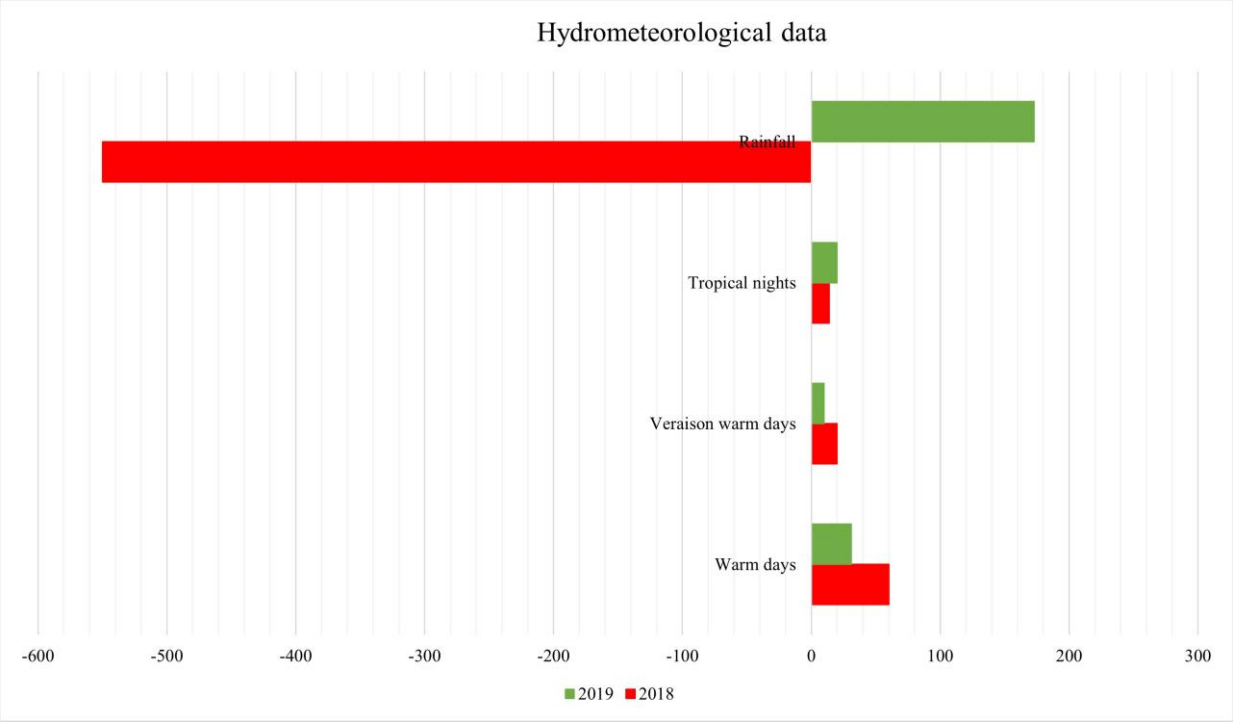

Figure 22. Hydroclimatic data of vintages 2018 and 2019. Rainfall data are expressed in mm, while the other data are expressed as number of days/nights.

Anthocyanins have several functions in plants, such as pollinator attraction, protection against pathogens and pests and UV light-induced damage (Landi et al., 2015; Sivankalyani et al., 2016). Indeed, environmental stresses may trigger the accumulation of anthocyanins (Downey et al., 2006). An increased temperature in plants improves the rate of metabolic processes, thus increasing both growth and metabolite accumulation (Ebadi et al. 1995, Dokoozlian and Kliewer 1996). Anthocyanin biosynthesis shows the maximum activity in the first weeks after veraison and it is regulated by both light exposure and temperature (Haselgrove et al., 2000). Nevertheless, metabolic processes can be stopped and/or remarkably reduced by high temperatures (Downey et al., 2006; Jones 1992). Probably, this threshold in grapevines is ~30 °C (Coombe 1987), while at 35 °C it starts the degradation of anthocyanins (Shaked-Sachray et al., 2002). Other environmental stresses that negatively affect anthocyanins content are UV radiation, water deficits, low temperatures, osmotic stress, wounding and pathogens (Alonso et al., 2016; Bonada et al., 2015; Kawahigashi et al., 2016). In fact, the grape peel is more affected than the juice by agronomic techniques and environmental conditions (Ribéreau-Gayon et al., 2006a). This negative effect is probably enhanced in organic farming since the use of pesticides and fertilizers is very limited (Reg. CE 834/07). Thus, these events prejudice anthocyanin and sugar accumulation, as well as the alcohol and the color content of wines (Sadras and Moran 2012). However, the effect of temperature is still widely discussed, but any definitive cause-and-effect relationship was found (Jones et al., 200; Vrsic et al., 2012). In addition to the vintage effect, the total content (from 500 mg kg^{-1} up to 3 g kg^{-1}) and the proportions of each anthocyanin are varietal characteristic and may be used to some extent as chemotaxonomy criteria (Mazza and Miniati, 1993; Roggero et al., 1988).

Moreover, polyphenols in general and anthocyanins in particular are a strong expression notonly of the cv. but also of the whole winemaking process as well as of the seasonal climate. Unfortunately, samples were collected in commercial wineries. For this reason, it is difficult taking into consideration the influence of the vinification practices and the age of the wines. Often the cogent necessity compels wineries to make unforeseen operation, such as racking or SO_2 adding, that compromise the scheduled experiments and we can only make obvious observations. In fact, as explained above, each winery can variate the process, especially the length of the maceration step, to accomplish a specific product, depending on the general quality of the grape and the vintage. Hence, the main consideration is that the anthocyanins content of all wines produced through the red winemaking process, which were Ancellota conventional and organic wines produced by Cantine Riunite & CIV and Festasio wine produced by CRPV, was higher than the white vinified ones, which were Rossissimo conventional and organic wines, L. Salamino conventional and organic wines produced by SMR, as expected. Concerning the wines Veruccese and Rossiola

produced by CRPV, they showed a low content of anthocyanins as compared to the other wines, suggesting that this difference is mainly due to the variety rather than the process. For what concern the Bertinora wine produced by CRPV, it showed a very low anthocyanins content, as expected, despite it was white vinified. Thus, these results demonstrated that this white variety contains traces of anthocyanins in the flesh of the berries. In addition, since the variety is characterized by a partially pigmented peel, it may be interesting to do further studies about the same wine produced through a red winemaking process.

According to previous studies and with the preliminary metabolomic results, conventional wines have a higher anthocyanins content than organic ones (Tassoni et al., 2014). However, the literature about organic wines and their discrimination by using HRMS analyses is still scarce (Cravero, 2019).

Regarding to the variety effect, Ancellotta conventional showed the highest values for the molecules 4, 8 9, 12, 13, 16, 25, 37, 39, 49, 68, 78, 82, 87, 91, as well as for the sum of 3-*O*-monoglucosides and the sum of -3-*O*-(6-*p*-coumaroylglucosides). Ancellotta organic showed a similar value to Ancellotta conventional for the molecules 37 and 49. Rossissimo organic showed the highest values for molecule 55 and for the (dp+cy+pt/pn+mv) × 10 activity. The high value of this ratio indicates the highest relative content of the anthocyanins with antioxidant properties, (Vasile Simone et al., 2013). Rossissimo conventional showed the highest values for molecules 55 and 76. L. Salamino conventional showed the highest value only for 3'5'OH activity, indicating a darker and more stable color (Mattivi et al., 2006). As expected, Ancellotta wines showed the highest anthocyanins content, especially the red vinified ones.

To the author's knowledge, this is the first study that anthocyanins molecules are reported for minor wines Festasio, Veruccese, Rossiola and Bertinora.

Festasio showed a content comparable to Ancellotta conventional for molecules 16, 39, 49, as well as for the sum of glucosides. Moreover, Festasio showed the highest values for molecules 48 and 69 and for the sum of 3-*O*-acetylmonoglucosides. However, Festasio showed a 3'5'OH activity higher than 3'OMT activity and 5'OMT activity, that is a typical trend of Ancellotta variety, due to the high content of delphinidin and petunidin derivatives (Mattivi et al., 2006; Vasile-Simone et al., 2013). Veruccese showed a value of molecule 82 comparable to Ancellotta conventional and the highest value for the 5'OMT activity, indicating a higher content of molecules 16 and 13 (Mattivi et al., 2006).

Compounds 16, 48 and 87 showed a good discriminant capacity of different wines and winemaking processes, according to Pisano et al. (2015).

Compounds 12 was detected in Ancellotta, in the form of monoglucoside, but usually it is rarely detected because of its low concentration (Garcia-Herrera et al., 2016; Maul et al., 2017; Trang et al., 2019). Thus, the use of HRMS techniques such as the Q-Exactive Orbitrap can enhance the detection of less concentrated compounds, since compound 12 was detected in all analyzed red wines.

Even if the acylated anthocyanins' content varies according to the variety, in *Vitis vinifera* wines the acylated anthocyanins disappear a few months after fermentation because of the presence of the ethanol, which reduce the copigmentation; thus, these compounds are not the most indicated to identify grape varieties (Ribéreau-Gayon et al., 2006b; Ribéreau-Gayon et al., 2018a).

To better explain the vintage effect and the differences between different varieties, PCA analysis for commercial wines (Figures 23 and 24) was done separately from PCA of minor wines (Figures 25 and 26). PCA for Ancellotta wines separated red vinified Ancellotta conventional (2019) along PC1, that explained 75.35% of total variance, according to data shown in table 18. PC2 explained 16.18% of total variance: in particular, PC2 separated red vinified wines (negative side of PC2) from white vinified wines (positive side of PC2).

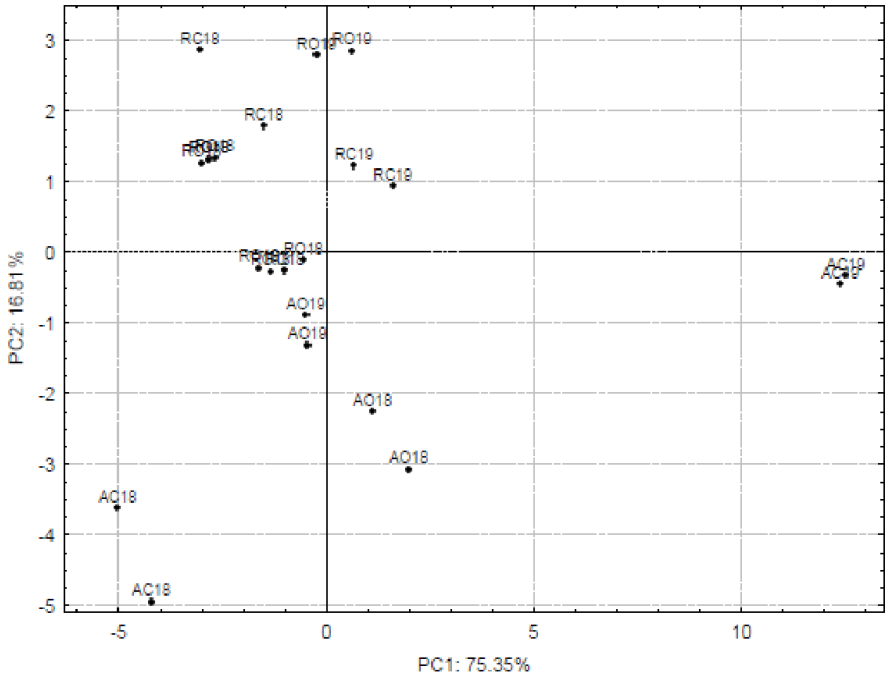

Figure 23. Scores plot for PC1 × PC2 of Ancellotta wines.

Red vinified Ancellotta conventional (2019) moved in the direction of all the main molecules along the PC1, according to the loading plot (Figure 24). All the other red vinified wines, especially Red vinified Ancellotta conventional (2018), oved along PC2 in the direction of 3'5'OH, 3'OMT and 5'OMT activities. All white vinified wines moved in the opposite direction of De+Cy+Pe/Mv+Pe × 10, even if the replication of 2019 also showed a higher level for malvidin-3-*O*-(6-*p*-coumaroylgalactoside) and petunidin-3-*O*-(6-*p*-coumaroylglucoside).

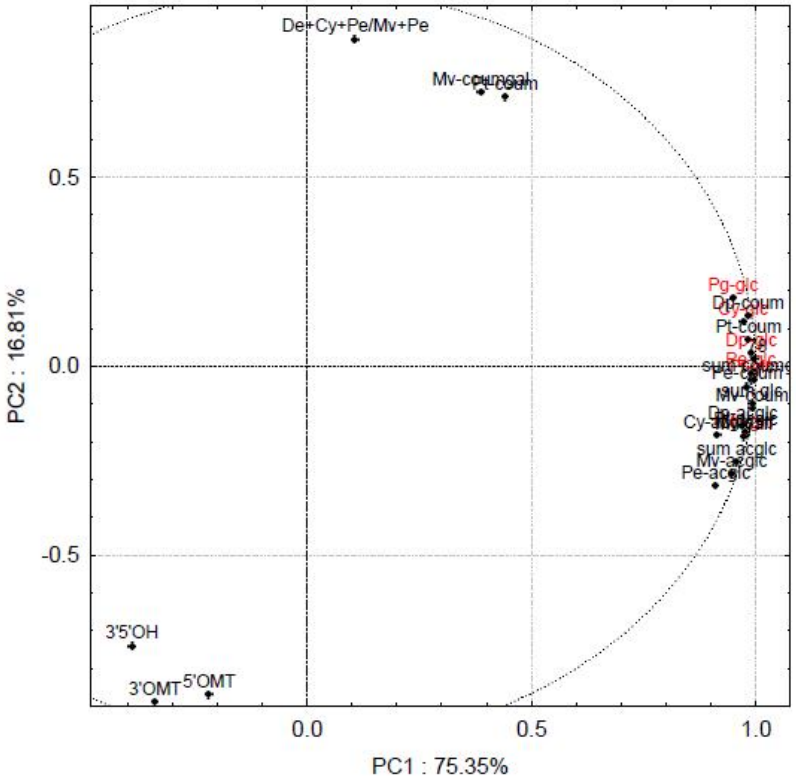

Figure 24. Loadings plot for PC1 × PC2. Main monoglucosides are highlighted with red labels.

Concerning minor wines, PCA analysis (Figure 25) explained 73.57% of total variance on PC1 and 13.17% of total variance on PC2. Bertinora and Rossiola showed similar characteristics in both vintages and resulted with the lowest anthocyanins content, even though they were produced through a white and red winemaking process, respectively. Veruccese showed different content of anthocyanins, that was higher during 2019, moving along PC2 in the direction of malvidin-3-*O*-(6-*p*-coumaroylgalactoside) and 5'OMT activity, as shown in the loadings plot (Figure 26). Festasio, even if it always showed a higher content of anthocyanins, in 2018 its content was not so different compared to the other wines, confirming the negative effect of 2018. However, during the second vintage the anthocyanins content was remarkably higher than the first one. Indeed, it moved in the direction of malvidin, petunidin and delphinidin-3-*O*-glucoside, their acetyl- and coumaroyl-derivatives and their sum (Figure 25).

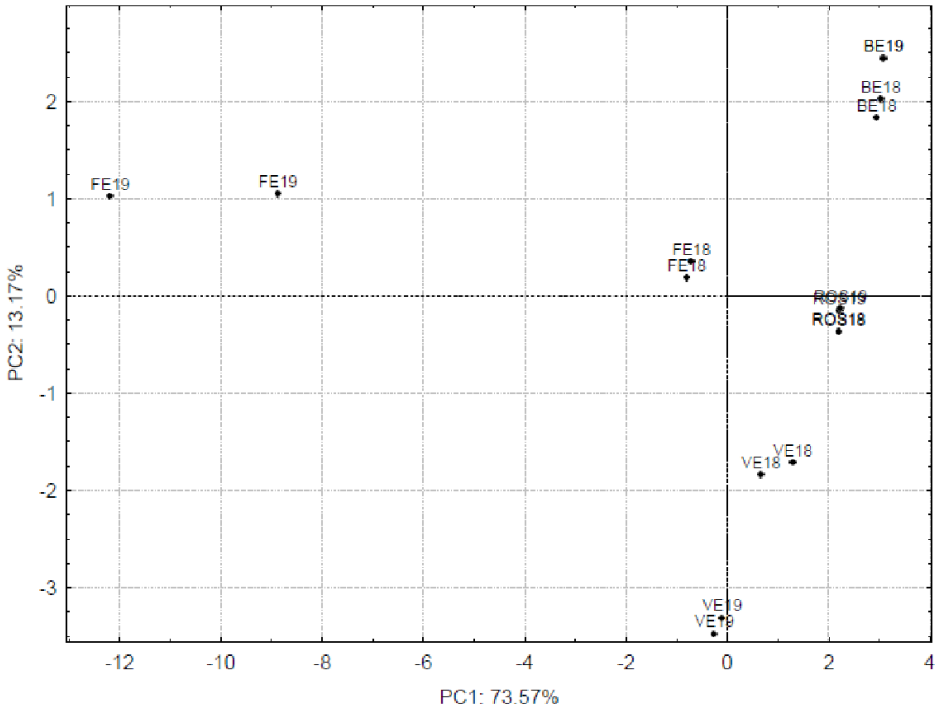

Figure 25. Scores plot for PC1 × PC2 of minor wines.

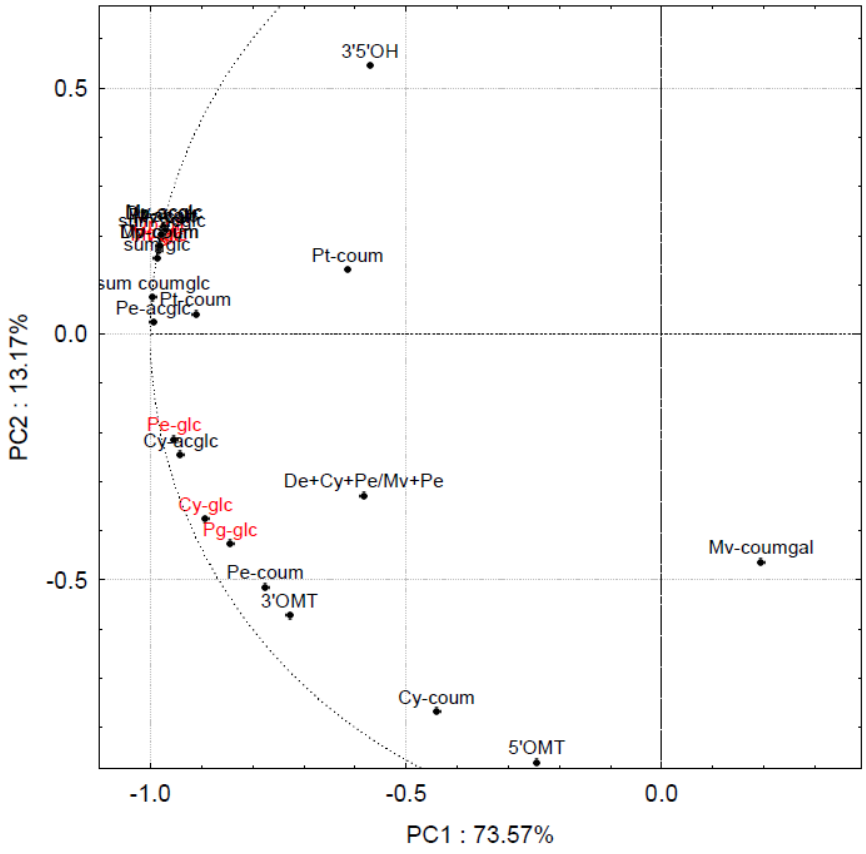

Figure 26. Loadings plot for PC1 × PC2 of minor wines.

3.3.3 XCMS analysis

Initially, raw data uploaded on XCMS platform led to the identification of more than 30,000 features, in accordance with other studies (Arapitsas et al., 2012, 2016). The application of the parameters listed in 2.9.3 allowed the untargeted analysis to reduce the identification down to 2,616 features with a *p*-value lower than 0.01. For this reason, an effective and fast processing of the data set was adopted through a more restrictive selection of the significant features, as an alternative to the download, post-processing and the subsequent statistical analysis, as suggested by Vaclavik et al., (2011). Nevertheless, this high number of statistically significant features was still too high to permit some statistical treatment via XCMS, such as the interactive heatmap, that admit a maximum number of features equal to 1,000.

Interactive PCA tool of the XCMS platform permitted to change the number of considered features in both scores and loadings plots and to set different scaling parameters. The PCA obtained using the Multigroup Job mode was shown in Figure 27. PC1 and PC2 explained 52% and 12% of the total variance, respectively. The relevant difference in anthocyanins' concentrations grouped the samples of the two vintages in two macro-clusters along the PC1 Despite the weaker difference shown by the samples, however, they maintained their identity and separated on the PC2.

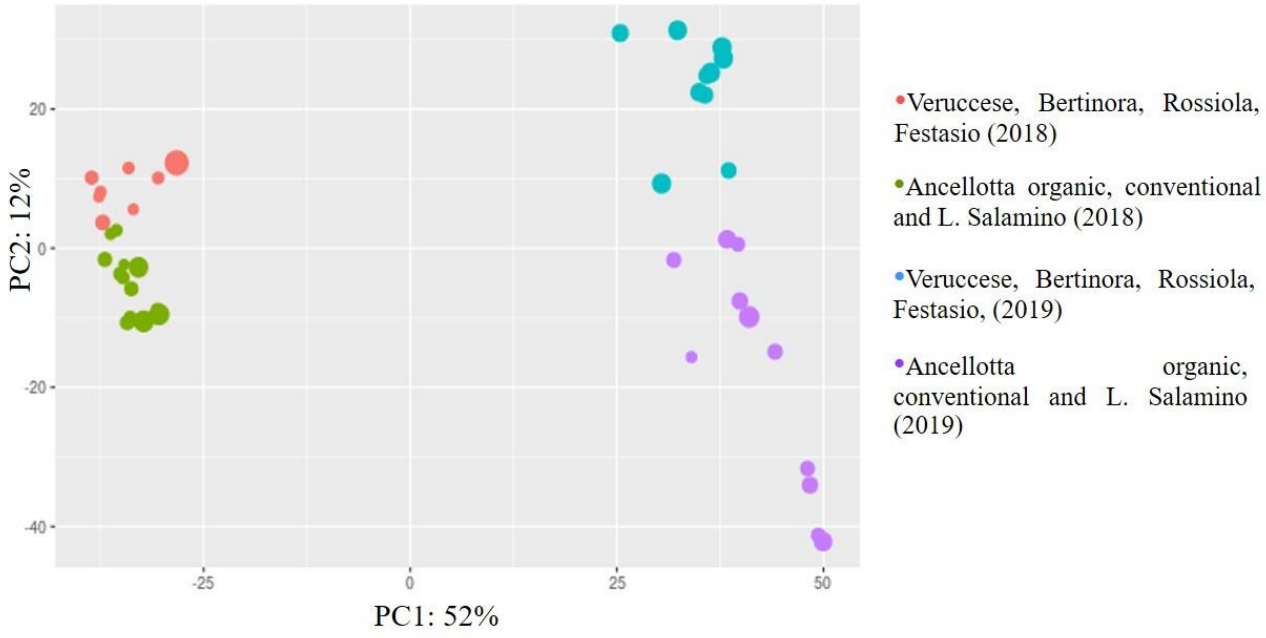

Figure 27. PCA analysis of multigroup analysis for PC1 × PC2. The dimension of each point represents the value Dmodx. The bigger it is, the higher it is the probability that the sample is a moderate outlier.

The features are more concentrated in the right part of the loading plot (where all the samples of the 2019 vintage are placed; Figure 28). This plot shows that the samples of the 2018 vintage are characterized by a lower number of features which are different from those that distinguish the 2019 vintage. This profile seems to be due to adverse weather conditions occurring in the 2018 vintage. Furthermore, in the 2019 vintage the samples showed a higher profile variability in comparison with the flattening of the peculiar characteristics occurred in 2018.

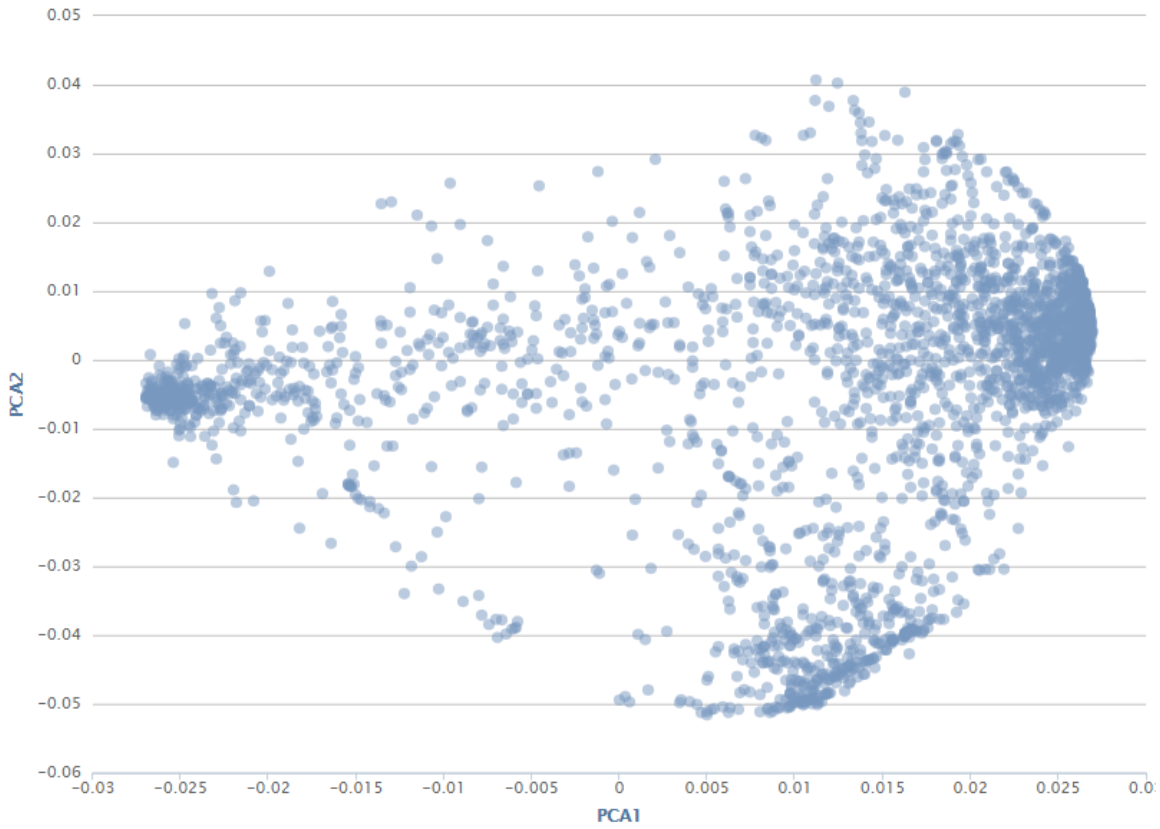

Figure 28. Loading plot for PC1 × PC2 of the 2,616 detected features.

A more careful observation allowed to confirm in both vintages the similarity of the Festasio anthocyanin profile with the Ancellotta wines vinified in red (Figure 29). However, it is clear that the vintage effect can seriously affect the quality of wines, thus reducing the peculiar differences among the varieties.

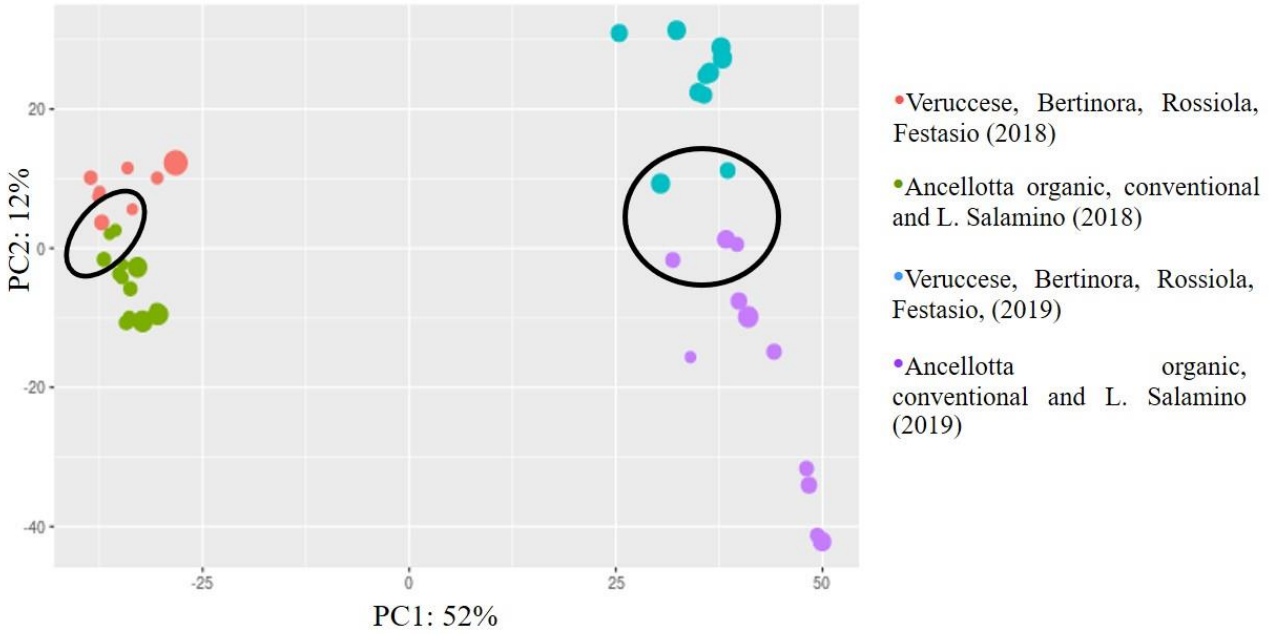

Figure 29. Location of Festasio and Ancellotta wines.

Metlin database (embedded in XCMS) permitted the identification of compounds rarely or never detected in wine. In fact, for each significant feature detected, the name, the retention time, the *m/z* ratio and the peak of each sample analyzed were indicated as output results. In particular, cyanidin-3-*O*-sambubioside (Rt 12.99, *m/z* = 582.1566) was detected in all the wines considered (Figure 30). This molecule is a trisaccharide anthocyanin found in flowers and fruits of herbaceous or shrubs plants (Andersen and Markham, 2006; Yousof et al., 2018) and it was a highly significant feature ($p<0.001$). Moreover, it was particularly abundant in commercial wines, especially in vintage 2019, while less abundant in minor wines (Figure 31).

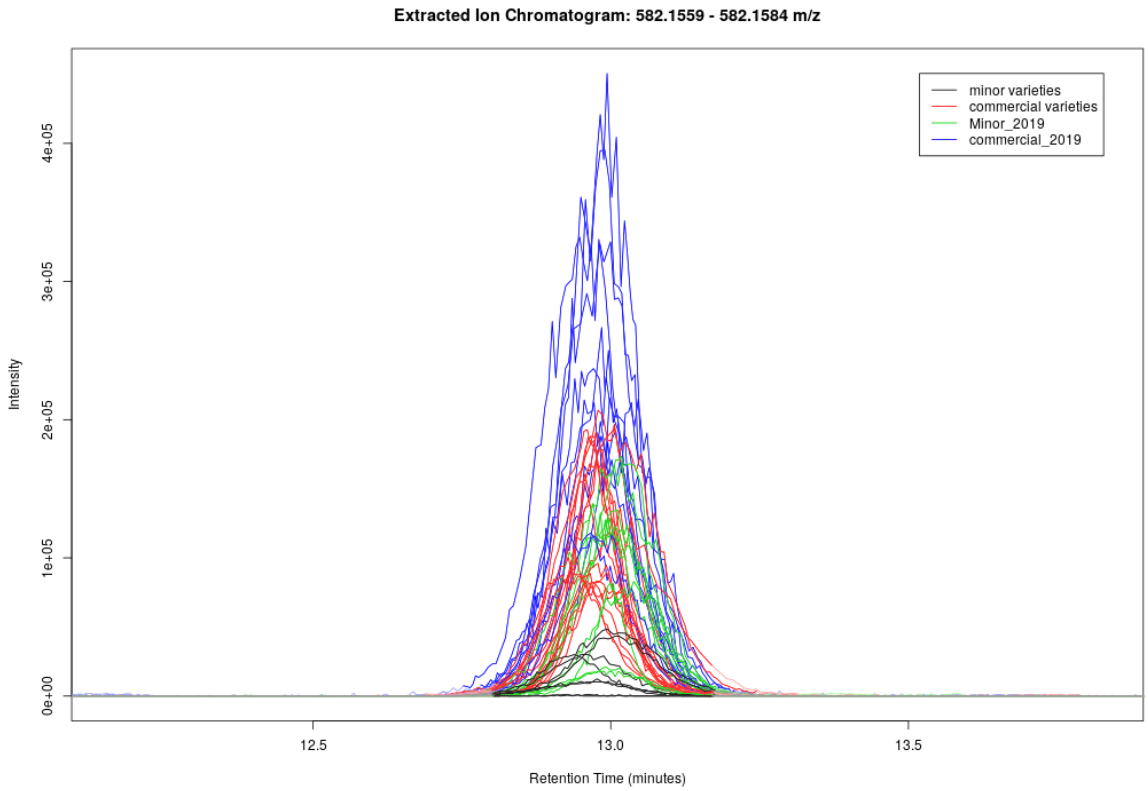

Figure 30. Aligned peaks of cyanidin-3-*O*-sambubioside of the whole dataset produced by the platform XCMS. Each peak represents a single sample, and each color represents a different dataset.

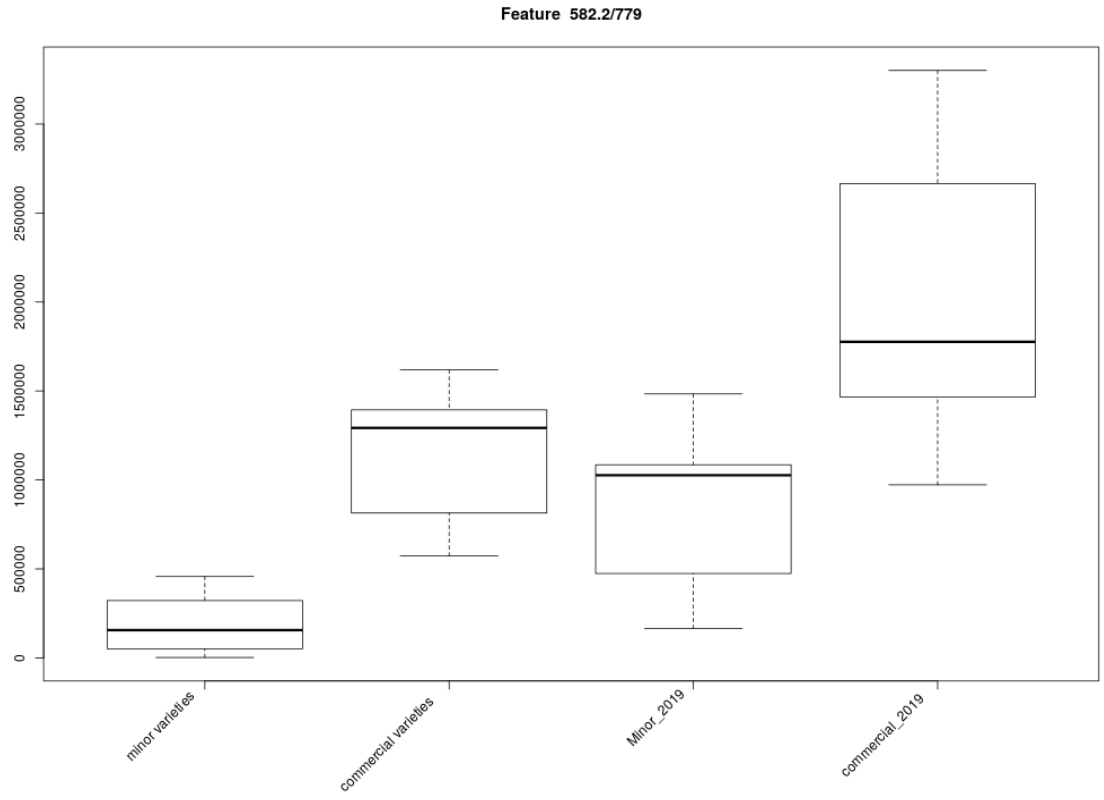

Figure 31. Error bars of the different analyzed group of wines for cyanidin-3-*O*-sambubioside.

Malvidin-3-*O*-glucoside-4-vinylphenol (Rt = 36.21, *m/z* = 609.1605) (Figure 32) was a highly significant feature (*p<0.001*) and particularly concentrated in commercial wines, meanwhile it showed a low concentration down to non-detection in minor ones (Figure 33). This is an anthocyanin-vinyl derivative, so its presence is not only related to the grape variety, but also to the conditions of aging and availability of the vinyl to form the adduct. Indeed, the low concentration of vinylphenol in red wines is principally due to the inhibition of cinnamate decarboxylase of yeasts by certain phenolic compounds of grape (Chatonnet et al., 1989, 1993). In the same figure, there is also a possible isomer of the molecule (Rt = 35.59, *m/z* = 609.1604), although it resulted as a non-significant feature (*p* = 0.035), according to the method.

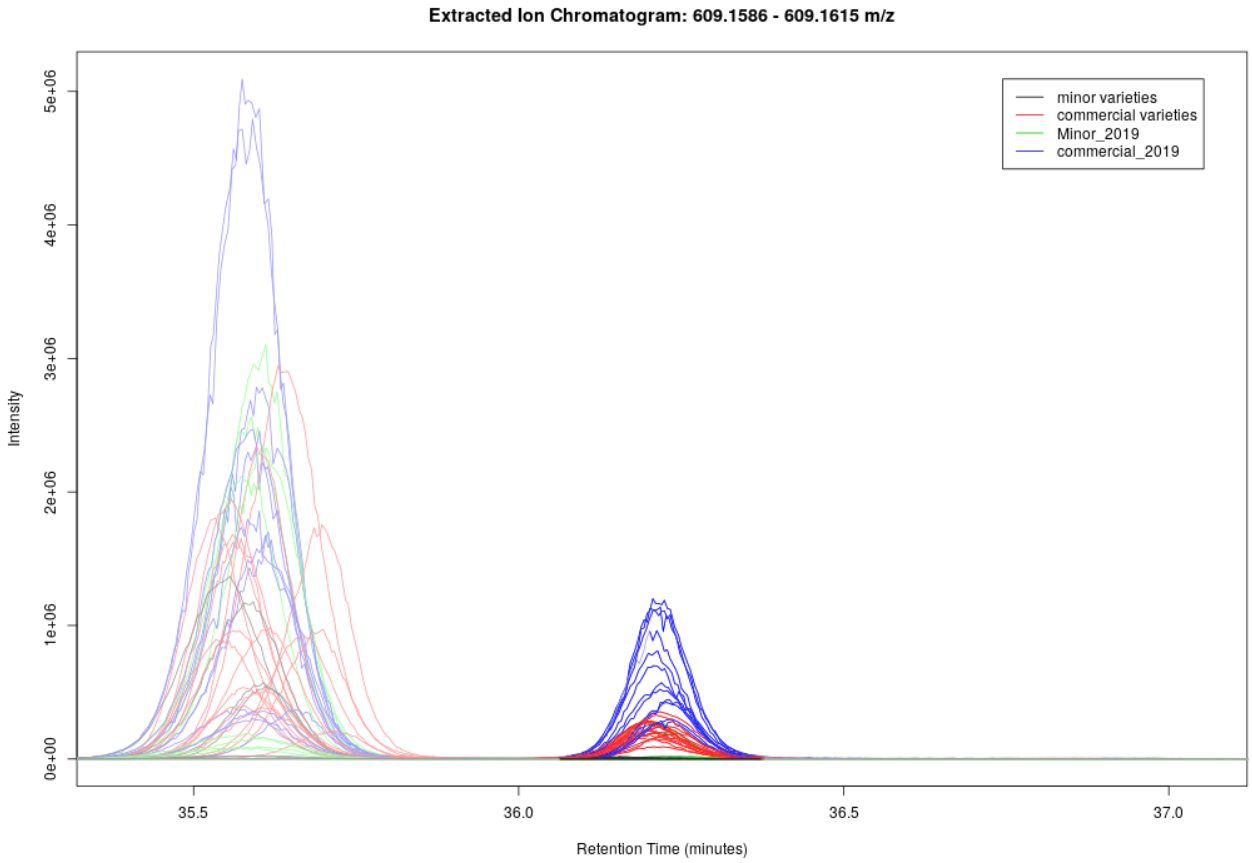

Figure 32. Aligned chromatograms of malvidin-3-*O*-glucoside-4-vinylphenol produced by the platform XCMS. Each peak represents a sample, and each color represents a different dataset.

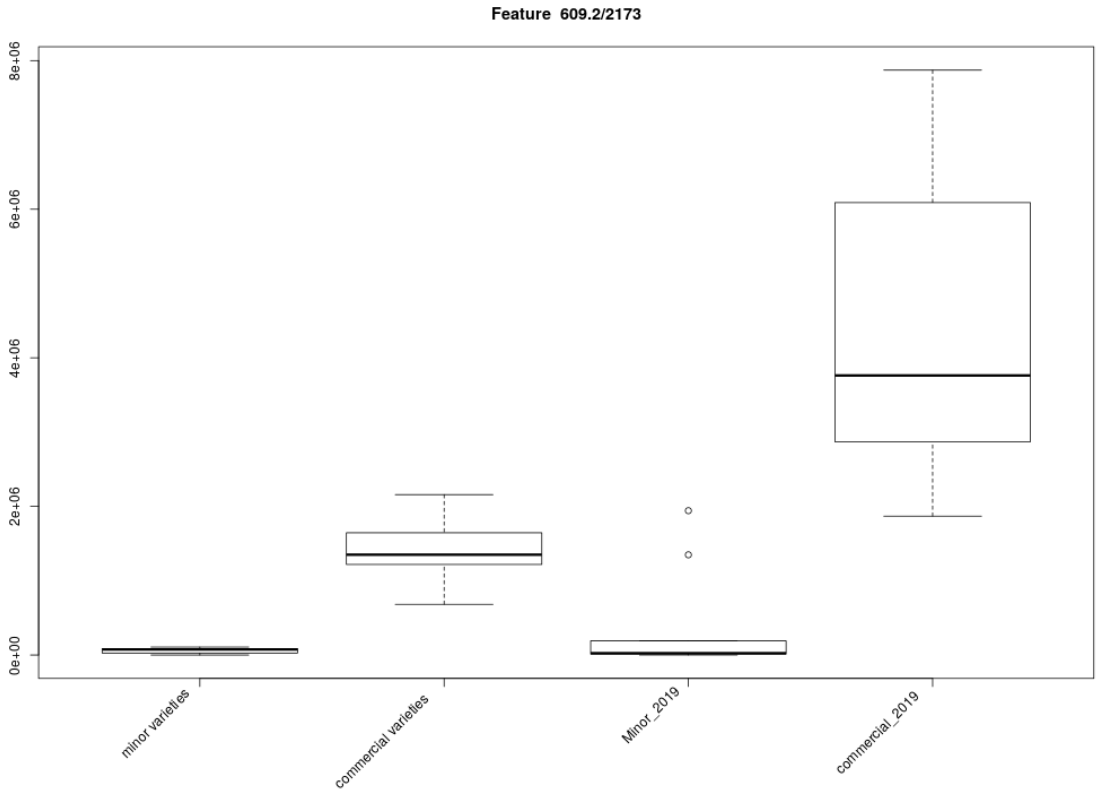

Figure 33. Error bars of the different analyzed group of wines for malvidin-3-*O*-glucoside-4-vinylphenol.

3.4 NMR analysis

3.4.1 NMR 400 MHz

Main components of wine present in the anomeric region (3.15-5.50 ppm) such as glycerol, organic acids, amino acids and residuals of ethanol and sugars, represented the most intense signals. PCA analysis (Figure 34) separated white wines from the red ones along PC1 (19.19%), while white wines separated along the PC2 (12.50). The low variance explained by each PC may be due to the large diversity of the dataset. Indeed, Vernaccina (19), Bertinora (20), Vernaccia del viandante (23), Melara (22) and Pignoletto of Riunite (Campegine) (33-34) showed similar characteristics. Compared to this group, Caveccia (24), Albariño (17) and Gewürztraminer (16) showed slight differences. Conversely, Pignoletto wines from Castelfranco E. winery (1-5) were completely separated from the other ones. In particular, Pignoletto (3-5) showed an interesting separation due to the higher content of sugars (9 g L^{-1}) compared to the base wine (1-2), which has only 3 g L^{-1}.

Concerning red wines, they completely gathered in the negative side of PC1, excepting for Veruccese (18) and Rossiola (21). Festasio (25) showed similar characteristics to L. Reggiano (6-7) and L. Grasparossa (8-9). Moreover, L. Salamino (31-32), red vinified Ancellotta (10-11), Cabernet Sauvignon (12), Tempranillo (13), Merlot (14) and Syrah (15) showed similar characteristics. In addition, white vinified Ancellotta conventional (30) showed very different characteristics compared to the organic ones (26-29). These differences can be explained by the vintage effect and by the different winemaking process (Section 3.3.2).

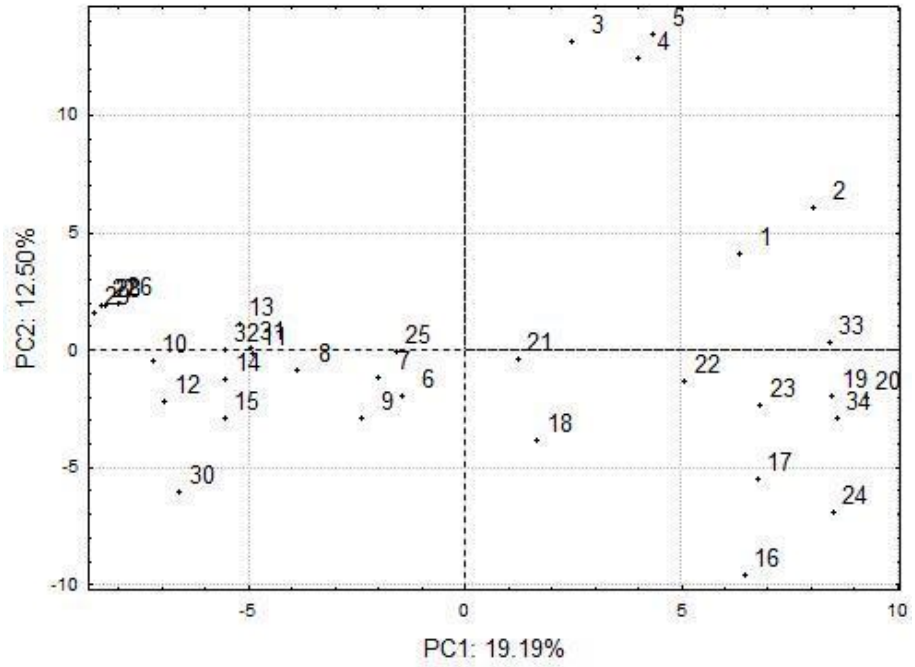

Figure 34. Scores plot of the whole dataset, considering the entire spectra.

Main compounds of the anomeric region (3.15−5.50 ppm), phenolic compounds of the aromatic region (5.5-8 ppm) and several minor compounds and were identified according to ^{1}H-NMR spectra (Table 13; Anastasiadi et al., 2009; Ali et al., 2011; Fotakis et al., 2013; López-Rituerto et al., 2012; Papotti et al., 2012).

ID	Compounds[a]	^{1}H chemical shifts (δ)[b]	Group
1	leucine	0.89 (d)	C_5H_3, C_6H_3
2	2,3-butanediol	1.15 (d)	C_1H_3, C_4H_3
3	lactic acid	1.38 (d) 4.31 (m)	C_3H_3 C_2H
4	threonine	1.49 (d) 4.57 (m)	C_4H_3 C_3H
5	alanine	1.55 (d)	C_3H_3
6	proline	2.01 (m) 2.13 (m) 2.36 (m)	C_4H_2 C_3H C_3·H
7	acetic acid	2.08 (s)	C_3H_3
8	succinic acid	2.63 (s)	C_2H_2, C_3H_2
9	citric acid	2.80 (d) 2.95 (d)	C_2H, C_4H C_2·H, C_4·H

10	malic acid	2.91 (dd) 2.96 (dd) 4.57 (dd)	C_2H $C_{2'}H$ C_3H
11	*β*-glucose	3.52 (t) 4.59 (d)	C_2H βC_1H
12	tartaric acid	4.68 (s)	C_2H, C_3H
13	*α*-glucose	5.20 (d)	αC_1H
14	ethanol	1.19 (t)	C_2H_3
15	glycerol	3.57 (m) 3.66 (m) 3.79 (m)	C_2H C_3H_2 C_1H_2
16	fructose	4.07 (m)	C_3H, C_4H, C_5H
17	gallic acid	7.07 (s)	H2, H6
18	(+)-catechin	2.51 (dd) 4.55 (d) 5.87 (d) 6.86 (d)	H4 H2 H8 H2’
19	kaempferol	6.58 (d) 8.08 (d)	H8 H2’, H6’
20	caftaric acid	5.34 (s)	
21	*p*-coumaric/*trans*-coutaric acid	6.43 (d)	αCH
22	*cis*-*p*-coutaric acid	6.94 (d)	C3H/C5H
23	unknown	7.15 (s)	
24	*cis*-resveratrol	7.18 (d)	H2’, H6’
25	2-phenylethanol	7.31 (m)	ring
26	*trans*-resveratrol	7.37 (d)	H2’, H6’
27	*p*-coumaric acid	7.45 (d) 7.50 (d)	H2, H6
28	*p*-coumaric acid/ *trans*-caftaric acid	7.56 (d)	C2H/C6H
29	quercetin	7.73 (d)	H2’
30	ferulic acid	7.68 (d)	H-α
31	malvidin-3-*O*-glucoside	7.96 (s)	6’ (aglycon)

		8.82 (s)	4 (aglycon)
32	delphinidin-3-*O*-glucoside	6.82 (s) 7.66 (s)	6 (aglycon) 2',6' (aglycon)
33	petunidin-3-*O*-glucoside	6.84 (s)	6 (aglycon)
34	unknown	7.97 (s)	
35	unknown	8.14 (s)	
36	unknown	8.58 (s)	
37	arginine	8.23 (s)	
38	niacine	8.81 (dd) 9.10 (s)	C4H, C6H C2H

Table 13. [a]Assignments were done according to the literature.[b]Peak multiplicities in parentheses: s, singlet; d, doublet; t, triplet; dd, doublet of doublets; m, multiplet

In Figure 35 the most abundant compounds are represented. Since the intensity of each signal is proportional to the number of nuclei (Sparkman et al., 2011), the most important compounds were glycerol, ethyl alcohol, succinic acid (8), lactic acid (3), acetic acid (7) and proline (6). Generally, the total amount of citric acid (9) and malic acid (10) was very low. As expected, the lyophilization process permitted the simplification of the spectra, limiting broadband signals. However, traces of alcohols such as 2,3-butendiol (2) and 2-phenethyl alcohol (24, Figure 33) were found.

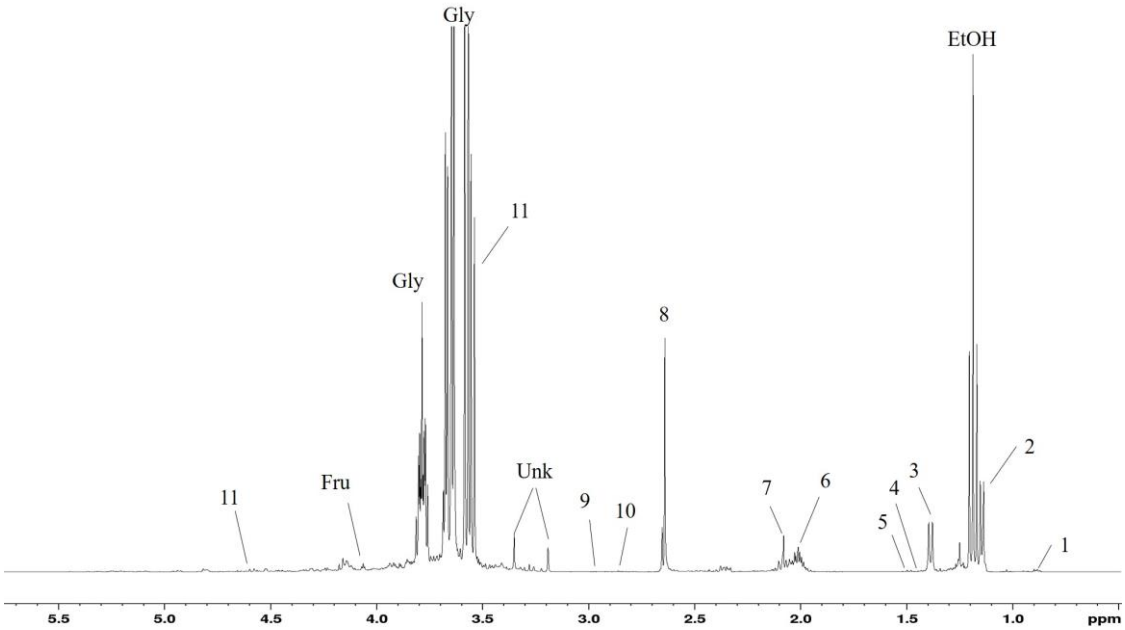

Figure 35. Main compounds of the anomeric region detected in Cabernet Sauvignon. Figure is out of scale in order to permit the identification of less concentrated compounds. Numbers are referred to table 13.

Low signal region after 5.5 ppm, where all molecules with aromatic rings (anthocyanins and flavonoids) are located permitted the identification of several polyphenols (Figure 36).

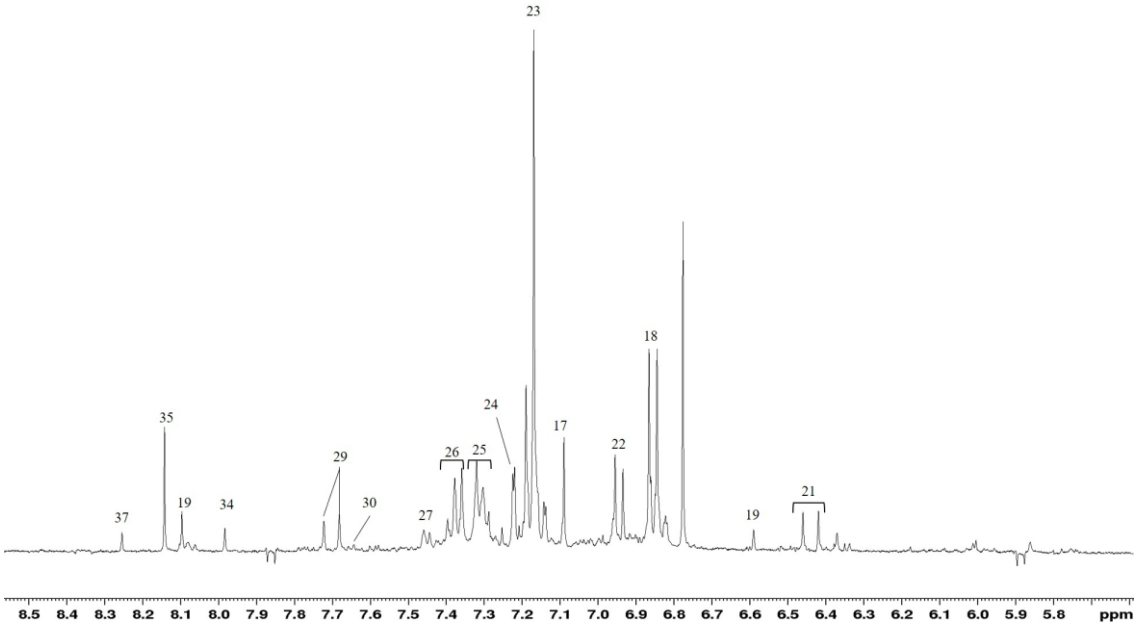

Figure 36. Main compounds of the aromatic region detected in Vernaccia del Viandante. Figure is out of scale in order to permit the identification of less concentrated compounds. Numbers are referred to table 13

As a consequence, PCA permitted to distinguish different groups in the dataset, according to the aromatic region of each spectra. In Figure 37, PC1 and PC2, which explained 22.32% and 11.77% of the total variance, respectively, is reported. In this case, Pignoletto wines from Castelfranco Emilia showed very similar characteristics, with slight differences between commercial wines (3-5) and base wines (1-2). Concerning all the other commercial and white wines, they showed similar characteristics, excepting for Bertinora (20), that was separated from the group along PC2. About red wines, more appreciable differences were shown. Indeed, the main group was near the origin of PCs, then dispersing along the negative side PC1 and lightly along PC2. Near the origin were located L. Reggiano conventional and organic (6 and 7, respectively), L. Grasparossa conventional and organic (8 and 9, respectively), Ancellotta conventional (11), Festasio (25), Cabernet Sauvignon (12), Tempranillo (13), Merlot (14) and Syrah (15). In particular, wine 7 showed similar characteristics to wine 14; wine 8 showed similar characteristics to wine 12; wine 9 showed similar characteristics to wine 15; wine 25 showed similar characteristics to wine 11. Ancellotta organic (10) differentiated from the main group exactly along PC1. However, L. Salamino (31-32) and all white vinified Rossissimo organic wines were clearly separated from the other red wines, confirming again the differences due to organic farming and oenological process. Rossiola (21), separated from the main group in the positive side of PC1, showing intermediate phenolic characteristics between red and white wines. Finally, Veruccese (18) and Rossissimo conventional

(30) showed a completely different quantity and quality of signals: in the first case, difference is probably due to the specific phenolic pattern of the variety; in the second one, the difference is mainly due to the specific batch and to the integrated farming, that permit to promptly manage the most of disease and nutrition lack, ensuring a good production.

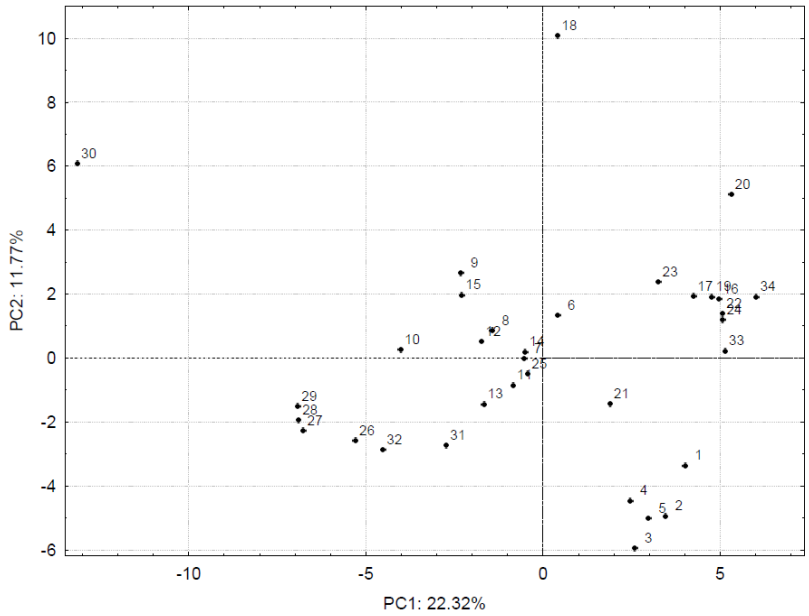

Figure 37. Scores plot for PC1 × PC2 of the aromatic region.

Regarding PC3, it explained 11.70% of the variance (Figure 38). Basically, all red and white wines were significantly separated, forming two isolated groups. Ancellotta organic (10) showed slightly different from other red wines. However, a substantial difference was demonstrated by L. Salamino (31-32), Rossissimo organic wines (26-29) and especially by Rossissimo conventional (30).

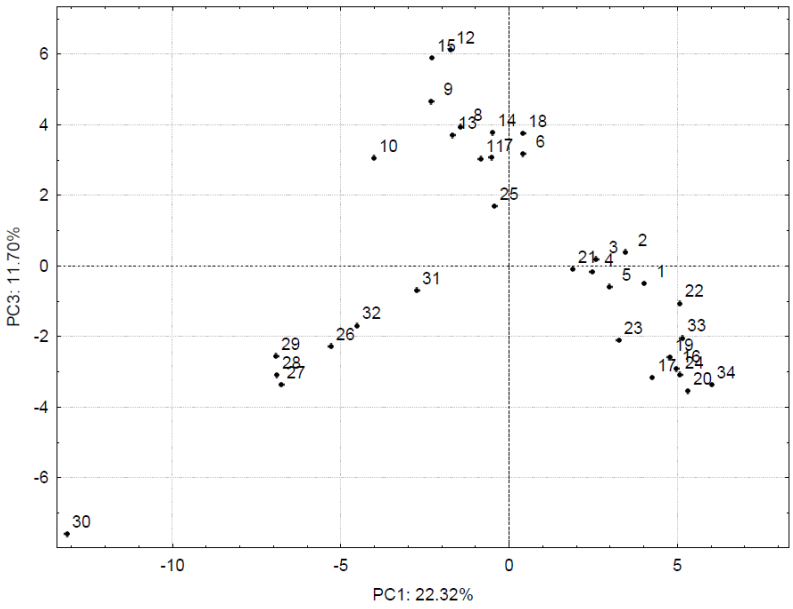

Figure 38. Scores plot for PC1 × PC3 of the aromatic region.

3.4.2 NMR 600 MHz

The analyzed spectra showed a good separation with PCA analysis. In fact, PC1 and PC2 explained the 73.58 % and the 14.88 % of the total variance, respectively. A first interpretation of the score plot permitted a macro-separation between sweet wines and dry Malvasia wines (Figure 39). This separation is due to the great abundance of signals located in the anomeric region (3.15−5.50 ppm), representing the most abundant compounds (alcohols, organic acids and sugars) of wine.

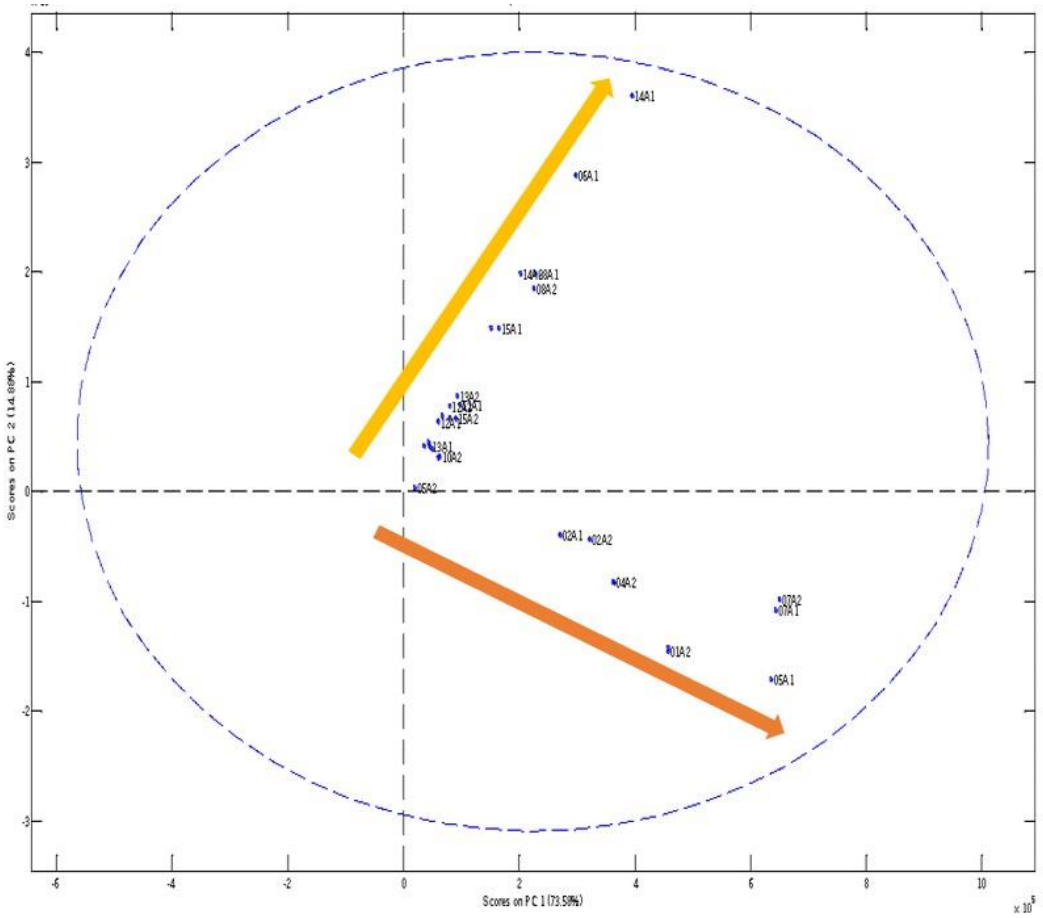

Figure 39. Differentiation between sweet wines (orange arrow) and dry wines (yellow arrow).

Subsequently, dry wines could be distinguished according to their oenological process (Figure 40). In fact, organic wine 14, produced by a soft pressing and a long Charmat process with *batonnage*, was completely separated from all the other wines. In particular, it was very different from wine 15, that was also refined for 6 months with *batonnage*, but with a shorter fermentation. Moreover, wine 06 was produced with 80% of a Charmat wine and 20% a long-aged wine in wood barrels, showing thus intermediate characteristics, as compared with wine 14 and wines produced through a short cryomaceration (08). Finally, all wines produced with a short Charmat winemaking (03, 09, 10, 11, 12, 13) showed very similar characteristics.

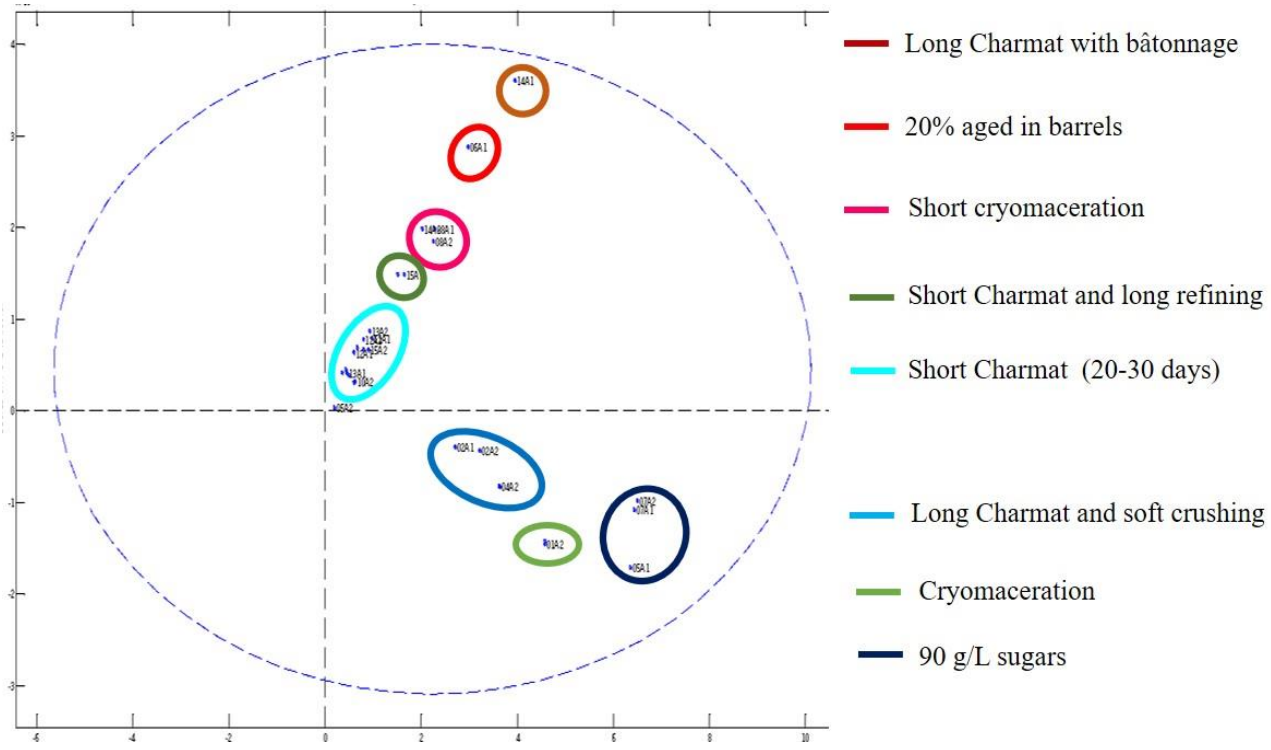

Figure 40. Separation of dry and sweet wines in PCA analysis.

Concerning the sweet wines (Figure 40), wines 05 and 07 were completely separated from all the other wines because of their extremely high content of sugars (90 g L^{-1}). Moreover, they had separated each other probably as a consequence of the different temperature of fermentation: 18 °C (05), while 07was produced at 15 °C for 3 months. Wine 01, produced through a soft pressing, a cryomaceration of 24 hours and a fermentation ranging from 16 to 18 °C, showed intermediate characteristics, as compared with wines with a high content of sugars and wines produced with a long Charmat process (02 and 04).

Main compounds of the anomeric region (3.15−5.50 ppm) are indicated in figure 41 and were identified according to ^{1}H-NMR spectra, while phenolic compounds of the aromatic region (5.5-8 ppm) and several minor compounds were confirmed through HSQC and HMBC experiments (Table 14; Anastasiadi et al., 2009; Ali et al., 2011; Fossen et al., 1998; Fotakis et al., 2013; Elegami et al., 2003; López-Rituerto et al., 2012; Papotti et al., 2012; Rayyan et al., 2005).

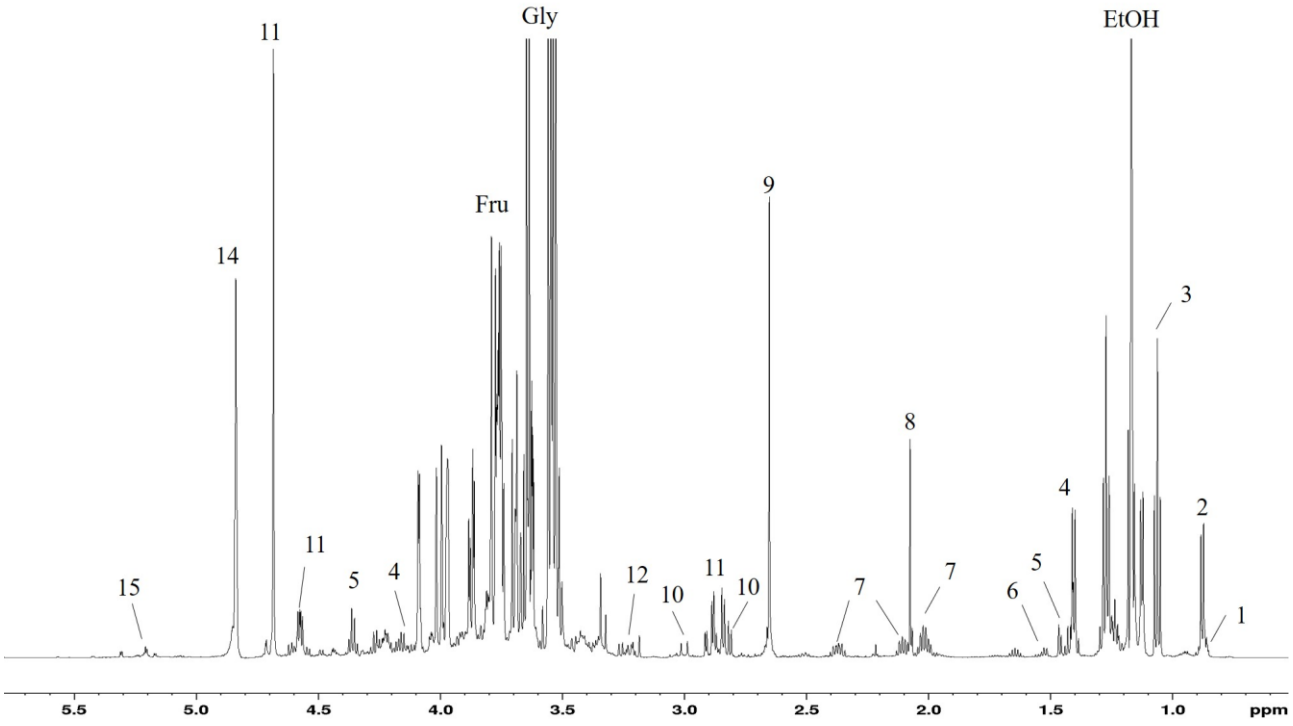

Figure 41. Identification of main components of Malvasia wine. Data are the results of a multi-suppression experiment of the sample 13A2. Numbers are referred to table 14.

ID	Compounds	^{1}H chemical shifts (δ)	Group
1	isobutanol/isopentanol/1-propanol	0.86 (d)	CH_3
2	leucine	0.88 (d)	C_5H_3, C_6H_3
3	2,3-butanediol	1.16 (d)	C_1H_3, C_4H_3
4	lactic acid	1.41 (d) 4.31 (q)	C_3H_3 C_2H
5	threonine	1.46 (d) 4.41 (m)	C_4H_3 C_3H
6	alanine	1.56 (d)	C_3H_3
7	proline	2.02 (m) 2.11 (m) 2.37 (m)	C_4H_2 C_3H $C_{3'}H$
8	acetic acid	2.08 (s)	C_3H_3
9	succinic acid	2.65 (s)	C_2H_2, C_3H_2
10	citric acid	2.81 (d) 3.00 (d)	C_2H, C_4H $C_{2'}H$, $C_{4'}H$
11	malic acid	2.85 (dd) 2.91 (dd)	C_2H $C_{2'}H$

		4.57 (dd)	C_3H
12	*β*-glucose	3.26 (t) 4.61 (d)	C_2H βC_1H
13	tartaric acid	4.68 (s)	C_2H, C_3H
14	unknown	4.84 (s)	
15	*α*-glucose	5.17 (d) 5.21 (d)	αC_1H
16	*γ*-glucose	5.24 (d)	
17	sucrose	5.42 (d)	
EtOH	ethanol	1.17 (t)	C_2H_3
Gly	glycerol	3.54 (m) 3.63 (m) 3.76 (m)	C_2H C_3H_2 C_1H_2
Fru	fructose	3.99 (m) 4.09 (d)	C_3H, C_4H, C_5H *α, β*
18	histidine	7.40 (s) 8.66 (s)	CH CH
19	uridine	7.87 (d)	C6H ring
20	gallic acid	7.13 (s)	H2, H6
21	(+)-catechin	2.51 (dd) 4.55 (d) 5.89 (d) 6.84 (d)	H4 H2 H8 H2’
22	*trans*-fertaric acid	6.88 (d)	
23	*cis-p*-coutaric acid	6.93 (d)	C3H/C5H
24	quercetin	7.73 (d)	H2’
25	ferulic acid	7.68 (d)	H-α
26	unknown	7.69 (s)	
27	kaempferol	6.58 (d) 8.10 (d)	H8 H2’, H6’
28	*p*-coumaric/*trans*-coutaric acid	6.43 (d)	αCH
29	unknown	5.31 (d)	
30	caftaric acid	5.33 (s)	

31	*trans*-caffeic acid	7.54 (d)	H-α
32	unknown	7.15 (s)	
33	*cis*-resveratrol	7.16 (d)	H2', H6'
34	*trans*-resveratrol	7.37 (t)	H2', H6'
35	2-phenylethanol	7.29 (m)	ring
36	phenylalanine	7.41 (d)	
37	*p*-coumaric acid	7.49 (d)	H2, H6
38	unknown	8.58 (s)	
39	unknown	8.11 (m)	
40	unknown	8.00 (s)	
41	arginine	8.23 (s)	
42	niacine	8.89 (t) 9.22 (s)	C4H, C6H C2H
43	ethanal	9.66 (s)	CHO

Table 14. Assignments were from HSQC and HMBC experiments. Peak multiplicities in parentheses: s, singlet; d, doublet; t, triplet; dd, doublet of doublets; m, multiplet.

In particular, figure 42 reports the HSQC experiment, representing the direct bound between carbon and hydrogen. As expected, cryoprobe permitted the detection of several volatile compounds, such as the 2-phenylethanol and 2,3-butanediol, that usually are the most commonly detected (López-Rituerto et al., 2012). Moreover, main organic acids (malic, citric, lactic, succinic), sugars and amino acids (proline, threonine, alanine) showed an easy detectable signal. However, other less abundant compounds such as isobutanol, isopentanol and 1-propanol typically show the signal at 0.88 ppm (López-Rituerto et al., 2012), thus complicating their detection.

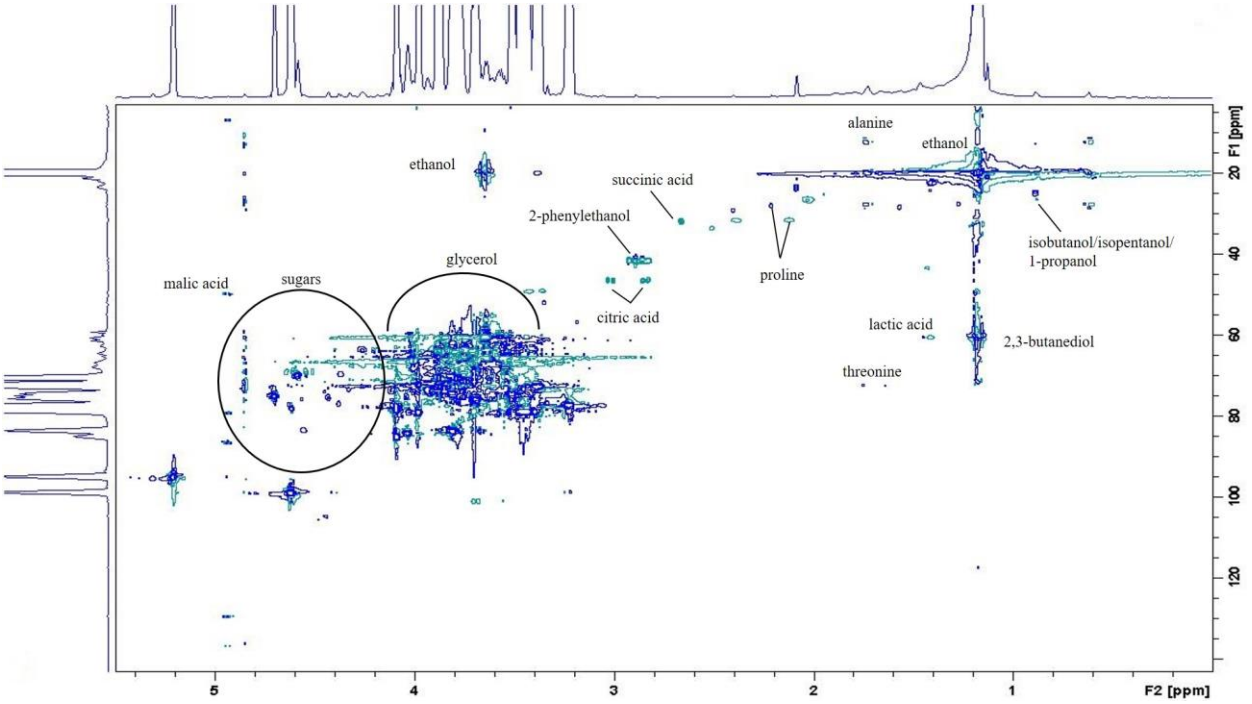

Figure 42. HSQC experiment of the anomeric region.

Then, the aromatic region of the 2D analysis of sample 05 was used for the same purpose, even if, as expected, the signal presented a very low intensity, typical of non-concentrated samples (Figure 43). Myricetin 3'-(6''-p-couglc) was referenced for 8 H at 6.80 ppm and 4' C at 140.5 ppm (Fossen et al., 1998). Quercetin 4'-glc and quercetin 3,4'-diglc were referenced for the 5' H at 7.35 ppm and 7.20 ppm respectively, while carbons were indicated at 137.89 ppm and 134.26 ppm, respectively (Rayyan et al., 2005).

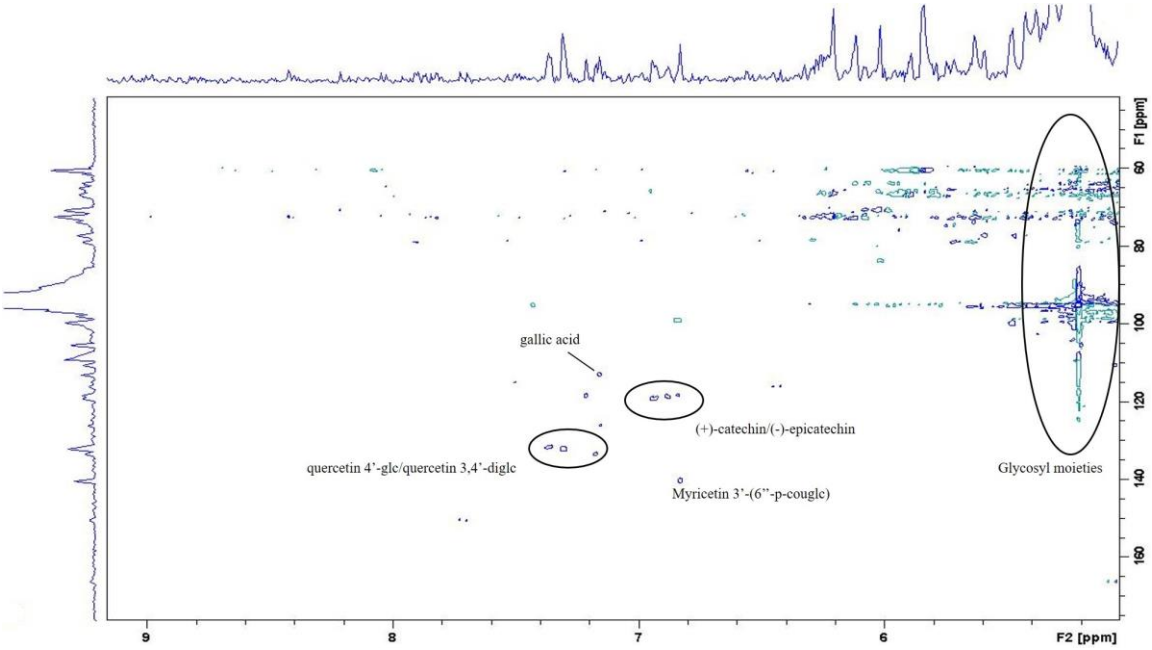

Figure 43. HSQC experiment of the aromatic region.

However, the region of polyphenols in ^{1}H-NMR spectra typically shows low intensity signals with overlapping peaks. In fact, similar compounds like (+)-catechin and (-)-epicatechin, or compounds with a different structure, such as *p*-benzoic, trans-caftaric and *cis*-*p*-coutaric acids showed a part their signal in the area between 6.82 and 6.94 ppm (Figure 44).

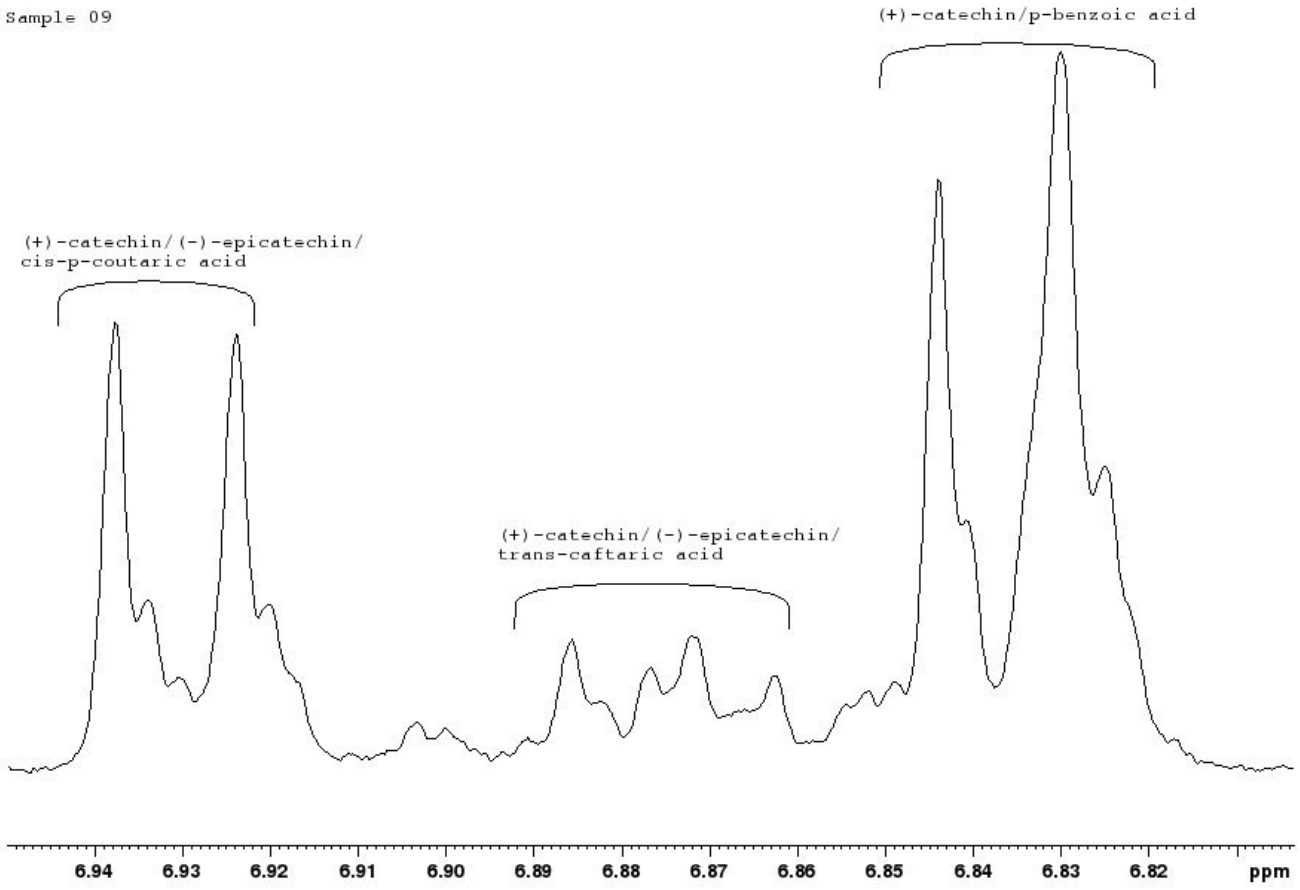

Figure 44. Example NMR spectrum in the region of phenolic compounds in wine 09. Different molecules show singlets, doublets, doublets of doublets in the same point of the spectra.

Other phenolic compounds typically found in wines are quercetin, *cis*- and *trans*-resveratrol, syringic acid, caffeic acid, and many others (Amargianitaki and Spyros, 2017). Many of these compounds were found after 7.10 ppm (Figure 45).

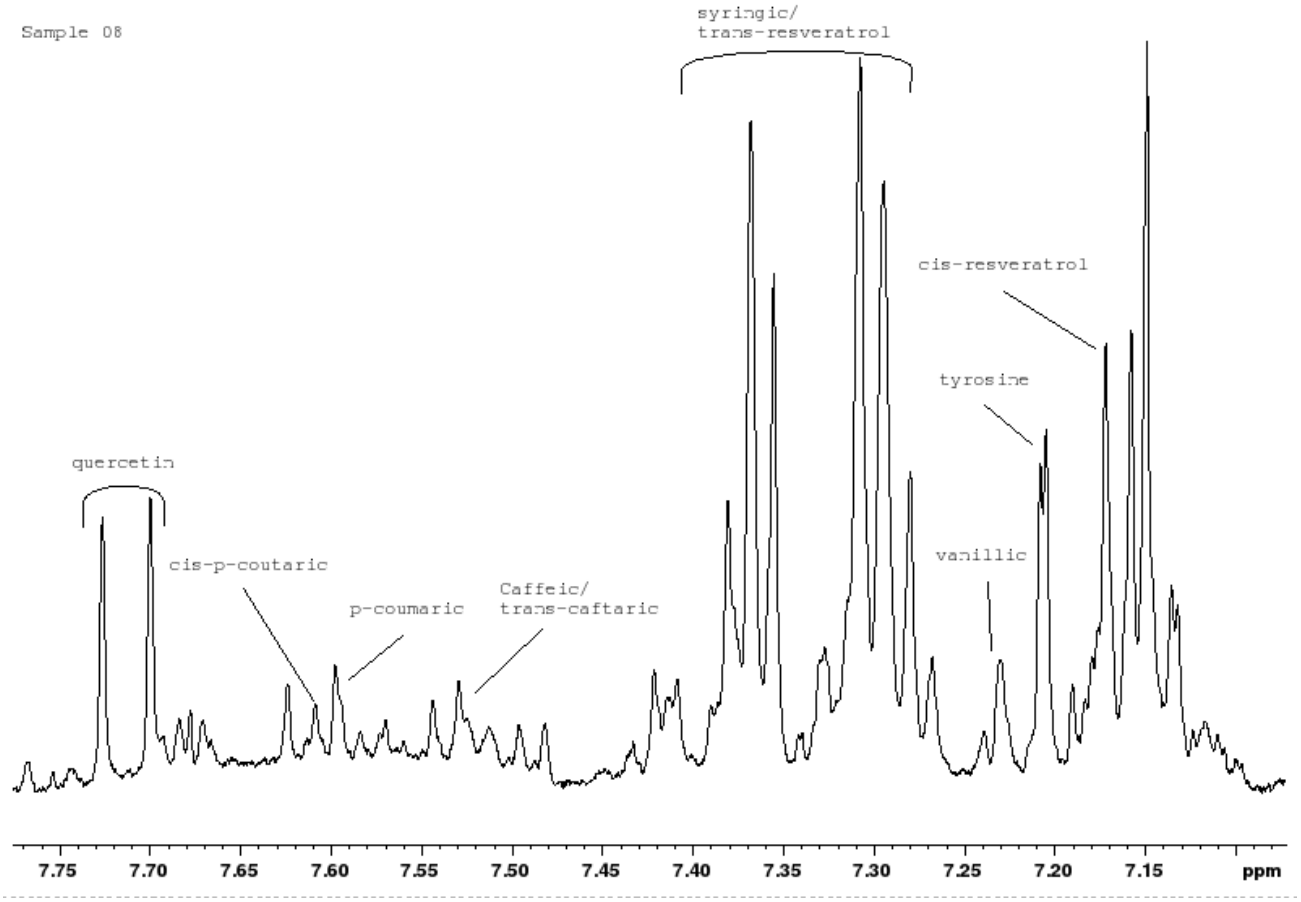

Figure 45. Aromatic region from 7.10 ppm to 7.75 ppm of sample 08.

For these reasons, a PCA of the aromatic region of all wines was done (Figure 46). Despite the pre-treatment of the whole dataset (phasing, calibration, and alignment), replication of several samples (07, 08, 09, 10 and 11) showed different characteristics. This behaviour is probably due to the extreme complexity and the low intensity of the aromatic region, that partially nullifies spectra pre-treatments. However, PCA analysis differentiated three wines: 13, 12 and 08. Wine 13 obtained from pellicular maceration at 7-8 °C for 4 h extracted an important quantity of most-soluble phenolic compounds. Probably, since grapes were produced according to the integrated farming, the good sanitary state of grapes permitted the application of this practice and the partial extraction of polyphenols that enhance the quality of dry wines (Ribéreau-Gayon et al., 2018b). However, the opinions about this process are still contradictory. In any case is well-separated from the main cluster and from the standard white-winemaking processing of the same cultivar (12; 20 days at 20°C). Better results were achieved for sample 08 coming from a cryomaceration at lower temperature, which increases the extraction of polyphenols and aromatic compounds (Ribéreau-Gayon et al., 2018b), where the extraction of polyphenols is comparable to sample 12. Unfortunately, the two replications are very separated but with an opposite direction on PC1, if compared with all the other wines. It is probable that wine 8a1 is an outlier as it is very unlikely that it contains less phenols than a classic white vinification (12).

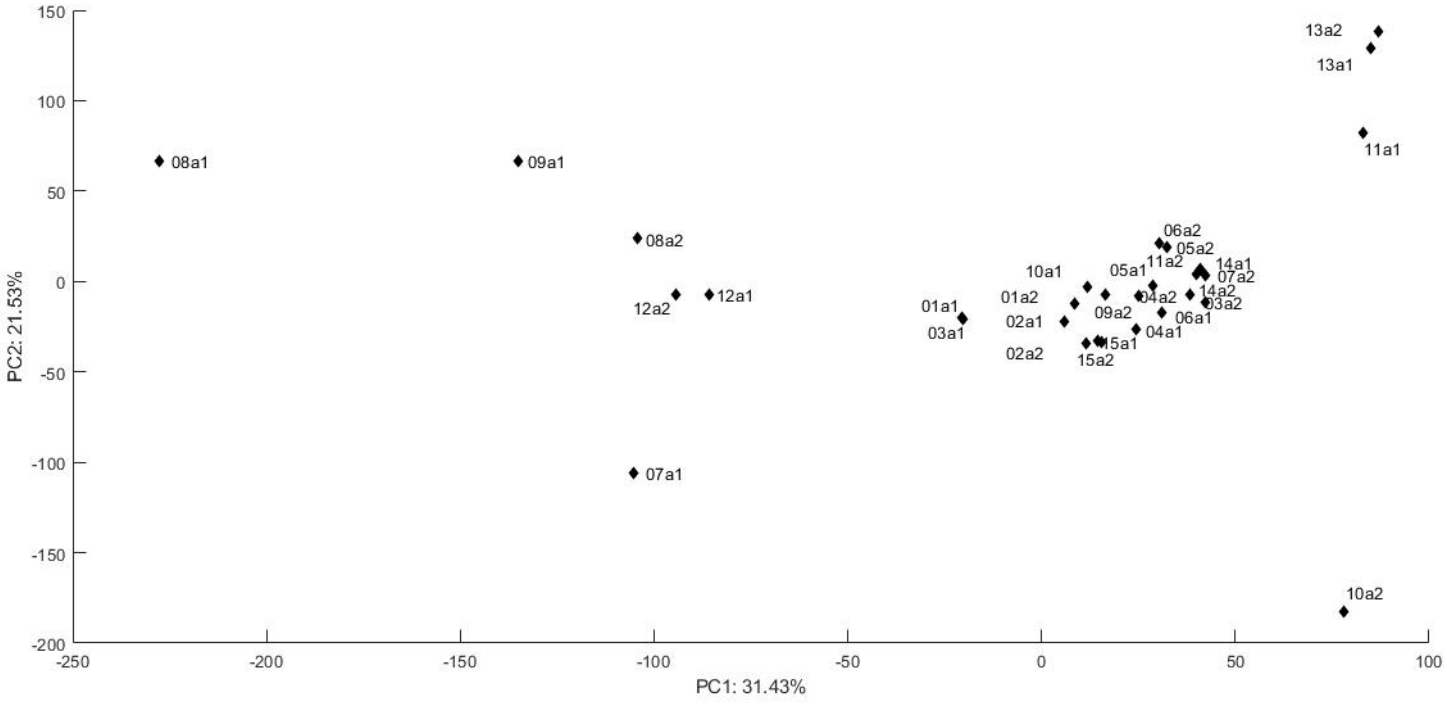

Figure 46. Scores plot for PC1 × PC2 of the aromatic region of Malvasia wines.

4. Conclusions

The evaluation of wines under investigation allowed to deepen and expand the researcher's knowledge in the wine sector. For the first time, the study describes the profile of free aromatic compounds of Festasio, L. di Fiorano, and Albana rosa. However, the aromatic profile deserves further deepening. In any case, the aromatic profile is similar to the commonest wines in Emilia-Romagna. Indeed, the analogy between L. Pellegrino and L. Grasparossa or between Festasio and L. Palamino are some examples, although some differences were highlighted in the content of total alcohols and the lower levels of total acids.

LC-MS Q-Exactive Orbitrap permitted the identification of 11 different classes of anthocyanins, for a total of 110 compounds. However, the scarce literature about the accurate mass assignments of several compounds do not allow the exact association between each condensed formula with its mass. Furthermore, any reference about the tentatively identified isomers was found. Regarding the quantitative results, the similarity of the anthocyanin profile of Festasio with that of Ancellotta wines vinified in red suggests a use of the former as a blending wine. Likewise, its performance could be tested as a grape to produce enocyanin. Indeed, Festasio can be used as a blending wine, due to the extremely high concentration of malvidin-3-O-glucosides, which is the most representative along with the significant abundance of acetyl, coumaroyl, and caffeoyl derivatives of malvidin, petunidin, and delphinidin, as well as their sum. Regarding the other minor wines, since they were cultivated in zones remarkably different from the Lambrusco production area, they showed an anthocyanins pattern completely different, as long as easily recognizable. Therefore, all minor wines can enrich the wine quality and quantity, particularly interesting for their anthocyanins content and nutraceutical properties. However, the high variability between different vintages needs to be in-deep studied to evaluate the necessity of genetic improvement of minor varieties. It is important to specify that also Ancellotta and other commercial Lambrusco wines showed a high variability due to the vintage effect. Hence, all minor wines need to be tested in different cultivation regimes (organic, integrated, biodinamic) and with different winemaking processes at commercial scale to evaluate their commercial potential.

The cloud platform XCMS Online is a fast and an easy way for statistical analysis and identification procedure for untargeted analysis purposes. Moreover, the presence of several studies in literature permits to compare the results and develop new identification and discrimination strategies. However, the quantity of identified compounds needs to be carefully managed, since the high number of features should be processed with specific and advanced software, such as MATLab or

PLS_Toolbox. By contrast, the reduction of the significant features through a restrictive method may reduce the detection of less abundant molecules. Nonetheless, the heterogeneous dataset analyzed was successfully classified in four different clusters, accordingly with different vintages, varieties, and winemaking processes.

Concerning the NMR results, 400 MHz instruments are among the most used. Thus, resulting spectra are easily comparable with the literature, permitting the identification of a wide range of compounds. Furthermore, the untargeted analysis of a particularly heterogeneous dataset permitted the differentiation of all wines, according to their winemaking process and winery of origin. Additionally, the composition analysis of the whole spectra and its aromatic region may help both characterization and discrimination of wines, in adulteration studies. The same approach applied to Malvasia wines dataset permitted their classification. Moreover, the use of a powerful instrument with an increased resolution, such as the 600-MHz NMR, allowed the identification of further compounds, compared to the 400-MHz instrument. Hence, the identification of a large number of sugars, organic acids, amino acids, volatile compounds and polyphenols enabled to clarify the influence of different enological practices affect the organoleptic properties of a single-varietal wine such as Malvasia di Candia aromatica. Indeed, processes like cryomaceration, pellicular maceration, wood barrels refining, *bâtonnage*, long and short Charmat winemaking gave different clusterization of wines.

Generally, further *ad hoc* studies are necessary to assess the role and the origin of minor secondary metabolites in grape and wine, as well as their peculiar characteristics. New metabolomic and challenging studies are crucial to comprehend the relationship among wine quality, agronomical practices, winemaking processes, environmental conditions and genetical characters. For these reasons, minor wines need to be constantly evaluated and compared with commercially established wines. To accomplish these targets, collaboration among farmers, producers, consumers and research centers is a crucial point.

References

Ablett, S., 1992. Overview of NMR applications in food science. Trends Food Sci. Technol. 3, 246–250.

Ackermann, S.M., Dolsophon, K., Monakhova, Y.B., Kuballa, T., Reusch, H., Thongpanchang, T., Bunzel, M., Lachenmeier, D.W., 2017. Automated multicomponent analysis of soft drinks using 1D ^{1}H and 2D ^{1}H-^{1}H J-resolved NMR spectroscopy. Food Anal. Method.3, 827–836.

Ageorges, A.; Fernandez, L.; Vialet, S.; Merdinoglu, D.; Terrier, N.; Romieu, C., 2006. Four specific isogenes of the anthocyanin metabolic pathway are systematically co-expressed with the red colour of grape berries. *Plant Sci.170*, 372–383.

Agiomyrgianaki, A., Dais, P., 2012a. Simultaneous determination of phenolic compounds and triterpenic acids in oregano growing wild in Greece by ^{31}P NMR spectroscopy. Magnetic Resonance Chem. 50, 739–748.

Agiomyrgianaki, A., Petrakis, P.V., Dais, P., 2012b. Influence of harvest year, cultivar and geographical origin on Greek extra virgin olive oils composition: A study by NMR spectroscopy and biometric analysis. Food Chem., 135, 2561–2568.

Aharoni, A., Ric de Vos, C.H., Verhoeven, H.A., Maliepaard, C.A., Kruppa, G., Bino, R., Goodenowe, D.B., 2002. Nontargeted metabolome analysis by use of Fourier Transform Ion Cyclotron Mass Spectrometry. Omics J. Integr. Biol. 6, 217–234.

Akanbi, T.O. and Barrow, C.J., 2018. compositionCompositional information useful for authentication of krill oil and the detection of adulterants. Food Anal. Method. 11, 178–187.

Albagnac, G., 1975. La décarboxylation des acides cinnamiques substitués par les levures. Annls Technol. Agric. 24 133-141.

Alberts, P., Stander, M.A., de Villiers, A., 2012. Advanced ultra high pressure liquid chromatography–tandem mass spectrometric methods for the screening of red wine anthocyanins and derived pigments. J. Chromatogr. A 1235, 92−102.

Alcalde-Eon, C., Boido E., Carrau, F., Dellacassa, E., Rivas-Gonzalo, J.C., 2006. Pigment profiles in monovarietal wines produced in Uruguay. Am. J. Enol. Vitic. 57, 449–459.

Ali, K., Maltese, F., Fortes, A.M., Pais, M.S., Choi, Y.H., Verpoorte, R., 2011a. Monitoring biochemical changes during grape berry development in Portuguese cultivars by NMR spectroscopy. Food Chem., 124, 1760–1769.

Ali, K., Maltese, F., Toepfer, R., Choi, Y.H., Veropoorte, R., 2011. Metabolic characterization of Palatinate German white wines according to sensory attributes, varieties, and vintages using NMR spectroscopy and multivariate data analyses. J. Biomol. NMR, 49, 255–266.

Ali, K., Maltese, F., Toepfer, R., Choi, Y.H., Verpoorte, R., 2011. Metabolic characterization of Palatinate German white wines according to sensory attributes, varieties, and vintages using NMR spectroscopy and multivariate data analyses. J. Biomol. NMR, 49, 255–266.

Ali, K., Maltese, F., Toepfer, R., Choi, Y.H., Verpoorte, R., 2011b. Metabolic characterization of Palatinate German white wines according to sensory attributes, varieties, and vintages using NMR spectroscopy and multivariate data analyses. J. Biomol. NMR. 49, 255–266.

Alonso, R., Berli, F.J., Piccoli, P., Bottini, R., 2016. Ultraviolet-B radiation, water deficit and abscisic acid: a review of independent and interactive effects on grapevines. Theor. Exp. Plant Physiol., 28, 11-22.

Alonso-Salces, R., Heberger, K., Holland, M., Moreno-Rojas, J., Mariani, C., Bellan, G., Guillou, C., 2010b. Multivariate analysis of NMR fingerprint of the unsaponifiable fraction of virgin olive oils for authentication purposes. Food Chem., 118, 956–965.

Alonso-Salces, R.M., Moreno-Rojas, J.M., Holland, M.V., Reniero, F., Guillou, C., Heberger, K., 2010a. Virgin olive oil authentication by multivariate analyses of ^{1}H NMR fingerprints and ^{13}C and ^{2}H data. J. Agric. Food Chem. 58, 5586–5596.

Amador-Noguez, D., Feng, X-J., Fan, J., Roquet, N., Rabitz, H., Rabinowitz, J.D., 2010. Systems-level metabolic flux profiling elucidates a complete, bifurcated tricarboxylic acid cycle in clostridium acetobutylicum. J. Bacteriol. 192, 4452–61.

Amargianitaki, M., and Spyros, A., 2017. NMR-based metabolomics in wine quality control and authentication. Chem. Biol. Technol. Agric. 9, 1-12.

Anastasiadi, M., Zira, A., Magiatis, P., Haroutounian, S.A, Skaltsounis, A.L., Mikros, E., 2009. 1H NMR-based metabolomics for the classification of Greek wines according to variety, region, and vintage. Comparison with HPLC data. J. Agric. Food. Chem. 57, 11067–74.

Arapitsas, P., Scholz, M., Vrhovsek, U., Di Blasi, S., Biondi Bartolini, A, Masuero, D., Perenzoni, D., Rigo, A., Mattivi, F., 2012. A Metabolomic Approach to the Study of Wine Micro-Oxygenation. PLoS ONE, 7, 1-11.

Arapitsas, P., Ugliano, M., Perenzoni, D., Angeli, A., Pangrazzi, P., Mattivi, F., 2016. Wine metabolomics reveals new sulfonated products in bottled whitewines, promoted by small amounts of oxygen. J. Chrom. A, 1429, 155-165.

Araujo, P., Tilahun, E., Zeng, Y., 2018. A novel strategy for discriminating marine oils by using the positional distribution (sn-1, sn-2, sn-3) of omega-3 polyunsaturated fatty acids in triacylglycerols. Talanta, 182, 32–37.

Arctander, S., 1969. Perfume and flavor chemicals. Montclaire N.J. Eds.

Arpae, 2019. Rapporto Idro-Meteo-Clima Emilia-Romagna: Rapporto annuale dati 2018. https://www.arpae.it/cms3/documenti/_cerca_doc/meteo/rapporti_annuali/2018_report_web.pdf (accessed November 17th 2020)

Arpae, 2020. Rapporto Idro-Meteo-Clima Emilia-Romagna: Rapporto annuale dati 2019. https://www.arpae.it/cms3/documenti/_cerca_doc/meteo/rapporti_annuali/idrometeoclima2019.pdf (accessed November 17th 2020)

Asimov, E. 2009. Brunello inquiry cites five wineries. 12 August. The New York Times D; Dining In, Dining Out/Style Desk:4.

Aursand, M., Standal, I.B., Axelson, D.E., 2007. High-resolution ^{13}C nuclear magnetic resonance spectroscopy pattern recognition of fish oil capsules. J. Agric. Food Chem. 55, 38–47.

Avakyants, S.P., Rastyannikov, E.G., Chernyaga, B.S., Navrotskii, V.J., 1981. Khromato-mass-spektrometricheskoe issledovanie letuchikh vesnchestv vina. Vinodel. Vinograd. SSSR 41 50-53.

Aznar, M., Lopez, R., Cacho, J.F., Ferreira, V., 2001. Identification and quantification of impact odorants of aged red wines from Rioja. GC-olfactometry, quantitative GC-MS, and odor evaluation of HPLC fractions. J. Agric. Food Chem. 49, 2924- 2929.

Baiano, A., Terracone, C., Longobardi, F., Ventrella, A., Agostiano, A., Del Nobile, M.A., 2012. Effects of different vinification technologies on physical and chemical characteristics of Sauvignon blanc wines. Food Chem. 135, 2694–2701.

Barnaba, C., Larchera, R., Nardin, T., Dellacassa, E., Nicolini, G., 2018. Glycosylated simple phenolic profiling of food tannins using high resolution mass spectrometry (Q-Orbitrap). Food Chem. 267, 196–203.

Baro, A.L., and Quiros Carrasco, LA., 1977. Les conditions de formation des aldehydes dans les vins. Relation et importance en rapport avec les phénomènes d'oxydation et les caractéristiques organoleptiques. Bull. O.I.V. 50 253-267.

Bartle, K.D. and Myers, 2002. History of gas chromatography. TrAC Trends Anal. Chem. 21, 547-557.

Bavaresco, L., Gatti, M., Pezzutto, S., Fregoni, M., Mattivi, F., 2008. Effect of leaf removal on grape yield, berry composition and stilbene concentration. Am. J. Enol. Vitic. 59, 292-298.

Bayer, E., 1966. Quality and flavor by gas chromatography. J. Gas Chromat. 4 67-73.

Bayonove, C., Cordonnier, R., Ratier, R., 1974. Localisation de l'arôme dans la baie de raisin: variétés Muscat d'Alexandrie et Cabernet Sauvignon. C.r. Acad. Agric. Fr. 60 1321-1328.

Beckmann, M., Enot, D.P., Overy, D.P., Draper, J., 2007. Representation, comparison, and interpretation of metabolome finger-print data for total composition analysis and quality trait investigation in potato cultivars. J. Agric. Food Chem. 55, 3444-3451.

Beckonert, O.E., Bollard, M., Ebbels, T.M., Keun, H.C., AnttI, H., Holmes, E., Nicholson, J.K., 2003. NMR-based metabonomic toxicity classification: Hierarchical cluster analysis and k-nearest-neighbour approaches. Anal. Chimica Acta, 490, 3–15.

Belton, P.S., Delgadillo, I., Holmes, E., Nicholls, A., Nicholson, J.K., Spraul, M., 1996. Use of high-field ^{1}H NMR spectroscopy for the analysis of liquid foods. J. Agric. Food Chem. 44, 1483–1487.

Beltran, G., Novo, M., Guillamón, J.M., Mas, A., Rozès, N., 2008. Effect of fermentation temperature and culture media on the yeast lipid composition and wine volatile compounds. Int. J. Food Microbiol. 121, 169-177.

Bensaid, F.F., Wietzerbin, K., Martin, G.J., 2002. Authentication of natural vanilla flavorings: Isotopic characterization using degradation of vanillin into guaiacol. J. Agric. Food Chem. 50, 6271–6275.

Benton, H.P., Ivanisevic, J., Mahieu, N.G., Kurczy, M.E., Johnson, C.H., Franco, L., Rinehart, D., Valentine, E., Gowda, H., Ubhi, B.K., Tautenhahn, R., Gieschen, A., Fields, M.W., Patti, G.J., Siuzdak G., 2014. Autonomous Metabolomics for Rapid Metabolite Identification in Global Profiling. Anal. Chem. 87, 884–891.

Beretta, G., Caneva, E., Regazzoni, L., Bakhtyari, N.G., Maffei, F.R., 2008. A solid-phase extraction procedure coupled to ^{1}H NMR, with chemometric analysis, to seek reliable markers of the botanical origin of honey. Analytica Chimica Acta, 620, 176–182.

Berke, B., Cheze, C., Vercauteren, J., Deffieux, G., 1998. Bisulfite addition to anthocyanins: Revisited structures of colourless adducts. Tetrahedron Letters, 39, 5771–5774.

Berregi, I., del Campo, G., Caracena, R., Miranda, J.I., 2007. Quantitative determination of formic acid in apple juices by ^{1}H NMR spectrometry. Talanta, 72, 1049–1053.

Bertelli, D., Lolli, M., Papotti, G., Bortolotti, L., Serra, G., Plessi, M., 2010. Detection of honey adulteration by sugar syrups using one-dimensional and two-dimensional high-resolution nuclear magnetic resonance. J. Agric. Food Chem. 58, 8495–8501.

Bertocchi, F. and Paci, M., 2008. Applications of high-resolution solid-state NMR spectroscopy in food science. J. Agric. Food Chem. 56, 9317–9327.

Bertrand, A., Thése, Université Bordeaux II, 1975.

Bettiga, L.J., Christensen, L.P., Dokoozlian, N.K., Golino, D.A., McGourty, G., Smith, R.J., Verdegaal, P.S., Walker, M.A., Wolpert, J.A., Weber, E., 2003. Wine grape varieties in California. University of California Agricultural and Natural Resources (publication no. 3419), Oakland.

Bharti, S.K., and Roy, R., 2012. Quantitative ^{1}H NMR spectroscopy. Trends Anal. Chem. 35, 5–26.

Biais, B., Allwood, J.W., Deborde, C., Xu, Y., Maucourt, M., Beauvoit, B., Moing, A., 2009. ^{1}H NMR, GC-EI-TOFMS, and data set correlation for fruit metabolomics: Application to spatial metabolite analysis in melon. Anal. Chem. 81, 2884–94.

Bicchi, C., Cagliero, C., Rubiolo, P., 2011. New trends in the analysis of the volatile fraction of matrices of vegetable origin: a short overview. A review. Flavour Fragr. J. 26, 321–325.

Bingol, K., Li, D. W., Bruschweiler-Li, L., Cabrera, O. A., Megraw, T., Zhang, F., Bruschweiler, R., 2015. Unified and isomer-specific NMR metabolomics database for the accurate analysis of ^{13}C-^{1}H HSQC spectra. Acs Chem. Biol. 10, 452–459.

Blay, P., Hui, J.P., Chang, J., Melanson, J.E., 2011. Screening for multiple classes of marine biotoxins by liquid chromatography–high-resolution mass spectrometry. Anal. Bioanal. Chem. 400, 577–85.

Boccacci, P., Torello Marinoni, D., Gambino, G., Botta, R., Schneider, A., 2005. Genetic Characterization of Endangered Grape Cultivars of Reggio Emilia Province. American J. Enol. Viticul. 56, 4.

Boido, E., Fariña, L., Barnaba, C. Arrieta, Y., Larcher, R., Nicolini, G., Carrau, F., Dellacassa, E., 2019. Chemical characterization and enological potential of less frequent red grape Uruguayan varieties by study secondary metabolites. BIO Web of Conferences 12, 02035.

Boidron, J.N., 1978. Relation entre les substances terpéniques et la qualité du raisin (Role du Botrytis cinerea). Annls Technol. agric. 27 141-145

Bonada, M., Jeffery, D., Petrie, P., Moran, M., Sadras, V., 2015. Impact of elevated temperature and water deficit on the chemical and sensory profiles of Barossa Shiraz grapes and wines. Aust. J. Grape Wine Res., 21, 240-253.

Borsa, D., Carniel, D., Asproudi, A, Ponticelli, L., Crespan, M., Costacurta, A., 2005. Characterization of Malvasia grapes by secondary metabolites. Riv. Vit. Enol. 2-3-4, 167-182.

Brenton, A.G. and Godfrey, A.R., 2010.Accurate Mass Measurement: Terminology and Treatment of Data. J. Am. Soc. Mass. Spectrom. 21, 1821–1835

Brown, S.C., Kruppa, G., Dasseux, J.L., 2005. Metabolomics applications of FT-ICR mass spectrometry. Mass Spectrom. Rev. 24, 223–231.

Bruker, 2012. ERETIC2 user's guide preliminary. Billerica, MA: Bruker.

Bucci, A., 2007. Vite e vino in Romagna. Le radici storiche della moderna vitivinicoltura romagnola. Ed. Sapim, Forlì.

Budde, W.L., 2001. Analytical Mass Spectrometry: Strategies for Environmental and Related Applications. Washington, DC: American Chemical Society and New York: Oxford.

Busch, K.L., 1995. Electron ionization, up close and personal. Spectroscopy (Eugene, OR), 10, 39–42.

Buttery, R.G., Seifert, R.M., Guadagni, D.G., Luig, L.C., 1971. Characterization of additional volatile components of tomato, J. Agric. Food Chem. 19 524-529.

Calò, A.; Scienza, A.; Costacurta, A., 2010. Vitigni d'Italia. Le varietà tradizionali per la produzione dei vini moderni. Edagricole.

Capitani, D., Sobolev, A.P., Di Tullio, V., Mannina, L., Proietti, N., 2017a. Portable NMR in food analysis. Chem. Biol. Technol. Agric. 4, 17.

Capitani, D., Sobolev, A.P., Mannina, L., 2017b. Nuclear magnetic resonance – metabolomics. In: C.A. Georgiou and G. P. Danezis (Eds.), Food authentication: Management, analysis and regulation (pp. 177–193). Chichester, UK; Hoboken, NJ: John Wiley & Sons.

Cavaliere, C., Antonelli, M., Capriotti, A.L., La Barbera, G., Montone, C.M., Piovesana, S., Laganà, A., 2019. A Triple Quadrupole and a Hybrid Quadrupole Orbitrap Mass Spectrometer in Comparison for Polyphenol Quantitation. J. Agric. Food Chem. 67, 4885−4896.

Caven-Quantrill, D.J. and Buglass, A.J., 2007. Determination of volatile organic compounds in English vineyard grape juices by immersion stir bar sorptive extraction–gas chromatography/mass spectrometry. Flavour Fragr. J. 22, 206–213.

Caytan, E., Botosoa, E.P., Silvestre, V., Robins, R.J., Akoka, S., Remaud, G.S., 2007. Accurate quantitative ^{13}C NMR spectroscopy: Repeatability over time of site-specific ^{13}C isotope ratio determination. Anal. Chem. 79, 8266–8269.

Charisiadis, P., Exarchou, V., Troganis, A.N., Gerothanassis, I.P., 2010. Exploring the "forgotten"-OH NMR spectral region in natural products. Chem. Communications, 46, 3589–3591.

Chatonnet, P., Boidron, J.-N., Pons, M., 1989. Incidence du traitement thermique du bois de chêne sur sa composition chimique. 2e partie : évolution de certains composés en fonction de l'intensité de brûlage. OENO One, 23, 223-250.

Chatonnet, P., Dubourdieu, D., Boidron, J.-N., Lavigne, V., 1993. Synthesis of volatile phenols by Saccharomyces cerevisiae in wines. J. Sci. Food Agric. 62, 191.

Chauhan, A., Goyal, M.K., Chauhan, P., 2014. GC-MS Technique and its Analytical Applications in Science and Technology. J. Anal. Bioanal. Tech. 5, 222.

Cheng, H.N., and Neiss, T.G., 2012. Solution NMR spectroscopy of food polysaccharides. Polymer Rev. 52, 81–114.

Chin, S.T. and Marriott, P.J., 2014. Multidimensional gas chromatography beyond simple volatiles separation, Chem. Commun., 50, 8819–8833.

Chinnici, F., Sonni, F., Natali, N., Galassi, S., Riponi, C., 2009. Colour features and pigment composition of Italian carbonic macerated red wines. Food Chem. 113, 651–657.

Choze, R., Alcantara, G.B., Alves, F.E.G., Silva, L.M., Faria, J.C., Liao, L.M., 2013. Distinction between a transgenic and a conventional common bean genotype by ^{1}H HR-MAS NMR. Food Chem. 141, 2841–2847.

Christophoridou, S., and Dais, P., 2009. Detection and quantification of phenolic compounds in olive oil by high resolution ^{1}H nuclear magnetic resonance spectroscopy. Anal. Chimica Acta, 633, 283–292.

Christophoridou, S., Dais, P., Tseng, L.H., Spraul, M., 2005. Separation and identification of phenolic compounds in olive oil by coupling high-performance liquid chromatography with postcolumn solid-phase extraction to nuclear magnetic resonance spectroscopy (LC-SPE-NMR). J. Agric. Food Chem. 53, 4667–4679.

Cifuentes, A., 2009. Advanced separation methods in food analysis. J. Chromatog. A, 1216, 7109–7358.

Clausen, M.R., Edelenbos, M., Bertram, H.C., 2014. Mapping the variation of the carrot metabolome using ^{1}H NMR spectroscopy and consensus PCA. J. Agric. Food Chem. 62, 4392–4398.

Cloarec, O., Dumas, M.E., Craig, A., Barton, R.H., Trygg, J., Hudson, J., Blancher, C.,Gauguier, D., Lindon, J.C., Holmes, E., Nicholson, J., 2005. Statistical total correlation spectroscopy: An exploratory approach for latent biomarker identification from metabolic ^{1}H NMR data sets. Anal. Chem. 77, 1282–1289.

Codorníu, 2020. https://www.codorniu.com/. (accessed on 08/12/2020)

Consonni, R., Cagliani, L., 2008a. Ripening and geographical characterization of Parmigiano Reggiano cheese by ^{1}H NMR spectroscopy. Talanta, 76, 200–205.

Consonni, R., Cagliani, L.R., 2008b. Geographical characterization of polyfloral and acacia honeys by nuclear magnetic resonance and chemometrics. J. Agric. Food Chem. 56, 6873–6880.

Conte, P., 2008. ^{1}H NMR spectroscopy with multivariate statistical analysis as a tool for a rapid screening of the molecular changes occurring during micro-oxygenation of an Italian red wine. The Open Magnetic Resonance Journal, 1, 77–80.

Cook, S.L., Methven, L., Parker, J.K., Khutoryanskiy, V.V., 2018. Polysaccharide food matrices for controlling the release, retention, and perception of flavours. Food Hydrocolloids, 79, 253–261.

Coombe, B.G., 1987. Influence of temperature on composition and quality of grapes. Acta Hortic. 206, 23-35.

Cordonnier, R. and Bayonove, C., 1978. Les composantes varietales et prefermentaires de l'arôme de vins. Extrait Parfum Cosmet. Armes 24 67-77.

Cordonnier, R. and Bayonove, C., 1981. Etude de la phase prefermentaire de la vinification: Extraction et formation de certain composé de l'arôme; cas des terpenol, des aldehydes et des alcools en C6. Conn. Vigne Vin 15 269-286.

Cortes, H.J., Winniford, B., Luong, J., Pursch, M., 2009. Comprehensive two dimensional gas chromatography review. J. Sep. Sci., 32, 883–904.

Costacurta, A., Calò, A., Carraro, R., Giust, M., Crespan, M., 2005. The Malvasias cultivated in Italy: Molecular, ampelographic, chemical profiles and pedigree relationships. Riv. Viticol. Enol. 58, 55-65.

Cotte, J.F., Casabianca, H., Lheritier, J., Perrucchietti, C., Sanglar, C., Waton, H., Grenier-Loustalot, M.F., 2007. Study and validity of ^{13}C stable carbon isotopic ratio analysis by mass spectrometry and ^{2}H site-specific natural isotopic fractionation by nuclear magnetic resonance isotopic measurements to characterize and control the authenticity of honey. Analytica Chimica Acta, 582, 125–136.

Craig, A., Cloarec, O., Holmes, E., Nicholson, J.K., Lindon, J.C., 2006. Scaling and normalization effects in NMR spectroscopic metabonomic data sets. Anal. Chem. 78, 2262–2267.

Crespan, M., Cabello, F., Giannetto, S., Ibáñez, J., Karoglan Kontić, J.K., Maletić, E., Pejić, I. Rodríguez-Torres, J. & Antonacci, D. (2006). Malvasia delle Lipari, Malvasia di Sardegna, Greco di Gerace, Malvasia de Sitges and Malvasia dubrovacka – Synonyms of an old and famous grape cultivar. Vitis 45(2), 69-73.

D'Agostina, A., Boschin, G., Bacchini, F., Arnoldi, A., 2004. Investigations on the high molecular weight foaming fractions of espresso coffee. J. Agric. Food Chem. 52, 7118–7125.

Dagan, S., 2000. Comparison of gas chromatography-pulsed ame photometric detection-mass spectrometry, automated mass spectral deconvolution and identification system and gas chromatography-tandem mass spectrometry as tools for trace level detection and identification, J. Chromatogr. A, 868, 229–247.

Dagan, S., 2000. Comparison of gas chromatography-pulsed ame photometric detection-mass spectrometry, automated mass spectral deconvolution and identification system and gas chromatography-tandem mass spectrometry as tools for trace level detection and identification, J. Chromatogr. A, 868, 229–247.

Dais, P., and Hatzakis, E., 2013. Quality assessment and authentication of virgin olive oil by NMR spectroscopy: A critical review. Anal. Chimica Acta, 765, 1–27.

Dais, P., Misiak, M., Hatzakis, E., 2015. Analysis of marine dietary supplements using NMR spectroscopy. Anal. Methods, 7, 5226–5238.

Dais, P., Plessel, R., Williamson, K., Hatzakis, E., 2017. Complete ^{1}H and ^{13}C NMR assignment and ^{31}P NMR determination of pentacyclic triterpenic acids. Anal. Method. 9, 949–957.

Dais, P., Spyros, A., 2007. ^{31}P NMR spectroscopy in the quality control and authentication of extra-virgin olive oil: A review of recent progress. Magnetic Resonance Chem. 45, 367–377.

Dais, P., Spyros, A., Christophoridou, S., Hatzakis, E., Fragaki, G., Agiomyrgianaki, A., Brenes, M., 2007. Comparison of analytical methodologies based on ^{1}H and ^{31}P NMR spectroscopy with

conventional methods of analysis for the determination of some olive oil constituents. J. Agric. Food Chem. 55, 577–584.

Dal Poggetto, G., Castanar, L., Adams, R.W., Morris, G.A., Nilsson, M., 2017. Relaxation-encoded NMR experiments for mixture analysis: REST and beer. Chemical Communic. 53, 7461–7464.

Damoc, E., Scigelova, M., Giannakopulos, A.E., Moehring, T., Pehal, F., Hornshaw, M., 2009. Direct Analysis of Red Wine Using Ultra-Fast Chromatography and High Resolution Mass Spectrometry. Thermo Fisher Scientific Inc.

De Moura Ribeiro, M.V., Boralle, N., Redigolo Pezza, H., Pezza, L., Toci, A.T., 2017. Authenticity of roasted coffee using ^{1}H NMR spectroscopy. J. Agric. Food Chem. 57, 24–30.

Decreto del Ministero delle Politiche Agricole Alimentari e Forestali, 24 giugno 2008 (in Gazz. Uff., 21 agosto, n. 195), Modifica del protocollo tecnico di selezione clonale della vite.

Dettmer, K., Aronov, P.A., Hammock, B.D., 2007. Mass spectrometry-based metabolomics. Mass Spectrom. Rev. 26, 51–78.

Dokoozlian, N.K., and Kliewer, W.M., 1996. Influence of light on grape berry growth and composition varies during fruit development. J. Am. Soc. Hortic. Sci. 121, 869-874.

Downey, M.O., Dokoozlian, N.K., Krstic, M.P., 2006. Cultural practice and environmental impacts on the flavonoid composition of grapes and wine: a review of recent research. Am. J. Enol. Vitic., 57, 257-268.

Drawert, F., and Schreier, P., 1978. Charactérisation des raisins et des vins à l'aide de certains constituants remarquables. Annls Technol. agric. 27 367-375.

Ducati, J.R., Bettú, V., Hoff, R., 2009. Remote sensing techniques in the characterization of viticultural terroirs in South Brazil: A case study on Malvasia. In: Proc. 3rd International Symposium Malvasia 23–27 May, Santa Cruz de Tenerife, Spain. pp. 1 – 18.

Dunn, W.B., Bailey, N.J., Johnson, H.E., 2005. Measuring the metabolome: current analytical technologies. Analyst, 130, 606–625.

Dunn, W.B., Bailey, N.J.C., Johnson, H.E., 2005. Measuring the metabolome: current analytical technologies. Analyst 130, 606–625.

Ebadi, A., May, P., Sedgley, M., Coombe, B.G., 1995. Fruit set on small Chardonnay and Shiraz vines grown under varying temperature regimes between budburst and flowering. Aust. J. Grape Wine Res. 1, 1-10.

Eichelberger, J.W., Harris, L.E., Budde, W.L., 1975. Reference compound to calibrate Ion abundance measurement in gas chromatography-mass spectrometry systems. Anal. Chem., 47, 995.

Ejsing, C.S., Sampaio, J.L., Surendranath, V., Duchoslav, E., Ekroos, K., Klemm, R.W., Simons, K., Shevchenko, A., 2009. Global analysis of the yeast lipidome by quantitative shotgun mass spectrometry. Proc. Natl. Acad. Sci. 106, 2136–41.

Elegami, A.A., Bates, C., Gray, A. I, Mackay, S.P., Skellern, G.G., Waigh, R.D., 2003. Two very unusual macrocyclic flavonoids from the water lily Nymphaea lotus. Phytochem., 63, 31-727.

Ellinger, J.J., Chylla, R.A., Ulrich, E.L., Markley, J.L., 2013. Databases and Software for NMR-Based Metabolomics. Current Metabolomics, 1, 1–22.

Ellis, D.I., Brewster, V.L., Dunn, W.B., Allwood, J.W., Golovanov, A.P., Goodacre, R., 2012. Fingerprinting food: Current technologies for the detection of food adulteration and contamination. Chem. Socie. Rev. 41, 5706–27.

Englert, G., 1995. NMR spectroscopy. In: G. Britton, S. Liaaen-Jensen, & H. Pfander (Eds.), Carotenoids, Vol. 1B: Spectroscopy (pp. 147–260). Basel, Switzerland: Birkhauser.

Erikson, U., Standal, I.B., Aursand, I.G., Veliyulin, E., Aursand, M., 2012. Use of NMR in fish processing optimization: A review of recent progress. Magnetic Resonance Chem. 50, 471–480.

Eriksson, L., Johansson, E., Kettaneh-Wold, N., Wold, S., 2001. Multi- and megavariate data analysis: Principles and applications. Umeå, Umetrics Academy. 533pp.

Esslinger, S., Riedl, J., Fauhl-Hassek, C., 2014. Potential and limitations of non-targeted fingerprinting for authentication of food in official control. Food Research International, 60, 189–204.

Everstinem, K., Spink, J., Kennedy, S., 2013. Economically Motivated Adulteration (EMA) of food: common characteristics of EMA incidents. J. Food Protect. 76, 723–735.

Falginella, L.; di Gaspero, G.; Castellarin, S.D., 2012. Expression of flavonoid genes in the red grape berry of “Alicante Bouschet” varies with the histological distribution of anthocyanins and their chemical composition. *Planta*. *236*, 1037–1051.

Fadzillah, N.A., Rohman, A., Salleh, R.A., Amin, I., Shuhaimi, M., Farahwahida, M.Y., Rashidi, O., Aizat, J.M., Khatib, A., 2017. Authentication of butter from lard adulteration using high-resolution of nuclear magnetic resonance spectroscopy and high-performance liquid chromatography. Int. J. Food Prop. 20, 2147–2156.

Fan, S., Zhong, Q., Fauhl-Hassek, C., Pfister, M. K.H., Horn, B., Huang, Z., 2018. Classification of Chinese wine varieties using ^{1}H NMR spectroscopy combined with multivariate statistical analysis. Food Control, 88, 113–122.

Farag, M.A., Labib, R.M., Noleto, C., Porzel, A., Wessjohann, L.A., 2018. NMR approach for the authentication of 10 cinnamon spice accessions analyzed via chemometric tools. LWT, 90, 491–498.

Felton, J.F., 2004. GC and Systems Biology. Today's Chemist at Work 13, 26–29.

Fernandes, A., Bras, N.F., Mateus, N., Freitas, V.D., 2015. A study of anthocyanin self-association by NMR spectroscopy. New J. Chem. 39, 2602–2611.

Ferreira, V., Ortin, N., Escudero, A., Lopez, R., Cacho, J., 2002. Chemical characterization of the aroma of Grenache Rose wines: Aroma extract dilution analysis, quantitative determination and sensory reconstitution studies. J. Agric. Food Chem. 2002, 50, 4048-4054.

Fiehn, O., 2002. Metabolomics – the link between genotypes and phenotypes. Plant Mol. Biol., 48, 155–171.

Fielden, C., 2003. The wines of Argentina, Chile and Latin America. Hachette UK, London.

Fontana M., Filippetti I., Pastore C., Intrieri C., 2007. Indagine ampelografica e molecolare su vitigni locali dell'Emilia-Romagna: primi risultati. Italus Hortus, 14, 49-53.

Forester, S.C., Waterhouse, A.L., 2009. Metabolites Are Key to Understanding Health Effects of Wine Polyphenolics, T.J. Nutr. 139, 1824–1831,

Fossen, T., Pedersen, A.T., and Andersen, Ø.M., 1998. Flavonoids from red onion (Allium cepa). Phytochem. 47, 281, 1998.

Fotakis, C., Christodouleas, D., Kokkotou, K., Zervou, M., Zoumpoulakis, P., Moulos, P., Liouni, M., Calokerinos, A., 2013a. NMR metabolite profiling of Greek grape marc spirits. Food Chemistry, 138, 1837–1846.

Fotakis, C., Christodouleas, D., Kokkotou, K., Zervou, M., Zoumpoulakis, P., Moulos, P., Liouni, M., Calokerinos, A., 2013. NMR metabolite profiling of Greek grape marc spirits. Food Chem. 138, 1837–1846.

Fotakis, C., Kokkotou, K., Zoumpoulakis, P., Zervou, M., 2013. NMR metabolite fingerprinting in grape derived products: An overview. Food Resear. Int. 54, 1184-1194.

Fotakis, C., Kokkotou, K., Zoumpoulakis, P., Zervou, M., 2013b. NMR metabolite fingerprinting in grape derived products: An overview. Food Research Int. 54, 1184–1194.

Franke, A.A., Custer, L.J., Morimoto, Y., Nordt, F.J., Maskarinec, G., 2011. Analysis of urinary estrogens, their oxidized metabolites, and other endogenous steroids by benchtop orbitrap LCMS versus traditional quadrupole GCMS. Anal. Bioanal. Chem. 401, 1319–30.

Fregoni, M., Zamboni, M., Colla, R., 2002. Caratterizzazione ampelografica dei vitigni autoctoni piacentini. Università Cattolica S.C. Cattedra di Viticoltura Piacenza.

G. A. Theodoridis, H. G. Gika, E. J. Want, Wilson, I.D., 2012. Liquid chromatography-mass spectrometry based global metabolite profiling: a review. Anal. Chim. Acta, 711, 7–16.

Gangwar, L., Singh, R., Deepak, D., 2018. Structure elucidation of a novel oligosaccharide (Medalose) from camel milk. J. Molecular Structure, 1153, 157–161.

García-García, A.B., Lamichhane, S., Castejon, D., Cambero, M.I., Bertram, H.C., 2018. ^{1}H HR-MAS NMR-based metabolomics analysis for dry-fermented sausage characterization. Food Chem. 240, 514–523.

Garcia-Herrera, P., Pérez-Rodríguez, M.-L., Aguilera-Delgado, T., Labari-Reyes, M.-J., Olmedilla-Alonso, B., Camara, M., de Pascual-Teresa, S., 2016. Anthocyanin profile of red fruits and black carrot juices, purees and concentrates by HPLC-DAD-ESI/MS-QTOF. Int. J. Food Sci. Technol. 51, 2290–2300.

Gemma, M., Clark, K.S., Barnett, N.W., Niere, J.O., Adams, M.J., 2008. Generalised 2D-correlation NMR analysis of a wine fermentation. Anal. Chim. Acta, 629, 128–135.

Gfintert, M., 1984. Gaschromatographisch-massenspektrometrische Untersuchungen flüchtiger Inhaltsstoffe des Weinaromas: Beitrag zur Sortencharakterisierung der Rebsorte Weisser Riesling. Thesis, Universität Karlsruhe, Karlsruhe.

Giraudeau, P., 2014. Quantitative 2D liquid-state NMR. Magnetic Resonance Chem. 52, 259–272.

Girelli, C.R., Del Coco, L., Fanizzi, F.P., 2016. ^{1}H NMR spectroscopy and multivariate analysis as possible tool to assess cultivars, from specific geographical areas, in EVOOs. Europ. J. Lipid Sci. Technol. 118, 1380–1388.

Giust, M., Costacurta, A., Carraro, R., Aggio, L., Morbin, E., 2005. Malvasias in the collection of Istituto Sperimentale per la Viticultura. Results of twenty years of phenologic and productive observations. Riv. Viticol. Enol. 58, 67-80.

Gniechwitz, D., Reichardt, N., Meiss, E., Ralph, J., Steinhart, H., Blaut, M., Bunzel, M., 2008. Characterization and fermentability of an ethanol soluble high molecular weight coffee fraction. J. Agric. Food Chem. 56, 5960–5969.

Godelmann, R., Fang, F., Humpfer, E., Schutz, B., Bansbach, M., Schäfer, H., Spraul, M., 2013. Targeted and nontargeted wine analysis by ^{1}H NMR spectroscopy combined with multivariate statistical analysis. Differentiation of important parameters: Grape variety, geographical origin, year of vintage. J. Agric. Food Chem. 61, 5610-5619.

Gómez-Plaza, E., Gil-Muñoz, R., Carreño-Espín, J., Fernández-López, J.A., Martínez-Cutillas, A., 1999. Investigation on the aroma of wines from seven clones of Monastrell grapes. Eur. Food Res. Technol. 209, 257-260.

González-Rodríguez, M.J., Garrido-Frenich, A., Arrebola, F.J., Martínez-Vidal, J.L., 2012. Evaluation of low-pressure gas chromatography linked to ion-trap tandem mass spectrometry for the fast trace analysis of multiclass pesticide residues. Rapid Comm. Mass Spectrom. 16, 1216-1224.

Griffiths, W.J., Hornshaw, M., Woffendin, G., Baker, S.F., Lockhart, A., Heidelberger, S., Gaustafsson, M., Sjövall, J., Wang, Y., 2008. Discovering oxysterols in plasma: a window on the metabolome. J. Proteome Res. 7, 3602–12.

Güntert, M., 1984. Gaschromatographisch-massenspektrometrische Untersuchungen flfichtiger Inhaltsstoffe des Weinaromas: Beitrag zur Sortencharakterisierung der Rebsorte Weisser Riesling. Thesis, Universitht Karlsruhe, Karlsruhe.

Güntert, M., 1984. Gaschromatographisch-massenspektrometrische Untersuchungen flüchtiger Inhaltsstoffe des Weinaromas: Beitrag zur Sortencharakterisierung der Rebsorte Weisser Riesling. Thesis, Universität Karlsruhe, Karlsruhe.

Guymon, J.F., and Crowell, E.A., 1972. GC-separated brandy components derived from French and American oaks. Am. J. Enol. Vitic. 23 114-120.

Hadi, N.I., Jamal, Q., Iqbal, A., Shaikh, F., Somroo, S., Musharraf, S.G., 2017. Serum Metabolomic Proles for Breast Cancer Diagnosis, Grading and Staging by Gas Chromatography-Mass Spectrometry. Sci. Rep., 7, 1715.

Hardman, M. and Makarov, A., 2003. Interfacing the orbitrap mass analyzer to an electrospray ion source. Anal. Chem. 75, 1699.

Haselgrove, L., Botting, D., van Heeswijck, R., Høj, P.B., Dry, P.R., Ford, C., Land, P,G,I,, 2000. Canopy microclimate and berry composition; the effect of bunch exposure on the phenolic composition of Vitis vinifera L cv Shiraz grape berries. Aust. Grape Wine Res. 6, 141.

Hatzakis, E. and Dais, P., 2008. Determination of water content in olive oil by ^{31}P NMR spectroscopy. J. Agric. Food Chem., 56, 1866–1872.

Hatzakis, E. and Dais, P., 2010. Detection and quantification of free glycerol in virgin olive oil by ^{31}P NMR Spectroscopy. J. American Oil Chemist. Soc. 87, 29–34.

Hatzakis, E., 2019. Nuclear Magnetic Resonance (NMR) Spectroscopy in Food Science: A Comprehensive Review. Comprehen. Rev. Food Sci. Food Safety 18, 189-220.

Hatzakis, E., 2019. Nuclear Magnetic Resonance (NMR) Spectroscopy in Food Science: A Comprehensive Review. Comprehen. Rev. Food Sci. Food Safety, 18.

Hatzakis, E., Archavlis, E., Dais, P., 2007. Determination of glycerol in wines using ^{31}P-NMR spectroscopy. J. American Oil Chemist. Soc. 84, 615–619.

Hatzakis, E., Koidis, A., Boskou, D., Dais, P., 2008. Determination of phospholipids in olive oil by ^{31}P NMR spectroscopy. J. Agric. Food Chem. 56, 6232–6240.

He, F., Liang, N.-N., Mu, L., Pan, Q.-H., Wang, J., Reeves, M. J., Duan, C.-Q., 2012. Anthocyanins and Their Variation in Red Wines II. Anthocyanin Derived Pigments and Their Color Evolution. Molecules, 17, 1483-1519.

He, J., Oliveira, J., Silva, A.M.S., Mateus, N., De Freitas, V., 2010. Oxovitisins: A New Class of Neutral Pyranone-anthocyanin Derivatives in Red Wines. J. Agric. Food Chem. 58, 8814-8819.

Heldman, D.R., 2006. IFT and the food science profession. (Heldman Associates; Institute of Food Technologists). Food Technol. 60, 11.

Heldman, D.R., 2006. IFT and the food science profession. (Heldman Associates; Institute of Food Technologists). Food Technol. 60, 11.

Hennig, K., and Villforth, F., 1942. Die Aromastoffe der Weine. Vorratspfl. Lebensmittelforsch. 5 181-200 and 313-333.

Henry, H., Sobhi, H.R., Scheibner, O., Bromirski, M., Nimkar, S.B., Rochat, B., 2012. Comparison between a high-resolution single-stage Orbitrap and a triple quadrupole mass spectrometer for quantitative analyses of drugs. Rapid Commun. Mass Spectrom. 26, 499–509.

Hills, B., 1998. Magnetic resonance imaging in food science. New York: Wiley.

Hopfgartner, G., Varesio, E., Tschäppät, V., Grivet, C., Bourgogne, C., Leuthold, L.A.J., 2004. Triple quadrupole linear ion trap mass spectrometer for the analysis of small molecules and macromolecules. J. Mass Spectrom. 39, 845.

Hornedo-Ortega, R., Álvarez-Fernández, M.A., Cerezo, A.B., Garcia-Garcia, I., Troncoso, A.M., Garcia-Parrilla, M.C., 2017. Influence of Fermentation Process on the Anthocyanin Composition of Wineand Vinegar Elaborated from Strawberry. J. Food Sci. 82, 364-372.

Hoult, D., 1976. Solvent peak saturation with single phase and quadrature fourier transformation. J. Magnetic Resonance, 21, 337–347.

http://catalogoviti.politicheagricole.it/result.php?codice=363 (accessed on 22/11/2020)

Hu, F., Furihata, K., Ito-Ishida, M., Kaminogawa, S., Tanokura, M., 2004. Nondestructive observation of bovine milk by NMR spectroscopy: Analysis of existing States of compounds and detection of new compounds. J. Agric. Food Chem. 52, 4969–4974.

Hu, F., Furihata, K., Kato, Y., Tanokura, M., 2007. Nondestructive quantification of organic compounds in whole milk without pretreatment by two-dimensional NMR spectroscopy. J. Agric. Food Chem. 55, 4307–4311.

Hu, Q., Noll, R.J., Li, H., Makarov, A., Hardman, M., Graham Cooks, R., 2005. The Orbitrap: a new mass spectrometer. J. Mass Spectrom. 40, 430–443.

Hu, Y., Wang, S., Wang, S., Lu, X., 2017. Application of nuclear magnetic resonance spectroscopy in food adulteration determination: The example of Sudan dye I in paprika powder. Sci. Rep. 7, 1–9.

Hwang, T. and Shaka, A., 1995. Water suppression that works. Excitation sculpting using arbitrary wave-forms and pulsed-field gradients. J. Magnetic Resonance, Series A, 112, 275–279.

Igarashi, T., Aursand, M., Hirata, Y., Gribbestad, I.S., Wada, S., Nonaka, M., 2000. Nondestructive quantitative determination of docosahexaenoic acid and n-3 fatty acids in fish oils by high-resolution ^{1}H nuclear magnetic resonance spectroscopy. J. American Oil Chemist. Soc. 77, 737–748.

International Organization for Standardization, 2002. Quality management systems-Fundamentals and vocabulary. ISO 9000:2000(E).

International Organization of Vine and Wine, 2006. Standards and technical documents. Retrieved from International Code of Oenological Practices; wines; basic definition (18/73): http://www.oiv.int

ISO/IEC 17025, 2005. General Requirements for Competence of Testing and Calibration Laboratories. Paragraphs 5.5-5.6.

Izquierdo-García, J.L., Villa, P., Kyriazis, A., Del Puerto-Nevado, L., Perez-Rial, S., Rodriguez, I., Hernandez, N., Ruiz-Cabello, J., 2011. Descriptive review of current NMR-based metabolomic data analysis packages. Progress in Nuclear Magnetic Resonance Spectrosc. 59, 263–270.

James, A.T. and Martin, A.J.P., 1956. Gas–liquid chromatography: the separation and identification of the methyl esters of saturated and unsaturated acids from formic acid to n-octadecanoic acid. Biochem. J. 63, 144–152.

Jennings, W., Mittlefehldt, E., Stremple, P., 1987. Analytical Gas Chromatography. Academic Press, Inc., San Diego, CA.

Jézéquel, T., Deborde, C., Maucourt, M., Zhendre, V., Moing, A., Giraudeau, P., 2015. Absolute quantification of metabolites in tomato fruit extracts by fast 2D NMR. Metabolomics, 11, 1231–1242.

Jia, W., Chu, X., Ling, Y., Huang, J., Lin, Y., Chang, J., 2014. Simultaneous determination of dyes in wines by HPLC coupled to quadrupole orbitrap mass spectrometry. J. Sep. Sci. 37, 782–791.

Jiang, W., Xue, J., Liu, X., Wang, D., Guo, Y., Wang, L., 2015. The application of SNIF-NMR and IRMS combined with C, H and O isotopes for detecting the geographical origin of Chinese wines. Int. J. Food Sci. Technol. 50, 774–781.

Jones, G.V., and Davis, R.E., 2000. Climate influences on grapevine phenology, grape composition, and wine production and quality for Bordeaux, France. Am. J. Enol. Vitic. 51, 249-261.

Jones, H.G., 1992. Plants and Microclimate. A Quantitative Approach to Environmental Plant Physiology. Cambridge University Press, Cambridge, UK.

Jung, Y., Lee, J., Kwon, J., Lee, K.S., Ryu, D.H., Hwang, G.S., 2010. Discrimination of the geographical origin of beef by ^{1}H NMR-based metabolomics. J. Agri. Food Chem. 58, 10458–10466.

Junot, C., Fenaille, F., Colsch, B., Becher, F., 2014. High resolution mass spectrometry based techniques at the crossroads of metabolic pathways. Mass Spectrom. Rev. 33, 471–500.

Kaffarnik, S., Ehlers, I., Grobner, G., Schleucher, J., Vetter, W., 2013. Two-dimensional ^{31}P, ^{1}H NMR spectroscopic profiling of phospholipids in cheese and fish. J. Agri. Food Chem. 61, 7061–7069.

Kanani, H., Chrysanthopoulos, P.K., Klapa, M.I., 2008. Standardizing GC-MS metabolomics. J. Chromatogr. B: Anal. Technol. Biomed. Life Sci., 871, 191–201.

Kang, J., Cui, S.W., Phillips, G.O., Chen, J., Guo, Q., Wang, Q., 2011. New studies on gum ghatti (Anogeissus latifolia) Part III: Structure characterization of a globular polysaccharide fraction by 1D, 2D NMR spectroscopy and methylation analysis. Food Hydrocolloids, 25, 1999–2007.

Kang, J., Guo, Q., Shi, Y.-C., 2018. Molecular and conformational properties of hemicellulose fiber gum from dried distillers grains with solubles. Food Hydrocolloids, 80, 53–59.

Kawahigashi, H., Kasuga, S., Sawada, Y., Jun, I., Ando, T.K.H., Wu, J., Mizuno, H., Momma, M., Fujimoto, Z., 2016. The sorghum gene for leaf color changes upon wounding (P) encodes a flavanone 4-reductase in the 3-deoxyanthocyanidin biosynthesis pathway. G3 Genesgen. 6, 1439-1447.

Kazalaki, A., Misiak, M., Spyros, A., Dais, P., 2015. Identification and quantitative determination of carbohydrate molecules in Greek honey by employing ^{13}C NMR spectroscopy. Anal. Methods, 7, 5962–5972.

Keeler, J., 2010. Understanding NMR spectroscopy. Chichester: John Wiley and Sons.

Keith, E.S., and Powers, J.J., 1968. Determination of flavour threshold levels and sub-threshold, additive and concentration effects. J. Food Sci. 33 213-218.

Kepner, R.E., Webb, A.D., Muller, C.J., 1972. Identification of 4-hydroxy-3-methyloctanoic acid gamma-lactone (5-butyl-4- methyl-dihydro-2-(3H)-furanone) as a volatile component of oakwood aged wines of Vitis vinifera var. 'Cabernet-Sauvignon'. Am. J. Enol. Vitic. 23 103-105.

Khodaei, N. and Karboune, S., 2013. Extraction and structural characterisation of rhamnogalacturonan I-type pectic polysaccharides from potato cell wall. Food Chem. 139, 617–623.

Kidric, J., 2008. Chapter 5. NMR study of beverages. Annual Reports on NMR Spectroscopy, 64, 61–171.

Kim, J., Jin, G., Lee, Y., Chun, H.S., Ahn, S., Kim, B.H., 2015. Combined analysis of stable isotope, ^{1}H NMR, and fatty acid to verify sesame oil authenticity. Journal of Agricultural and Food Chemistry, 63, 8955–8965.

Kim, J., Jung, Y., Song, B., Bong, Y.S., Ryu, D.H., Lee, K.S., Hwang, G.S., 2013. Discrimination of cabbage (Brassica rapa ssp. pekinensis) cultivars grown in different geographical areas using ^{1}H NMR-based metabolomics. Food Chem. 137, 68–75.

Kirchner, M., Matisová, E.,, Otrekal, R., Hercegová, A., de Zeeuw, J., 2005. Search on ruggedness of fast gas chromatography–mass spectrometry in pesticide residues analysis. J. Chrom. A 1084, 63-70.

Kiser, R.W., 1965. Introduction to Mass Spectrometry and Its Application. Englewood Cliffs, NJ: Prentice-Hall.

Ko, W.-C., Cheng, J.-Y., Chen, P.-Y., Hsieh, C.-W., 2013. Optimized extraction method of acetic acid in vinegar and its effect on SNIF-NMR analysis to control the authenticity of vinegar. Food Bioproc. Technol. An International J. 6, 2202–2206.

Korytár, P., Janssen, H.-G., Matisová, E., Brinkman, U.A.Th., 2002. Practical fast gas chromatography: methods, instrumentation and applications. TrAC Trends Anal. Chem. 21, 558-572.

Košir, I.J., Kocjančič, M., Ogrinc, N., Kidrič, J., 2001. Use of SNIF-NMR and IRMS in combination with chemometric methods for the determination of chaptalisation and geographical origin of wines (the example of Slovenian wines). Anal. Chimica Acta, 429, 195–206.

Kotseridis, Y. and Baumes, R., 2000. Identification of impact odorants in Bordeaux red grape juice, in the commercial yeast used for its fermentation, and in produced wine. J. Agric. Food Chem. 48, 400-406.

Kritioti, A., Menexes, G., Drouza, C., 2018. Chemometric characterization of virgin olive oils of the two major Cypriot cultivars based on their fatty acid composition. Food Research Int. 103, 426–437.

Kuballa, T., Brunner, T.S., Thongpanchang, T., Walch, S.G., Lachenmeier, D.W., 2018a. Application of NMR for authentication of honey, beer, and spices. Current Opinion in Food Sci. 19, 57–62.

Kuballa, T., Hausler, T., Okaru, A.O., Neufeld, M., Abuga, K.O., Kibwage, I.O., Rehm, J., Luy, B., Walch, S.G., Lachenmeier, D.W., 2018b. Detection of counterfeit brand spirits using ^{1}H NMR fingerprints in comparison to sensory analysis. Food Chemistry, 245, 112–118.

Kuehnbaum, N.L. and Britz-McKibbin, P., 2013. New advances in separation science for metabolomics: Resolving chemical diversity in a post-genomic era. Chem. Rev., 113, 2437–2468.

Lachenmeier, D.W., Humpfer, E., Fang, F., Schutz, B., Dvortsak, P., Sproll, C., Spraul, M., 2009. NMR-spectroscopy for nontargeted screening and simultaneous quantification of health-relevant compounds in foods: The example of melamine. J. Agric. Food Chem. 57, 7194–7199.

Lacombe, T., Boursiquot, J.-M., Laucou, V., Dechesne, F., Varès, D., This, P., 2007. Relationships and genetic diversity within the accessions related to Malvasia held in the domaine de vassal grape germplasm repository. Am. J. Enol. Vitic. 58, 124-131.

Laghi, L., Picone, G., Capozzi, F., 2014. Nuclear magnetic resonance for foodomics beyond food analysis. Trend. Anal. Chem. 59, 93–102.

Laghi, L., Versari, A., Marcolini, E., Parpinello, G.P., 2014. Metabonomic investigation by ^{1}H-NMR to discriminate between red wines from organic and biodynamic grapes. Food Nutr. Sci. 05, 52–59.

Lambert, J., Mazzola, E., Ridge, C., 2018. Nuclear magnetic resonance spectroscopy: An introduction to principles, applications, and experimental methods (2nd Ed). Chichester, England: John Wiley & Sons, Ltd.

Landi, M., Tattini, M., Gould, K.S., 2015. Multiple functional roles of anthocyanins in plant-environment interactions. Environ. Exp. Bot. 119, 4-17.

Larice, J.-L., Archier P., Rocheville-Divorne, C., Coen, S., Roggero, J.-P., 1989. Composition anthocyanique des cépages. II — Essai de classification sur trois ans par analyse en composantes principales et étude des variations annuelles de cépages de même provenance. Rev. Fr. Oenol. 121, 7.

Le Gall, G., Colquhoun, I.J., Davis, A.L., Collins, G J., Verhoeyen, M.E., 2003. Metabolite profiling of tomato (Lycopersicon esculentum) using ^{1}H NMR spectroscopy as a tool to detect potential unintended effects following a genetic modification. J. Agric. Food Chem. 51, 2447–2456.

Lee, J.E., Lee, B.J., Chung, J.O., Hwang, J.A., Lee, S.J., Lee, C.H., Hong, Y.-S., 2010. Geographical and climatic dependencies of green tea (Camellia sinensis) metabolites: A ^{1}H NMR-based metabolomics study. J. Agric. Food Chem. 58, 10582.

Lee, J.E., Lee, B.J., Chung, J.O., Kim, H.N., Kim, E.H., Jung, S., Lee, H., Lee, S.J., Hong, Y.-S., 2015. Metabolomic unveiling of a diverse range of green tea (Camellia sinensis) metabolites dependent on geography. Food Chem. 174, 452–459.

Lei, Z., Huhman, D.V., Sumner, L.W., 2011. Mass spectrometry strategies in metabolomics. J. Biol. Chem. 286, 25435–25442.

Levitt, M., 2005. Spin dynamics. Chichester: John Wiley & Sons.

Leydet, Y., Gavara, R., Petrov, V., Diniz, A.M., Jorge Parola, A., Lima, J.C., Pina, F., 2012. The effect of self-aggregation on the determination of the kinetic and thermodynamic constants of the network of chemical reactions in 3-glucoside anthocyanins. Phytochem. 83, 125–135.

Li, J., Liu, X., Han, S., Li, J., Xu, Q., Xu, H., Wang, Y., Liu, F., Zhang, Z., 2012. Analysis of Ochratoxin A in wine by high-resolution UHPLC-MS. Food Anal. Method. 5, 1506–1513.

Li, Q., Yu, Z., Zhu, D., Meng, X., Pang, X., Liu, Y., Frew, R., Chen, H., Chen, G., 2017. The application of NMR-based milk metabolite analysis in milk authenticity identification. J. Sci. Food Agric. 97, 2875–2882.

Li, X. and Franke, A.A., 2011. Improved LC-MS method for the determination of fatty acids in red blood cells by LC-Orbitrap MS. Anal. Chem. 83, 3192–98.

Lim, H.K., Chen, J., Sensenhauser, C., Cook, K., Subrahmanyam, V., 2007. Metabolite identification by datadependent accurate mass spectrometric analysis at resolving power of 60,000 in external calibration mode using an LTQ/Orbitrap. Rapid Commun. Mass Spectrom. 21,1821–32

Longobardi, F., Ventrella, A., Bianco, A., Catucci, L., Cafagna, I., Gallo, V., Mastrorilli, P., Agostiano, A., 2013. Non-targeted ^{1}H NMR fingerprinting and multivariate statistical analyses for the characterisation of the geographical origin of Italian sweet cherries. Food Chem. 141, 3028–3033.

Lopez, M.I., Trullols, E., Callao, M. P., Ruisánchez, I., 2014. Multivariate screening in food adulteration: Untargeted versus targeted modelling. Food Chem. 147, 177–181.

Lovegrove, A., Edwards, C.H., De, N.I., Patel, H., El, S.N., Grassby, T., Zielke, C., Ulmius, M., Nilsson, L., Butterworth, P.J., Ellis, P.R., Shewry, P.R., 2017. Role of polysaccharides in food, digestion, and health. Critical Rev. Food Sci. Nutr. 57, 237–253.

M.C. Cravero, 2019. Organic and biodynamic wines quality and characteristics: A review. Food Chem. 294, 334-340.

Madalinski, G., Godat, E., Alves, S., Lesage, D., Genin, E., Levi, P., Labarre, J., Tablet, J.C., Ezan E., Junot, C., 2008. Direct introduction of biological samples into a LTQ-Orbitrap hybrid mass spectrometer as a tool for fast metabolome analysis. Anal. Chem. 80, 3291–303.

Maher, A.D. and Rochfort, S.J., 2014. Applications of NMR in dairy research. Metabolites, 4, 131–141.

Majchrzak, T., Wojnowski, W., Lubinska-Szczygeł, M., Różańska, A., Namieśnik, J., Dymerski, T., 2018. PTR-MS and GC-MS as complementary techniques for analysis of volatiles: A tutorial review. Analyt. Chim. Acta. 1035, 1-13.

Majchrzak, T., Wojnowski, W., Lubinska-Szczygeł, M., Różańska, A., Namieśnik, J., Dymerski, T., 2018. PTR-MS and GC-MS as complementary techniques for analysis of volatiles: A tutorial review. Analyt. Chim. Acta. 1035, 1-13.

Makarov, A. and Denisov, E.J., 2009. Am. Soc. Mass Spectrom. 20, 1486.

Makarov, A. and Scigelova, M., 2010. Coupling liquid chromatography to Orbitrap mass spectrometry. J. Chromatogr. A 1217, 3938–3945.

Makarov, A., 1999. Mass spectrometer. U.S. Patent 5, 886, 346.

Makarov, A., 2000. Electrostatic axially harmonic orbital trapping: a high-performance technique of mass analysis. Anal. Chem. 72: 1156.

Makarov, A., 2000. Electrostatic axially harmonic orbital trapping: a high-performance technique of mass analysis. Anal. Chem. 72: 1156.

Makarov, A., Hardman, M., Schwartz, J., Senko, M., 2002. PCT Patent Appl.W002078046.

Malmendal, A., Amoresano, C., Trotta, R., Lauri, I., De Tito S., Novellino, E., Randazzo, A., 2011. MR spectrometers as “magnetic tongues”: Prediction of sensory descriptors in canned tomatoes. J. Agric. Food Chem. 59, 10831–10838.

Mandery, H., 1983. Gaschromatographisch-massenspektrometrische Untersuchungen fl/ichtiger Inhaltsstoffe des Traubenmost- und Weinaromas: Auswirkung der Sfissung auf die Aromazusammensetzung. Dissertation, Universit/it Karlsruhe, Karlsruhe.

Mandery, H., 1983. Gaschromatographisch-massenspektrometrische Untersuchungen flüichtiger Inhaltsstoffe des Traubenmost- und Weinaromas: Auswirkung der Sfissung auf die Aromazusammensetzung. Dissertation, Universität Karlsruhe, Karlsruhe.

Mannina, L., Marini, F., Antiochia, R., Cesa, S., Magrì, A., Capitani, D., Sobolev, A.P., 2016. Tracing the origin of beer samples by NMR and chemometrics: Trappist beers as a case study. Electrophoresis, 37, 2710–2719.

Mannina, L., Sobolev, A.P., 2011. High resolution NMR characterization of olive oils in terms of quality, authenticity and geographical origin. Magnetic Resonance in Chemistry, 49, 3–11.

Mannina, L., Sobolev, A.P., Lorenzo Di, A., Vista, S., Tenore, G.C., Daglia, M., 2015. Chemical composition of different botanical origin honeys produced by sicilian black honeybees (Apis mellifera ssp. sicula). J. Agric. Food Chem. 63, 5864–5874.

Mannina, L., Sobolev, A.P., Viel, S., 2012. Liquid state ^{1}H high field NMR in food analysis. Progress in Nuclear Magnetic Resonance Spectrosc. 66, 1–39.

Marcone, M.F., Wang S., Albabish W., Somnarain D., Hill A., Nie S., 2013. Diverse food-based applications of nuclear magnetic resonance (NMR) technology. Food Resear. Int. 51, 729–747.

Mariette, F., 2009. Investigations of food colloids by NMR and MRI. Current Opinion in Colloid & Interface Sci. 14, 203–211.

Marquez, A., Duenas, M., Serratosa, M.P., Merida, J., 2013. Pyranoanthocyanin derived pigments in wine: structure and formation during winemaking. J. Chem. 2013, 1−7.

Marshall, A.G. and Verdun, F.R., 1990. Fourier transforms in nmr, optical, and mass spectrometry: a user's handbook, Elsevier: Amsterdam, 450.

Martin, G., Akoka, J.S., Martin, M.L., 2006. SNIF-NMR—Part 1: Principles. In G. A. Webb (Ed.), Modern magnetic resonance, part 3 (pp. 1629). Dordrecht, the Netherlands: Springer.

Masino, F., Montevecchi, G., Arfelli, G., Antonelli, A., 2008. Evaluation of the Combined Effects of Enzymatic Treatment and Aging on Lees on the Aroma of Wine from *Bombino bianco* Grapes. J. Agric. Food Chem., 56, 9495-9501.

Massart, D., 1988. Chemometrics. Amsterdam: Elsevier.

Maštovská, K. and Wylie, P.L., 2012. Evaluation of a new column backflushing set-up in the gas chromatographic–tandem mass spectrometric analysis of pesticide residues in dietary supplement. J. Chrom. A 1265, 155-164.

Masuda, M., and Nishimura, K., 1971. Branched nonalactones from some Quercus species. Phytochemistry 10 1401-1402.

Masuda, M., Okawa, E., Nishimura, K., Yunome, H., 1984. Identification of 4, 5-dimethyl-3-hydroxy-2(SH)-furanone (Sotolone) and ethyl-9-hydroxy-nonanoate in botrytised wine and evaluation of the roles of compounds characteristic of it. Agric. biol. Chem. 48 2707-2710.

Matisová, E., Horouzková, S., 2012. Analysis of Endocrine Disrupting Pesticides by Capillary GC with Mass Spectrometric Detection. Int. J. Environ. Res. Public Health 9, 3166-3196.

Mattivi, F., Guzzon, R., vrhovsek, U., Stefanini, M., Velasco, R., 2006. Metabolite Profiling of Grape: Flavonols and Anthocyanins. J. Agric. Food Chem. 54, 7692−7702.

Mattivi., F., Zulian, C., Nicolini, G., Valenti, L., 2002. Wine, Biodiversity, Technology, and Antioxidants. Annals New York Academy of Sciences, 37-56.

Maul, E., Carka, F., Cunha, J., José Eduardo Jorge Eiras Dias, Gardiman, M., Gazivoda, A., Ivanišević, D., Maletić, E., Maraš, V., Muñoz Organero, G., Nikolić, D., Regner, F., Röckel, F., Schneider, A., Zdunić, G., Ziegler, M., Lacombe, T., 2017. On-farm inventory of minor grape varieties in the European Vitis Database. ECPGR Activity Grant Scheme.

Mayr, C.M., Geue, J.P., Holt, H.E., Pearson, W.P., Jeffery, D.W., Francis, I.L., 2014. Characterization of the Key Aroma Compounds in Shiraz Wine by Quantitation, Aroma Reconstitution, and Omission Studies. J. Agric. Food Chem. 62, 4528−4536.

Mazza, G. and Miniati, E., 1993. Grapes. In Anthocyanins in Fruits, Vegetables and Grains (eds G. Mazza and E. Miniati), CRC Press, Boca Raton, FL, p. 149.

Mazzei, P. and Piccolo, A., 2012. ^{1}H HRMAS-NMR metabolomic to assess quality and traceability of mozzarella cheese from Campania buffalo milk. Food Chem. 132, 1620–1627.

Mazzei, P., Spaccini, R., Francesca, N., Moschetti, G., Piccolo, A., 2013. Metabolomic by ^{1}H NMR spectroscopy differentiates “Fiano di Avellino” white wines obtained with different yeast strains. J. Agric. Food Chem. 61, 10816–10822.

McGovern, P., Jalabadze, M., Batiuk, S., Callahan, M.P., Smith, K.E., Hall, G.R., Kvavadze, E., Maghradze, D., Rusishvili, N., Bouby, L., Failla, O., Cola, G., Mariani, L., Boaretto, E., Bacilieri, R., This, P., Walesk, N., Lordkipanidz, D., 2017. Early Neolithic wine of Georgia in the South Caucasus. PNAS PLUS, 309-318.

McKay, R.T., 2011. How the 1D-NOESY suppresses solvent signal in metabonomics NMR. Spectroscopy: An examination of the pulse sequence components and evolution. Concepts in Magnetic Resonance Part A, 38A, 197–220.

Meiboom, S. and Gill, D., 1958. Modified spin-echo method for measuring nuclear relaxation times. Rev. Sci. Instrument. 29, 688–691.

Meneghetti, S., Poljuha, D., Frare, E., Costacurta, A., Morreale, G., Bavaresco, L., Caló, A., 2012. Inter- and intra-varietal genetic variability in Malvasia cultivars. Mol. Biotechnol. 50, 189-199.

Merchak, N., El, B.E., Bou, K.R., Rizk, T., Akoka, S., Bejjani, J., 2017. Geoclimatic, morphological, and temporal effects on Lebanese olive oils composition and classification: A ^{1}H NMR metabolomic study. Food Chem. 217, 379–388.

Merchak, N., Rizk, T., Silvestre, V., Remaud, G.S., Bejjani, J., Akoka, S., 2018. Olive oil characterization and classification by ^{13}C NMR with a polarization transfer technique: A comparison with gas chromatography and ^{1}H NMR. Food Chem. 245, 717–723.

Merchak, N., Silvestre, V., Rouger, L., Giraudeau, P., Rizk, T., Bejjani, J., Akoka, S., 2016. Precise and rapid isotopomic analysis by ^{1}H–^{13}C 2D NMR: Application to triacylglycerol matrices. Talanta, 156-157, 239–244.

Merkx, D.W.H., Hong, G.T.S., Ermacora, A., van, D.J.P.M., 2018. Rapid quantitative profiling of lipid oxidation products in a food emulsion by ^{1}H NMR. Anal. Chem. 90, 4863–4870.

Miyazaki, T., Okada, K., Yamashita, T. ,Miyazaki, T., 2017. Two dimensional gas chromatography time-of-flight mass spectrometry-based serum metabolic fingerprints of neonatal calves before and after first colostrum ingestion. J. Dairy Sci., 100, 4354–4364.

Moco, S., Capanoglu, E., Tikunov, Y., Bino, R.J., Boyacioglu, D., Hall, R.D., Vervoort, J., de Vos, R.C., 2007. Tissue specialization at the metabolite level is perceived during the development of tomato fruit. J. Exp. Bot. 58, 4131–4146.

Molina, A.M., Swiegers, J.H., Varela, C., Pretorius, I.S., Agosin, E., 2007. Influence of wine fermentation temperature on the synthesis of yeast-derived volatile aroma compounds. Appl. Microbiol. Biotechnol. 77, 675-687.

Mommers, J., Knooren, J., Mengerink, Y., Wilbers, A., Vreuls, R., 2011. Retention time locking procedure for comprehensive two-dimensional gas chromatography. J. Chromatog. A. 1218, 3159-3165.

Monaci, L., Losito, I., Palmisano, F., Godula, M., Visconti, A., 2011a. Towards the quantification of residual milk allergens in caseinate-fined white wines using HPLC coupled with single-stage Orbitrap mass spectrometry. Food Addit Contam Part A. 28, 1304–1314.

Monaci, L., Losito, I., Palmisano, F., Visconti, A., 2011b. Reliable detection of milk allergens in food using a high-resolution, stand-alone mass spectrometer. J AOAC Int. 94, 1030–1042.

Monakhova, Y.B. and Diehl, B.W., 2016a. Authentication of the origin of sucrose-based sugar products using quantitative natural abundance ^{13}C NMR. J. Agric. Food Chem. 96, 2861–2866.

Monakhova, Y.B. and Diehl, B.W.K., 2016b. Quantitative analysis of sunflower lecithin adulteration with soy species by NMR spectroscopy and PLS regression. J. American Oil Chemist. Soci. 93, 27–36.

Monakhova, Y.B., Kuballa, T., Lachenmeier, D.W., 2013. Chemometric methods in NMR spectroscopic analysis of food products. J. Anal. Chem. 68, 755–766.

Montevecchi, G., Masino, F., Vasile Simone, G., Cerretti, E., Antonelli, A., 2015. Aromatic profile of white sweet semi-sparkling wine from malvasia di candia aromatica grapes. S. Afr. J. Enol. Vitic., 36, 2.

Mora-Gutierrez, A. and Baianu, I.C., 1991. Carbon-13 nuclear magnetic resonance studies of chemically modified waxy maize starch, corn syrups, and maltodextrins. Comparisons with potato starch and potato maltodextrins. J. Agric. Food Chem. 39, 1057–1062.

Mostafa, A., Edwards, M., Gorecki, T., 2012. Optimization aspects of comprehensive two-dimensional gas chromatography. J. Chromatogr. A, 1255, 38–55.

Moulard, Y., Bailly-Chouriberry, L., Boyer, S., Garcia, P., Popot, M.A., Bonnaire, Y., 2011. Use of benchtop exactive high resolution and high mass accuracy Orbitrap mass spectrometer for screening in horse doping control. Anal. Chim. Acta 700, 126–36.

Murgia, S., Mele, S., Monduzzi, M., 2003. Quantitative characterization of phospholipids in milk fat via ^{31}P NMR using a monophasic solvent mixture. Lipids, 38, 585–591.

Nagornov, K.O., Gorshkov, M.V., Kozhinov, A.N., Tsybin, Y.O., 2014. High-resolution Fourier transform ion cyclotron resonance mass spectrometry with increased throughput for biomolecular analysis. Anal. Chem. 86, 9020–9028.

Nagy, S., and Dinsmore, H.C., 1974. Relationship of furfural to temperature abuse and flavor change in commercially canned single-strength orange juice. J. Food Sci. 39 1116-1119.

Nagy, S., and Randall, V., 1973. Use of furfural content as an index of storage temperature abuse in commercially processed orange juice. J. Agric. Food Chem. 21 272-275.

Naves, Y.R., 1947. Sur la presence d'ionones darts les produits végétaux. Helv. claim. Acta 30 956-957.

Neudoerffer, T.S., Sandler, S., Zubechis, E., Smith, M.D., 1965. Detection of an undesirable anormally in concord grape by gas chromatography. J. Agric. Food Chem. 13 584-588.

Nicolini, G., Moser, S., Larcher, R., Versini, G. & Fedrizzi, B., 2009. Technological characterization of Malvasia colli di Parma doc juice and wine. In: Malvasias (ed.): Proc. 3rd Internat. Symp. "Malvasias", May 2009, La Palma, Canary Islands, Spain. p. 10.

Nigro, G., Filippetti I., Melotti, M., Simoni, M., Vespignani, G., 2010. Vitigni autoctoni: Veruccese e Vernaccina Riminese. L'informatore agrario. n.10.

Nigro, G., Melotti, M., Simoni, M., 2013. Festasio e Lambrusco di Fiorano. Agricoltura. Novembre: 67-68.

Nilsson, G.S., Gorton, L., Bergquist, K.-E., Nilsson, U., 1996. Determination of the degree of branching in normal and Amylopectin type potato starch with ^{1}H-NMR spectroscopy improved resolution and two-dimensional spectroscopy. Starch-Starkë, 48, 352–357.

Nilsson, M., Duarte, I.F., Almeida, C., Delgadillo, I., Goodfellow, B.J., Gil, A.M., Morris, G.A., 2004. High-resolution NMR and diffusion-ordered spectroscopy of port wine. J. Agric. Food Chem. 52, 3736–3743.

Nishimura, K., and Masuda, M., 1971. Minor constituents of whiskey fusel oils. I. basic, phenolic, and lactonic compounds. J. Food Sci. 36 819-822.

Nunes, F.M., Reis, A., Silva, A.M., Domingues, M.R., Coimbra, M.A., 2008. Rhamnoarabinosyl and rhamnoarabinoarabinosyl side chains as structural features of coffee arabinogalactans. Phytochem. 69, 1573–1585.

Ogrinc, N., Kosir, I.J., Kocjancic, M., Kidric, J., 2001. Determination of authenticity, regional origin, and vintage of Slovenian wines using a combination of IRMS and SNIF-NMR analyses. J. Agric. Food Chem. 49, 1432–1440.

Ohloff, G., 1978. Recent developments in the field of naturally-occurring aroma components. Fortschr. Chem. org. NatStoffe 35 431-527.

Ohtsuki, T., Tada, A., Tahara, M., Suematsu, T., Sugimoto, N., 2016. Applications of NMR Spectroscopy, 4, 222–262.

Olszewski, K.L., Mather, M.W., Morrisey, J.M., Garcia, B.A., Vaidya, A.B., Rabinowitz, J.D., Llinás, M., 2010. Branched tricarboxylic acid metabolism in Plasmodium falciparum. Nature 466, 774–78.

Orfanakis, A., Hatzakis, E., Kanaki, K., Pergantis, S. A., Rizos, A., Dais, P., 2013. Characterization of polyglycerol polyricinoleate formulations using NMR spectroscopy, mass spectrometry and dynamic light scattering. J. American Oil Chemists' Society, 90, 39–51.

Otsuka, K., Zenibayashi, Y., Itoh, M., Totsuka, A., 1974. Presence and significance of two diastereomers β-methyl-γ-octalactone in aged distilled liquores. Agric. biol. Chem. 38 485-490.

Otte, D.A., Borchmann, D.E., Lin, C., Weck, M., Woerpel, K.A., 2014. ^{13}C NMR spectroscopy for the quantitative determination of compound ratios and polymer end groups. Organic Letters, 16, 1566–1569.

Özdemir, I.S., Dağ, C., Makuc, D., Ertaş, E., Plavec, J., Bekiroğlu, S., 2018. Characterisation of the Turkish and Slovenian extra virgin olive oils by chemometric analysis of the presaturation ^{1}H NMR spectra. LWT, 92, 10–15.

Pacifico, D., Casciani, L., Ritota, M, Mandolino, G., Onofri, C., Moschella, A., Parisi, B., Valentini, M., 2013. NMR-based metabolomics for organic farming traceability of early potatoes. J. Agric. Food Chem. 61, 11201–11211.

Papadimitriou, A., Ketikidis, I., Stathopoulou, M.-E., Banti, C., Papachristodoulou, C., Zoumpoulakis, L., Agathopoulos, S., Vagenas, G.V., Hadjikakou, S., 2018. Innovative material containing the natural product curcumin, with enhanced antimicrobial properties for active packaging. Materials Sci. Engineer. C, 84, 118–122.

Papotti, G., Bertelli, D., Graziosi, R., Silvestri, M., Bertacchini, L., Durante, C., Plessi, M., 2013. Application of one- and two-dimensional NMR spectroscopy for the characterization of protected designation of origin Lambrusco wines of Modena. J. Agric. Food Chem. 61, 1741–1746.

Papoušková, B., Bednář, P., Hronb, K., Stávekc, J., Balíkc, J., Myjavcová, R., Bartáka, P., Tománkovác, E., Lemr, K., 2011. Advanced liquid chromatography/mass spectrometry profiling of anthocyanins in relation to set of red wine varieties certified in Czech Republic. J. Chromatogr. A, 2018, 7581–7591

Paris, P. W. 2002. Top French wine diluted and sold with fake labels. 24 February. The Observer 22.

Paul, W. and Raether, M., 1955. Das Elektrische Massenfilter. Z. Physik., 140, 262–71.

Paul, W. and Steinwedel, H., 1953, Ein neues Massenspektrometer ohne Magnetfeld. Z. Naturforsch A, 8, 448–450.

Perini, M., Giongo, L., Grisenti, M., Bontempo, L., Camin, F., 2018. Stable isotope ratio analysis of different European raspberries, blackberries, blueberries, currants and strawberries. Food Chem. 239, 48–55.

Petersen B.O., Bojstrup M., Hindsgaul O., Meier S., Nilsson M., 2014. ^{1}H NMR spectroscopy for profiling complex carbohydrate mixtures in non-fractionated beer. Food Chem. 150, 65–72.

Petrakis, E.A., Cagliani, L.R., Polissiou, M.G., Consonni, R., 2015. Evaluation of saffron (Crocus sativus L.) adulteration with plant adulterants by ^{1}H NMR metabolite fingerprinting. Food Chem. 173, 890–896.

Petrakis, E.A., Cagliani, L.R., Tarantilis, P.A., Polissiou, M.G., Consonni, R., 2017. Sudan dyes in adulterated saffron (Crocus sativus L.): Identification and quantification by ^{1}H NMR. Food Chem. 217, 418–424.

Picone, G., Babini, E., Placucci, G., Capozzi, F., Mezzetti, B., Capocasa, F., 2011. Unsupervised principal component analysis of NMR metabolic profiles for the assessment of substantial equivalence of transgenic grapes (vitis vinifera). J. Agric. Food Chem. 59, 9271–9279.

Picone, G., Trimigno, A., Tessarin, P., Donnini, S., Rombola, A. D., Capozzi, F., 2016. ^{1}H NMR foodomics reveals that the biodynamic and the organic cultivation managements produce different grape berries (Vitis vinifera L. cv. Sangiovese). Food Chem. 213, 187–195.

Pineau, B., J.-C., Barbe, van Leeuwen, C., Dubourdieu, D., 2007. Which Impact for β-Damascenone on Red Wines Aroma? J. Agric. Food Chem. 55, 4103−4108.

Piotto, M., Saudek, V., Sklenar, V., 1992. Gradient-tailored excitation for single-quantum NMR spectroscopy of aqueous solutions. J. Biomol. NMR, 2, 661–665.

Pisano, P.L., Silva, M.F., Olivieri, A.C., 2015. Anthocyanins as markers for the classification of Argentinean wines according to botanical and geographical origin. Chemometric modeling of liquid chromatography–mass spectrometry data. Food Chem. 175, 174–180.

Price, S.F., Breen, P.J., Valladao, M., Watson, B.T., 1995. Cluster sun exposure and quercetin in pinot noir grapes and wine. Am. J. Enol. Vitic. 46, 187.

Ramakrishnan, V., Luthria D.L., 2017. Recent applications of NMR in food and dietary studies. J. Sci. Food Agric. 97, 33–42.

Ramey, D.D., and Ough, C.S., 1980. Volatile ester hydrolysis or formation during storage of model solutions and wines. J. Agric. Food Chem. 28 928-934.

Ramshaw, E.H. and Hardy, P.J., 1969. Volatile compounds in dried grapes. J. Sci. Food Agric. 20 619-621.

Rapp, A. & Mandery, H., 1986. Wine aroma. Experientia 42, 873-884.

Rapp, A., 1980. Flfichtige Komponenten in edelfaulen Trauben, Niederschrift fiber die Tagung des Bundesausschusses ffir Weiuforschung; Freiburg.

Rapp, A., Almy, J., Güntert, M., 1985a. Identification of several sulfur-containing components in wine. Am. J. Enol. Vitic. 36 219-221.

Rapp, A., and Hastrich, H., 1978. Gaschromatographische Untersuchungen über die Aromastoffe von Weinbeeren III. Die Bedeutung des Standortes für die Aromastoffzusammensetzung der Rebsorte 80 Riesling. Vitis 17 288-298.

Rapp, A., and Knipser, W., 1980. Eine neue Methode zur Anreicherung von Dampfraumkomponenten. Dargestellt am Beispiel des Weines. Chromatographia 13 698-702.

Rapp, A., Güntert, M., Heimann, W., 1985. Beitrag zur Sortencha-rakterisierung des Weines der Rebsorte Riesliug. II. Untersuchung der Aromastoffzusammensetzung deutscher Weissweine der Rebsorten Riesling, Müller-Thurgau und Silvaner. Vitis 24 139-150.

Rapp, A., Güntert, M., Rieth, W., 1985. Einfluss der Maischestandzeit auf die Aromazusammensetzung des Traubenmostes und Weines. Dt. Lebensm. Rdsch. 81 69-72.

Rapp, A., Mandery, H., Güntert, M., 1984. Terpene compounds in wine. Flavour research of alcoholic beverages, pp. 255-274. Eds L. 85 Nykänen and P. Lektonen. Foundations for biotechnical and industrial fermentation research 3, Helsinki.

Raterink, R.-J., Kloet, F.M., Li, J., Wattel, N.A., Schaaf, M.J.M., Spaink, H.P., Berger, R., Vreeken, R.J., Hankemeier, T., 2013. Rapid metabolic screening of early zebrafish embryogenesis based on direct infusion-nanoESI-FTMS. Metabolomics 9, 864–873.

Rayyan, S., Fossen, T., Nateland, H.S., Andersen, Ø.M., 2005. Isolation and identification of flavonoids including flavone rotamers from the herbal drug ‘‘Crataegi folium cum flore,’’ hawthorn, Phytochem. Anal. 16, 41-334.

Razzaq, H.A.A., Pezzuto, M., Santagata, G., Silvestre, C., Cimmino, S., Larsen, N., Duraccio, D., 2016. Barley β-glucan-protein based bioplastic film with enhanced physicochemical properties for packaging. Food Hydrocol. 58, 276–283.

Remaud, G.S., Akoka, S., 2017. A review of flavors authentication by position-specific isotope analysis by nuclear magnetic resonance spectrometry: The example of vanillin. Flav. Fragranc. J. 32, 77–84.

Ribéreau-Gayon, P., 1971. Recherches technologiques sur les composés phénoliques des vins rouges. III. Influence du mode de logement sur Ies caractères chimiques et organoleptiques des vins rouges, plus particulièrement sur leur couleur. Conn. Vigne Vin 5 87-97.

Ribéreau-Gayon, P., 'Wine-Flavor' in flavor of foods and beverages. Eds G. Charalambous and G. E. Inglett. Academic Press, New York/San Francisco/London 1978.

Ribéreau-Gayon, P., Boidron, J.H., and Terrier, A., 1975. Aroma of muscat grape varieties, J. Agric. Food Chem. 23 1042-1047.

Riberéu-Gayon, P., Glories, Y., Maujean, A., Dubourdieu, D., 2018a. Trattato di Enologia: Chimica del vino, Stabilizzazione e trattamenti. Vol. 2. Quarta Edizione italiana. Edagricole.

Ribéreau-Gayon, P., Dubourdieu, D., Donèche, B., Lonvaud, A., 2018b. Trattato di Enologia:Microbiologia del vino e vinificazioni. Vol. 1. Quarta Edizione italiana. Edagricole.

Rieth, W., 1984. Gaschromatographisch-massenspektrometrische Untersuchungen flüchtiger Inhaltsstoffe des Traubenmost- und Weinaromas: Einfluss önologischer Verfahren und Behandlungsstoffe auf die Aromazusammensetzung. Dissertation, Universität Karlsruhe, Karlsruhe.

Rigaud, J., Cheynier, V., Asselin, C., Brossaud, F., Moutounet, M., 1996. Caractérisation des flavonoïdes de la baie de raisin. Application à une étude terroir. In Oenologie 95 (ed. A. Lonvaud-Funel), Lavoisier, Paris, p. 137.

Roberts, L.D., Souza, A.L., Gerszten, R.E., Clish, C.B., 2012. Targeted metabolomics. Current Protocols in Molecular Biology, 98, 30.2.1–30.2.24.

Robinson, A.L., Adams, D.O., Boss, P.K., Heymann, H., Solomon, P.S., Trengove, R.D., 2012. Influence of Geographic Origin on the Sensory Characteristics and Wine Composition of Vitis vinifera cv. Cabernet Sauvignon Wines from Australia. Am. J. Enol. Vitic. 63-4.

Robinson, A.L., Boss, P.K., Heymann, H., Solomon, P.S., Trengove, R.D., 2011. Development of a sensitive non-targeted method for characterizing the wine volatile profile using headspace solid-phase microextraction comprehensive two-dimensional gas chromatography time-of-flight mass spectrometry. J. Chromatogr. A 1218 504–517.

Robinson, J., Harding, J., Vouillamoz, J., 2012. Wine Grapes: A complete guide to 1,368 vine varieties, including their origins and flavours. Penguin Random House UK. 1248 pages.

Roggero, J.-P., Coen, S., Ragonnet, B., 1986. High performance liquid chromatography survey on changes in pigment content in ripening grapes of Syrah. An approach to anthocyanin metabolism. Am. J. Enol. Vitic. 37, 77.

Roggero, J.P., Larice, J.-L., Rocheville-Divorne, C., Archier P., Coen, S., 1988. Composition anthocyanique des cépages. I: Essai de classification par analyse en composantes principales et par analyse factorielle discriminante. Rev. Fr. Oenol. 112, 41.

Rojas-Cherto, M., Peironcely, J.E., Kasper, P.T., van der Hooft, J.J., de Vos, R.C., Vreeken, R., Hankemeier, T., Reijmers, T., 2012. Metabolite identification using automated comparison of high-resolution multistage mass spectral trees. Anal. Chem. 84, 5524–5534.

Roman, T., Barp, L., Malacarne, M., Nardin, T., Nicolini, G., Larcher, R., 2019. Mono- and di-glucoside anthocyanins extraction during the skin contact fermentation in hybrid grape varieties. European Food Resear. Technol. 245, 2373–2383.

Rose, R., Damoc, E., Denisov, E., Makarov, A., Heck, A., 2012. High-sensitivity Orbitrap mass analysis of intact macromolecular assemblies. Nat. Methods, 9, 1084.

Ruan, Q., Ji, Q.C., Arnold, M.E., Humphreys, W.G., Zhu, M., 2011. Strategy and its implications of protein bioanalysis utilizing high-resolution mass spectrometric detection of intact protein. Anal. Chem. 83, 8937–44.

Rubiolo, P., Liberto, E., Sgorbini, B., Russo, R., Veuthey, J.-L., Bicchi, C., 2008. Fast-GC–conventional quadrupole mass spectrometry in essential oil analysis. J. Sep. Sci. 31, 1074.

Rudell, D.R., Mattheis, J.P., Curry, F.A., 2008. Prestorageultraviolet-white light irradation alters apple peel metabolome. J. Agric. Food Chem. 56, 1138-1147.

Ruffa, P., Raimondi, S., Boccacci, P., Abbà, S., Schneider, A., 2016. The key role of “Moscato bianco” and “Malvasia aromatica di Parma” in the parentage of traditional aromatic grape varieties. Tree Genet. Genomes 12(3), 114.

Rusilowicz, M., O’Keefe, S., Wilson, J., Charlton, A., 2014. Chemometrics applied to NMR analysis. In R. A. Meyers (Ed.), Encyclopedia of analytical chemistry. John Wiley & Sons, Ltd, NJ, USA.

Ryan, D., Morrison, P., Marriott, P., 2005. Orthogonality considerations in comprehensive two-dimensional gas chromatography. J. Chromatogr. A, 1071, 47–53.

Ryu, S., Koda, M., Miyaka, W.A.T., Tanokura, M., 2017. Quantitation of minor components in mango juice with band-selective excitation NMR spectroscopy. J. Agric. Food Chem. 65, 9547–9552.

Sadras, V.O., and Moran, M.A., 2012. Elevated temperature decouples anthocyanins and sugars in berries of Shiraz and Cabernet Franc. Australian J. Grape Wine Resear. 18, 115-122.

Saha, D., Bhattacharya, S., 2010. Hydrocolloids as thickening and gelling agents in food: A critical review. J. Food Sci. Technol. 47, 587–597.

Saito, Y., Kodama, S., Kodama,S., Matsunaga, A., Yamamoto, A., 2004. Multiresidue Determination of Pesticides in Agricultural Products by Gas Chromatography/Mass Spectrometry with Large Volume Injection. J. AOAC Int. 87, 1356–1367.

Sanchez-Ilarduya, M. B., Sanchez-Fernandez, C., Garmon-Lobato, S., Abad-Garcia, B., Berrueta, L. A., Gallo, B., Vicente, F., 2014. Detection of non-coloured anthocyanin–flavanol derivatives in Rioja aged red wines by liquid chromatography–mass spectrometry. Talanta, 121, 81−88.

Savorani, F., Tomasi, G., Engelsen, S.B., 2010. icoshift: A versatile tool for the rapid alignment of 1D NMR spectra. J. Magnetic Resonance, 202, 190–202.

Scalabrelli, G., Ferroni, G., Zinnai, A., Venturi, F., Andrich, G., 2008. Sensorial characteristics of wines obtained from late harvest of grapevine variety Malvasia di Candia aromatica in Tuscany. Riv. Viticol. Enol. 2, 409-422.

Scano, P., Anedda, R., Melis, M.P., Dessi', M.A., Lai, A., Roggio, T., 2011. ^{1}H- and ^{13}C-NMR characterization of the molecular components of the lipid fraction of pecorino sardo cheese. J. American Oil Chemists' Society, 88, 1305–1316.

Schauer, N., Steinhauser, D., Strelkov, S., Schomburg, D., Allison, G., Moritz, T., Lundgren, K., Roessner-Tunali, U., Forbes, M.G., Willmitzer, L., Fernie, A.R., Kopka, J., 2005. GC-MS libraries for the rapid identification of metabolites in complex biological samples. FEBS Lett. 579: 1332–1337.

Schauer, N., Steinhauser, D., Strelkov, S., Schomburg, D., Allison, G., Moritz, T., Lundgren, K., Roessner-Tunali, U., Forbes, M.G., Willmitzer, L., Fernie, A.R., Kopka, J., 2005. GC–MS libraries for the rapid identification of metabolites in complex biological samples. FEBS Letters, 579, 1332-1337.

Schievano, E., Stocchero, M., Morelato, E., Facchin, C., Mammi, S., 2012. An NMR-based metabolomic approach to identify the botanical origin of honey. Metabolomics, 8, 679–690.

Schievano, E., Tonoli, M., Rastrelli, F., 2017. NMR quantification of carbohydrates in complex mixtures. A challenge on honey. Anal. Chem. 89, 13405–13414.

Schmitt, C., Turgeon, S.L., 2011. Protein/polysaccharide complexes and coacervates in food systems. Advances in Colloid and Interface Science, 167, 63–70.

Schneider, A., Torello Marinoni, D., 2003. Analisi con marcatori molecolari microsatelliti di vitigni autoctoni della provincia di Reggio Emilia. Convegno "Recupero e valorizzazione di vitigni autoctoni". Correggio RE, 12 dicembre 2003.

Schreier, P., 1979. Flavor composition of wines: a review, CRC. Food Sci. Nutr. 12 59-111.

Schreier, P., 1979. Flavor composition of wines: a review, CRC. Food Sci. Nutr. 12 59-111.

Schreier, P., and Drawert, F., 1974. Gaschromatographisch-massenspektrometrische Untersuchung flüchtiger Inhaltsstoffe des Weines. I. Unpolare Verbindungen des Weinaromas, Z. Lebensmittelunters. -Forsch. 154, 273.

Schreier, P., Drawert, F., Junker, A., 1976. Identification of volatile constituents from grapes. J. Agric. Food Chem. 24 331-336.

Schreier, P., Drawert, F., Junker, A., and Reiner, L., 1976. Anwendung der multiplen Diskriminanzanalyse zur Differenzierung vou Rebsorten anhand der quantitativen Verteilung flfichtiger Weininhaltsstoffe. Mitt. Klosterneuburg 26 225-234.

Schreier, P., Drawert, f., Junker, A., Barton, H., Leupotd, G., 1976b. Über die Biosynthese von Aromastoffen durch Mikroorganismen. II. Bildung von Schwefelverbindungen aus Methionin dutch Saccharomyces cerevisiae, Z. Lebensmittelunters. -Forsch. 162 279-284. 71

Schreier, P., Drawert, F., Kerenyi, Z., Junker, A., 1976d. Gaschromatographisch-massenspektrometrische Untersuchung flfichtiger Inhaltsstoffe des Weines. VI. Aromastoffe in Tokajer Trockenbeerenauslese (Aszu) Weinen, a) Neutralstoffe, Z. Lebensmittelunters. -Forsch. 161 249-258.

Schreier, P., Drawert, F., Winkler, A., 1979. Composition of neutral volatile constituents in grape brandies. J. Agric. Food Chem. 27 365-372.

Schueuermann, C., Khakimov, B., Balling Engelsen, S., Bremer, P., Silcock, P., 2016. GC-MS Metabolite Profiling of Extreme Southern Pinot noir Wines: Effects of Vintage, Barrel Maturation, and Fermentation Dominate over Vineyard Site and Clone Selection. J. Agric. Food Chem. 64, 2342−2351.

Schueuermann, C., Steel, C.C., Blackman, J.W., Clark, A.C., Schwarz, L.J., Moraga, J., Collado, I.G., Schmidtke, L.M., 2019. AGC–MS untargeted metabolomics approach for the classification of chemical differences in grape juices based on fungal pathogen. Food Chem. 270, 375–384376.

Schuhmann, K., Almeida, R., Baumert, M., Herzog, R., Bornstein, S.R., Shevchenko, A., 2012. Shotgun lipidomics on a LTQ Orbitrap mass spectrometer by successive switching between acquisition polarity modes. J. Mass Spectrom. 47, 96–104.

Schuhmann, K., Herzog, R., Schwudke, D., Metelmann-Strupat, W., Bornstein, S.R., Shevchenko, A., 2011. Bottom-up shotgun lipidomics by higher energy collisional dissociation on LTQ Orbitrap mass spectrometers. Anal. Chem. 83, 5480–87.

Schwartz, J.C., Wade, A.P., Enke, C.G., Cooks, R.G., 1990. Systematic delineation of scan modes in multidimensional mass spectrometry. Anal. Chem. 62, 1809.

Schwarz, M., Wabnitz, T.C., Winterhalter, P., 2003. Pathway Leading to the Formation of Anthocyanin−Vinylphenol Adducts and Related Pigments in Red Wines. J. Agric. Food Chem. 51, 3682-3687.

Schwudke, D., Liebisch, G., Herzog, R., Schmitz, G., Shevchenko, A., 2007. Shotgun lipidomics by tandem mass spectrometry under data-dependent acquisition control. Methods Enzymol. 433, 175–91.

Scienza, A., Failla, O., Toninato, L., Cardetta, A., Fabrizio, C., Pastore, R., Lanati, D., 2004. Dizionario dei vitigni antichi minori italiani. Ci.Vin. Editore, Siena.

Sciubba, F., Capuani, G., Di, C.M.E., Avanzato, D., Delfini, M., 2014. Nuclear magnetic resonance analysis of water soluble metabolites allows the geographic discrimination of pistachios (Pistacia vera). Food Resear. Intern. 62, 66–73.

Scotter, M., 2009. The chemistry and analysis of annatto food colouring: A review. Food Additives & Contaminants: Part A, 26, 1123–1145.

Segurel, M.A., Razungles, A.J., Riou, C., Salles, M., Baumes, R.L., 2004. Contribution of Dimethyl Sulfide to the Aroma of Syrah and Grenache Noir Wines and Estimation of Its Potential in Grapes of These Varieties. J. Agric. Food Chem. 52, 7084-7093.

Self, R.L., Wu, W.H., Marks, H,S., 2011. Simultaneous quantification of eight biogenic amine compounds in tuna by matrix solid-phase dispersion followed by HPLC-Orbitrap mass spectrometry. J. Agric. Food Chem. 59, 5906–13.

Senko MW, Canterbury JD, Guan S, Marshall AG. A high performance modular data system for fourier transform ion cyclotron resonance mass spectrometry. Rapid Commun. Mass Spectrom. 1996; 10: 1839

Shaka, A., Barker, P., Freeman, R., 1985. Computer-optimized decoupling scheme for wideband applications and low-level operation. J. Magnetic Resonance, 64, 547–552.

Shaka, A., Keeler, J., Frenkiel, T., Freeman, R., 1983. An improved sequence for broadband decoupling: WALTZ-16. J. Magnetic Resonance, 52, 335–338.

Shaked-Sachraya, L., Weissb, D., Reuveni, M., Nissim-Leviaand, A., Oren-Shamir, M., 2002. increased anthocyanin accumulation in aster flowers at elevated temperatures due to magnesium treatment. Physiol. Plant. 114, 559-565.

Sheehan, T.L., 2002. The best MS Option: GC-MS and LC-MS. Am. Lab. September, 40 – 43.

Shi, T., Zhu, M.T., Chen, Y., Yan, X.L., Chen, Q., Wu, X.L., Lin, J., Xie, M., 2018. ^{1}H NMR combined with chemometrics for the rapid detection of adulteration in camellia oils. Food Chem. 242, 308–315.

Shimizu, J., Nokara, M., Watanabe, M., 1982. Transformation of terpenoids in grape must by Botrytis ciuerea. Agric. biol. Chem. 46 1339-1344.

Shinohara, T., 1985. Gas chromatographic analysis of volatile fatty acids in wines. Agr. Biol. Chem. 49, 2211-2212.

Shumilina, E., Ciampa, A., Capozzi, F., Rustad, T., Dikiy, A., 2015. NMR approach for monitoring post-mortem changes in Atlantic salmon fillets stored at 0 and 4 °C. Food Chem. 184, 12–22.

Siddiqui, N., Sim, J., Silwood, C.J., Toms, H., Iles, R.A., Grootveld, M., 2003. Multicomponent analysis of encapsulated marine oil supplements using high-resolution ^{1}H and ^{13}C NMR techniques. J. Lipid Resear. 44, 2406–2427.

Silipo, A., Larsbrink, J., Marchetti, R., Lanzetta, R., Brumer, H., Molinaro, A., 2012. NMR spectroscopic analysis reveals extensive binding interactions of complex xyloglucan oligosaccharides with the cellvibrio japonicus glycoside hydrolase family 31 α-xylosidase. Chem. European J. 18, 13395–13404.

Simpson, R.F., 1978b. 1,1,6-Trimethyl-1,2-dihydronaphthalene: an important contributor to the bottle aged bouquet of wine, Chemy Ind. 37.

Simpson, R.F., 1980. Volatile aroma components of Australian port wines. J. Sci. Food Agric. 31 214-222.

Simpson, R.F., Strauss, C.R., Williams, P.J., 1977. Vitispirane: a C13 spirt-ether in the aroma volatiles of grape juice, wines and distilled grape-spirits. Chemy Ind. 663-664.

Simpson, R.F., Strauss, C.R., Williams, P.J., 1977. Vitispirane: a C_{13} spirt-ether in the aroma volatiles of grape juice, wines and distilled grape-spirits. Chemy Ind. 663-664.

Sinanoglou, V.J., Kokkotou, K., Fotakis, C., Strati, I., Proestos, C., Zoumpoulakis, P., 2014. Monitoring the quality of γ -irradiated macadamia nuts based on lipid profile analysis and chemometrics. Traceability models of irradiated samples. Food Resear. Int. 60, 38–47.

Singh, M., Kumar, A., Srivastava, G., Deepak, D., Singh, M.P.V.V., 2016. Isolation, structure elucidation and DFT study on two novel oligosaccharides from yak milk. J. Molecular Structure, 1117, 69–78.

Sivankalyani, V., Feygenberg, O., Diskin, S., Wright, B., Alkan, N., 2016. Increased anthocyanin and flavonoids in mango fruit peel are associated with cold and pathogen resistance. Postharvest Biol. Technol. 111, 132-139.

Skogerson, K., Runnebaum, R., Wohlgemuth, G., de, R.J., Heymann, H., Fiehn, O., 2009. Comparison of gas chromatography-coupled time-of-flight mass spectrometry and ^{1}H nuclear magnetic resonance spectroscopy metabolite identification in white wines from a sensory study investigating wine body. J. Agric. Food Chem. 57, 6899–907.

Šmejkalova, D. and Piccolo, A., 2010. High-power gradient diffusion NMR spectroscopy for the rapid assessment of extra-virgin olive oil adulteration. Food Chem. 118, 153–158.

Smolinska, A., Blanchet, L., Buydens, L.M., Wijmenga, S.S., 2012. NMR and pattern recognition methods in metabolomics: From data acquisition to biomarker discovery: A review. Analytica Chimica Acta, 750, 82–97.

Sobolev, A.P., Testone, G., Santoro, F., Nicolodi, C., Iannelli, M.A., Amato, M.E., Ianniello, A., Brosio, E., Mannina L., 2010. Quality traits of conventional and transgenic lettuce (Lactuca sativa L.) at harvesting by NMR metabolic profiling. J. Agric. Food Chem. 58, 6928–6936.

Soltow, Q.A., Strobel, F.H., Mansfield, K.G., Wachtman, L., Park, Y., Jones, D.P., 2013. High-performance metabolic profiling with dual chromatography-Fourier-transform mass spectrometry (DC-FTMS) for study of the exposome. Metabolomics 9, S132–S143.

Son, H.S., Hwang, G.S., Kim, K.M., Ahn, H.J., Park, W.M., Van Den Berg, F., Hong, Y.S., Lee, C.H., 2009. Metabolomic studies on geographical grapes and their wines using ^{1}H NMR analysis coupled with multivariate statistics.J. Agric. Food Chem. 57, 1481–1490.

Sparkman, O.D., Penton, Z., Kitson, F.G., 2011. Gas Chromatography and Mass Spectrometry: A Practical Guide. 2nd edition, Pages: 632, Academic Press, San Diego, CA.

Spyros, A. and Dais, P., 2013. NMR spectroscopy in food analysis. Cambridge: Royal Society of Chemistry.

Steinke, R.D., and Paulson, M.C., 1964. The production of steam-volatile phenols during the cooking and alcoholic fermentation of grain. J. Agric. Food Chem. 12 381-387.

Stern, D.J., Lee, A., Mc Fadden, W.H., Stevens, K.L., 1967. Volatiles from grapes. Identification of volatiles from concord essence. J. Agric. Food Chem. 15 1100-1103.

Storm, J., Perner, J., Aparicio, I., Patzewitz, E-M., Olszewski, K., Llines, M., Engel, P.C., Müller, S., 2011. Plasmodium falciparum glutamate dehydrogenase a is dispensable and not a drug target during erythrocytic development. Malar. J. 10, 193.

Strupat, K., Scheibner, O., Bromirski, M., 2016. High-Resolution, Accurate-Mass Orbitrap Mass Spectrometry –Definitions, Opportunities, and Advantages. Thermo Fisher, Technical Note 64287.

Sun, J., Lin L.-z., Chen, P., 2012. Study of the mass spectrometric behaviors of anthocyanins in negative ionization mode and its applications for characterization of anthocyanins and non-anthocyanin polyphenols. Rapid Commun. Mass Spectrom. 26, 1123–1133.

t'Kindt, R., Morreel, K., Deforce, D., Boerjan, W., Van Bocxlaer, J., 2009. Joint GC–MS and LC–MS platforms for comprehensive plant metabolomics: Repeatability and sample pre-treatment. J. Chromatog. B. 877, 3572–3580.

Tassoni, A., Tango, N., Ferri, M., 2014. Polyphenol and Biogenic Amine Profiles of Albana and Lambrusco Grape Berries and Wines Obtained Following Different Agricultural and Oenological Practices. Food Nutri. Sci., 5, 8-16.

Tautenhahn, R., Cho, K., Uritboonthai, W., Zhu, Z., Patti, G.J., Siuzdak, G., 2012. An accelerated workflow for untargeted metabolomics using the METLIN database. Nature Biotechnol. 30, 826–828.

Tavares, M.I.B., 2017. NMR Relaxometry Applied to Food Samples', In A. Rahman & I. Choudhary (Eds.), Applications of NMR spectroscopy (pp.151–176). United Arab Emirates: Bentham Science Publishers.

Teleman, A., Kruus, K., Ammälahti, E., Buchert, J., Nurmi, K., 1999. Structure of dicarboxyl malto-oligomers isolated from hypochlorite-oxidised potato starch studied by ^{1}H and ^{13}C NMR spectroscopy. Carbohydrate Research, 315, 286–292.

Tengku-Rozaina, T.M. and Birch, E.J., 2014. Positional distribution of fatty acids on hoki and tuna oil triglycerides by pancreatic lipase and ^{13}C NMR analysis. European J. Lipid Sci. Technol. 116, 272–281.

Terrier, A., Boidron, J.N., Ribéreau-Gayon, P., 1972. Teneurs en composés terpéniques des raisins de V. vinifera. C.r. Acad. Sci.Ser. D. 275 941-944.

Terrier, A., Thèse Docteur-ingénieur, UniversitéUniversit6 de Bordeaux II, Bordeaux 1972.

Thomas, A., Geyer, H., Schanzer, W., Crone, C., Kellmann, M., Moehring, T., Thevis, M., 2012. Sensitive determination of prohibited drugs in dried blood spots (DBS) for doping controls by means of a benchtop quadrupole/Orbitrap mass spectrometer. Anal. Bioanal. Chem. 403, 1279–89.

Tikunov, Y., Lommen, A., de Vos, C.H.R., Verhoeven, H.A., Bino, R.J., Hall, R. D., Bovy, A.G., 2005. A novel approach for non-targeted data analysis for metabolomics. Large-scale profiling of tomato fruit volatiles. Plant Physiol. 139, 1125-1137.

Tociu, M., Todasca, M.-C., Bratu, A., Mihalache, M., Manolache, F., 2018. Fast approach for fatty acid profiling of dairy products fats using ^{1}H-NMR spectroscopy. International Dairy J. 83, 52–57.

Tsiafoulis, C.G., Skarlas, T., Tzamaloukas, O., Miltiadou, D., Gerothanassis, I.P., 2014. Direct nuclear magnetic resonance identification and quantification of geometric isomers of conjugated linoleic acid in milk lipid fraction without derivatization steps: Overcoming sensitivity and resolution barriers. Analytica Chimica Acta, 821, 62–71.

Vaclavik, L., Lacina, O, Hajslova, J., Zweigenbaum, J., 2011. The use of high performance liquid chromatography–quadrupole time-of-flight mass spectrometry coupled to advanced data mining and chemometric tools for discrimination and classification of red wines according to their variety. Anal. Chim. Acta, 685, 45-51.

Vallverdú-Queralt, A., Boix, N., Piqué, E., Gómez-Catalan, J., Medina-Remon, A., Sasot, G., Mercader-Martí, M., Llobet, J.M., Lamuela-Raventos, R.M., 2015. Identification of phenolic compounds in red wine extract samples and zebrafish embryos by HPLC-ESI-LTQ-Orbitrap-MS. Food Chem. 181, 146–151.

Vaysse, J., Balayssac, S., Gilard, V., Desoubdzanne, D., Malet-Martino, M., Martino, R., 2010. Analysis of adulterated herbal medicines and dietary supplements marketed for weight loss by DOSY 1H-NMR. Food Additives & Contaminants: Part A, 27, 903–916.

Venkatachalam, M., Zelena, M., Cacciola, F., Ceslova, L., Girard-Valenciennes, E., Clerc, P., Dugo, P., Mondello, L., Fouillaud, M., Rotondo, A., Dufosse, L., 2018. Partial characterization of the pigments produced by the marine-derived fungus Talaromyces albobiverticillius 30548. Towards a new fungal red colorant for the food industry. J. Food Comp. Analysis, 67, 38–47.

Vermathen, M., Marzorati, M., Baumgartner, D., Good, C., Vermathen, P., 2011. Investigation of different apple cultivars by high resolution magic angle spinning NMR: A feasibility study. J. Agric. Food Chem. 59, 12784–12793.

Viggiani, L., Castiglione Morelli, M.A. 2008. Characterization of Wines by Nuclear Magnetic Resonance: A Work Study on Wines from the Basilicata Region in Italy. J. Agric. Food Chem., 56, 8273–8279.

Virus, E.D., Sobolevsky, T.G., Rodchenkov, G.M., 2008. Introduction of HPLC/Orbitrap mass spectrometry as screening method for doping control. J. Mass Spectrom. 43, 949–57.

Vlahov, G., 1998. Regiospecific analysis of natural mixtures of triglycerides using quantitative ^{13}C nuclear magnetic resonance of acyl chain carbonyl carbons. Magnetic Resonance Chem. 36, 359–362.

Vlahov, G., 1999. Application of NMR to the study of olive oils. Progress in Nuclear Magnetic Resonance Spectroscopy, 35, 341–357.

Vogels, J.T.W.E., Terwel, L., Tas, A.C., Van Den Berg, F., Dukel, F., Van Der Greef, J., 1996. Detection of adulteration in orange juices by a new screening method using proton NMR spectroscopy in combination with pattern recognition techniques. J. Agric. Food Chem. 44, 175–180.

Vrsic, S., and Vodovnik, T., 2012. Reactions of grape varieties to climate changes in North East Slovenia. Plant Soil Environ. 58, 34-41.

Vu, T.N. and Laukens, K., 2013. Getting your peaks in line: A review of alignment methods for NMR spectral data. Metabolites, 3, 259–276.

W. B. Dunn, D. Broadhurst, P. Begley, Zelena, E., Francis-McIntyre, S., ANderson, N., Brown, M., Knowles, J.D., Halsall, A., Haselden, J.N., Nicholls, A.W., Wilson, I.D., Kell, B.D., Goodacre, R., The Human Serum Metabolome (HUSERMET) Consortium, 2011. Procedures for large-scale metabolic profiling of serum and plasma using gas chromatography and liquid chromatography coupled to mass spectrometry. Nat. Protoc., 6, 1060–1083.

Wang, S., Li, C., Copeland, L., Niu, Q., Wang, S., 2015. Starch retrogradation: A comprehensive Review. Comprehen. Rev. Food Sci. Food Safety, 14, 568–585.

Wang, Y., Zhang, T., Xu, J., Du, W., 2011. Comparison of the binding affinity of chlorogenic acid with two serum albumins. Int. J. Biolog. Macromol. 48, 81–86.

Wei, F., Furihata, K., Koda, M., Hu, F., Kato, R., Miyakawa, T., Tanokura, M., 2012. ^{13}C NMR-based metabolomics for the classification of green coffee beans according to variety and origin. J. Agric. Food Chem. 60, 10118–10125.

Welch, R.C., Johnston, J.C., Hunter, G.L.K., 1982. Volatile constituents of the Muscadine grape (V. rotundifolia). J. Agric. Food Chem. 30 681-684.

Werner, E., Croixmarie, V., Umbdenstock, T., Ezan, E., Chaminade, P., Tablet, J.C., Junot, C., 2008. Mass spectrometry based metabolomics: accelerating the characterization of discriminating signals by combining statistical correlations and ultrahigh resolution. Anal. Chem. 80, 4918–32.

Wider, G. and Dreier, L., 2006. Measuring protein concentrations by NMR spectroscopy. J. American Chemical Soc. 128, 2571–2576.

Wildenradt, H.L., and Singleton, V.L., 1974. The production of aldehydes as a result of oxydation of polyphenolic compounds and its relation to wine aging. Am. J. Enol. Vitic. 25 119-126.

Willemse, C.M., Stander, M.A., Vestner, J., Tredoux, A.G. J., de Villiers, A., 2015. Comprehensive Two-Dimensional Hydrophilic Interaction Chromatography (HILIC) × Reversed-Phase Liquid Chromatography Coupled to High-Resolution Mass Spectrometry (RP-LC-UV-MS) Analysis of Anthocyanins and Derived Pigments in Red Wine. Anal. Chem. 87, 12006-12015.

Williams, P.J., Strauss, C.R., Wilson, B., Massy-Westropp, R.A., 1982. Novel monoterpene disaccharide glycosides of Vitis vinifera grapes and wines. Phytochem. 21 2013-2020.

Williamson, K. and Hatzakis, E., 2017. NMR spectroscopy as a robust tool for the rapid evaluation of the lipid profile of fish oil supplements. J. Visualized Experiments 123, e55547.

Wold, H., 1966. Estimation of principal components and related models by iterative least squares. In P. R. Krishnaiah (Ed.), Multivariate analysis. New York: Academic Press.

Wong,Y.F., Hartmann, C., Marriott, P.J., 2014. Multidimensional gas chromatography methods for bioanalytical research. Bioanal. 6, 2461–2479.

Xia, J., Psychogios, N., Young, N., Wishart, D.S., 2009. MetaboAnalyst: a web server for metabolomic data analysis and interpretation. Nucl. Acids Res. 37, W652-660.

Xiao, C., Dai, H., Liu, H., Wang, Y., Tang, H., 2008. Revealing the metabonomic variation of rosemary extracts using ^{1}H NMR spectroscopy and multivariate data analysis. J. Agric. Food Chem. 56, 10142–10153.

Yan, B., Huang, J., Dong, F., Yang, L., Huang, C., Gao, M., Shi, A., Zha, W., Shi, L., Hu, X., 2016. Urinary metabolomic study of systemic lupus erythematosus based on gas chromatography/mass spectrometry, Biomed. Chromatogr., 30, 1877–1881.

YannoniNord, L.I., Vaag, P., Duus, J.Ø., 2004. Quantification of organic and amino acids in beer by ^{1}H NMR spectroscopy. Anal. Chem. 76, 4790–4798.

Yousof, N.S.A.M., Xynos, N., Dina, E., Omar, M.H., Keong, C.Y., Wasiman, M.I., Aligiannis, N., 2018. Comparison of Standard Elution and Displacement Modes in Centrifugal Partition Chromatography for an Efficient Purification of Four Anthocyanins from Hibiscus sabdariffa L. J. Pharm. Pharmacol. 6, 701-711.

Zachariasova, M., Cajka, T., Godula, M., Malachova, A., Veprikova, Z., Hajslova, J., 2010. Analysis of multiple mycotoxins in beer employing (ultra)-high-resolution mass spectrometry. Rapid Commun. Mass Spectrom. 24, 3357–67

Zamboni, M., Fregoni, M., Civardi, S., 2009. Terroirs and wines of Malvasia di Candia aromatica. Riv. Viticol. Enol. 2, 25-35.

Zamora, R., Navarro, J.L., Hidalgo, F.J., 1994. Identification and classification of olive oils by high-resolution ^{13}C nuclear magnetic resonance. J. American Oil Chemists' Society, 71, 361–364.

Zhang, A., Liu, Q., Zhao, H., Zhou, X., Sun, H., Nan, Y., Zou, S., Ma, C.W., Wang, X., 2016. Phenotypic characterization of nanshi oral liquid alters metabolic signatures during disease prevention, Sci. Rep., 6, 19333.

Zhang, J., Maloney, J., Drexler, D.M., Cai, X., Stewart, J., Mayer, C., Herbst, J., Weller, H., Shou, W.Z., 2012. Cassette incubation followed by bioanalysis using high-resolution MS for in vitro ADME screening assays. Bioanalysis 4, 581–93.

Zhang, X.L., Wang, C., Chen, Z., Zhang, P.Y., Liu, H.B., 2016. Development and validation of quantitative ^{1}H NMR spectroscopy for the determination of total phytosterols in the marine seaweed sargassum. J.Agric. Food Chem. 64, 6228–32.

Zhang, Y., Zhao, Y., Shen, G., Zhong, S., Feng, J., 2018. NMR spectroscopy in conjugation with multivariate statistical analysis for distinguishing plant origin of edible oils. J. Food Compos. Analysis, 69, 140–148.

Zhao, L., Ni, Y., Su, M., Li, H., Dong, F., Chen, W., Weis, R., Zhang, L., Guiraud, S.P., Martin, F.-P., Rajani, C., Xie, G., Jia, W., 2017. High Throughput and Quantitative Measurement of Microbial Metabolome by Gas Chromatography/Mass Spectrometry Using Automated Alkyl Chloroformate Derivatization. Anal. Chem., 89, 5565–5577.

Zhao, Y., Chen, H., Feng, J., Chen, Z., Cai, S., 2017. ^{1}H NMR-based compositioncompositional identification of different powdered infant formulas. Food Chem. 230, 164–173.

Zheng, H., Lorenzen, J.K., Astrup, A., Larsen, L.H., Yde, C.C., Clausen, M.R., Bertram, H.C., 2016. Metabolic effects of a 24-week energy-restricted intervention combined with low or high dairy intake in overweight women: An NMR-based metabolomics investigation. Nutrients, 8, 108.

Zhou, L.L., Li, C., Weng, X.C., Fang, X.M., Gu, Z.H., 2015. ^{19}F NMR method for the determination of quality of virgin olive oil. Grasas Y Aceites, 66, 102–106.

Zubarev, R.A. and Makarov, A., 2013. Orbitrap Mass Spectrometry: Orbitrap is the newest addition to the family of high-resolution mass spectrometry analyzers. With its revolutionarily new, miniature design, Orbitrap combines high speed with excellent quantification properties, ranking favorably in many analytical applications. Anal. Chem. 85, 5288-5296.